LOWER PALAEOZOIC GEOLOGY OF THE GALA AREA, BORDERS REGION, SCOTLAND

Kassi, Akhtar Mohammad

A Thesis Submitted for the Degree of PhD
at the
University of St Andrews

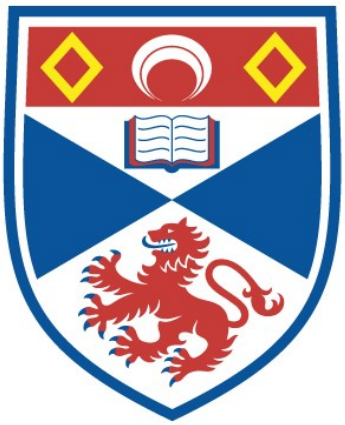

1985

LOWER PALAEOZOIC GEOLOGY OF THE GALA AREA BORDERS REGION, SCOTLAND.

by

Akhtar Mohammad Kassi

Thesis presented for the degree of Doctor of Philosophy in the Faculty of Science of the University of St Andrews

September 1984

ProQuest LLC.
789 East Eisenhower Parkway
P.O. Box 1346
Ann Arbor, MI 48106 – 1346

CERTIFICATE

I certify that AKHTAR MOHAMMAD KASSI has been engaged in research at the university of St. Andrews, and that he has fulfilled the conditions of Ordinance General No. 12, and he is qualified to submit the accompanying thesis in application for the degree of Doctor of Philosophy. He was admitted under this ordinance in may 1981.

I certify that the following thesis is based on the results of research carried out by me, that it is my own composition, and that it has not previously been presented for a higher degree.

WITH THE NAME OF ALLAH

THE COMPASSIONATE, THE MERCIFUL

TO DEAR FRIENDS

CONTENTS

LIST OF FIGURES

LIST OF PLATES

LIST OF TABLES

LIST OF APPENDICES

ABSTRACT

The Lower Palaeozoic succession of the Gala area, Southern Uplands, comprises two contrasting facies, a pelagic/hemipelagic sequence, the Moffat Shales, and overlying turbidite sandstone (greywacke) successions variously of Ordovician and Silurian age. The area is divided into fault blocks bounded by a series of major strike faults, leading to contrasting sequences within successive fault blocks; pelagic/hemipelagic facies are replaced by turbidites progressively later southeastwards. Turbidites in the two northernmost blocks are of Ordovician age, and include two formations. Blocks to the south are formed of three successively younger formations of the Gala Group (Upper Llandovery), with Moffat Shales spanning the Upper Llandeilo - Upper Llandovery interval, whilst the southernmost block includes one formation representing the Hawick Group (?Wenlock). Two formations within the Gala Group have been further subdivided into members. In most instances, formations crop out within discrete fault blocks, though in one instance successively higher levels within a single formation form three separate blocks, whilst another block includes an interdigitating intraformational contact, attributed to the overlapping of two turbidite fans of contrasting source areas.

Whereas blocks display successively younger flysch sequences to the SE, strata within each block young dominantly to NW. The structural style is comparable to areas elsewhere in the Southern

Uplands; showing evidence of prolonged and continuous deformation. Though these observations would support formation of an accretionary prism on an active continental-oceanic margin in response to a northwestward subduction of an oceanic plate, lack of consistent variation in dip attitudes and axial overturning may dispute this proposition.

Palaeocurrents suggest a combination of axial and lateral derivation of rudites and associated fine-grained lithologies with contrasting zones of facies associations, representing environments ranging from inner- to outer-fan (fringe) and basin plain, and suggesting at least three cycles of progression and regression of turbidite fans. Greywacke petrography suggests mainly a magmatic-arc and ophiolitic derivation for 'basic-clast' greywackes and a dominantly Highland type derivation for `silicic` greywackes, with recycling becoming increasingly significant in the higher levels, and indicating elevations of parts of the succession already accreted.

Mineral assemblages, illite crystallinity and b_0 values of illites establishes the anchizone of metamorphism withuot a significant areal variation increase in grade.

1. INTRODUCTION

1.1 Location of the Area

The purpose of this study was to investigate the stratigraphy, petrology, structure, sedimentation, provenance and metamorphism of the Gala Area. The area covers about 250 Km^2, and is located in the southern part of Midlothian (Lothian Region); part of SE Peeblesshire; and the northeastern part of Selkirkshire, (Borders Region), SE Scotland (Fig. 1.1). The area covers the Northern Belt and part of the Central Belt of the Southern Uplands of Scotland (Peach & Horne 1899). The approximate boundaries of the studied area are as follows:

The northern boundary is marked by the Southern Uplands Fault whilst the southern boundary is an arbitrary E-W line about 3 km south of Selkirk. The eastern boundary follows approximately the Edinburgh-Galashiels road (A7) whilst the southwestern and western boundary is marked by the River Tweed; the Gatehopeknowe Burn between [NS 388 376] and [NS 408 376]; northwards through Caddonhead and Ladyside Heights, and thence along the Middleton-Innerleithen road (B7007) to the Southern Uplands Fault.

The rocks exposed are mainly very fine to very coarse grained greywackes interbedded with shales, siltstones and conglomerates. Associated black and grey mudstones, some associated with cherts, represent the Moffat Shale Group. The

Fig. 1.1: Map of the Southern Uplands showing location of the Gala area.

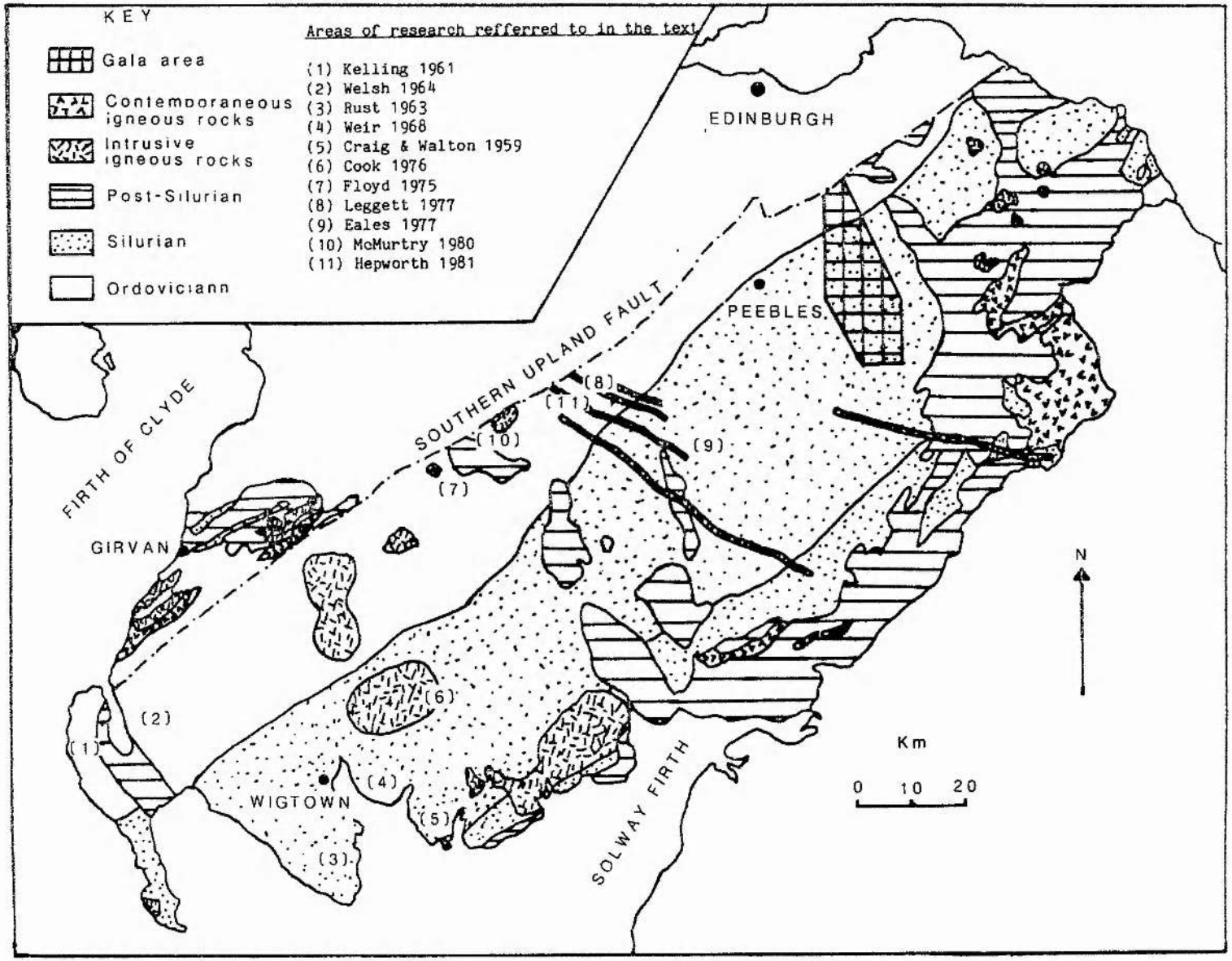

strata are mostly steeply dipping and the strike is NE-SW.

The topography of the area is characteristic of the Southern Uplands as a whole, consisting of a tableland around 700 m high dissected by major rivers having strong geological controls on their trends. The main foci of drainage are the River Tweed and its tributaries the Gala Water and Caddon Water, which approximately follow the regional dip. Tributaries to all three are numerous, and follow the appropriate trends, several being controlled by faults in whole or in part. Some of these are dip faults, others (the majority) strike faults, whilst N-S alignments relate to sinistral strike-slips and NW-SE, to dextral strike slips. Valley floors and slopes carry a thin but obscuring cover of drift, and exposures are confined largely to stream beds, sporadic slope-break crags, and artificial exposures including quarries, and road and railway cuttings. Exposure is probably less than 1 percent of the total area, and its distribution uneven; eastward of the A7 road exposure fails totally under a wide expanse of hill-peat cover.

The area was mapped on a scale of 6 inches to the statute mile.

1.2 History of Previous Research

The pioneers of the research in the Southern Uplands of Scotland were Nicol (1848), Sedgwick (1850), Harkness (1851), Murchison (1851), Geikie (1871) and Lapworth (1870, 1874, 1878).

Lapworth's paper "The Moffat Series" published in 1878 laid down the basic stratigraphy of the Southern Uplands - Longford-Down inlier as a whole. Peach & Horne (1899) revised and further extended Lapworth's work and published the massive Southern Uplands Memoir " Silurian Rocks of Britain": Vol. I, Scotland. Lapworth (1878) and Peach & Horne (1899) established the local stratigraphy, which was based mainly on studies of graptolites occurring in the interbedded black shale sequences and associated, though not interbedded, occurrences of the Moffat Shale Group. Very little information was revealed about the greywackes which form the bulk of the succession.

Lapworth and Peach & Horne regarded the area as being isoclinally folded and arranged as an anticlinorium in the north and a synclinorium in the south. This structural concept persisted for more than half a century.

Research languished until Kuenen (1953) interpreted the rocks of the Southern Uplands as turbidites. Interest was renewed when Walton (1955, 1956), Craig & Walton (1959) and Kelling (1961, 1962) in succession reinterpreted the stratigraphy and structure of the area using sedimentary structures as "way up" criteria. Walton (1955) subdivided the Silurian succession of the Peeblesshire area into three lithostratigraphic units based on the petrology of greywackes. Craig & Walton (1959) extrapolating the structural pattern of the Kirkcudbrightshire coast, reinterpreted the structure of the Southern Uplands as a whole as a succession of monoclinal folds, in which the steep

limbs face consistently NW and are bounded by steep reverse faults which roughly cancel out the descents of the structural profile imposed by the monoformal limbs, to sustain approximately constant stratigraphical Levels across wide cross-strike tracts. Kelling (1961, 1962) demonstrated that the area in the Rhinns of Galloway consists of a series of large complex monoclines rather than an anticlinorium, and subdivided the area into lithostratigraphic units based on the petrological studies of greywackes. Comparable petrographic criteria were employed by other workers, including Gordon (1962); Rust (1963, 1965); Warren (1963); Welsh (1964). Rust (1965), followed by Weir (1968), diagnosed polyphase deformation, recognizing five distinguishable episodes. Subsequent studies, including Floyd (1975), Cook & Weir (1979) and Hepworth (1981), confirmed the validity of petrographic criteria as a basis for establishing lithostratigraphical units displaying widespread lateral continuity. These studies accepted in essence the structural framework of Craig & Walton (1959) and the deformational sequence of Rust (1965).

Meanwhile, in a pioneering study of the Girvan area of Ayrshire (tectonically north of the Southern Uplands), Williams (1958) analysed fault patterns, and interpreted oblique slips as being related to rotation of stress systems during continuing deformation. Stringer & Treagus (1980, 1981) adopted the implication of continuity of deformation, simplifying the deformational sequence to partly discrete though merging F_{1-2} phases (F_{1-2} of Rust 1965) and a late kink-band phase (F_5 of

Rust).

Most recently, Webb (1983) has refined both the `faulted monoform` concept of Craig and Walton (1959) and the detail of the postulated accretionary prism (Mckerrow et al. 1977; Leggett et al. 1979), proposing that a pattern of imbricate faulting in the Ettrick area, related to shearing of early folds under the influence of variable response to lithological contrasts within the succession, is widely and perhaps universally applicable within the Southern Uplands.

Application of the theory of plate tectonics to the Scoto-Irish sector of the Caledonide orogen (Wilson 1966; Dewey 1969a,b; 1971) led to a re-appraisal of the structural framework of the Southern Uplands, and to a wider appreciation of the process of structural evolution therein, in which the deformation pattern was equated with that of modern oceanic sediments deposited above existing subduction zones. Mitchell (1974) compared the structural style with those of modern and ancient examples from the Pecific and Caribbean, and suggested a northwestward subduction of an oceanic plate beneath the site of the present Midland Valley. McKerrow et al. (1977) suggested that the Lower Palaeozoics of the Southern Uplands represents an accretionary prism which developed on an active continental margin where the oceanic plate had a thick sedimentary cover, developing this theme on the following grounds:

a) Contrasting sequences in the Southern Uplands are separated by

major strike faults; adjacent fault-bounded sequences display contrasts in sedimentary facies and composition, suggesting deposition in dissociated localities which may have been widely separated.

b) Fault-bounded sequences become progressively younger to the south, whilst individual fault blocks display an overall northward younging. Within the area studied, sequences range in age from mid-Caradoc to high Llandovery or perhaps Wenlock. Most blocks consists of sparsely fossiliferous or unfossiliferous turbidite/shale sequences conformably overlying Moffat Shales, which persist to successively higher levels southeastwards.

2. STRATIGRAPHY

The Ordovician and Silurian turbidite (flysch) succession of the Gala and Selkirk area overlies representatives of the Moffat Shale Group conformably, and crops out within a number of strikewise-orientated fault blocks (Hepworth 1981). Within the two northwest fault blocks, turbidite deposition took place in the Caradoc epoch, and within the successively higher levels of the more southeasterly blocks in the Llandovery epoch. The Silurian succession was divided (Lapworth 1870; Lapworth & Wilson 1870) into a) the Gala Group and b) the Hawick Group. In the present thesis it is proposed to subdivide the Ordovician succession into two formations and the Gala Group (Lapworth 1870) into three formations. The mapped portion of the Hawick Group (Lapworth 1870) is designated as the Selkirk Formation (Fig. 2.1). These subdivisions are based on lithological characters observable in the field and greywacke petrography. There are subtle colour variations in the rocks of successive formations; fresh hand specimens were accordingly compared with the Rock-Colour Chart (Geol. Soc. Amer., 1980.) and Munsell notation numbers assigned to rock colours (given in brackets). The detailed characters of each formation are as follows:

2.1 ORDOVICIAN SUCCESSION

The Ordovician flysch succession is probably equivalent to the Lowther Group as proposed by Geikie (1871). The stratigraphic position of the group was uncertain, being based on

Fig. 2.I: Geological map of the Gala area

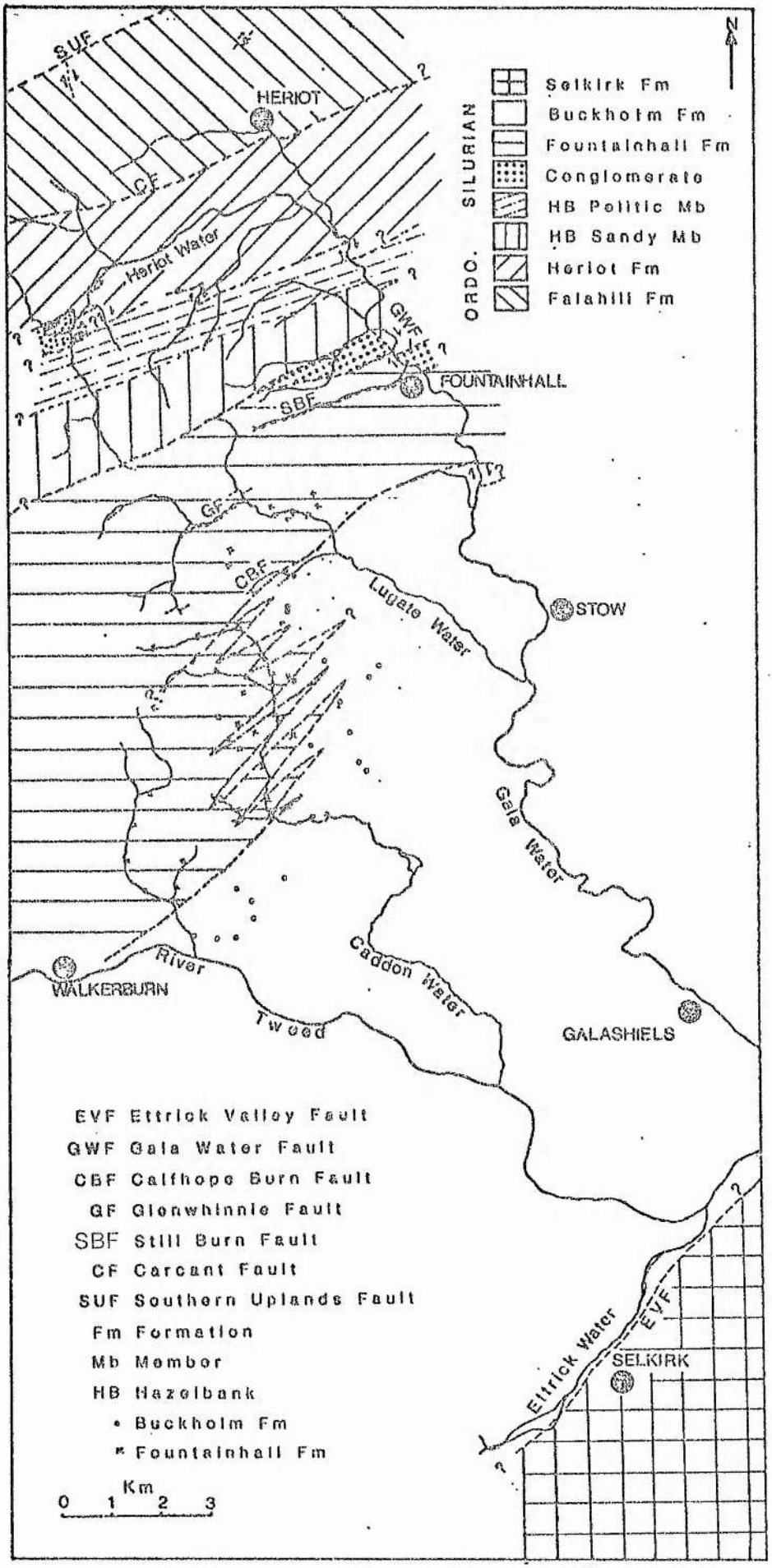

Fig. 2.2: Map showing localities mentioned in text

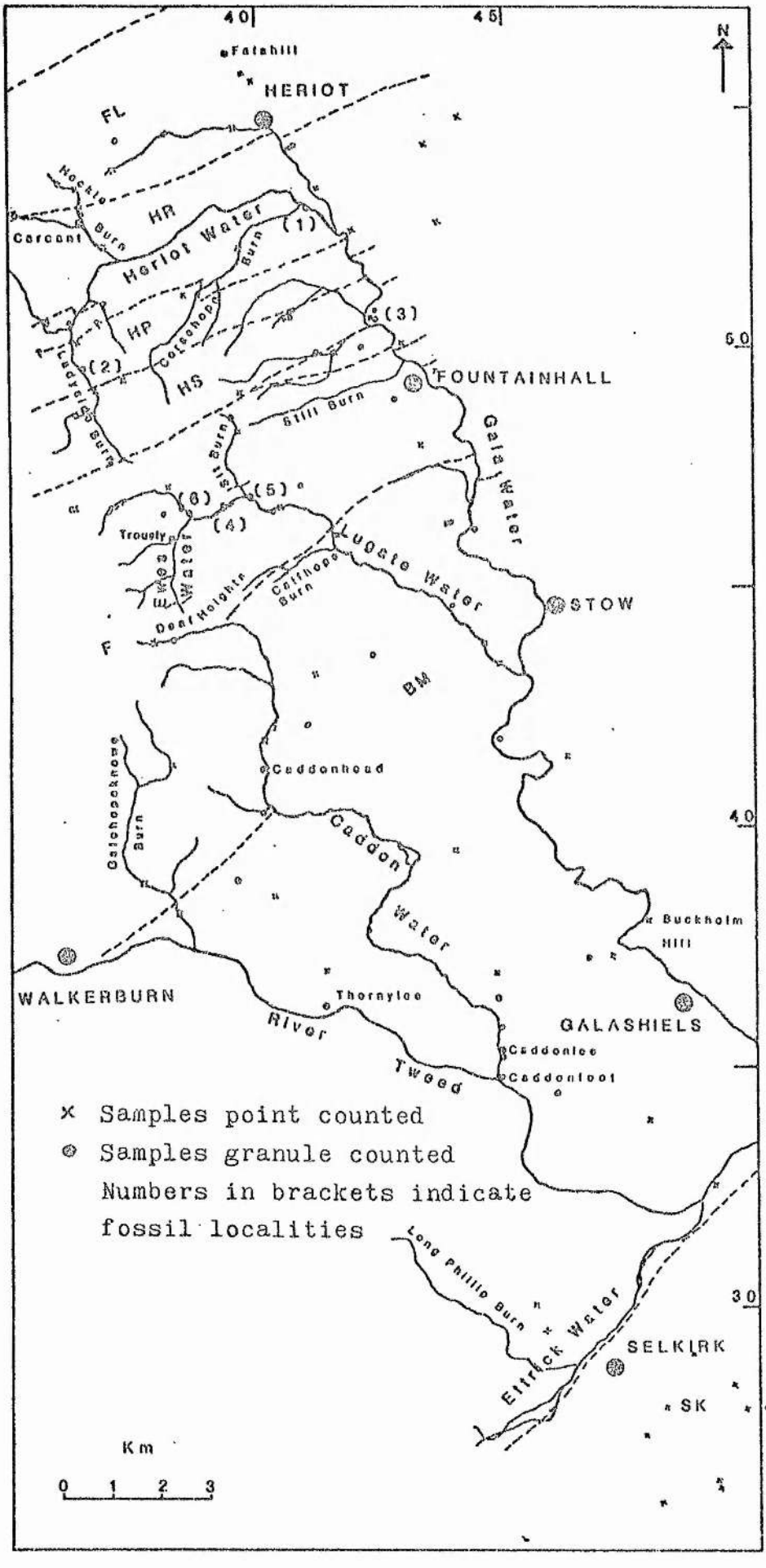

what is now known as a mis-interpretation of the regional structure. The definition of the group being unsatisfactory for this reason, the name was resurrected neither by McMurtry (1980) nor by Hepworth (1981), working in the adjacent (and eponymous) area. For this reason it is not proposed to employ the name in this study, nor is it considered necessary to establish an alternative name of Group status, as the Ordovician flysch succession is less completely represented than in areas to the SW.

2.1.1 Falahill Formation

This formation is named after Falahill, situated on the Forth-Tweed watershed about 2 km N of the now closed Heriot Station [NS 404 546]. The formation is characterized by the presence of dark grey (N3) greywackes which are rich in basic igneous fragments, feldspars, clinopyroxenes and green and brown amphiboles. Garnet and blue amphiboles of the glaucophane group also occur, the latter being the unique characteristic of the Falahill Formation. The greywackes are interbedded with brownish grey (5 YR 4/1) and medium dark grey (N4) shales. The greywackes are very thinly- to thickly-bedded (20 cm to 110 cm), with some beds up to 4 m thick. The beds are mostly massive and poorly graded, and graded units are commonly amalgamated. No notably thick succession of shales was found, though interbedded thin shaly and silty horizons occur.

The northern (upper) limit of the formation is defined by

the Southern Uplands Fault. The southern (lower) contact can be seen about 300 m north of Carcant farmhouse [NS 364 526], crossing the small reservoir in Heckle Burn. The contact is represented by highly sheared and broken greywackes, indicating a fault, the Carcant Fault. Eastwards the contact is not exposed, but is deduced to pass a short distance S of Heriot Station [NS 404 546]. The width of exposure of the Falahill Formation is around 2000 m.

2.1.2 Heriot Formation

a) Greywacke succession

The formation is named after the Heriot Water, and is exposed mostly in its tributaries. It is best exposed in a quarry on the east side of A7 road about 500 m S of Heriot Station [NS 404 546]. This is an 'acid-clast' formation (sensu Kelling 1962), and consists of medium dark grey (N4) greywackes dominated by quartz, acid igneous and metamorphic rock fragments, with subordinate basic igneous and sedimentary clasts and feldspars. The formation is garnetiferous. By contrast with the Falahill Formation, ferromagnesian fragments are notably deficient. The succession is dominated by greywackes which are medium to very coarse grained, thin to very thick (ranging between 3 cm and 230 cm, mostly 50 cm - 2 m), with some thick amalgamated units up to 5 m thick.

b) Moffat Shales associated with Heriot Formation

Two isolated successions of cherts, shales and siltstones represent Moffat Shales underlying the Heriot Formation. In each case the contact is unexposed, but is assumed to be conformable. One succession of olive brown (5 Y 5/6) to moderate olive brown (5 Y 4/4) cherts, medium grey (N5) siltstones and silty shales of up to about 100 m thick is exposed in a stream on the eastern side of the Edinburgh-Innerleithen road just opposite Garvald farmhouse [NS 352 512]. Chert horizons are highly weathered to olive brown (5 Y 5/6) and moderate olive brown (5 Y 4/4), highly friable and broken, and interbedded with very thin (1-3 cm), friable and medium grey (N5) weathered shales. The thickness of the chert beds ranges between 3 cm and 20 cm with a modal thickness of 4-5 cm. Siltstones are also highly broken, weathered and thinly bedded (4-6 cm). Some of these beds are bioturbated; others are parallel laminated. No fossils were found in these shales and siltstones. The second succession of medium grey (N5) siltstones crops out N of Little Dod [locality, NS 369 515] in Heriot Water and can be traced eastwards as far as Hangingshaw Hill, E of the Gala Water near Heriot Station. Within the present area chert horizons are associated only with this level of Moffat Shales.

The northern (upper) contact (described above) of the Heriot Formation with the Falahill Formation is faulted, while the southern (lower) contact of the underlying Moffat Shales with the southeastward-succeeding Hazelbank Formation is not exposed. It is inferred to cross the Corsehope Burn near the Corsehope

farmhouse [NS 387 510]. The shattered state of the Moffat Shales indicates that one or both contacts are tectonic; the southern contact of the Moffat Shales of Caradoc age is also with the Llandovery succession, and is inferentially a major thrust. The width of exposure of the Heriot Formation is over 2000 m.

2.2 GALA GROUP

Also in 1871, Lapworth & Wilsons gave a definition of the Gala Group which is much more satisfactory, as it implies the Llandovery arenaceous succession into which the Moffat Shales pass in the Moffat area. As this definition applies to the post-Ordovician, pre-Hawick Group flysch succession of the present area which, being eponymous, can be accepted as the type area for the group in Lapworth & Wilsons sense, it is considered appropriate to resurrect the name, and to divide it into three formations in accordance with established principles (Harland et al. 1972, Holland et al. 1978).

2.2.1 Hazelbank Formation

This formation is named after Hazelbank Quarry [NS 427 498], on the eastern side of the A7 road about 600 m N of the now closed Fountainhall Station. It can be divided into three members on the basis of lithology (Fig. 2.1):

(a) Conglomeratic Member

This member comprises massive and obscurely bedded conglomerates of 'basic-clast' character which contain copious amounts of rip-up clasts, locally reaching up to several cm in length, occassionally showing their original lamination. The pelitic rip-up clasts are roughly aligned parallel to the strike, but no imbrication was observed. Clasts range from a few mm to 1 cm in size, subangular to subrounded and supported by very coarse to fine grained sandy matrix. Sporadic, uneven horizons of sandy texture which may locally reach up to 1 m in thickness, and are roughly parallel to the strike also occur, but the nature of their contacts with the conglomerate was not determined. Their mineral composition is closely comparable to the Sandy Member (page 13). No cross laminations or current ripples were observed.

These conglomerates occur in only a limited number of exposures (5) in which neither internal nor external contacts are revealed. The upper contact of the member is faulted with the Moffat Shales underlying the Heriot Formation, and the lower contact (inferentially conformable) is with the Pelitic Member of the Hazelbank Formation. The thickness of the member may reach over 500 m.

b) Pelitic Member

In this division pelitic sequences (Bouma Tcde, Tde) dominate over thickly bedded and massive (Bouma Tae) sequences (Zone 2; Chapter 5). The lithology and petrology of sporadic

thick greywacke horizons (Bouma Tae sequences) occurring within the pelitic sequences is the same as in the succeeding Sandy Member, which suggests the same source area, whilst the dominance of pelitic sequences indicates a more distal (probably outer-fan, fringe) association (Chapter 5).

c) Sandy Member

This member is characterized by thickly bedded dark grey (N3) 'basic-clast' greywackes (Kelling 1962), typified by basic igneous fragments, feldspars and ferromagnesian minerals including green clinopyroxenes and green and brown amphiboles. These rocks are correspondingly depleted in quartz, acid igneous, metamorphic and sedimentary clasts. The beds are thin to very thick (3 cm to 1.5 m, with a modal thickness between 20 cm to 1 m), locally up to more than 4.5 m thick, and medium to coarse grained. The interbedded shales range between few cm and 1 m in thickness, and calcareous bands occur sporadically.

The lower contact of the Hazelbank Formation with the Fountainhall Formation follows the course of Comely Burn opposite Hazelbank Quarry, and cuts across the Comely Burn at [NS 417 499]. The contact is inferred to continue westwards between Ladyside Heights [NS 366 473] and Dewar Hill [NS 353 474] but is not visible. East of the Gala Water the contact has been displaced about 800 m southwards by the Gala Water Fault, resuming at Allen Haugh [NS 432 495] and continuing to Cortleferry [NS 440 495].

2.2.2 Fountainhall Formation

The formation is named after Fountainhall village and is exposed in a railway cutting about 500 m NE of Burnhouse [NS 435 495]. It is widely exposed in different localities throughout the reach of the Lugate Water N of Calfhope Burn, and further SW in the higher reaches of Gatehopeknowe Burn between [NS 383 386] and [NS 376 408], NE of Walkerburn. Lithologically it is divisible into following two members:

(a) Sandy and Pelitic Member

This member consists of medium to coarse grained, medium grey (N5) greywackes, sporadic conglomerates and dark grey (N3) and light olive to olive grey (5 Y 5/1) mudstones, siltstones and greyish black (N2) shales. The greywackes are medium to thick bedded (3 cm - 1.5 m), with some massive beds up to 10 m thick, and are again 'acid-clast', being typified by quartz, acid igneous fragments and feldspars. Basic igneous, metamorphic and sedimentary fragments are present in minor amounts. This formation is non-garnetiferous, comparatively less siliceous and richer in feldspars and basic igneous fragments than the Heriot Formation and the succeeding Buckholm Formation.

(b) Conglomeratic Member

This member consists of a thick, massive and obscurely

bedded horizon of conglomerate, which may reach up to nearly 500 m in thickness. Neither internal nor external contacts are exposed. The member lenses out westwards across the Comely Burn between [NS 414 492] and [NS 418 500].

These conglomerates are obscurely bedded, showing sporadic grading to sand size and almost uniformly distributed rip-up clasts. Uneven coarse sandy horizons which may reach up to nearly 1 m in thickness are closely comparable to the greywackes of the lower Sandy and Pelitic Member. The clasts are subangular to subrounded and range from a few mm to over 1 cm in size. Pelitic clasts are aligned parallel to the strike. No imbrication of the clasts was observed. Clasts are supported by a coarse to fine sandy matrix which sometimes exceeds the amount of pebbles.

Again the upper and lower contacts of the conglomerates are not exposed. However, the petrological characters of the conglomerate and associated greywackes are closely comparable to the greywackes of the underlying Sandy Member, and the Conglomeratic Member is therefore regarded as a unit of the Fountainhall Formation.

c) Moffat Shales associated with Fountainhall Formation

Three mappable sequences of pelitic rocks occur within the outcrop of the Fountainhall turbidite facies. The northernmost, which is structurally the highest, is exposed throughout the

course of the Still Burn west of Fountainhall, between [NS 426 492] and [NS 402 484]. This outcrop is of black shales. The second pelitic sequence crops out about 2.5 km to the southwest, and is exposed in the Lugate Water between its junctions with the Sit Burn at [NS 389 468] and the Ewes Water at [NS 387 463]. This consists of medium grey (N5) siltstones and silty shales. The third and the southernmost pelitic sequence crops out about 2 km SE of the Lugate Water outcrop, and follows the course of the Calfhope Burn between [NS 404 454] and [NS 399 451]. This is a succession more than 100 m in thickness of greyish black (N2) shales, brownish grey (5 YR 4/1) siltstones and greenish grey (5 GY 6/1) mudstones and siltstones. A comparably thick sequence of brownish grey (5 YR 4/1) siltstones and mudstones is also exposed (along strike) in the upper reaches of the Ewes Water between [NS 883 453] and [NS 376 443]. This outcrop marks the southeastern limit of the outcrop of the Fountainhall Formation.

As with the pelitic sequence at the base of the Heriot Formation (q.v.), these pelitic sequences represent the pelagic/hemipelagic Moffat Shale successions conformably overlain by turbidites of the Fountainhall facies. Lithological contrasts among the three outcrops are born out by faunal records from the three outcrops (Peach & Horne 1899 and supplementary information herein, and I. Strachan pers. comm.- see Chapter 4, Age and Correlation). These contrasts indicate that the three outcrops represent successively higher levels of the Birkhill Shales.

All the outcrops are highly sheared and disturbed. The

southern outcrop is limited southwards by a fault, which is exposed in the Calfhope Burn and continues into the Ewes Water outcrop. Inferentially the disruption of the two northern pelitic outcrops is likewise related to fault shearing. Three successive fault blocks are thus defined within the Fountainhall outcrop, each having the appropriate level of Birkhill Shales succeeded by turbidites, drawn from a constant source area that span the time. The northern shale outcrop is thus associated with the Still Burn Fault, the central outcrop with the Glenwhinnie Fault, and the southern with the Calfhope Burn Fault.

d) Buckholm-Fountainhall Contact

The lower contact of the lowest shale sequence is faulted in the Calfhope Burn and the fault continues southeastwards across the high reaches of Ewes Water. The fault may be inferred to continue northeastwards beyond the Caddon Water. Relationships between the Fountainhall Formation and the Buckholm Formations become complicated in the vicinity of the Caddon Water. The contact roughly follows the course of the river, on a N-S trend and is highly irregular, the two formations appearing to interdigitate (Fig. 2.1). Southwards the contact again resumes its NE-SW trend, cutting across the Gatehopeknowe Burn. This relationship suggests the interdigitation of two overlapping turbidite fans in the vicinity of the present Caddon Water, carrying material from contrasting source areas, potentially far removed. This suggestion is supported by the following

supplementary observations:

a) Although the Caddon Water follows the sinistral strike-slip trend, there is no evidence of major faulting along the Caddon Water; yet a strike-slip displacement of nearly 4 km would be necessary if interdigitation were not responsible. The north boundary of the Fountainhall and Hazelbank Formations are not offset, and a large strike slip movement would have to be accommodated by thrusting and/or differential buckle-folding in each formation. There is no evidence of differential deformation on an appropriate scale.

b) The strata across the Caddon Water represent comparable facies associations (Zone 5; Chapter 5).

c) Divergence of erosional currents by as much as 90^{o} in successive turbidite sequences is most logically explained by the interdigitation of fans.

d) The occurrence of comparable faunas (Peach & Horne 1899) within the contrasting facies on both sides of the Caddon Water (noting that whereas the Peach & Horne identifications are considerably out-dated, the age determinations remain valid, at least in a broad context).

To the SW extreme of the mapped area, the Fountainhall and Buckholm contact is not exposed and inferentially cuts across the Gatehopeknowe Burn at [NS 383 385] about 2.5 km NW of Walkerburn (Fig. 2.1). Fossil records (Peach & Horne 1899) show that the Buckholm Formation and the southwestern part of the Fountainhall Formation (Fig. 2.1), stratigraphically underlie the level of the

Birkhill Shales exposed in Calfhope Burn and Ewes Water, and constitute one block (see Age and Correlation, Chapter 4), the lower contact of which is along the Ettrick Water. Although unexposed, the contact of the Buckholm and Fountainhall Formations across the Gatehopeknowe Burn at [NS 383 385] is thus considered to be stratigraphical rather than tectonic, though of course there may have been minor shearing related to the contrast in faces between the formations. The 'block' covers a cross-strike width of over 15 km, consists mostly of the Buckholm Formation.

2.2.3 Buckholm Formation

This formation is named after Buckholm Hill (Buckholm Sandstone, Lapworth & Wilson 1870a) N of Galashiels. It consists of very thick and massive, medium dark grey (N4) and dark grey (N3) greywackes (ranging from a few cm up to more than 15 m , and mostly 20 cm to 2 m). In places these greywackes are conglomeratic and in others interbedded with thin to thick (40 cm to 3 m) horizons of greenish grey (5 GY 6/1), brownish grey (5 YR 4/1), greenish olive (10 Y 4/2) mudstones, and medium grey (N5) shales and siltstones. The greywackes are silicic, being notably enriched in quartz, in association with acid igneous and metamorphic rock fragments. Garnet is commonly visible megascopically and is valuable as horizon index. Feldspars, sedimentary and basic igneous clasts are subordinate, and the prevalence of quartz imparts a vitreous lustre to fresh frectured surfaces. The profusion of garnet readily distinguishes the

Buckholm Formation from the otherwise compositionally comparable Fountainhall and Selkirk Formations. The greywackes are interbedded with greenish grey (5 GY 6/1), greyish red (5 R 4/2), brownish grey (5 YR 4/1), greyish olive (10 Y 4/2) and pale brown (5 YR 5/2) mudstones, and medium grey (N5) shales and siltstones. These mudstones are prolific in trace fossils, mostly burrows of Dictyodora (Benton 1982) and are exposed in three localities in Glentanner Burn between [NS 424 411] and [NS 421 415], near Thornylee [NS 401 376] and near Bowshank [NS 460 416] to the E of the A7 road. In Glentanner Burn one locality [NS 424 411] is dominated by greyish red (5 R 4/2) mudstones with subordinate brownish grey (5 YR 4/1) and occasional thin (1 - 3 cm) bands of green mudstones. The second locality [NS 421 415] has a prevalence of greyish olive (10 Y 4/2) mudstones. These mudstones are occasionally silty and show parallel lamination, and contain only a few trace fossils. The thickness of the mudstones ranges between 1 cm and 5 cm, with a mode between 2 - 3 cm. Sporadic thin (2 - 4 cm) silty bands are also present. The thickness of the mudstone horizons in Glentanner Burn is more than 2 m and the contacts are not exposed. Near Thornylee [NS 401 376] the mudstones are dominantly greyish red (5 R 4/2) but brownish and dark grey mudstones are also present interbedded with thickly bedded garnetiferous greywackes (which range 5 cm to 2 m, and mostly between 20 and 40 cm). The mudstone horizons are 2 to 3 m thick, and include sporadic thin (4 - 10 cm), Tcde, Tbcde, Bouma sequences. The Dictyodora burrows denote the Nereites subfacies (thick accumulations of mudstones and siltstones deposited by weak turbidity currents; (cf. Walton

1956, Seilacher 1974), and are concentrated especially within the greyish-red and medium grey mudstones. The environmental controls on these fossils are not certain but oxygen content of the sediment may be involved (Benton 1982) since these are mostly associated with primary red or purple mudstones and some with grey-green mudstones. The red or purple colour of some Gala Group and Hawick Rocks mudstones has been explained in terms of rapid deposition of oxidized source material, inferred as contemporary andesitic volcanics exposed to the coastal erosion during periods of transgression (Ziegler & McKerrow 1975). These authors point out that 'organic productivity can inferred to be low in the areas of red bed accumulation', but the abundance of trace fossils at certain levels suggest considerable biological activity.

The outcrop of the formation is anomalously wide, covering a cross-strike width in excess of 15 km. This width is considered to reflect folding and imbrication, rather than anomalously large stratigraphical thickness (an unfaulted succession with this width of outcrop would record a thickness of more than 8 km; cf. Webb 1983). Its lower contact is with the Selkirk Formation and roughly follows the Ettrick Water north of Selkirk. The contact is inferentially the Ettrick Valley Thrust (Toghill 1970).

2.3 HAWICK GROUP

The Hawick Group was first proposed as a field name, Ardwell Group ('Hawick Rocks'), in the servey of 1860's. The name was

established as the Hawick Rocks (Lapworth & Wilson 1871), considered as basal to the succession. Subsequently resurrected (Warren 1964), the unit was subdivided into two formations by Rust (1965), thus attaining the status of a Group on established procedure (Harland et al. 1972; Holland et al. 1978).

2.3.1 Selkirk Formation

This formation (Selkirk beds, Lapworth & Wilson 1870a) is named after Selkirk town, to the E and SE of which the rocks are exposed in various localities near Bell Hill and Selkirk Common. Originally proposed as a unit overlying the Hawick Rocks, the formation is considered to be a unit within the Hawick Group. The formation consists of medium grey (N5) to medium dark grey (N4), fine grained, flaggy, and thin to moderately thick (ranging from 4 cm to 2.5 cm, and mostly 10 to 75 cm) greywackes interbedded with thin to thick (a few cm to 1m) sequences of medium grey (N5) to olive grey (5 Y 4/1) mudstones, siltstones and shales. The greywackes are characteristically fine grained and siliceous with acid igneous fragments, and a copious matrix which is mostly carbonate. Sporadic coarse grained horizons are not rich in carbonate matrix and tend to be garnetiferous. Metamorphic, basic igneous and sedimentary rock fragments are present in subordinate amounts. In the Selkirk Formation as a whole, interbedded pelitic horizons (Tcde, Tde) are comparatively more abundant (see Zone 6, Chapter 5) and the proportion of the matrix is conspicuously higher than the other formations.

Mapping was terminated within the formation. The lower contact is not exposed in the area, being located probably farther southwards; as noted above, the upper and inferentially faulted contact with the Buckholm Formation coincides approximately with the Ettrick Water. An apparent thickness of at least 3 km was mapped.

3. PETROLOGY

This chapter deals with the petrology of the greywackes, and includes an account of point counting, granule counting and heavy mineral counting of selected specimens. Almost all have more than 15% matrix and most contain more than 20%. The majority correspond to lithic greywackes as defined by Pettijohn (1957) (cf. Fig. 3.3b). The analysed specimens of the Selkirk Formation were not plotted on Pettijohn's diagram because the major portion of the matrix is secondary carbonate (range: 24-40%; mean: 32%) and replacement of other components most probably selective. Specimens of the Selkirk Formation deficient in carbonate matrix do, however, correspond to lithic greywackes. The matrix of the greywackes is partly detrital and partly authigenic (Plates 3.1-3.2), supporting the conclusion that greywacke matrix is at least partly diagenetic in origin (Cummins 1962). The main clastic constituents are quartz, alkali and plagioclase feldspars, rock fragments in variety and ferromagnesian minerals, set in fine grained clastic and secondary phyllosilicate matrix, with or without carbonate. Mineral chemistry and classification of the more complex minerals are considered in detail in chapter 8.

3.1 DOMINANT CLASTIC MINERALS

QUARTZ: This occurs as poorly-sorted detrital grains in all formations. Quartz clasts are typically large in any sample. Grains often display marked corrosion of the boundaries with

replacement by authigenic minerals, dominantly phyllosilicates with a localised development of carbonate. Clay minerals may grow perpendicular to the grain surface, corroding its original boundaries (Plate 3.1). Corrosion of quartz by calcite, by increasing clast angularity (Plate 3.2), contributes to the textural immaturity of the greywackes. Most grains contain inclusions, mostly of the irregular, globular, and regular types (Plate 3.3-3.6; Mackie 1896; Keller and Littlefield 1950); acicular inclusions also occur, but are rare. Identifiable inclusions are mainly of quartz, zircon, apatite, rutile, micas, vermicular chlorite and liquid/gas globules. 100 quartz grains were examined in 5 specimens from each formation and the inclusions present recorded (Table 3.1). In most grains there are two or more types of inclusions, irregular inclusions being ubiquitous and globular occurring in more than 75% of grains. The regular type is subordinate and the acicular type least abundant. As irregular and globular inclusions characterize the quartz of igneous origin (Keller & Littlefield 1950), and regular and acicular inclusions the rocks of metamorphic origin, the study (Table 3.1) suggests that igneous quartz dominate over the metamorphic quartz. The distribution of inclusions is almost the same in all formations (Table 3.1) and is therefore of little value in differentiating between the formations and in discriminating sources, confirming the findings of Kelling (1961) and Floyd (1975). Globular inclusions contain both liquid and gas, and may occur in bands (presumably secondary) or isolated (presumably primary). Liquid inclusions are dominantly of monophase and 2-phase types (Yermakov, 1965, p.25) but isolated

Table 3.1: Inclusions in quartz grains

R = Regular I = Irregular
A = Acicular G = Globular

Sp No	Gr Ref	R	I	A	G
SELKIRK FORMATION					
730	487 291	09	100	06	84
748	480 259	15	100	06	79
785	492 264	08	100	05	87
745	478 273	14	100	06	80
738	481 279	16	100	05	79
mean		12.4	100	5.6	81.8
BUCKHOLM FORMATION					
700	362 359	15	100	03	81
771	456 300	14	100	07	78
159	416 459	11	100	10	79
056	483 378	21	100	06	73
048	460 398	12	100	08	80
mean		14.6	100	6.8	78.2
FOUNTAINHALL FORMATION					
555	376 456	08	100	09	79
680	383 413	10	100	07	81
501	385 465	13	100	05	80
507	396 482	17	100	03	80
654	383 386	14	100	03	83
mean		12.4	100	5.4	80.6
HAZELBANK FORMATION					
390	359 504	20	100	05	69
438	368 490	19	100	01	77
090	429 501	13	100	01	77
2-b	424 506	14	100	06	86
357	388 507	12	100	04	83
mean		15.6	100	04	78.2
HERIOT FORMATION					
617	436 539	18	100	03	77
334-a	365 528	15	100	07	78
81	419 543	17	100	04	79
397	368 508	19	100	04	77
331	366 526	16	100	06	78
mean		17	100	4.8	77.8
FALAHILL FORMATION					
343	352 525	16	100	03	81
340	361 352	12	100	06	82
334	365 528	14	100	06	82
337	365 530	10	100	05	85
80-a	395 554	15	100	10	75
mean		13.4	100	06	80.6

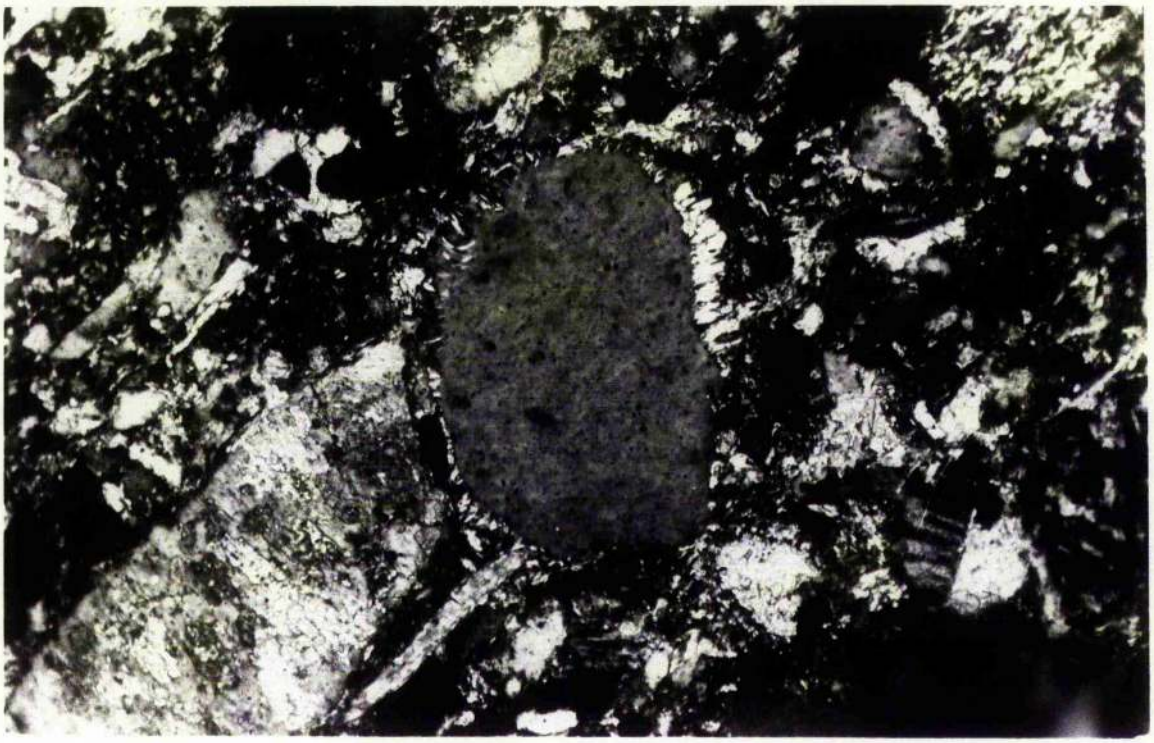

Plate 3.1: Photomicrograph of greywacke from Selkirk Formation showing corrosion of quartz grains by diagenetic (clay) minerals, X250, cross polars.

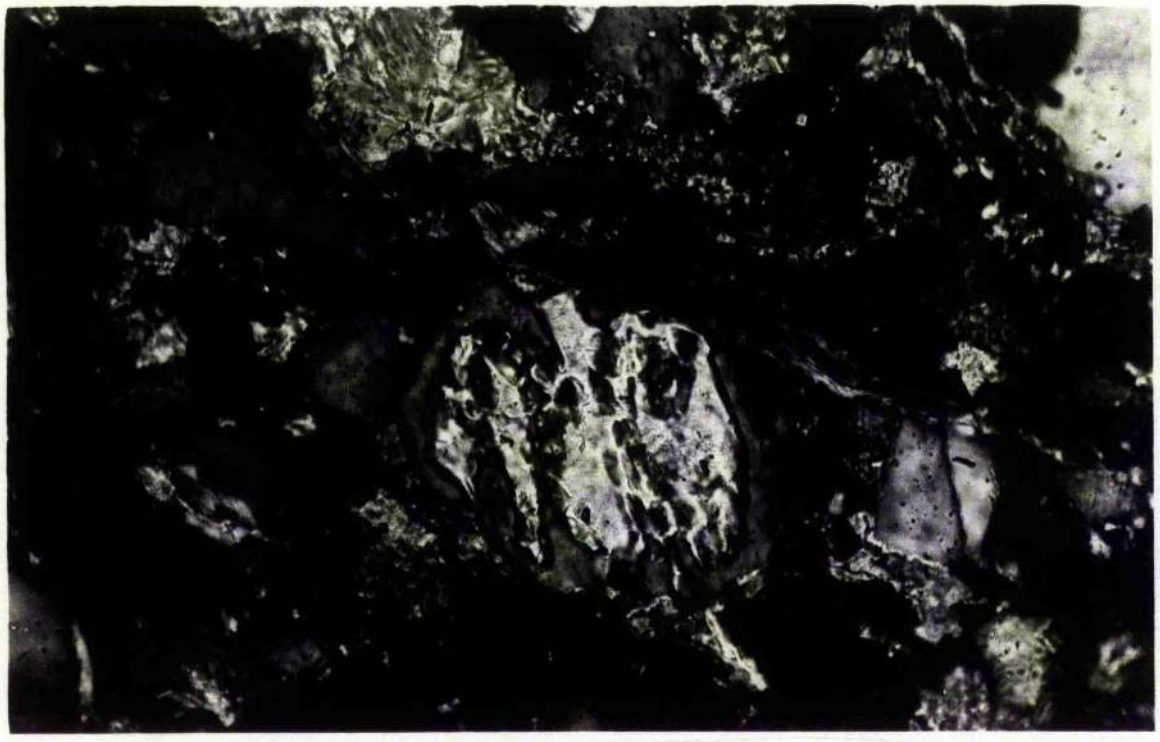

Plate 3.2: Photomicrograph of greywacke from Selkirk Formation showing replacement of quartz grain by calcite, X250, cross polars.

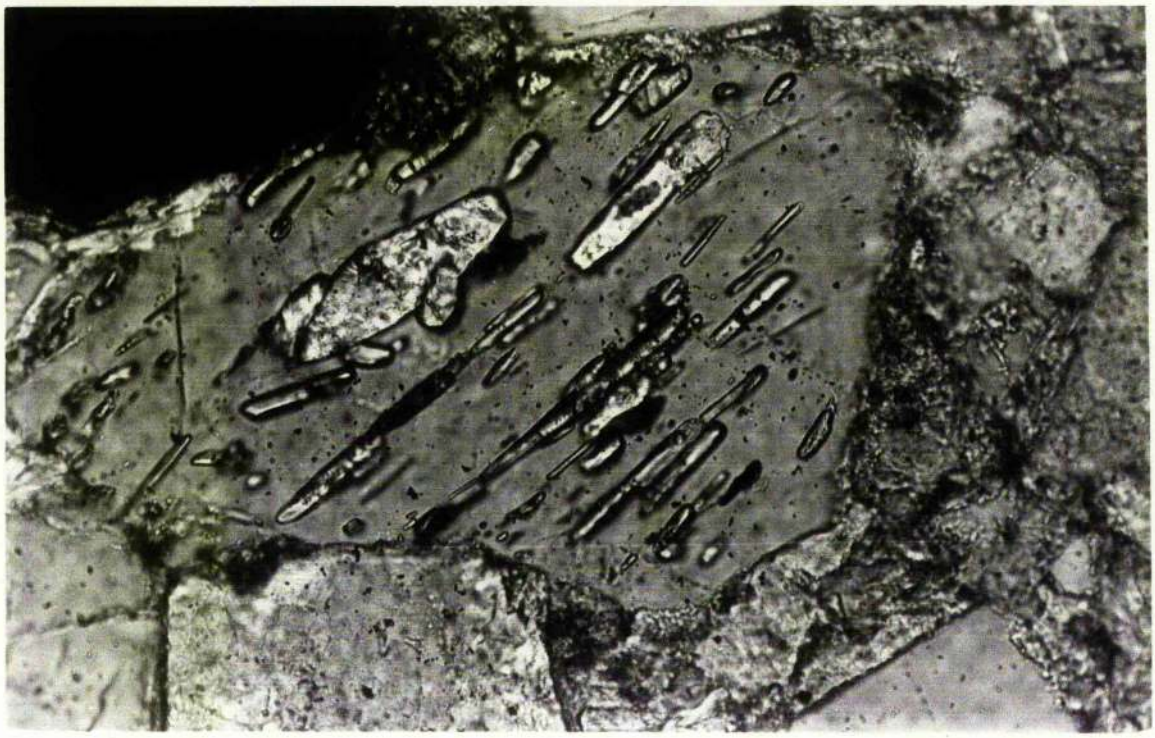

Plate 3.3: Photomicrograph of greywacke from Hazelbank Formation showing regular inclusions in quartz grain, X250, cross polars.

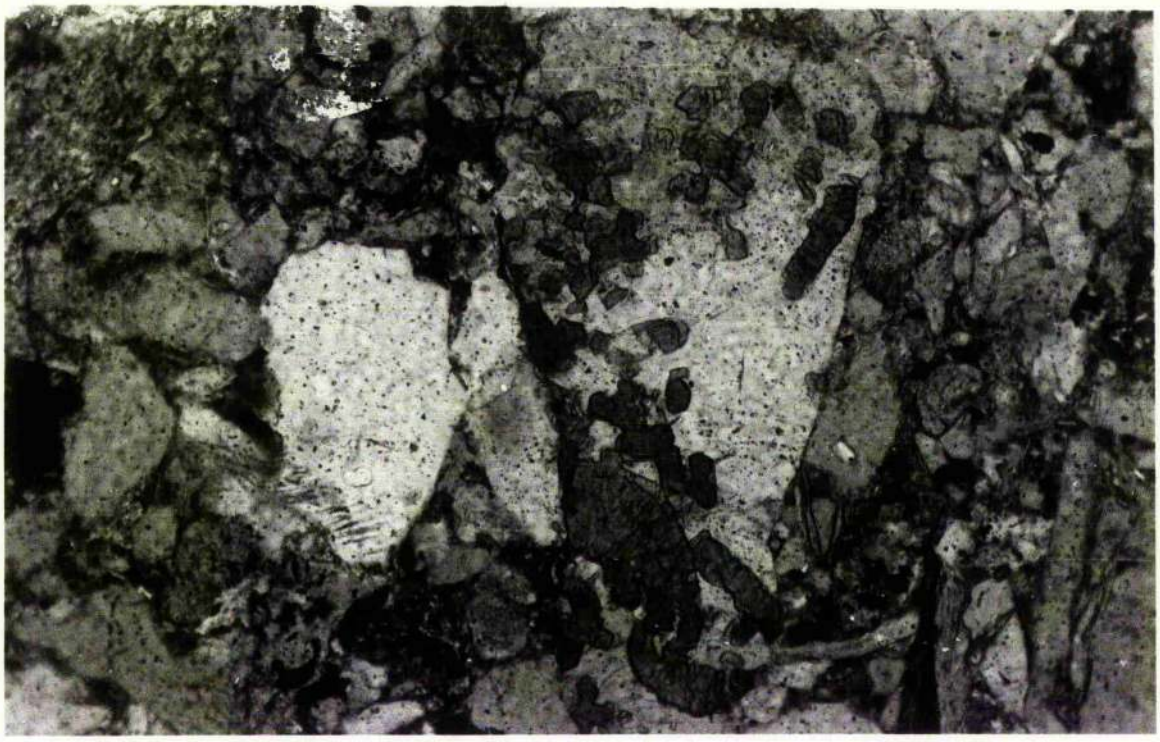

Plate 3.4: Photomicrograph of greywacke from Buckholm Formation showing vermicular inclusions of chlorite in quartz grain, X100, cross polars.

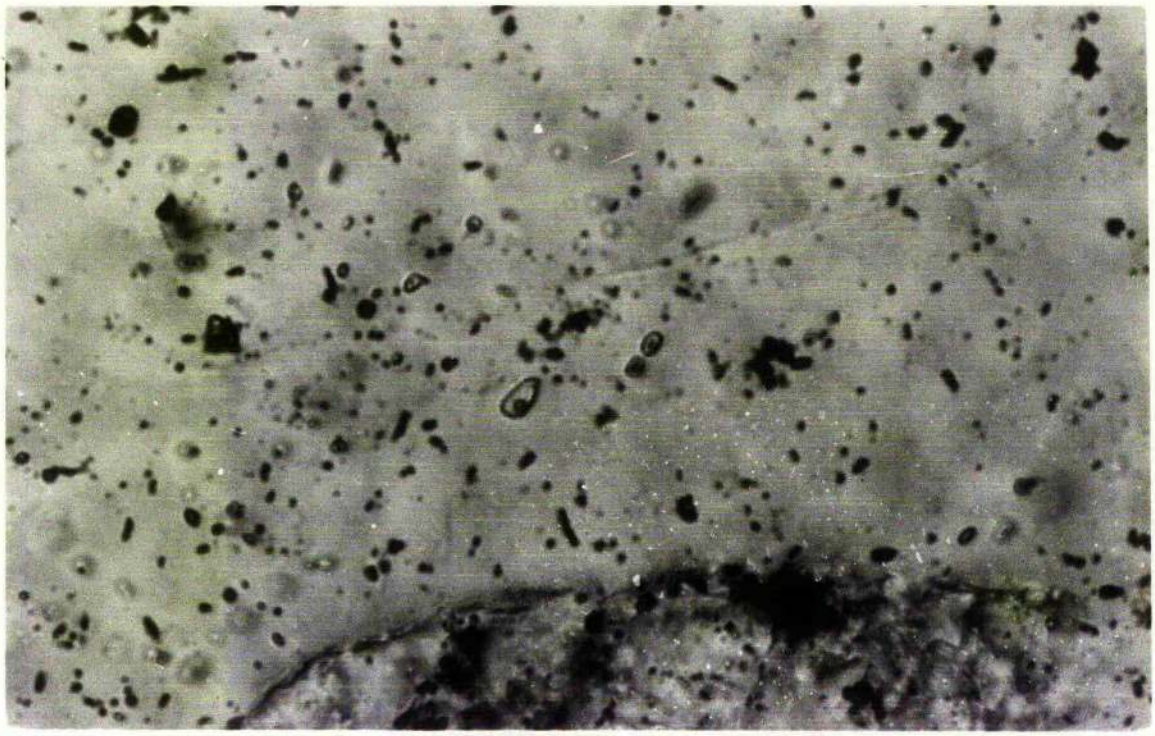

Plate 3.5: Photomicrograph of greywacke from Buckholm Formation showing globular liquid/gas (biphase) and irregular inclusions in quartz grain, X250, plane polarized light.

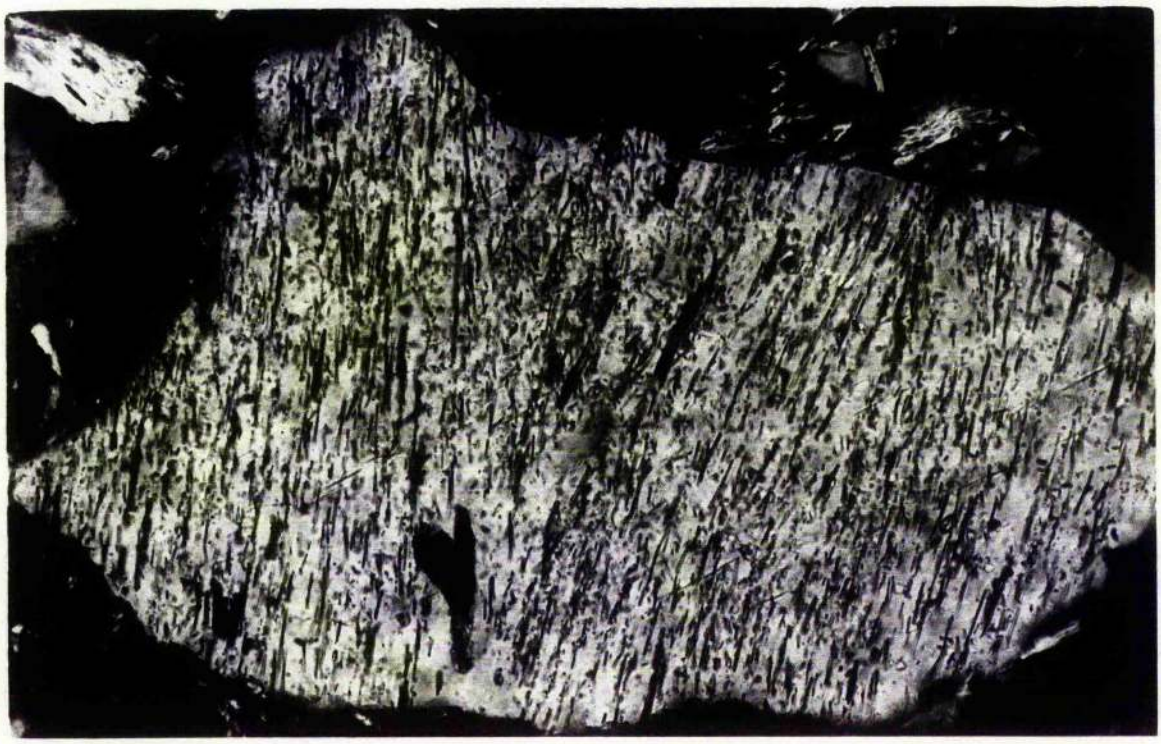

Plate 3.6: Photomicrograph of greywacke from Fountainhall Formation showing acicular inclusions in quartz grain, X250, cross polars.

3-phase inclusions may be found. Modern freezing and thawing techniques, not then available locally, would have considerable potential in diagnosing the early history of the mineral clasts, and in adding on the geology of the source area.

Straining effect in quartz:

Detrital quartz grains in three specimens from each formation were studied by means of thin-section traverses. Grains were classified as unstrained, slightly strained, strongly strained and polycrystalline (Blatt and Christie 1963). It was found out that quartz-enriched formations (Heriot, Fountainhall and Buckholms) are dominated by strongly strained and polycrystalline grains, whereas 'basic-clast' formations (Hazelbank and Falahill Formations) have high proportions of unstrained or slightly strained quartz grains. The high proportion of strained quartz is held to reflect the mixed igneous and metamorphic source of the Heriot, Fountainhall and Buckholm Formations (Fig 3.1), whilst the dominance of unstrained or slightly strained quartz in the Hazelbank and Falahill Formation is ascribed to a volcanic source.

FELDSPARS: Feldspar is the second most abundant mineral group in the rocks of the Gala area. The Falahill, Hazelbank and Fountainhall Formations are notably feldspathic, whereas the Heriot, Buckholm and Selkirk Formations are feldspar-depleted. Sodic plagioclase is the most common and orthoclase, microcline and microperthite are also present in minor amounts. A few

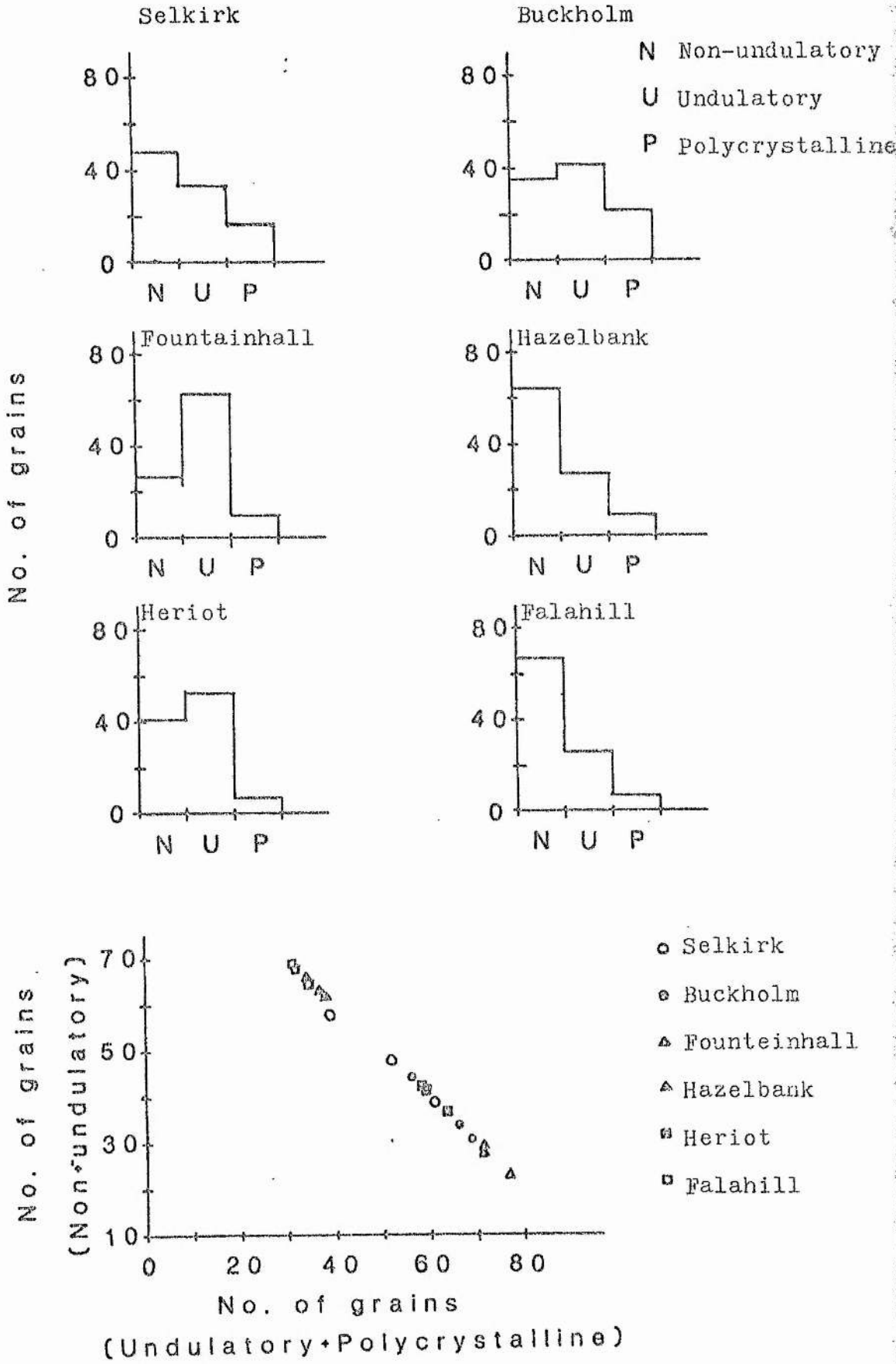

Fig. 3.1: Study of the extinction in quartz grains.

grains of albite also display chessboard zoning. Microprobe analyses of plagioclase (Chapter 8; Section 8.3.4) show that all the analysed plagioclase grains correspond to albite (An0-An9).

Feldspars are particularly susceptible to alteration which ranges from slight cloudiness to almost complete replacement by carbonates, clay minerals and locally epidote. In zoned types the cores are more altered than the surrounding rims.

FERROMAGNESIAN MINERALS: Ferromagnesian minerals are common in the 'basic-clast' Falahill and Hazelbank Formations and rare in other formations. They include pyroxenes and amphiboles in variety.

Pyroxenes: Two types of pyroxene may be found both in the Falahill and Hazelbank Formations: a) Faintly pleochroic, colourless to light green, with extinction angle 30-45°, biaxial positive and polarization colour of 3rd order orange. In these instances, the slower ray makes the smaller angle with cleavage traces in longitudinal sections. These properties denote augite. b) A colourless, non-pleochroic variety with extinction angle 26-45°, biaxial positive with polarization colour of 3rd order yellow. These presumably correspond to salite/diopsidic augite. Intergrowths of both these types are also present.

Amphiboles: Two types of amphiboles occur commonly: a) Colourless to pale green, yellowish, dark green to brownish green with extinction angle 12-23°, biaxial negative; these correspond most

closely to hornblende. This amphibole is very common in the Falahill and Hazelbank Formations. b) A bluish green to violet and inky blue type, with extinction angle of 4-17° which belongs to the glaucophane group. This amphibole is confined to the Falahill Formation. In amphiboles present in situ within the Ballantrae Complex, blue amphibole mantles normal green amphibole. Purely blue amphiboles are entirely detrital, and restricted to melanges.

Epidote: Epidotes are colourless to pale green and bright yellow, non-pleochroic to very weakly pleochroic, showing parallel extinction and are biaxial negative. They occur mostly as irregular detrital grains, as aggregates (epidosite) and as subhedral to euhedral columnar and psudohexagonal inclusions in quartz and feldspars. Certain detrital grains contain quartz inclusions, i.e, they exhibit "sieve structure".

MICAS: Micas are widespread in all the formations. Muscovite and biotite are the commonest, and are widely distributed. Biotite is typically yellowish brown to dark brown and occasionally red in colour. It is mostly detrital but the bright red type is very likely to be authigenic. Biotite flakes show various degrees of alteration to chlorite and in some instances the grains are completely altered. Muscovite is universally present and exclusively detrital. The flakes are in some instances very coarse, and tend to be deformed and twisted by compaction. It has been observed commonly in greywackes of the Falahill Formation that newly formed prehnite grows perpendicular to the

basal cleavage of the mica flakes (particularly muscovite) and thus disrupts the flakes. Flakes of authigenic white mica occurring in matrix show preferred orientation.

CHLORITE: Chlorite occurs in all formations, being especially abundant in the Falahill and Hazelbank Formations. It is pleochroic with colours ranging from light pale green to dark green and bluish-green. It occurs mostly as irregular patches in the matrix, replacing the original detrital matrix minerals and in some instances replacing detrital grains partly or wholly. Although much of the matrix in the Selkirk Formation is calcite, chlorite is also a significant component. Chlorite also replaces biotite, partially or wholly. Clasts of chlorite schist also occur, and might have furnished as a source for the detrital chlorite at least on a minor scale. Vermicular inclusions of chlorite in quartz grains (Plate 3.4) are also present in all the formations.

MATRIX: Matrix is taken conventionally as consisting of all material having a grain size of less than 0.01 mm. This size range includes the finer detrital grains along with diagenetically formed phyllosilicates and calcite (Plate 3.1-3.2). Of these chlorite is the most abundant, associated with a lesser proportion of illite, and in some cases kaolinite (Chapter 8; Section 8.2).

In the greywackes of the Selkirk Formation the matrix is mainly calcite (Chapter 8; Section 8.4.10; Appendix 8.17) with

subordinate phyllosilicates. The amount of calcite in the Selkirk Formation ranges from 24 to 40% (mean = 32%). The carbonates have replaced a variety of detrital grains and matrix as well (Plate 3.2), and may approach 50% by volume; in such instances massive replacement is complete, and partially-replaced clasts remain suspended in a coarsely crystalline carbonate matrix.

Detrital pelitic clasts, being incompetent, are extensively deformed by compaction (Plate 3.15). In some cases deformation may be so extensive as to bring about their total incorporation with the matrix, to give rise to "pseudo-matrix" (Dickinson 1970).

3.2 HEAVY MINERALS

Thin sections of the greywackes were used to study the heavy minerals. Five thin sections from each formation were selected, each section being traversed to cover an area of 1x2.2 cm. 8 types of heavy mineral were counted; apatite, epidote, garnet, glaucophane, chrome spinel, tourmaline, rutile, and zircon. The results (Fig. 3.2) appear reasonably consistent within formations and provide at least a semi-quantitative measure of the various species present.

The Falahill Formation is rich in garnet, apatite, chrome spinel and glaucophane. Chrome spinel and glaucophane are more likely to have been derived from a subduction complex, as chrome

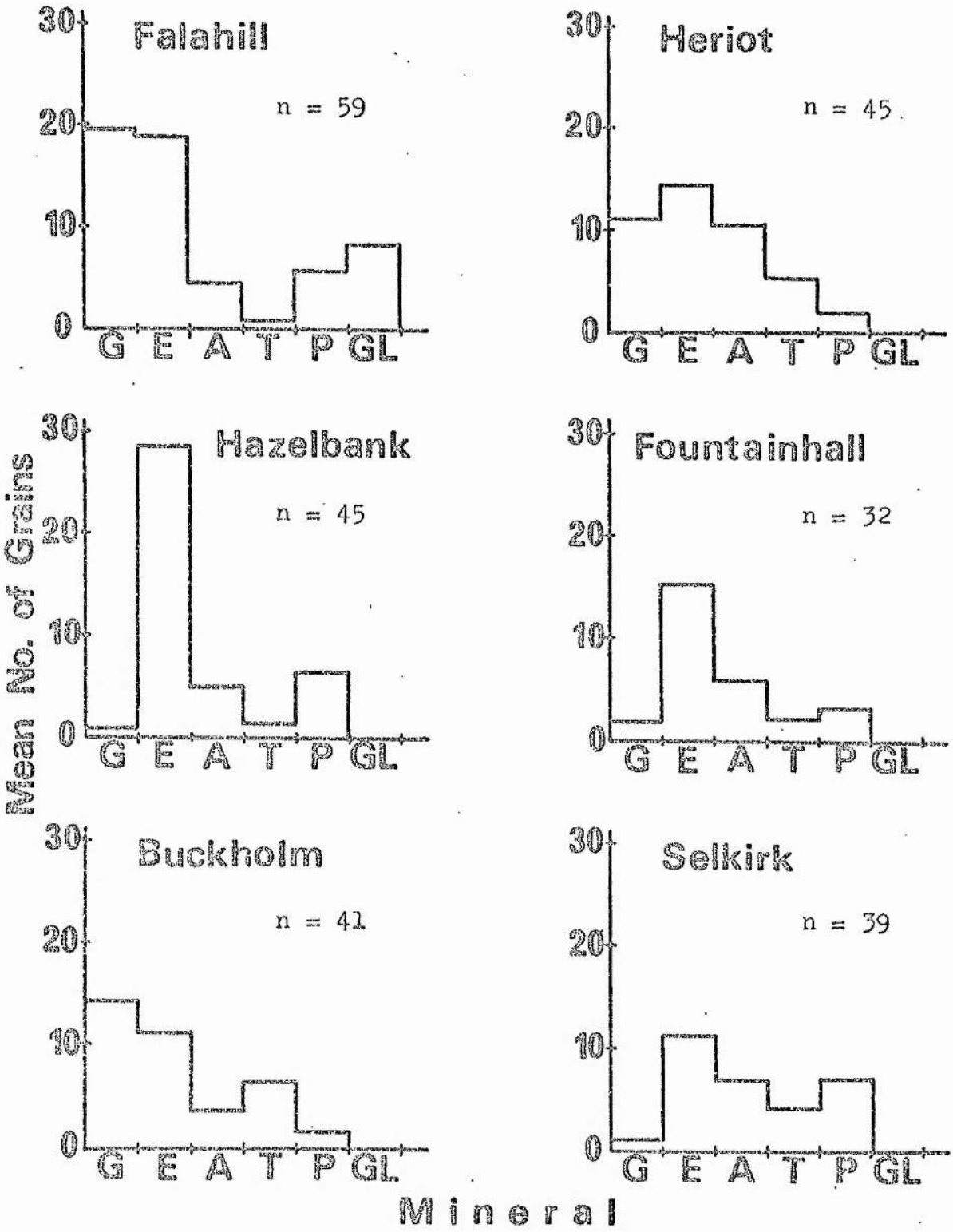

Fig. 3.2: Results of the heavy mineral count. G= garnet; E= epidote; A= apatite; T= tourmaline; P= picotite; GL= glaucophane n = mean of the number of grains counted in 5 thin sections.

spinel is characteristic of basic and ultrabasic rocks and glaucophane is characteristic of high T&P metamorphism, whereas the garnet, showing 'sieve structure' (Plate 3.7) may have been derived from a high grade regional metamorphic terrain (presumably Dalradian). The Hazelbank Formation is characterized by epidote, chrome spinel and apatite but devoid of glaucophane and garnet. Chrome spinel and apatite again reflect a mixed acid and basic igneous source.

In the Heriot and Buckholm Formations, garnet, tourmaline (Plate 3.8) and apatite are consistently present, which supports a dominantly metamorphic and acid igneous source area. In the Fountainhall Formation, apatite, chrome spinel and epidote prevail, suggesting a dominantly acid igneous and partly basic igneous source with some contribution from a metamorphic area. In the Selkirk Formation apatite, chrome spinel and tourmaline are again present, suggesting a source area comparable to that of the Fountainhall Formation.

3.3 OPAQUE MINERALS

Pyrite is the most common mineral among the opaques, occurring in all the formations as aggregates of cubes, as spheres and in some instances as irregular patches in the matrix. Its association displays a tendency to replace both matrix (carbonate and phyllosilicates) and clasts, suggesting that it has formed late in the diagenetic history of the rocks.

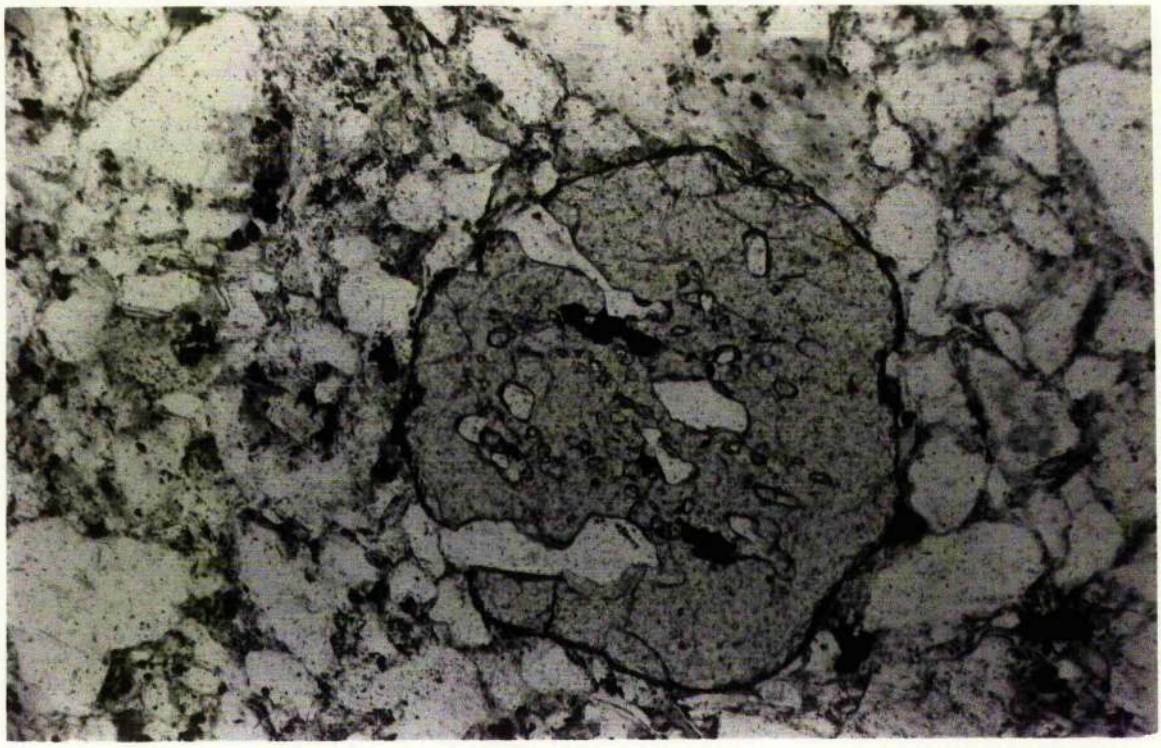

Plate 3.7: Photomicrograph of greywacke from Buckholm Formation showing 'sieve-structure' in garnet grain; islands inside the grain represent quartz, X100, plane polarized light.

Plate 3.8: Photomicrograph of greywacke from Hazelbank Formation showing 'sieve-structure' in tourmaline grain, X100, plane polarized light.

3.4 ROCK FRAGMENTS

Igneous (Plates 3.9-3.11), metamorphic (Plates 3.12-3.13) and sedimentary (Plates 3.14-3.16) clasts are all represented (Table 3.2), in order of decreasing abundance, acid volcanic clasts being the most abundant. Detailed descriptions of rock fragments are given in Appendix No. 3.4. Igneous (spilite, volcanic glass, rhyolite porphyry) and sedimentary fragments (siltstone, greywacke, chert and shale) are universally present. The Buckholm, Heriot and Selkirk Formations are typified by a profusion of acid volcanic, granitic and metamorphic clasts (mostly quartzite and mica schist); the Fountainhall Formation by granite, rhyolite porphyry, diorite and limestone fragments; and the Falahill and Hazelbank Formations by andesite, dolerite, dacite and epidosite, with occasional sandstone and shell fragments. Glaucophane schist fragments (Plate 3.13) are confined to the Falahill Formation, as are monomineralic blue-amphibole grains.

3.5 MODAL ANALYSIS

There are slight variations in the megascopic characters (colour, amount of siliceous grains, presence or absence of megascopic garnets, lustre) of the greywackes throughout the area, though the contrasts are not adequate in all cases to be diagnostic for subdividing the succession. Petrographical studies on Ordovician rocks (Kelling 1961; Welsh 1964; Floyd 1975; and others) and Silurian rocks (Walton 1955; Gordon 1962;

Table No 3.2: Types of rock fragments observed

IGNEOUS	SEDIMENTARY	METAMORPHIC
spilite	siltstone	quartzite
rhyolite porphyry	greywacke	muscovite-schist
volcanic glass	shale	muscovite-biotite-schist
trachyte	cherts	chlorite-schist
keratophyre	limestone	garnet-schist
granite	sandstone	glaucophane-schist
granodiorite	black shale	epidosite
dacite	shell fragments	amphibolite
diorite/dolerite		epidote-amphibolite
andesite/basalt		?kyanite schist

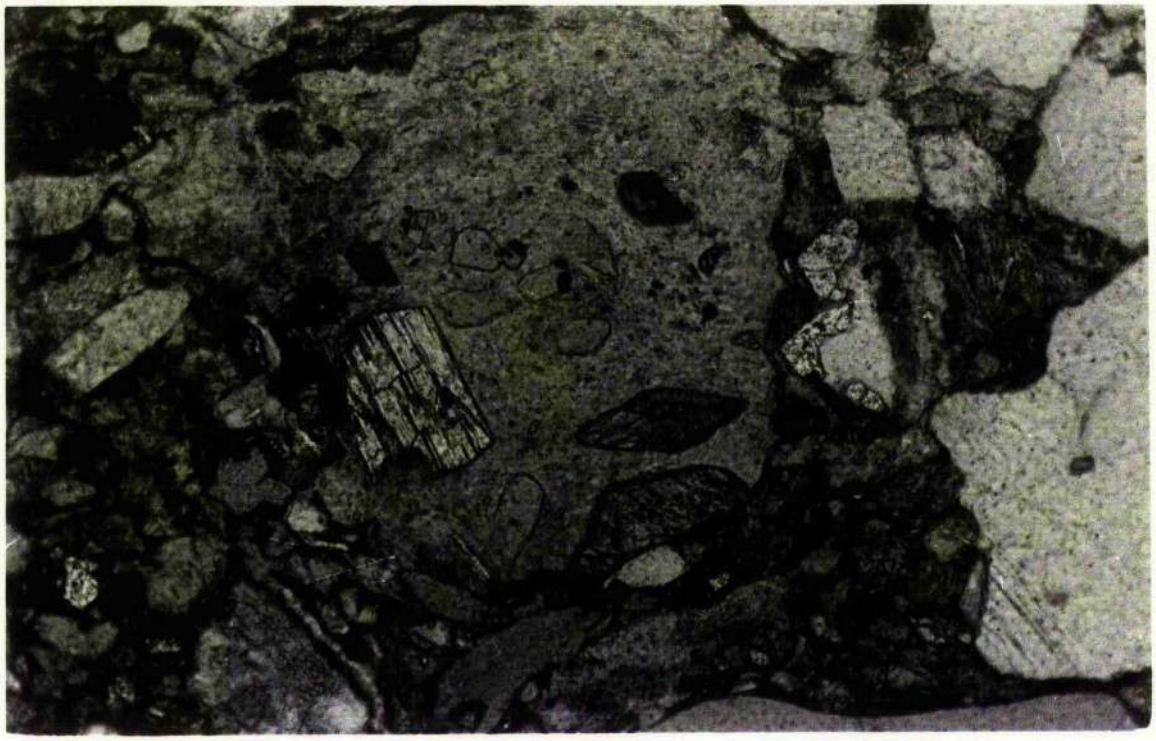

Plate 3.9: Photomicrograph of greywacke from Falahill Formation showing andesite fragment consisting amphibole phenocrysts, X250, plane polarized light.

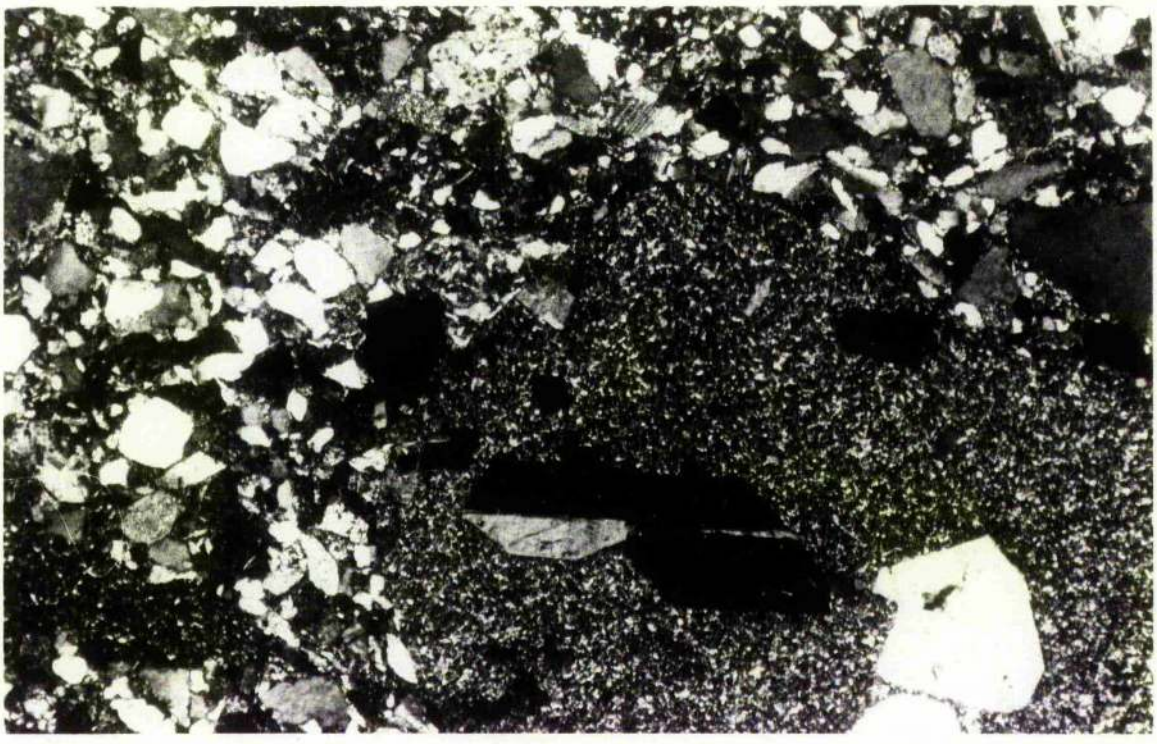

Plate 3.10: Photomicrograph of greywacke from Fountainhall Formation showing rhyolite fragment consisting feldspar phenocrysts, X025, cross polars.

Plate 3.11: Photomicrograph of greywacke from Fountainhall Formation showing granite fragment consisting micrographic intergrowths of quartz and plagioclase, X100, cross polars.

Plate 3.12: Photomicrograph of greywacke from Buckholm Formation showing strong quartzo-micaceous alignment in schist fgragment, X250, cross polars.

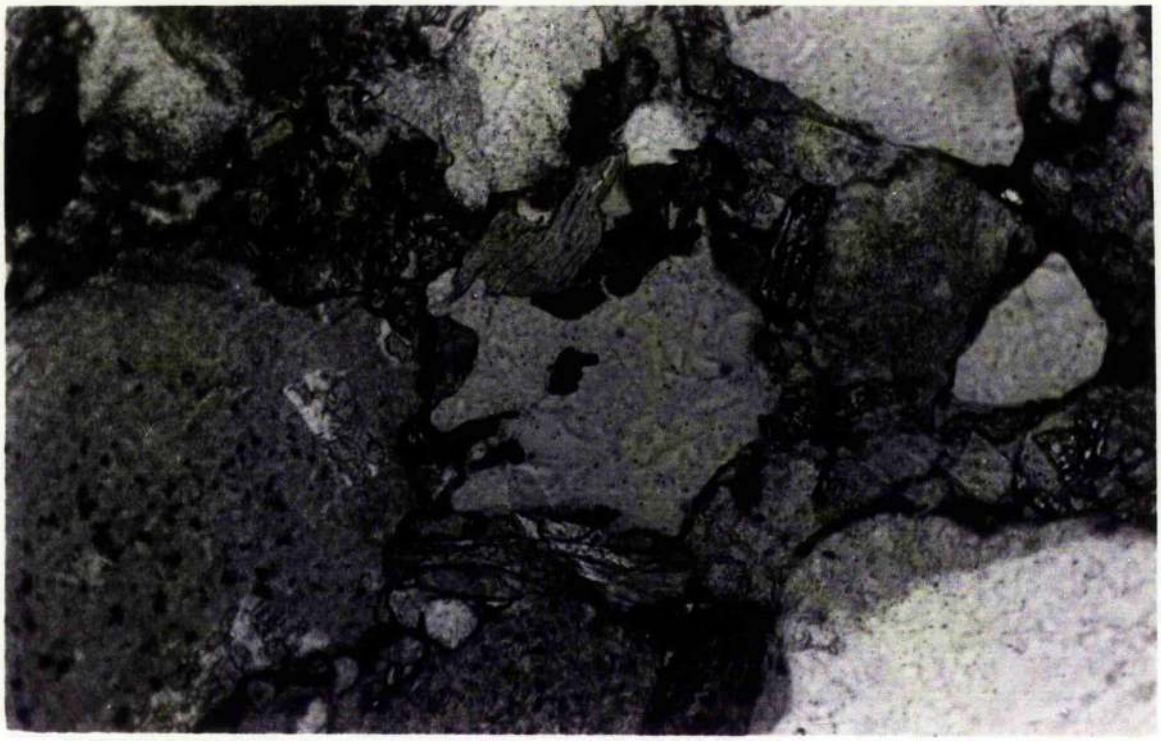

Plate 3.13: Photomicrograph of greywacke from Falahill Formation showing aggregate of minute glaucophane crystals in blueschist fragment (centre), X250, cross polars.

Plate 3.14: Photomicrograph of greywacke from Buckholm Formation showing quartz overgrowths in detrital sandstone fragment, X250, cross polars.

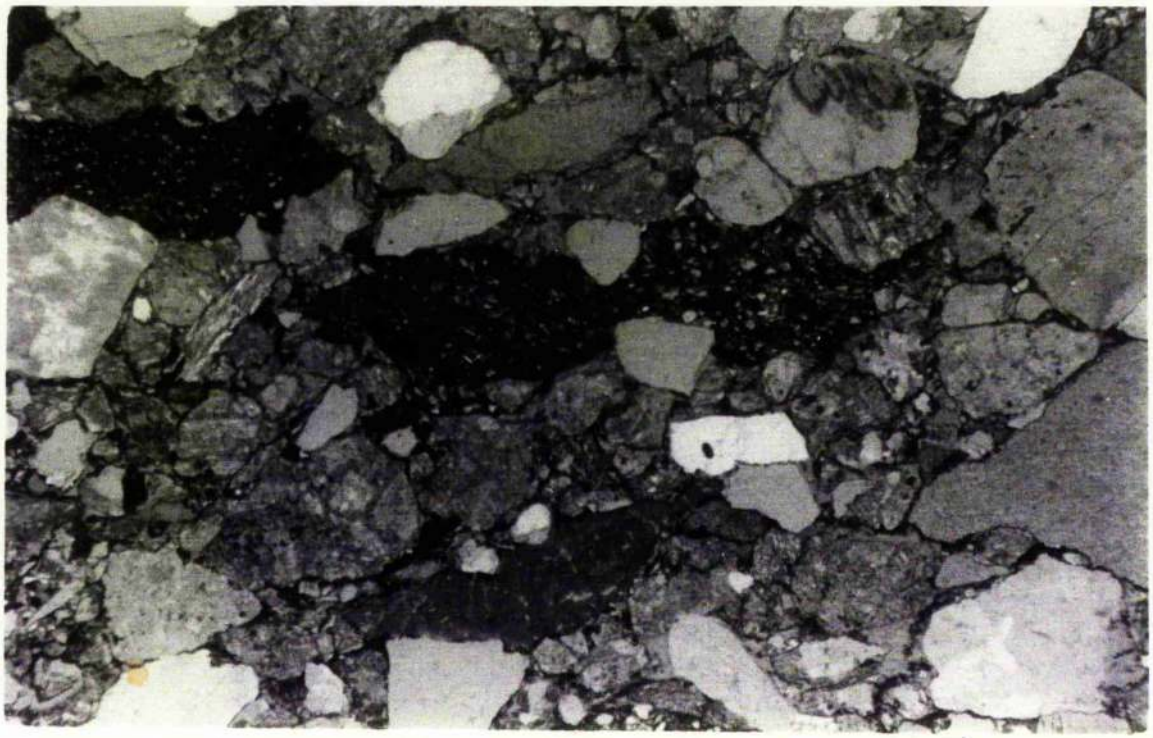

Plate 3.15: Photomicrograph of greywacke from Hazelbank Formation showing incompetent pelitic sedimentary fragments compressed and deformed between competent fragments, X025, cross polars.

Plate 3.16: Photomicrograph of greywacke from Hazelbank Formation showing impunctate brachiopod fragment derived presumably from a shallow marine environment, X100, cross polars.

Warren 1963; and others), have shown that the Southern Uplands greywacke sequences can be subdivided into laterally extensive and mappable units, mostly with the status of formations, on the basis of mineralogical characteristics. The rocks of the Gala area have been divided on this basis into six lithostratigraphic units and have been correlated with those in the adjacent area of Peeblesshire (Walton 1955) and with West Nithsdale (Floyd 1975).

As the Gala area is poorly and unevenly exposed, it is unrealistic to attempt to collect samples according to a pre-planned grid pattern. Fresh samples were accordingly collected wherever available. Qualitative estimation of thin sections was generally adequate to differentiate the formations. In order to confirm this proposition, and also to assess any horizontal and lateral variations, appropriate specimens of each formation were selected (Fig. 2.2, Chapter 2) for point counting. Very coarse and very fine grained specimens were excluded except in the preponderantly fine-grained Selkirk Formation. The samples were counted using a Swift Automatic Point Counter, Model C, for eight components: quartz, feldspar, acid igneous, basic igneous, sedimentary and metamorphic rock fragments, ferromagnesian minerals and matrix, as defined above. A test of comparison between the percentages of components for 500 and 1000 point counts in 9 specimens (Appendix 3.2) shows that the percentages obtained for the components in each count are ranked in the same order. Tests of correlation, and significance of correlation, were carried out a) between component minerals among the 9 samples and b) between 8 component

minerals within the individual samples counted, for one 500-count and the 1000-count data sets respectively (Table 3.3). In each instance, the product moment correlation coefficient (R) approaches, or more usually exceeds, 0.9 (where 1.0 denotes perfect correlation). Significance (T) exceeds 3.0 in each case, implying <0.1% chance of the correlations not being significant for 6 degrees of freedom. It was thus considered justifiable to count only 500 points in most of the samples since these counts yielded contrasts adequate to confirm the qualitative differentiation of the formations. The count interval was 1/3 mm, and the traverses interval 1mm apart, avoiding multiple counting of the large clasts.

3.6 Comparison with other areas

The results (Appendix 3.1, 3.2) of the point counting were plotted on triangular diagrams (Fig. 3.3a, b) with the three end members as: Q (quartz, acid igneous and metamorphic clasts); M (matrix, sedimentary fragments and mica); and F (feldspar, basic igneous fragments and ferromagnesian minerals).

Comparison of the QMF plots of the Ordovician succession of the Gala area with plots from the Rhinns of Galloway (Kelling 1962) and West Nithsdale (Floyd 1975); (Fig. 3.4a), and the Silurian succession of the Gala area with plots from Peeblesshire (Walton 1955) and Hawick (Warren 1963) (Fig. 3.4b), shows that although the plots are not strictly comparable, (probably through operator bias), the formations maintain their relative

Table 3.3: Test of correlation between the results of 500 and 1000 point counts.

a) Correlation between samples (n=9)

Component	R	T
Quartz	0.99	10.75
Feldspar	0.99	13.13
Acid igneous	0.99	10.61
Basic igneous	0.97	07.55
Sedimentary	0.94	05.12
Ferromass	0.87	03.08
Matrix	0.95	05.54
Total sample	0.99	34.87

b) 'Within-sample' correlation (partly independent, less reliable)

Sp No	R	T
58	1.00	17.66
2-c	0.96	04.01
90	0.99	14.53
320	0.97	06.48
21	1.00	85.14
3-a	0.97	06.52
81	1.00	32.83
218	0.99	12.29
322	0.97	06.80

All very highly significant (>1000:1 in favour)

R = Correlation coefficient

T = T test

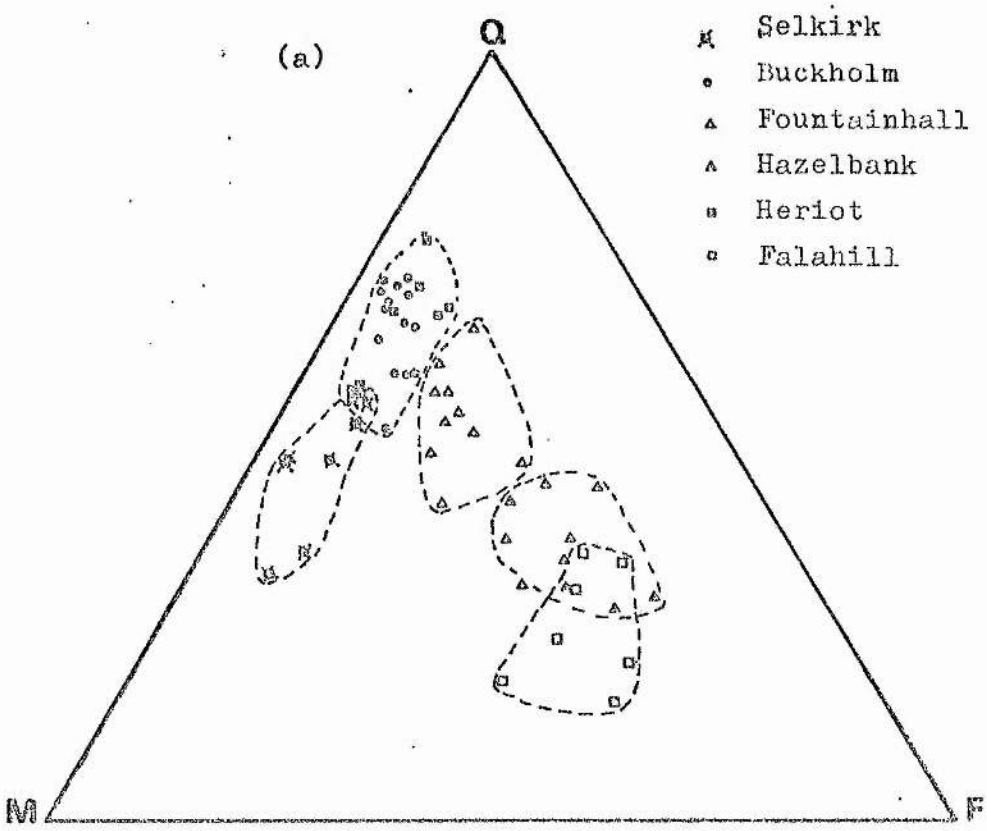

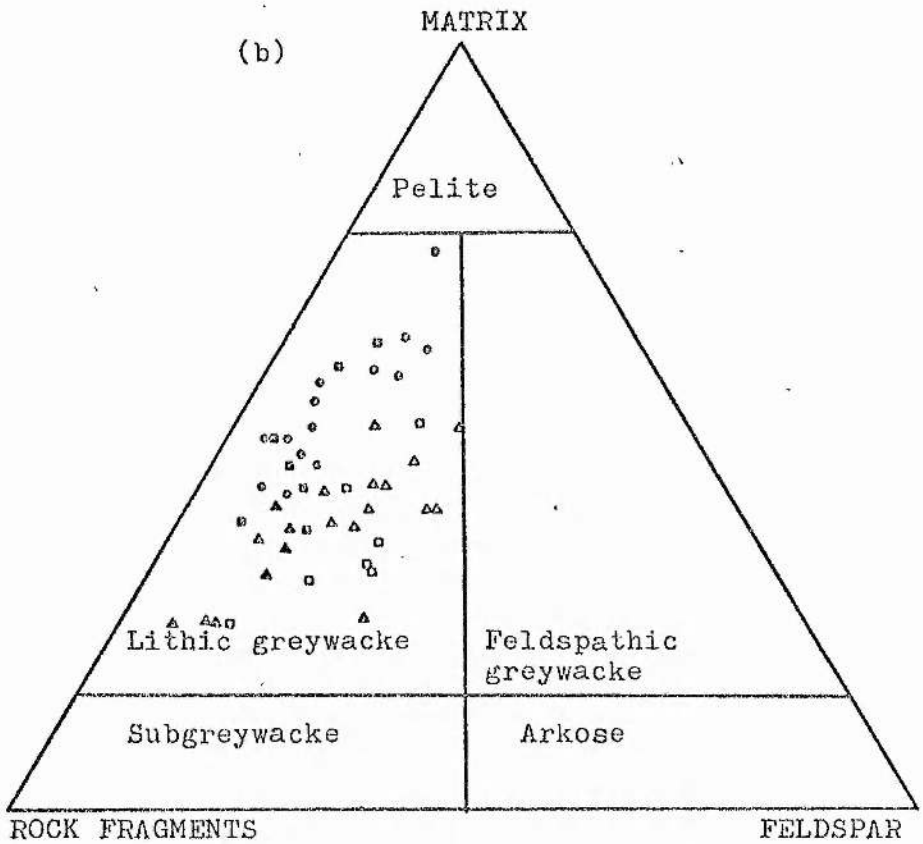

Fig. 3.3: (a) QMF plot and (b) MRF plot (after Pettijohn 1957). Q= Quartz + acid igneous + metamorphic; F= Feldspar + basic igneous + ferromagnisian minerals; M= Matrix + sedimentary.

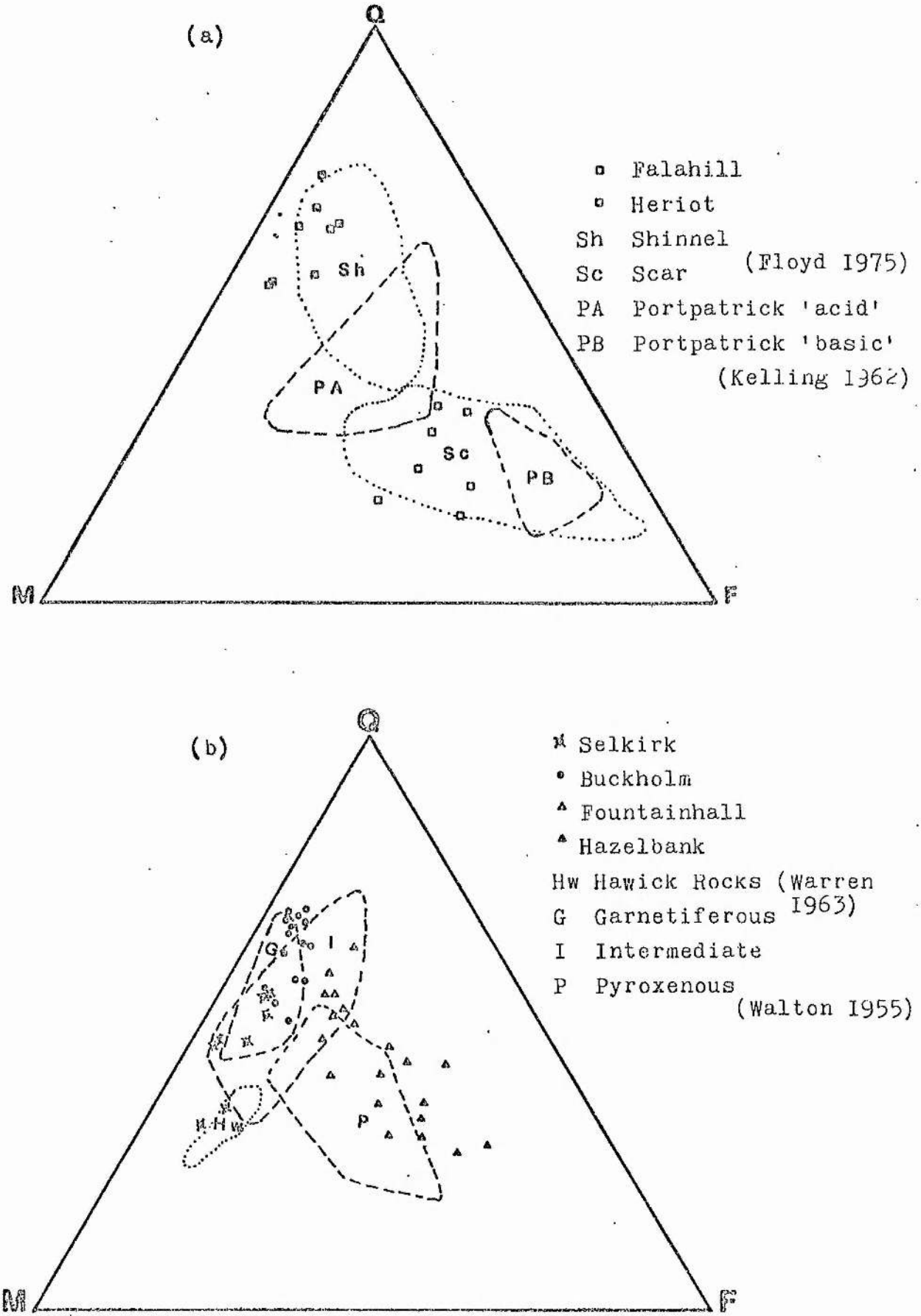

Fig. 3.4: Comparison of QMF triangular plots.

compositions within the succession as a whole, effectively throughout their outcrop in the Southern Uplands.

3.7 GRANULE COUNTS (Appendix 3.3)

A minimum of 75 granules (grains more than 1 mm across) were counted in the coarser grained specimens, and classified as quartz, feldspar, acid volcanic, acid plutonic, basic volcanic, basic plutonic, sedimentary and metamorphic. The acid plutonic class includes granite and granodiorite; the acid volcanic class comprises rhyolite, and volcanic glass. The basic plutonic class incorporates gabbro, dolerite and diorite, and the basic volcanic class consists of spilite, keratophyre, andesite, and ?trachyandesite. Metamorphic and sedimentary rock fragments include the components outlined above (Section 3.5).

The results (Appendix 3.3, Fig. 3.5a) show a marked spread and give a less clear differentiation of the formations than the point counts. Although comparisons of the Ordovician formations (Fig. 3.5b) with their proposed equivalents in the Rhinns of Galloway (Kelling 1962) and West Nithsdale (Floyd 1975) are less precise than the grain counts, the formations maintain their relative positions within the plot.

3.8 SUMMARY OF THE PETROLOGY

A) ORDOVICIAN SUCCESSION

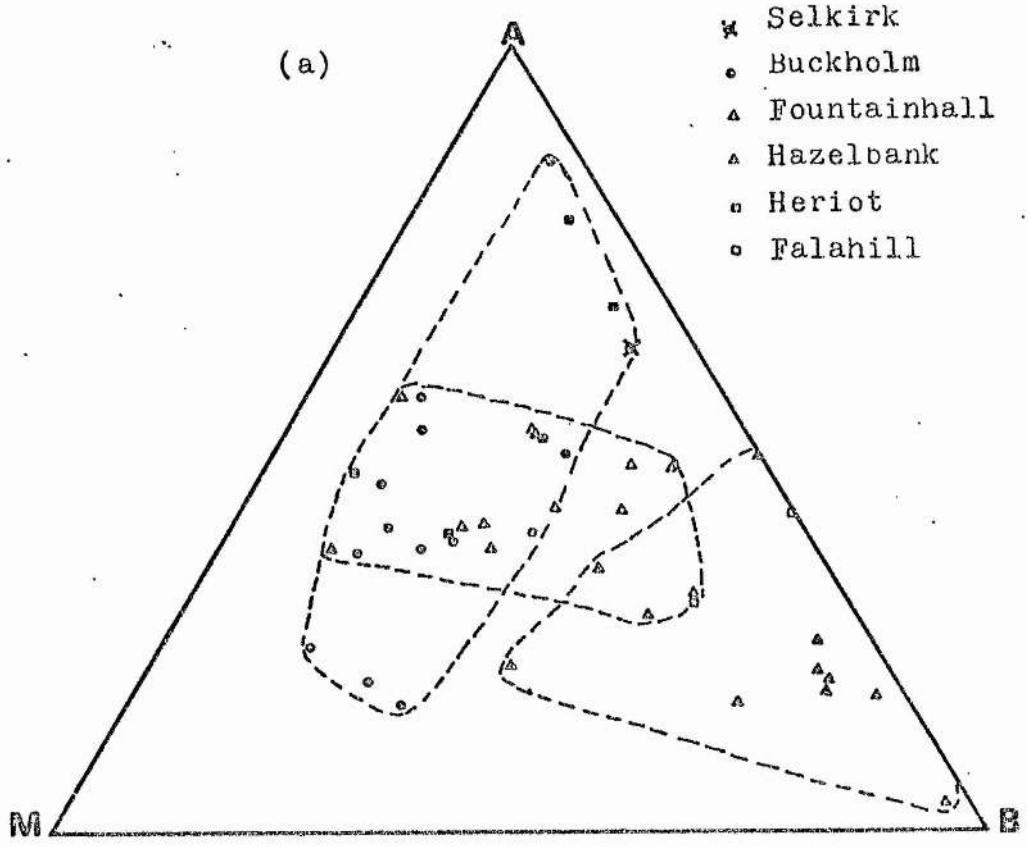

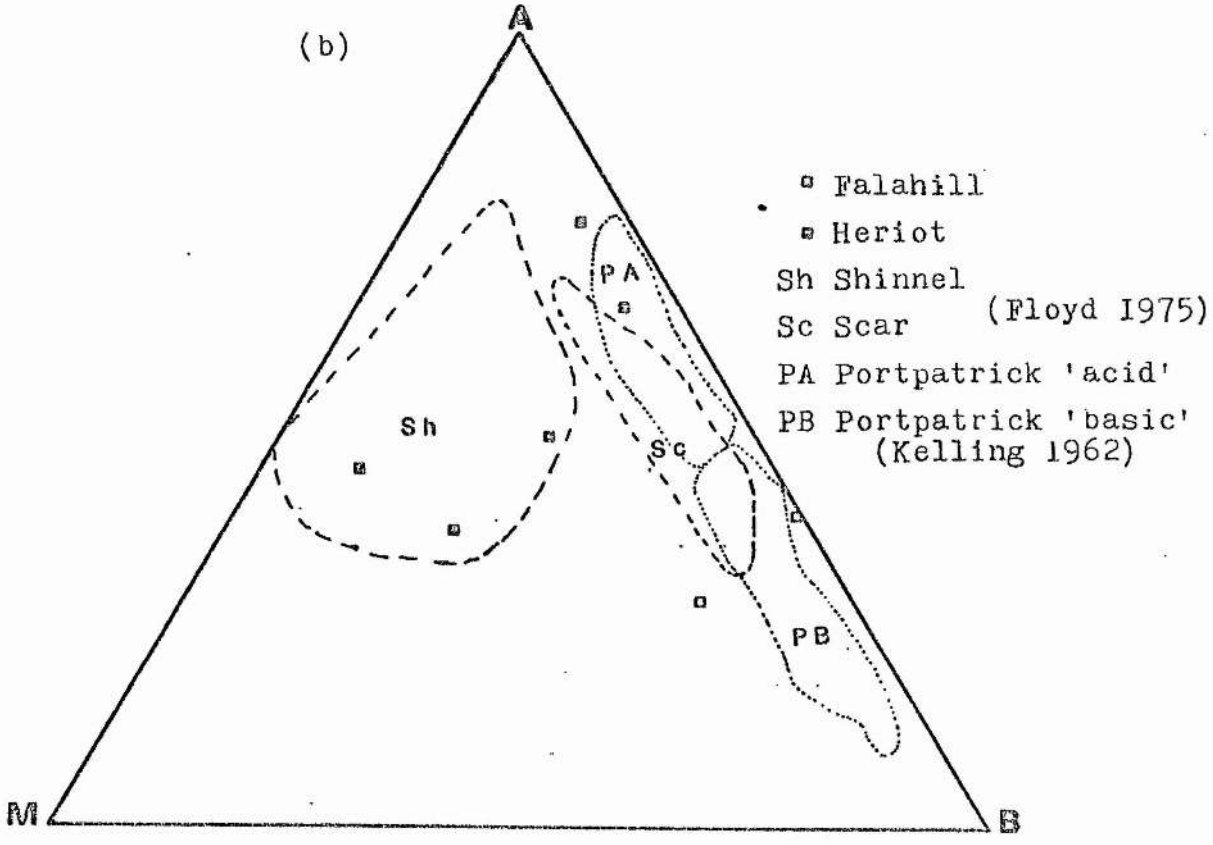

Fig. 3.5: (a) Results of the granule counts plotted on AMB triangular diagram. A= Acid igneous; B= Basic igneous; M= Metamorphic. (b) Comparison of AMB plot with other areas.

Falahill Formation

The greywackes of the Falahill Formation are "basic clast" sensu Kelling (1961), being quartz-depleted and feldspathic, and having in particular an abundance of basic igneous rock fragments and ferromagnesian minerals (Fig. 3.3a; 3.6), mostly clinopyroxenes and green, brown and blue amphiboles. The presence of garnet and blue amphiboles of the glaucophane group is diagnostic of the Falahill Formation.

Heriot Formation

These greywackes are 'garnetiferous' in the sense of Walton (1955). The rocks are quartz-enriched, reflecting the high content of acid igneous and metamorphic rock fragments. Feldspars and basic igneous fragments are subordinate, with a consequential lack of ferromagnesian minerals (Fig. 3.3a; 3.6). Most of the bed are garnetiferous, although some beds lack garnets. After garnet, apatite and tourmaline are the most abundant heavy minerals, again reflecting the high acid igneous and metamorphic contribution.

B) GALA GROUP

Hazelbank Formation

The Hazelbank Formation is again a 'basic-clast' unit, comparable to the Falahill Formation but contrasting

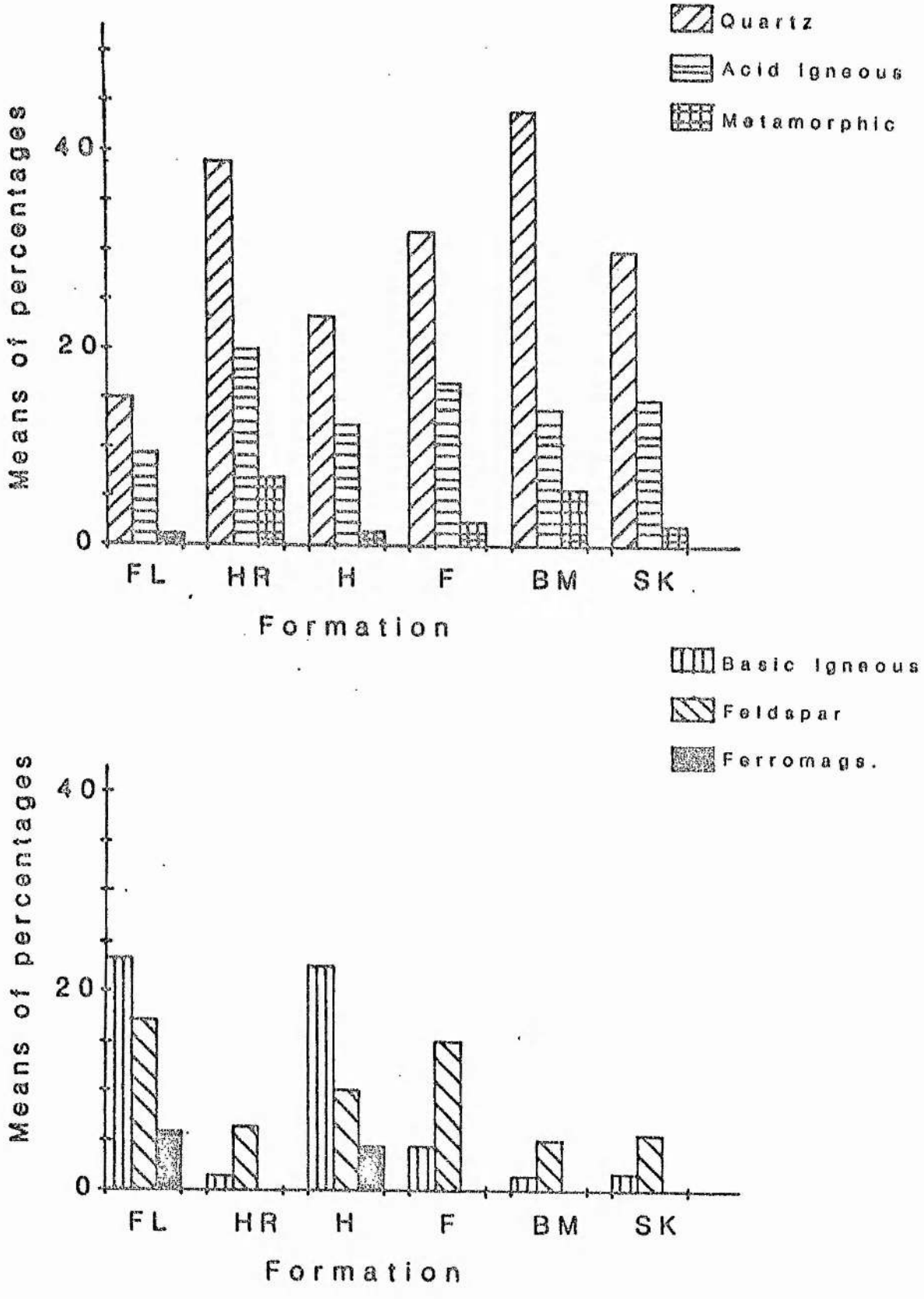

Fig. 3.6: Histograms of the formation means; FL =Falahill, HR =Heriot, H =Hazelbank, F =Fountainhall, BM =Buckholm, SK =Selkirk.

significantly in the lack of blue amphiboles and poverty in garnet, and in having a relatively high content of silicic and sedimentary fragments.

Fountainhall Formation

The Fountainhall Formation is an 'intermediate' unit in terms of Walton (1955), having abundant acid igneous fragments, a significant proportion of basic igneous fragments, and a high content of quartz (derived dominantly from acid igneous source) and feldspar (from the acid and basic igneous sources). This formation is non-garnetiferous and is compositionally intermediate between the 'highly siliceous' and 'highly basic' formations (Fig. 3.3a; 3.6).

Buckholm Formation

This formation is again quartzose, garnetiferous, rich in acid igneous and metamorphic rock fragments and depleted in feldspar and basic igneous clasts. It contrasts with the Heriot Formation in its relatively high epidote, apatite and zircon content.

C) HAWICK GROUP

Selkirk Formation

The Selkirk Formation is a 'silicic' formation (cf. Cook

1976), especially abundant in quartz, acid igneous and metamorphic fragments (Fig. 3.3a; 3.6). Feldspar occurs in subordinate amounts. These greywackes are characteristically very fine grained, thinly bedded and flaggy with a matrix dominated by authigenic carbonates. Certain coarser beds are garnetiferous and poorer in carbonates. The dominant heavy minerals are epidote, chrome spinel, apatite and tourmaline, again suggesting derivation from a granite-injected metamorphic terrain. The presence of chrome spinel presumably points to recycling of the 'basic-clast' greywackes.

4. AGE AND CORRELATION

4.1 ORDOVICIAN SUCCESSION

4.1.1 Falahill Formation

Graptolite species recorded by Peach & Horne (1899) from a road-side section lying on the strike of the Falahill Formation, on the Middleton-Innerleithen road (B7007) at Wull Muir (NT 347 533), include Diplograptus foliaceous (Murchison), `Lasiograptus` (Neurograptus) margaritatus (Lapworth) and Dicellograptus sp. On the basis of these determinations an Arenig age was assigned to cherts. Associated mudstones and black shales were attributed to the Glenkiln, and greywackes to the Hartfell. Walton (1961) considered that the cherts are interbedded with the argillaceous rocks, and proposed a Glenkiln age for the whole chert-mudstone sequence, though without the backing of fossil evidence. Subsequently Amplexograptus perexcavatus (Lapworth) and Dicranograptus nicholsoni (Hopkinson) were reported (Walton & Weir 1974) from the black shales.

Though these determinations have been disputed in detail (I. Strachan, pers. comm. to J.A. Weir), a high Ordovician age is still supported. No fossiliferous black shales were found in association with the greywackes of the Falahill Formation. It is correlated with the Portpatrick Basic-clast 'Division' of Kelling (1961) and the Scar Formation of Floyd (1975), on the basis of petrological characteristics (Fig. 3.4a; Chapter 3) and

strike-wise continuity. A Caradoc age has been assigned to the Scar Formation on the basis of occurrence of graptolites of the Dicranograptus clingani Zone near the base of the Scar Formation. A Caradoc age is thus valid both for the Falahill and for the Portpatrick Basic-clast 'Division'.

4.1.2 Heriot Formation

The following graptolites were recorded (Peach & Horne 1899), from a locality (Locality 1; Fig. 2.2; Chapter 2) about 240 metres south of Corsehope Burn, about 2 km S of Heriot Station, on the west side of the Gala Water which falls within the outcrop of the Heriot Formation.

Diplograptus foliaceous (Murchison)
Cryptograptus tricornis (Carruthers)
Dicellograptus sextans (Hall)
`Diplograptus` (Glyptograptus) euglyphus (Lapworth)
`Climacograptus` (Pseudoclimacograptus) scharenbergi (Lapworth)
C. cf. bicornis (Hall)

An Arenig age was again proposed for these shales. However, 'Diplograptus foliaceous' sensu Peach & Horne is effectively a 'basket name' for every large diplograptid; D. sextans and C. bicornis are typically Glenkiln species, whilst Cl. scharenbergi appears later and ranges well into the Lower Hartfell. D. euglyphus is not a reliable identification, diplograptids being notoriously difficult to identify unless preserved with the

proximal ends intact. The above evidence suggests a Caradoc age. On the basis of petrological characteristics (Fig. 3.4a; Chapter 3) and continuity of strike the formation is correlated with the Shinnel Formation of Floyd (1975), the Portpatrick Acid-Clast 'Division' of Kelling (1961) and the Boreland Formation of Welsh (1964). Of these, a Caradoc age has been assigned to the Shinnel Formation of Floyd (1975), again on the basis of fossils recorded by Peach & Horne (1899), which range from the Nemagraptus gracilis to the Dicranograptus clingani Zones. The Portpatrick 'Acid-Clast' Division has likewise been assigned an Upper Glenkiln-Lower Hartfell age, on the basis of graptolites recovered from shales interbedded with greywackes of its basal levels (Kelling 1961).

It has also been suggested (Kelling 1961) that in view of its great thickness, the uppermost part of the unit in the Rhinns may extend into the Silurian. In the present area, however, the width of the outcrop alone does not suggest an abnormal thickness, and there is no evidence to suggest that other than Lower Hartfell equivalents are included.

4.2 GALA GROUP

4.2.1 Hazelbank Formation

Peach & Horne (1899) recorded Climacograptus normalis Lapworth, Monograptus attenuatus Hopkinson and Monograptus tenuis (Portlock) from a locality about a mile upstream from the junction of the Ladyside Burn (Fig. 2.2; Locality 2; Chapter 2)

with the Heriot Water, within the outcrop of the Pelitic Member of the Hazelbank Formation. Proximal portions of either Monograptus or Dimorphograptus were also recorded. These fossils suggest the Coronograptus cyphus Zone (Middle Llandovery age).

Climacograptus normalis Lapworth, Diplograptus sp. and unattributable siculae were recovered (Peach & Horne 1899) from bluish flaky shales interbedded with thick greywacke beds in Hazelbank Quarry (Locality 3; Fig. 2.2; Chapter 2), close to the base of the Sandy Member of the Hazelbank Formation. This assemblage suggests the Parakidograptus acuminatus Zone (basal Llandovery), and that the formation as represented in the area ranges from this level to at least the Coronograptus cyphus Zone (Middle Llandovery).

The Hazelbank Formation is correlated with the Pyroxenous Group of Walton (1955) on the basis of petrological characters (Fig. 3.4b; Chapter 3), and the lower contact of the Hazelbank Formation with the Fountainhall Formation can be matched with the contact of the Pyroxenous Group and the Intermediate Group of Walton (1955) in the Peeblesshire area.

4.2.2 Fountainhall Formation

The following graptolites were obtained by the author from an outcrop of Upper Birkhill Shales exposed in the high reaches of Calfhope Burn (identifications by Dr. I. Strachan).

Diversograptus runcinatus (Lapworth)

Monograptus capis Hutt 1975

M. cf. exiguus (Nicholson) or cf. crispus Lapworth

M. cf sedgwickii (Portlock) (=spinigerus of Peach & Horne)

Pristiograptus nudus (Lapworth) (? = M. tenuis (Portlock) of Peach & Horne 1899)

At least two different Monograptus of spiralis type (subgenus Spirograptus Guerich).

The above fauna suggests the sedgwickii or maximus Zones, though rastritids are lacking (found in the comparable succession of the Ewes Water by Peach & Horne 1899). The following species were recorded (Peach & Horne 1899) from the blue sandy shale and flags in Ewes Water, from a point where the Ewes Water take a bend to the SW, about half a mile south of Trously (Fig. 2.2, Chapter 2):

Monograptus spinigerus (Nicholson) (? cf. sedgwickii (Portlock)

M. cf. attenuatus Hopkinson

M. cf. lobiferus (McCoy)

`M.` (Lagarograptus) cf. tenuis (Portlock)

Rastrites sp.

Climacograptus normalis Lapworth

Peach & Horne found Climacograptus normalis in Sit Burn and `Lugate` elsewhere (exact localities not mentioned). About 800 m up the Lugate Water from the junction with the Sit Burn in a section (Locality 4; Fig. 2.2; Chapter 2) they found suites of

fossils (details not given) indicating the Coronograptus gregarius Zone. From a locality (Locality 5; Fig. 2.2; Chapter 2) about 32 metres below the forkings of Sit Burn and Lugate Water in gray sandy and platy shales Peach & Horne (1899) recorded the following fauna:

`Monograptus` (Coronograptus) gregarius Lapworth
M. cf. attenuatus (Hopkinson)
M. (Demirastrites) cf. triangulatus (Harkness)
`M.` (Pristiograptus) cf. concinnus Lapworth
M. cf. lobiferus (McCoy)
`Diplograptus` (Glyptograptus) tamariscus (Nicholson)
Petalograptus palmeus (Barrande)
Climacograptus normalis Lapworth
Rastrites peregrinus Barrande
Discinocaris browniana Woodward
Peltocaris aptychoides Salter

About 100 metres up from the junction of Lugate Water with the Ewes Water (Locality 6; Fig. 2.2; Chapter 2) on the west bank Peach & Horne (1899) found `Monograptus spinigerus`, M. cf. attenuatus and M. cf. tenuis.

The above evidences suggests that faunas found in the black shales of Calfhope Burn and Ewes Water are comparable, i.e. they belong to the sedgwickii or maximus Zones of the Llandovery, whilst the faunas found in Sit Burn and Lugate Water (Peach & Horne 1899) indicate the C. gregarius Zone. Further north, in

Still Burn, Lapworth (1870) has recognized graptolites of Parakidograptus acuminatus Zone (Peach & Horne 1899; details not given).

The above evidence indicates that black shales exposed in Calfhope Burn, Lugate Water, Sit Burn and Still Burn are of different ages, suggesting that although the lithology and petrology of the greywackes remains the same, the formation can be subdivided into at least three 'blocks' bounded by major thrusts, the blocks being successively younger to the SE.

The formation lies on the strike of the Intermediate Group of Walton (1955) in Peeblesshire, has comparable petrological characteristics, and can be correlated (Fig. 3.4b; Chapter 3).

4.2.3 Buckholm Formation

Peach & Horne (1899) have obtained the following species from the Tweed Valley, Long Phillips Burn (NW of Selkirk), Buckholm Hill, Clovenfords, Caddonfoot, Caddonlee, Thornylee and the basin of Caddon Water, all within the outcrop of the Buckholm Formation (Fig. 2.2, Chapter 2):

Monograptus turriculatus (Barrande)

M. cf. exiguus Nicholson

M. cf. crispus Lapworth

`M.` (Monoclimacis) cf. galaensis Lapworth

M. cf. priodon (Bronn)

M. cf. convolutus (Hisinger)

`M.` (Diversograptus) cf. runcinatus Lapworth

M. cf. communis Lapworth

`M. cf. spinigerus (Nicholson)` (?sedgwickii or cf. sedgwickii (Portlock)

Myrianites sp.

Crossopodia sp.

In Thornylee [NS 401 369] a specimen of Protovirgularia was obtained (identified by Dr. I. Strachan). These faunas suggest that the rocks of the Buckholm Formation are of Tarannon (Upper Llandovery) age (turriculatus to crispus Zones).

The formation lies on the strike of the Garnetiferous Group of Walton (1955), has comparable petrological characteristics (Fig. 3.4b; Chapter 3) and is correlated. Peach & Horne (1899) have recorded comparable faunas in the high reaches of the Caddon Water, near Caddonhead [NS 401 411] and second 'Deaf Heights' [NS 385 445]. Near the farmhouse of Caddonhead about 4 miles NW of Clovenfords certain grey shales have furnished Monograptus exiguus (Nicholson), M. cf. spinigerus and Petalograptus folium (Toernquist) (Peach & Horne 1899).

Two localities near the head waters of Caddon immediately to the south of Deaf Heights [NS 305 445], one a scar on the north bank of the burn (exact locality not mentioned) shows drab coloured shales with dark or blue-black seams, and the other an exposure of grey and yellow shales a short distance west of the

above locality (exact locality not mentioned) yielded Monograptus exiguus (Nicholson) and M. cf. pandus Lapworth; the second yielded Monograptus turriculatus (Barrande), M. spiralis Geinitz, Myrianites and Crossopodia in addition. Still farther west, M. cf. exiguus (Nicholson), M. cf. convolutus (Hisinger) and M. cf. communis Lapworth have been obtained by Peach & Horne (1899) from grey sandy shales.

It is of significance to the facies interpretation (Chapter 5) to note that although the petrological characteristics of greywackes across the Caddon Water vary laterally, their faunas show no significant variation.

4.3 HAWICK GROUP

4.3.1 Selkirk Formation

No fossils have been reported from the Selkirk Formation. Its petrological characteristics (Fig. 3.4b; Chapter 3), especially the profusion of carbonate matrix and thin bedded and flaggy nature and geographic position are comparable to the Hawick Rocks (most probably with the Carghidown Formation of Rust (1965) into which the Selkirk Formation continues. The age of the Hawick Rocks remains controversial, estimates ranging between high Llandovery and Wenlock (Clarkson, Craig and Walton 1975).

5. SEDIMENTOLOGY

This chapter discusses the criteria used for the interpretation of the sedimentary facies and facies associations, and some examples of depositional cycles within the area. As the area is very poorly exposed and exposures are very restricted and laterally discontinuous, interpretation is necessarily limited and tentative.

5.1 REGIONAL FACIES ANALYSIS

The area has been subdivided into zones of contrasting facies associations (Fig. 5.1, 5.2). Sedimentary structures and details of Bouma sequences (Bouma 1962) allowed recognition of the A1, C1, C2 and D1 facies of Mutti & Ricci-Lucchi (1975). Brief details of each facies are given below:

Facies A1: thick, massive, chaotic and disorganized conglomerates with profusion of rip-up clasts.

Facies C1: thick (40 cm - 5 m), massive or poorly graded, Tae and/or Ta(?bc)e sequences.

Facies C2: medium thick (10 cm - 40 cm), well graded Tabcde, Tbcde, Tcde, Tacde sequences.

Facies D1: thin bedded (mostly >10 cm), Tcde, Tde and/or T?bcde sequences.

The distribution of various facies was plotted on the map and boundaries between the most contrasting facies associations

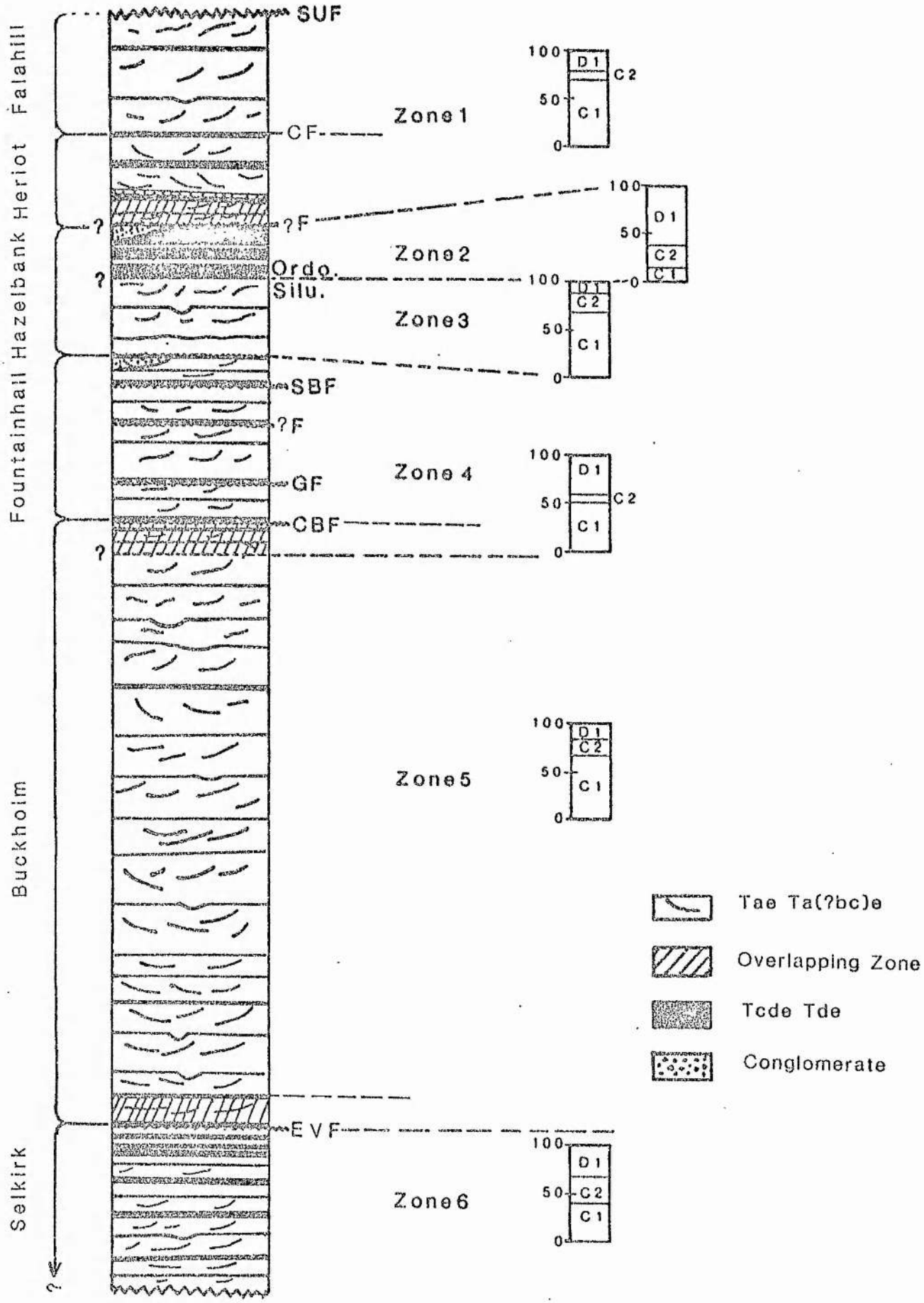

Fig. 5.1: Idealized columnar profile of the whole area with histograms of facies proportions.

Fig. 5.2: Map of the facies associations.

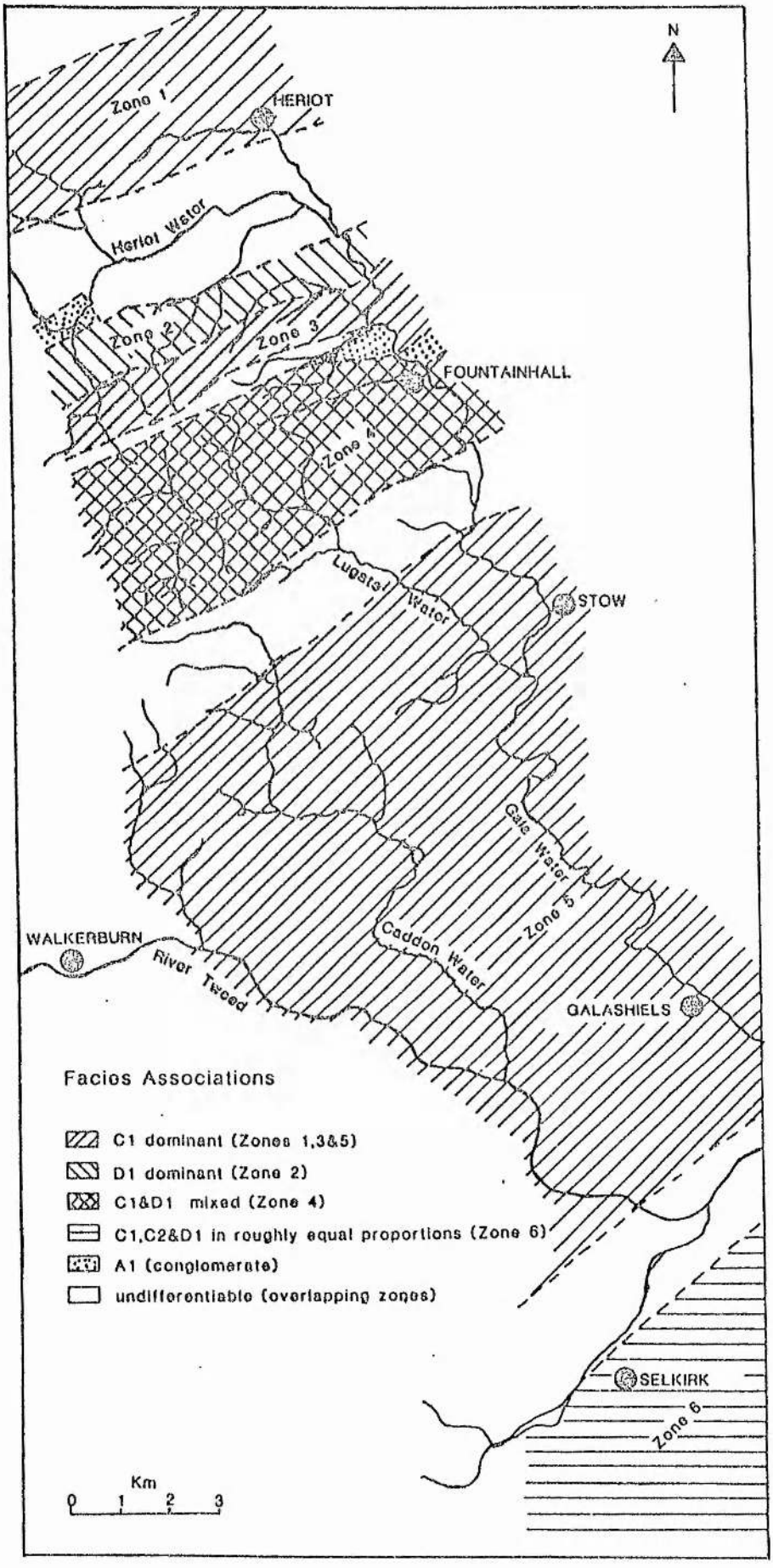

assessed (Fig. 5.2) by visual discrimination. The zones are not sharply bounded, and gradational zones of overlap are indicated.

Histograms of the proportion of facies in each zone (Fig. 5.1) show strongly contrasting facies associations. These contrasts reflect progressive changes in depositional environment through the succession. The dominant younging direction is northwestwards; minor folding and faulting within each block is considered not to be so intense as to influence the distribution of second order cycles ('megasequences': Ricci-Lucchi 1975a) and have accordingly been ignored. Detailed characteristics of the zones are as follows:

5.1.1 Zone 1 (includes the Falahill and Heriot Formations)

a) Bouma sequences

The rocks of this zone consist mainly of very thick (up to several metres) Tae and Ta(?bc)e sequences which are mostly poorly graded, but generally well graded towards the top of the succession. The sequences are commonly amalgamated, and localized horizons of very coarse texture can be observed. Tcde, Tde sequences are also present and may attain thicknesses of several metres. In some localities e.g. [NS 403 534] and [NS 395 526], thick bedded (Tae) sequences are followed by medium thick and thin Tcde and Tde sequences which suggest fining upwards cycles on a minor scale (< 7 m thick: Ricci-Lucchi 1975a).

b) Sole markings

Only a few longitudinal ridges and flute marks of parabolic (narrow) type were observed.

c) Channels

Thick bedding (40 cm to 4 m), the occasional occurrence of lenticular bedding, very coarse grain size (0.5-2 mm), the common occurrence of amalgamated units and profusion of mud clasts in thick Tae sequences suggest that the sandstones represent channel fill deposits. The lateral discontinuity of exposure does not allow observation of the detailed geometry of the sequences.

d) Facies Association

Facies C1 (thick and massive Tae Bouma sequences) is the most abundant (70%) (Fig. 5.1), suggesting a channelized mid-fan facies association.

Conglomerates (Facies A1)

This facies occurs at two distinct levels, each attaining a thickness approaching 500 m, and consists of massive, obscurely bedded conglomerates having a profusion of rip-up clasts which locally attain a length of several cm. These rip-up clasts are aligned roughly parallel to the bedding, and thus to the bedding

of the conglomerates. Uneven sandy horizons reaching up to 1 m in thickness occur locally. The nature of their contact with the conglomerate was not determined. No cross lamination or current ripples were observed. These conglomerates are formed by mass deposition of extremely concentrated dispersions (Mutti & Ricci-Lucchi 1975) and represent inner-fan association.

5.1.2 Zone 2 (includes upper part of Hazelbank Formation)

a) Bouma sequences

In this zone thin 'base cut out' Tcde and Tde sequences dominate, with a subordinate proportion of medium-thick (5-40 cm) Tabcde sequences. Thick (>40 cm) and amalgamated Tae sequences are the least abundant in this zone.

b) Sole marks

Sole marks are very rare. In some instances, thick Tae sequences gradually turn to thin Tcde and Tde units, suggesting fining-upward cycles on a minor scale (a few metres thick; Ricci-Lucchi 1975a).

c) Facies association

In this zone, facies D1 (thin Tcde, Tde sequences) is the most abundant, being found in up to 60% of exposures. Facies C2 (medium thick, well graded Tabcde sequences) is subordinate and C1 least abundant (Fig. 5.1). This association suggests outer-fan and fan fringe deposits. The columnar profile of the locality [NS 419 543] (Fig. 5.3) gives an instance of an association of this type.

5.1.3 Zone 3 (includes lower part of Hazelbank Formation)

The rocks of this zone consists of very thick (up to several metres) Tae, Ta(?bc)e sequences which are commonly amalgamated. The sequences are poorly graded, lenticular and very coarse grained with a profusion of rip-up clasts. Certain sequences show reverse grading near the base and normal grading near the top (C1 of Mutti and Ricci-Lucchi 1975). Some sequences (up to 20%) are relatively thin and well graded Tabce, Tabcde or Tacde units, representing the 'classic' turbidites (C2 of Mutti and Ricci-Lucchi 1975). These thick bedded and massive sequences represent a channelized mid-fan facies association. Occasional (up to 12%) packets of thin Tcde and Tde sequences, ranging between 40 cm and 2 m in thickness, are present within the thick Tae sequences, and probably represent overbank deposits.

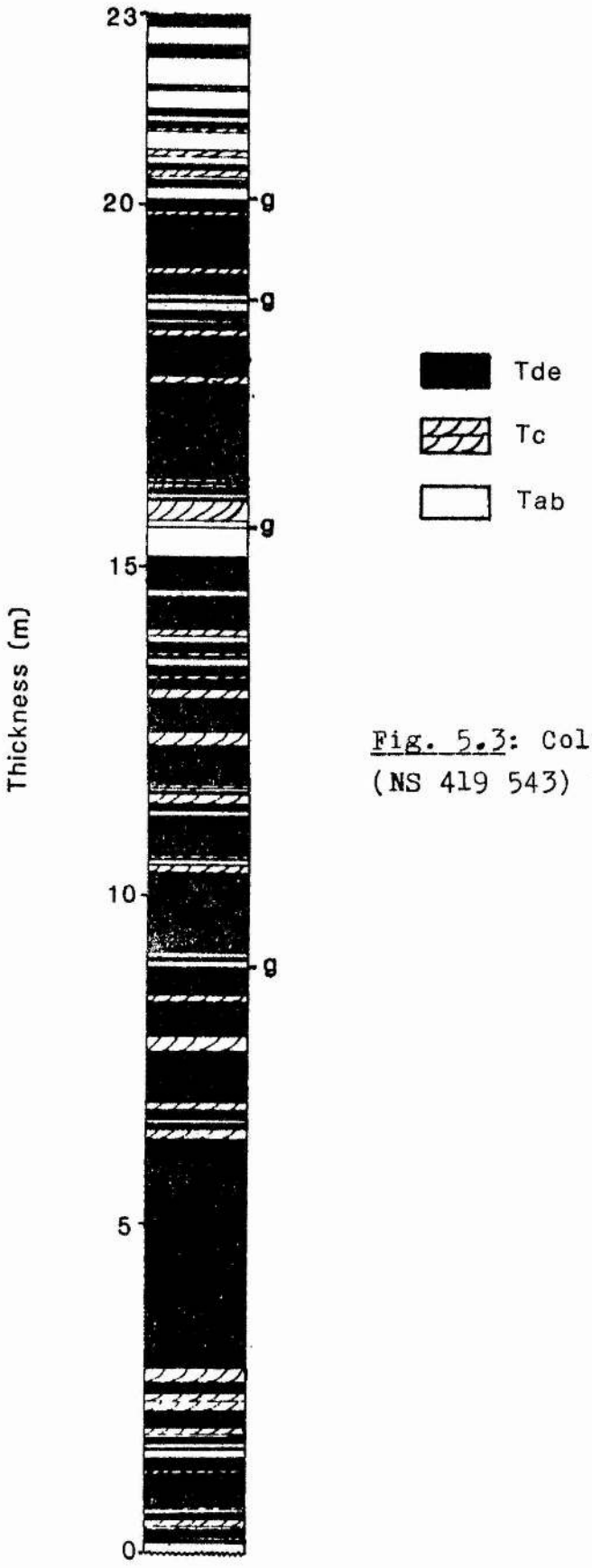

Fig. 5.3: Columnar profile of a locality (NS 419 543) in Zone 2.

b) Sole marks

Groove casts and longitudinal ridges are commonly present and bounce, brush and prod marks also occur. Load structures, associated flame structures and convolute lamination are also developed locally.

c) Facies associations

Up to 68% of the exposures (Fig. 5.1) in this zone are C1 (channelized Tae sequences), whilst C2 ('classic' Tabcde) facies are subordinate and D1 (thin Tcde and Tde) facies are the least abundant, suggesting a channelized mid-fan facies association.

5.1.4 Zone 4 (includes Fountainhall Formation and upper part of Buckholm Formation)

a) Bouma sequences

This zone represents a mixture of thick Tae (up to 50%) and thin Tcde and Tde (up to 42%) sequences. Thick sequences are poorly graded and locally display amalgamation, and are dispersed through the thin Tcde and Tde sequences which locally form successions up to several metres thick. Ta-e sequences of intermediate thickness (5 cm to 40 cm) are rare. The zone is highly disturbed by faulting and tight folding and displays a mixture of both thick (>40 cm) Tae, and thin (<10 cm) Tcde, Tde

sequences, the relationship of which are largely obscured by the structural complexity.

b) Sole marks

Longitudinal ridges ranging between a few cm and 3 cm wide are common. Occasional very fine lineations can been seen on the upper surfaces of the pelitic units. Groove and flute marks also occur.

c) Facies association

In this zone a mixture of C1 and D2 facies are present (Fig. 5.1), and although it can be deduced that these facies indicate environments varying between mid-fan and ocean floor, any depositional trend is obscured by the prevalence of faulting and tight folding.

Massive conglomerate (A1) similar to one described in Section 5.1.1 are again exposed on top of the zone.

5.1.5 Zone 5 (includes remainder of the Buckholm Formation)

a) Bouma sequences

This zone is characterised by very thick Tae sequences which may attain several metres in thickness with only a few millimetres of 'e' unit. Bouma c and d-units are generally

poorly developed, in some instances well developed ripples (wavelength a few cm - 10 cm; Plate 5.4) being visible on exposed top surfaces. Many are amalgamated 'top-cut-out' units. Lenticles of very coarse grained texture and ripped up mud clasts are common. In Buckholm Hill for instance, the sequences are exceptionally coarse grained and thick (Gala Grits of Lapworth & Wilson 1870a). Apart from the thick sequences which are ubiquitous, packets of dominantly thin pelitic Tcde and Tde sequences (up to 23%), locally reaching thicknesses of several metres, are also present. Such pelitic sequences are typified by mottled lamination, trace fossils and occasional fine upper surface current lineation. The medium thick Tabcde, Tacde sequences are only locally present.

b) Sole marks

Longitudinal ridges (Plate 5.2) are commonly present, whilst grooves and flute marks are subordinate. Other irregular sole marks (Plate 5.3) are also on record. Other sedimentary structures include load structures and their associated flame structures, convolute lamination, and occasional calcareous nodules. In one locality near Caddonlee [NS 449 356] calcareous nodules are present in a very coarse grained matrix rich in rip-up clasts. Intra-bed groove marks are also present in one locality [NS 399 371], revealed by an internal parting of a thick Ta(?bc)e sequence, a few cm above the sole of the bed, showing comparable trends of current direction to the sole marks. Such structures have been reported elsewhere (Hubert et al. 1966;

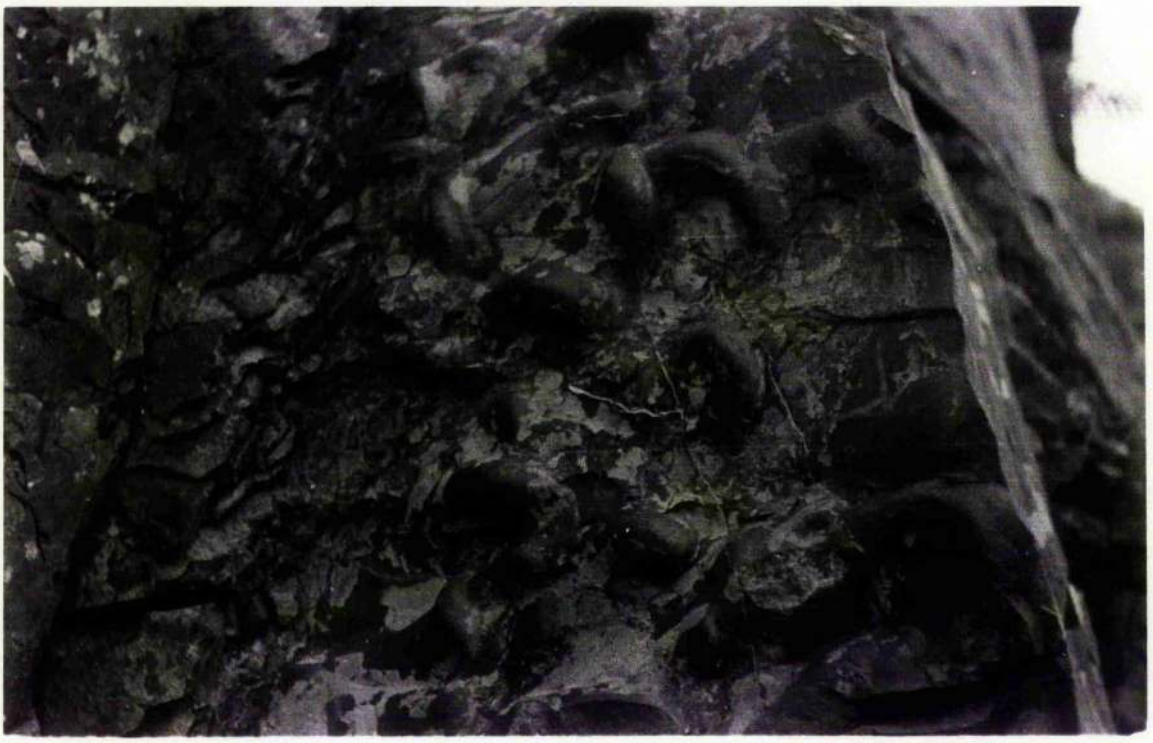

Plate 5.1: Linguiform shaped flute moulds in Selkirk Formation.

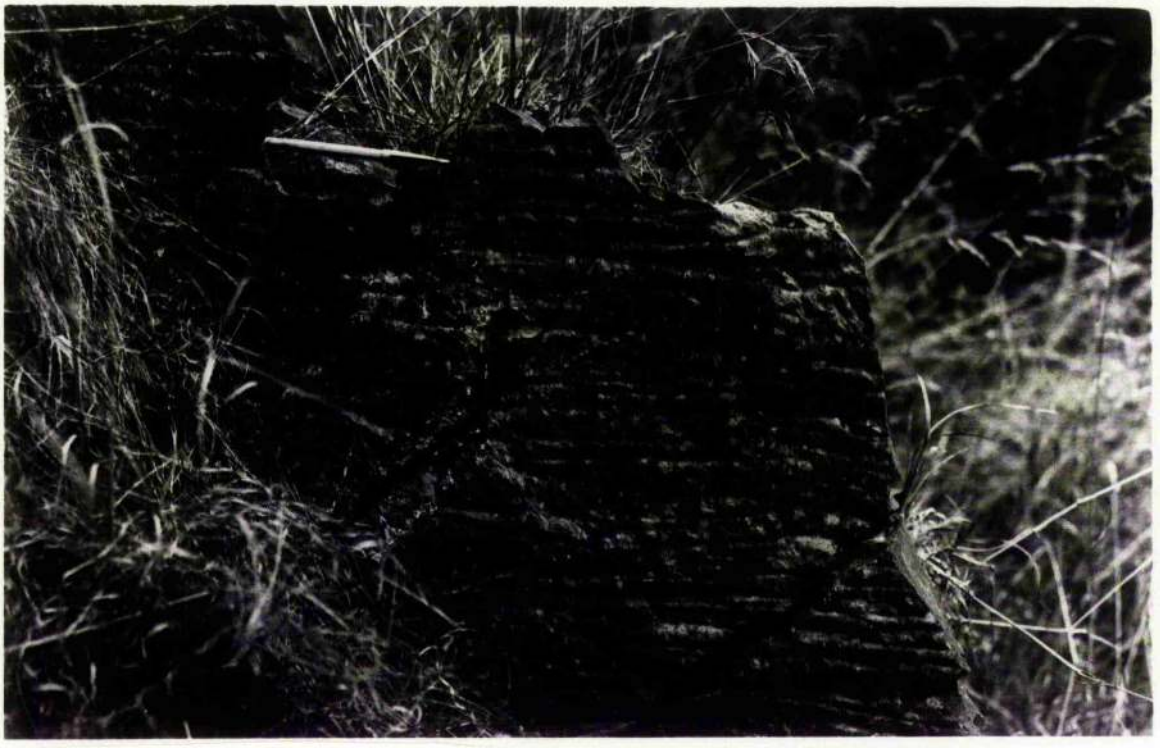

Plate 5.2: Closely spaced longitudinal ridge moulds in uckholm Formation.

Plate 5.3: Irregular sole marks close to scaly-pattern flute moulds in Buckholm Formation.

Plate 5.4: Current ripples in Buckholm Formation.

Dzulynski and Radomski 1955). It seems likely that such beds represent pulses of deposition from a single turbidity current influx.

The (Tae) units are very thickly bedded and locally lenticular, and very coarse grained with abundant rip-up mud clasts. These features again suggest channelized fan deposits.

c) Facies association

This zone again displays the C1 facies (Mutti & Ricci-Lucchi 1975) in up to 75% of the observed localities, suggesting a channelized mid-fan association. Successions of the D1 facies interspersed among the thick C1 successions suggest channel migration and the occasional introduction of interchannel deposits.

5.1.6 Zone 6 (includes mostly Selkirk Formation)

In this zone thin Tcde, Tde, and thick Tae sequences are equally abundant. Medium thick (5 cm - 40 cm) Ta-e sequences also occur and though subordinate, attain their greatest frequency in this zone. Thick Tae sequences rarely show amalgamation and are mostly medium to fine grained. Channels are rarely discernible and are shallow (less than 1.5 m deep). The southern and sequentially lower part of the zone tends to be richer in thick Tae sequences than the northern part.

b) Sole Marks

Thick sequences commonly display longitudinal ridges and sporadic flute marks (Plate 5.1). The pelitic sequence sometimes shows upper-surface longitudinal ridge marks. In some localities thick bedded Tae sequences are followed by medium thick Ta-e, and thin Tcde and Tde sequences which suggests fining-upwards cycles on a minor scale (a few metres thick).

c) Facies association

In this zone C1 and D1 facies are almost equally abundant. C2, although subordinate, reaches its maximum development in this zone. The C1 facies is more typical of the southern part and D1 the northern part of the zone, suggesting an overall retrogression of the fan from a mid-fan to an outer-fan (fringe) environment.

5.2 DEPOSITIONAL CYCLES

Individual Bouma sequences were measured in some of the best exposed localities of the area to evaluate the trend of second-order 'megasequences' (Ricci-Lucchi 1975a; Walker 1967; Figs. 5.4-5.8). A proximality index (Walker 1967) was calculated for the succession at each locality (Table 5.1). No definable trend could be discerned.

The combined columnar profile and bed thickness variation

Table 5.1: Proximality index of measured localities

S/No	Locality and Formation	Gr Ref	A		C		P
			No	%	No	%	
1	7-Buckholm	442 462	74	65	39	35	65
2	46-Buckholm	454 411	84	89	10	11	89
3	39-Buckholm	461 415	0	0	21	100	0
4	40-Buckholm	461 415	16	70	07	30	70
5	22-Buckholm	449 417	14	100	0	0	100
6	34-Buckholm	449 434	22	51	21	49	51
7	03-Heriot	450 408	28	93	02	07	93
8	81-Hazelbank	419 543	36	46	43	54	46
9	83-Hazelbank	424 510	17	88	02	12	88
10	02-Hazelbank	424 506	30	94	02	6	94
11	88-Hazelbank	426 506	117	93	13	7	93
12	86-Hazelbank	426 505	84	90	09	10	90
13	89-Hazelbank	426 505	59	94	03	06	94
14	84-Hazelbank	407 504	30	91	03	09	91
15	90-Hazelbank	429 501	73	96	03	04	96
16	08-Fountainhall	435 495	14	82	03	18	82
17	09-Fountainhall	436 494	07	100	0	0	100

A = sequences starting from Bouma unit-a

C = sequences starting from Bouma unit-c

P = Proximality index (ABC index) = $\frac{A}{A + C} \times 100$

(after Walker 1967)

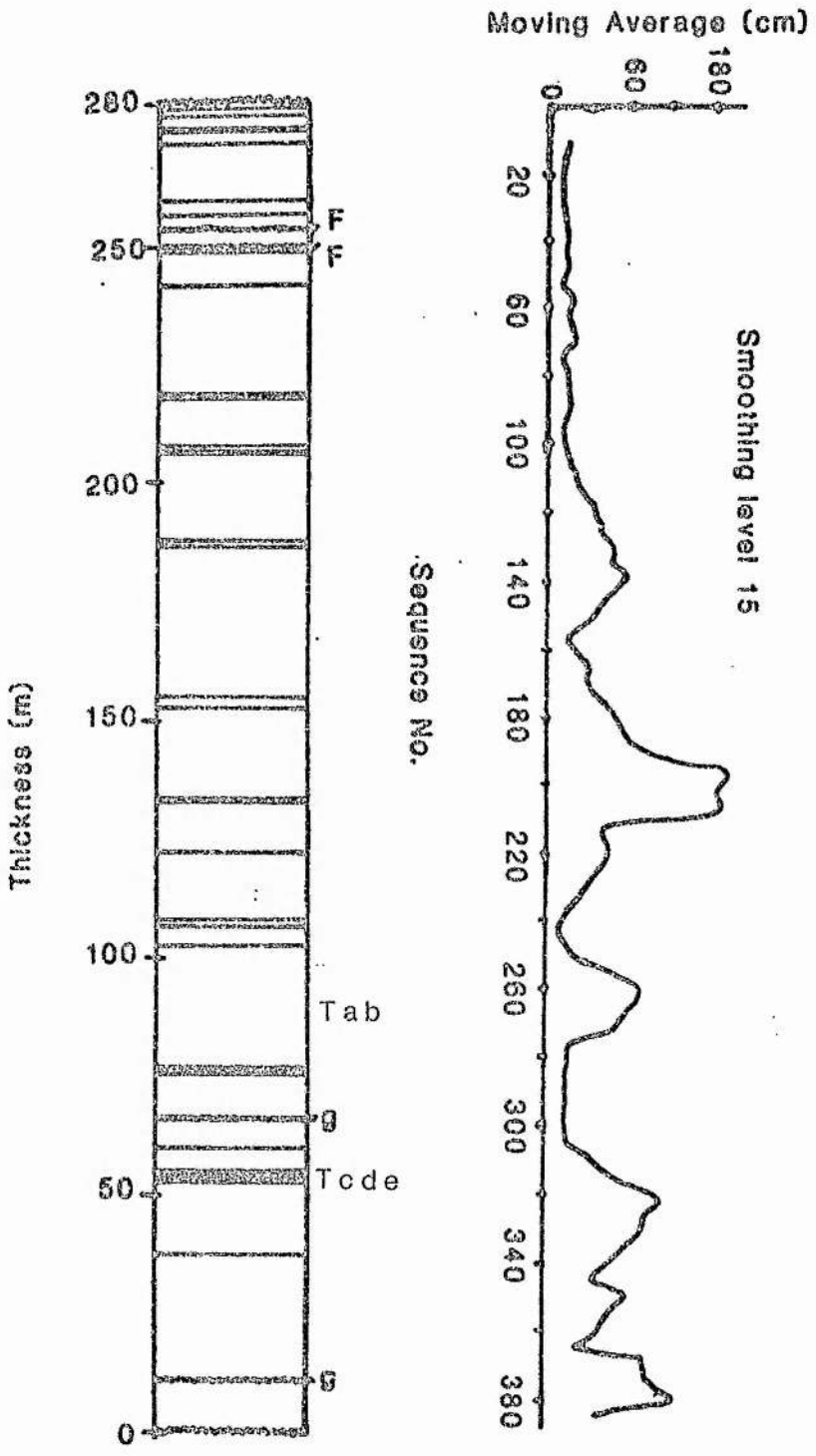

Fig. 5.4: Columnar profile and thickness diagram of the Hazelbank Quarry (Zone 3).

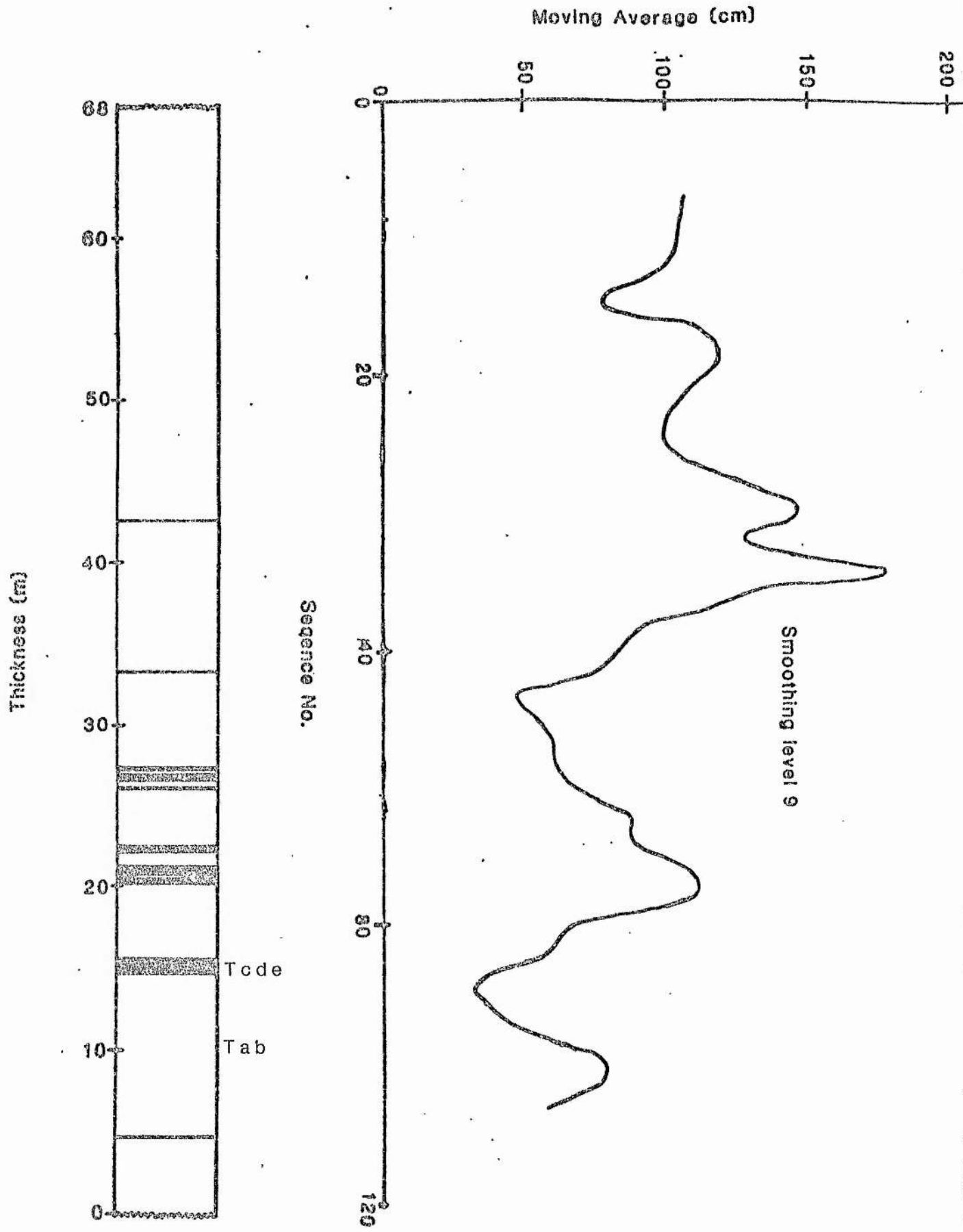

Fig. 5.5: Columnar profile and bed thickness digram of a locality (NS 429 501) in Zone 3.

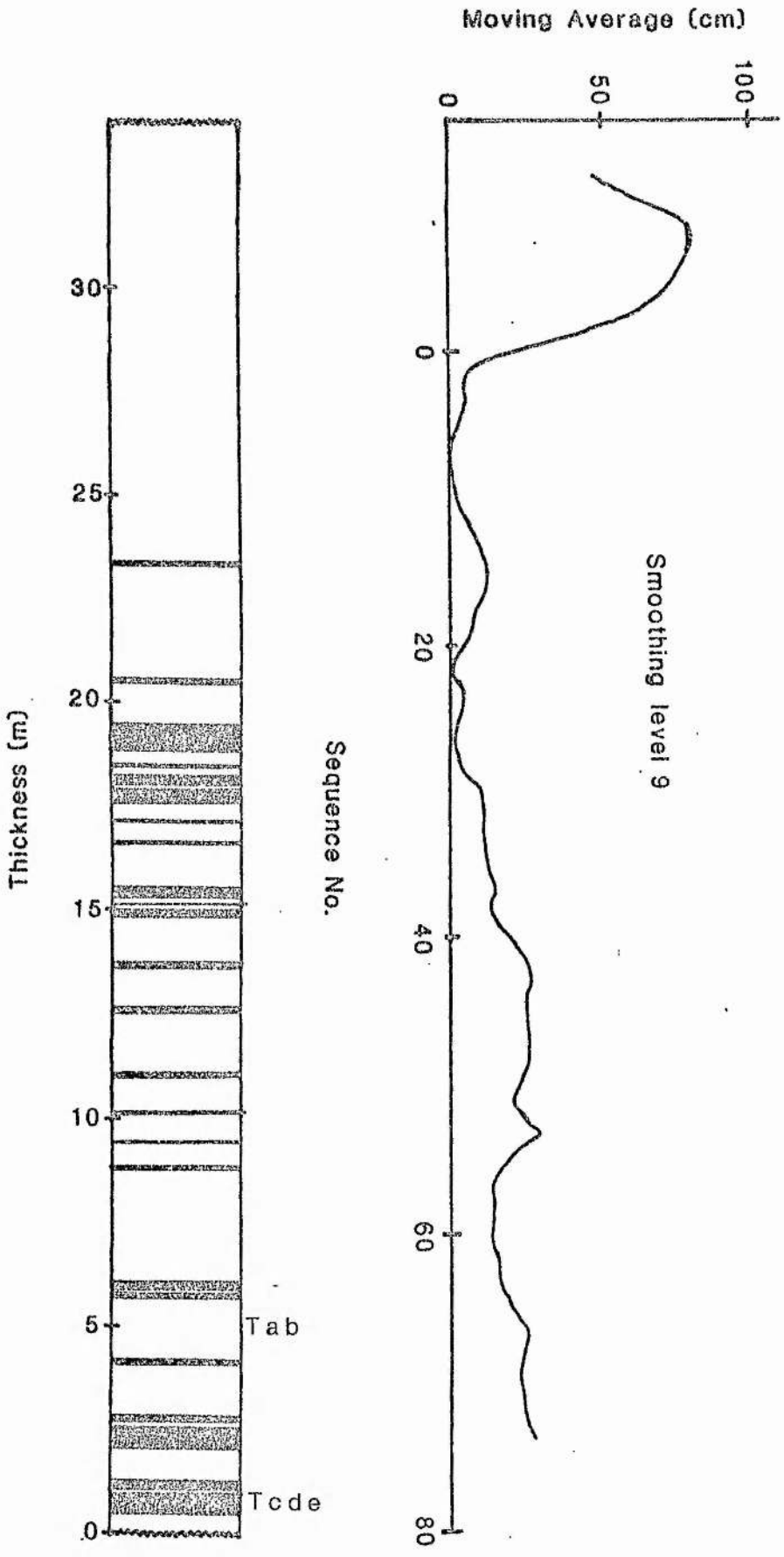

Fig. 5.6: Columnar profile and thickness diagram of a locality (NS 454 411) in Zone 5.

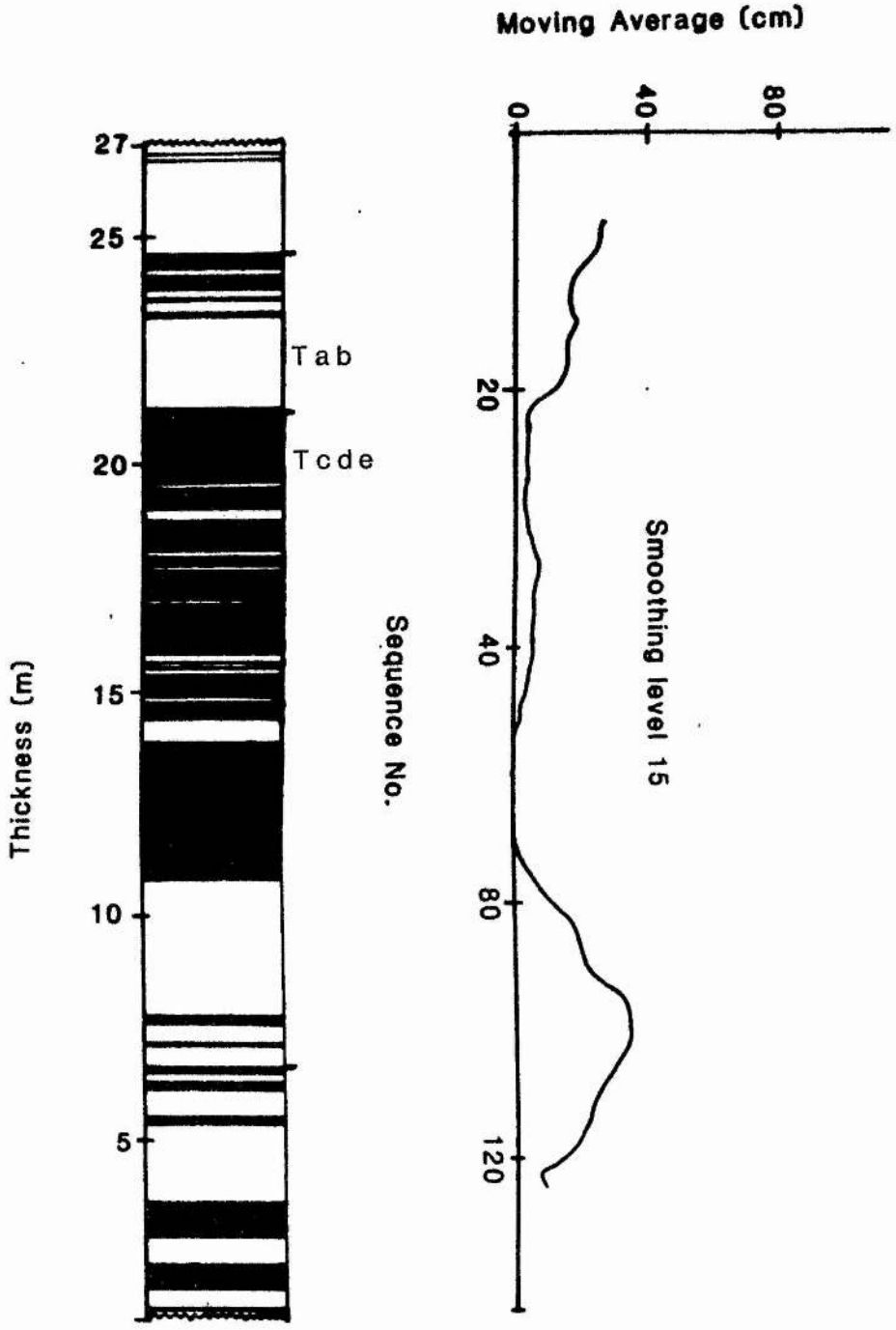

Fig. 5.7: Columnar profile and bed thickness diagram of a locality (NS 422 462) in an overlapping zone.

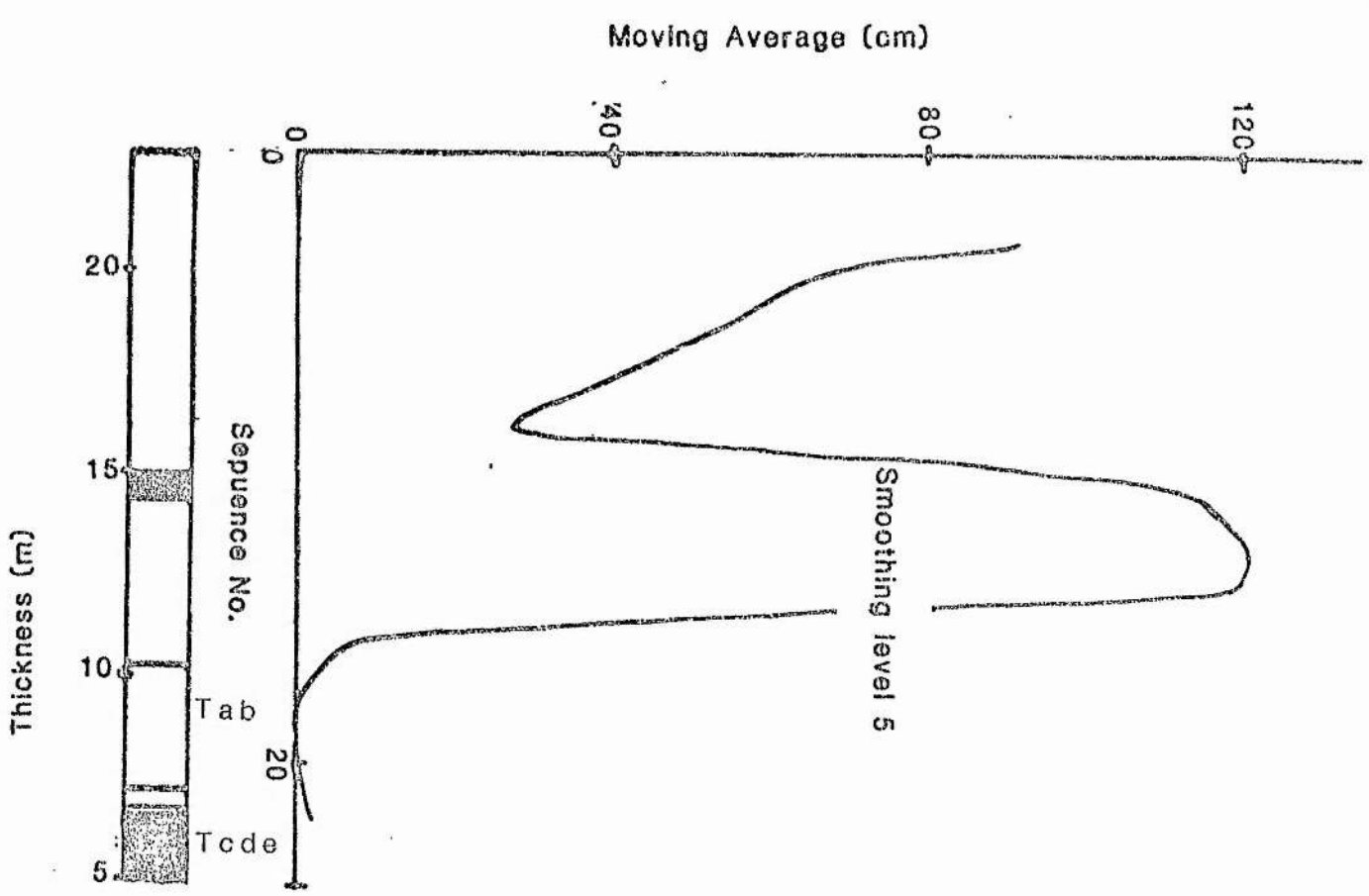

Fig. 5.8: Columnar profile and bed thickness diagram of a locality (NS 461 415) in Zone 5.

diagram of the Hazelbank quarry (Fig. 5.4) shows that thick and massive channelized sequences dominate, with a proximality index of 91.5% (Walker 1967). The diagram demonstrates that influxes of higher concentration mass depositions were followed by relatively lower density dispersions (Mutti & Ricci-Lucchi 1975). Five major cycles (Ricci-Lucchi 1975a) are exposed, and show neither positive (fining upwards) nor negative (coarsening upwards) trends. Likewise the thickness diagrams of the other localities (Figs. 5.5-5.8) also show comparable characters. Several example of similar cycles occur in the Apennines (Ricci-Lucchi 1975a) in which the trend is ambiguous. The cycles in the Apennines are also of comparable order of thickness (range: 6 m - 62 m) with those in the Gala area (range: 10 m - nearly 60m). The profile of the locality [NS 419 543], taken as representative of Zone 2 (Fig. 5.3; Section 5.1.2) shows traction current and fallout deposits, characteristic either of basin plain or outer fan (fringe) association (Ricci-Lucchi 1975a).

5.3 CONCLUSIONS

The area display facies associations ranging from inner fan (Facies A1, Zone 2 and 4) to outer fan (fringe) and basin plain environments (Facies D1, Zone 2, 4 and 6; Fig. 5.1).

In Zone 1, a channelized facies (C1) appears to persist throughout the zone. Zones 2 and 3 together display a retrogression from a mid-fan facies dominated by C1 in Zone 3, to

an outer-fan type in zone 2, in which the D1 facies prevails. Chaotic conglomerates of facies A1 at the top of Zone 2, having a source area comparable to the lower successions of Zone 2 and 3, suggest that the first, retrogressive cycle was followed by a rapid progression of the fan. These isolated exposures of chaotic, massive conglomerates, devoid of external contacts, provide the only evidence for rapid progression. Zone 4 displays a mixture of the C1 and D1 facies, suggesting a range of mid-fan to basin-floor associations, with no clearly discernible trend. Again the thick, chaotic and massive conglomerate of comparable composition and source area terminate Zone 4, suggesting another rapid progression.

In zone 5, facies C1 is distributed almost uniformly, with the intervening packets of D1 representing the inter-channel deposits, the whole constituting a channelized mid-fan association. Again no depositional trend is evident.

It has been concluded (Chapter 2 & 3) that overlapping turbidite fans were active during the deposition of Zone 5, being borne out by the change in the petrological characters of the greywackes across the Caddon Water, and the complex interdigitation of the contrasting facies along the Caddon Water (Fig. 2.1). Notwithstanding the petrographical contrast, the facies (Fig. 5.2) are closely comparable channelized mid-fan associations.

In Zone 6, facies C1, D1 and C2 are almost equally abundant.

Channels occur only sporadically, and are shallower. The C1 facies tends to decrease northwards and upwards, being replaced by the inter-channel D1 facies. The occurrence of 'classic' turbidites (C2), though in subordinate amount, partly suggests a proportion of relatively sluggish flows which show traction and fall-out deposits (Mutti & Ricci-Lucchi 1975). These suggest that the zone represent a relatively slow retrogression from a lower mid-fan to outer-fan (fringe) position.

6. PALAEOCURRENTS AND PROVENANCE

6.1 PALAEOCURRENT ANALYSIS

To analyse the palaeocurrents three categories of sedimentary structure were considered: sole marks (longitudinal ridges, groove marks, flute marks, bounce and brush marks), cross lamination and current ripples. Sole marks and current ripples were examined in the field by measuring the angle of pitch and noting whether the angle opens clockwise or anticlockwise relative to the strike, and the sense of direction of flow if possible. Only one reading was taken for each exposed sole with bottom structures unless two or more intersecting sets were found. In the case of cross lamination, orientated samples were taken and cut perpendicularly across and along the strike to ascertain the dip direction of the foreset laminae, the observed directions being marked and the azimuths measured. In order to bring the measured current directions into their original positions, the measured trends were rotated about the strike to horizontality. No correction for plunge was applied, partly because plunges are rarely observable directly, and partly since observed and deduced plunges are very low and the modal plunge horizontal. The regional orientation of the current structures may also have been affected by fault drag, especially in the vicinity of wrench faults. It should be noted that the method used is preferentially applicable to concentric folding, and errors may be introduced by its application to similar folds (cf. Ramsay 1960, 1961). As the axial thickening ratio is low

in the present area, an essentially concentric fold style is assumed, and the error introduced is considered to be acceptably small.

Accepting these limitations, it is evident that the current directions show convincing preferred orientations (Fig. 6.1). Erosional structures have a modal NE-SW trend, parallel to the regional strike, whilst depositional structures indicate a NW-SE palaeocurrent flow, with a lesser number showing a NE-SW trend. This divergence of directions is evident even within single bedding planes, in which groove casts may diverge by up to 40°, or in one example, by as much as 90°. Two bedding planes exposed in Hazelbank Quarry show grooves cutting minute longitudinal ridges, dragging the ridges round through angles of 90° (cf. Craig & Walton 1962). These divergences are clearly primary and are in themselves responsible for the wide spread of palaeocurrent azimuths, apart from those which may have been superimposed subsequently by tectonism. The divergent flow pattern may also be related to successions of currents generated within overlapping turbidite fans, or to the overlap of axial and lateral currents. The proposal of overlapping fans is also supported by the interdigitation of the contrasting greywackes of the Buckholm and Fountainhall Formations in Caddon Water (Chapters 2, 3 and 4). The dominance of 'strike-parallel' palaeocurrent trends denotes a corresponding dominance of flow parallel to the trench axis. Variability of the palaeocurrent directions may correspond to the localized irregularities within the submarine fan system. Although the number of current ripple

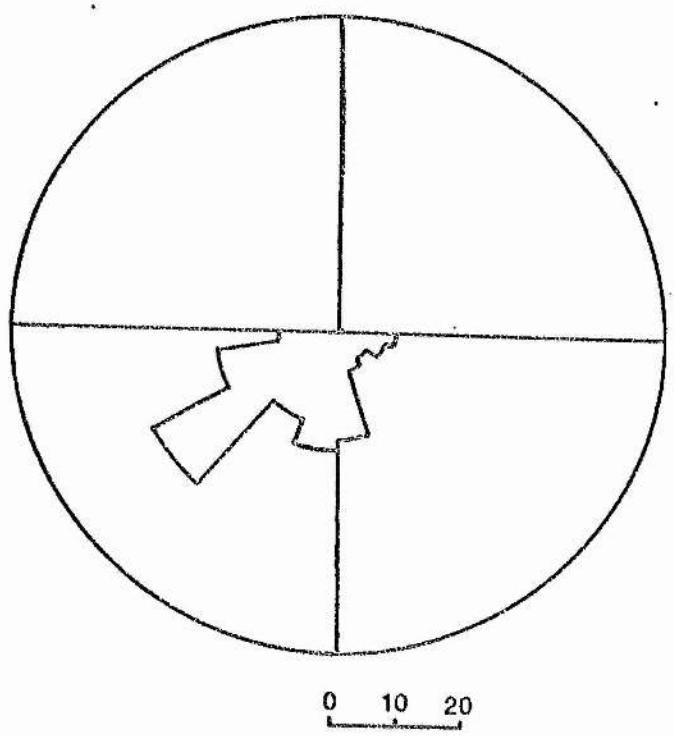

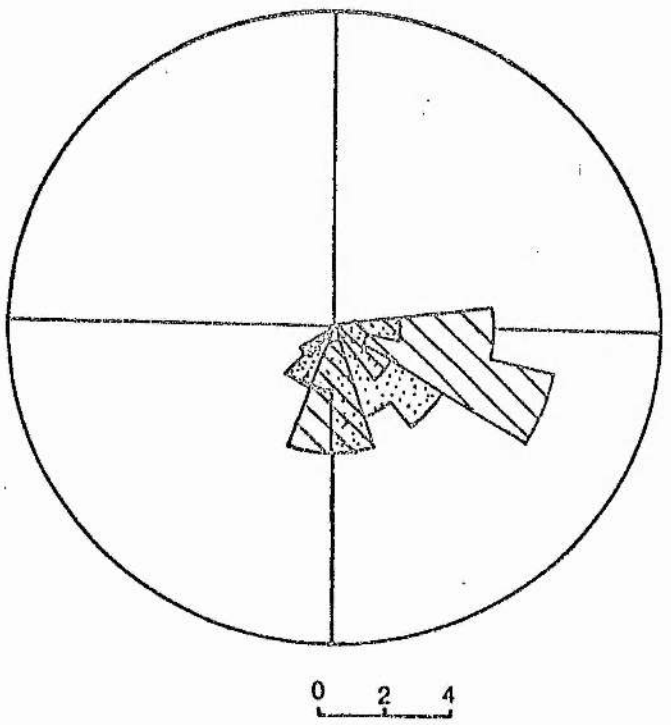

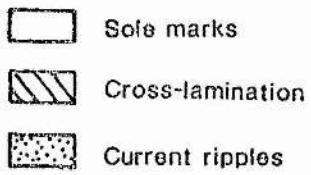

Fig. 6.1: Palaeocurrent pattern of the whole area.

readings (18) and cross-lamination readings (28) available for examination is significantly lower than the data set for sole markings, their inferred palaeocurrent trend is from NW to SE. This difference between erosional and depositional directions is comparable with that observed in the Hawick Rocks of SE Wigtownshire (Rust 1965b), the coast west of Gatehouse, Kirkcudbrightshire (Weir 1974a), and the Riccarton Beds and Hawick Rocks in Kirkcudbrightshire (Craig & Walton 1962), supporting Rust's postulation of longitudinal scour allied to transverse depositional currents.

The dominance of a NE-SW palaeocurrent trend is consistent through much of the Silurian succession (Figs. 6.2, 6.3), though the restricted data available from the Hazelbank Formation (Fig. 6.2a) suggest that there may be minor divergences both in the erosional and in the depositional structures.

Palaeocurrent data for the Ordovician succession of the two very poorly exposed blocks in the Gala area are restricted to only three readings, from the Heriot Formation only. One reading for cross-lamination shows a SSE palaeocurrent flow, whilst the two available readings of longitudinal ridge marks give a current flow from SW to NE. This direction is effectively opposite to the dominant vector for the Silurian succession (from NE to SW).

6.2 PROVENANCE

A plot of mean percentages of commonly occurring minerals

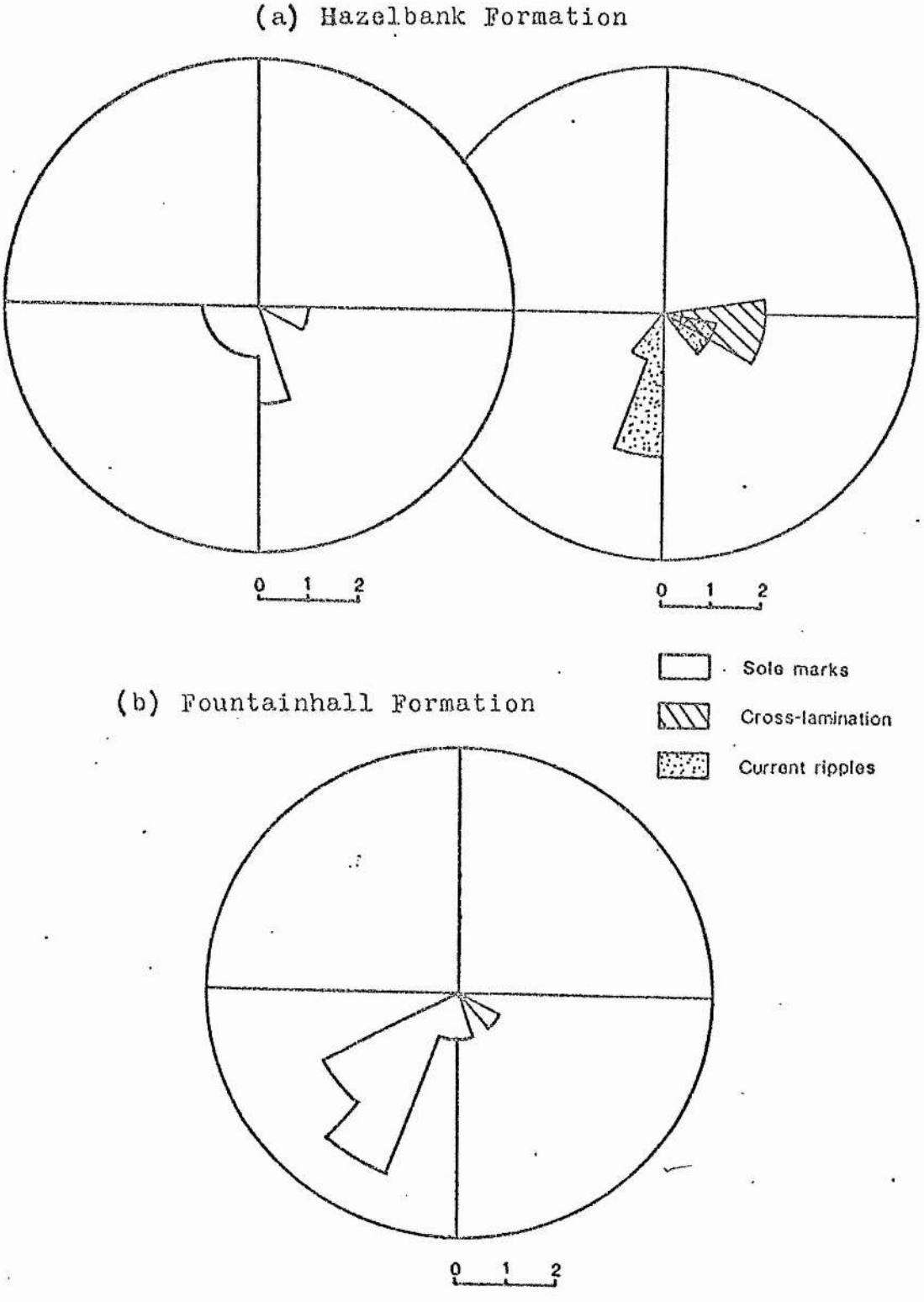

Fig. 6.2: Palaeocurrent pattern in the Hazelbank and Fountainhall Formations.

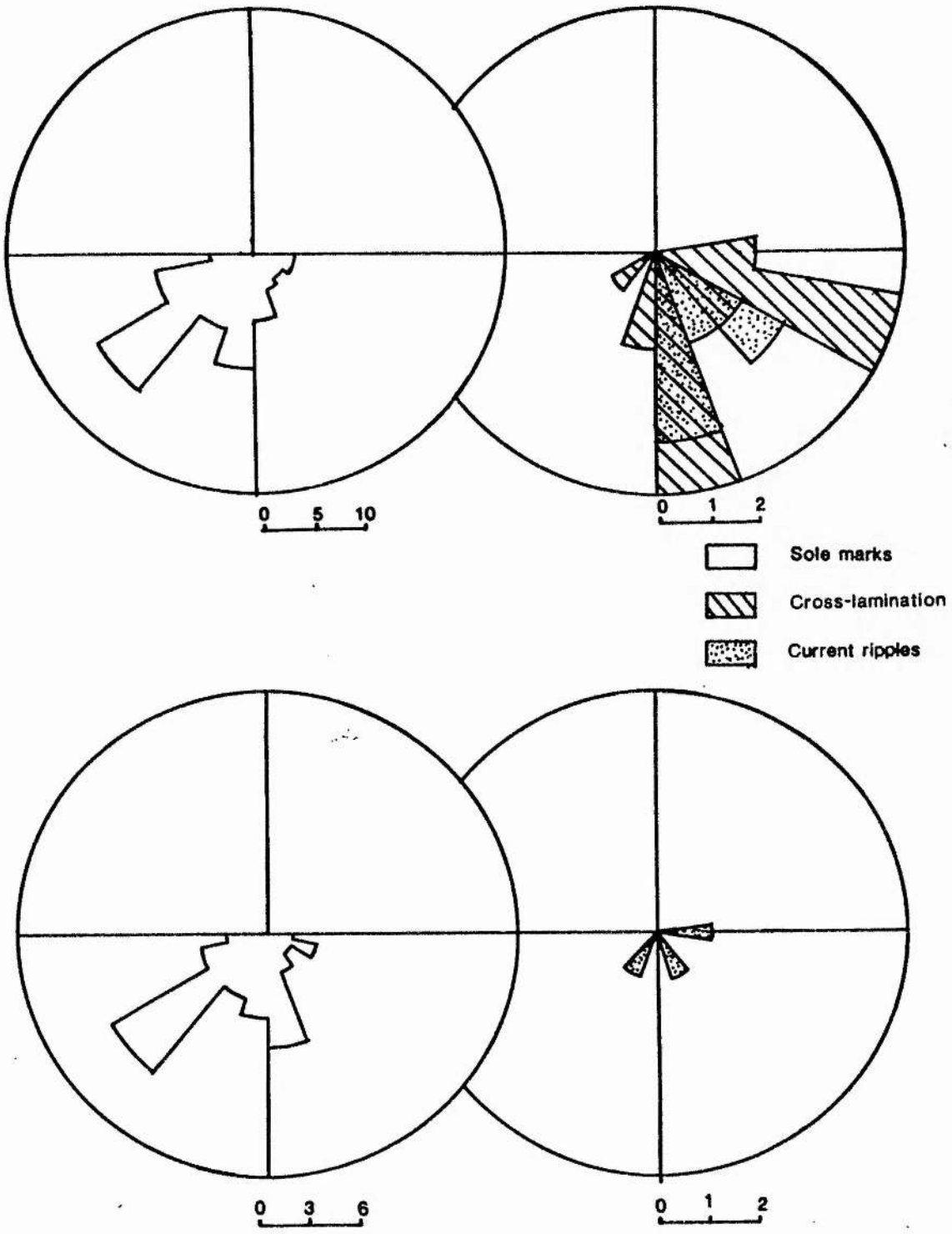

Fig. 6.3: Palaeocurrent pattern in the Buckholm and Selkirk Formations. Dominance of longitudinal transport against strong provinance contrasts indicates re-distribution following primarily transverse input.

and rock fragments from each formation (Fig. 6.4, next page) reveals that the distributions of quartz, acid igneous and metamorphic fragments are comparable in the Heriot, Fountainhall, Buckholm and Selkirk Formations. Quartz content increases with the increase in acid and metamorphic clasts, apart from a minor deficit of acid igneous clasts in the Buckholm Formation. This compatibility of relationships suggest that quartz clasts have been derived both from igneous and from metamorphic sources throughout the depositional history of the sequence. The dominance of the irregular and globular inclusions over the regular and acicular inclusions is probably related to the dominance of igneous quartz over the metamorphic quartz (Keller & Littlefield 1950).

The basic igneous fragments and ferromagnesian minerals are distributed inversely to the quartz, acid igneous and metamorphic fragments. Feldspars also show a crude inverse relation to silicic fragments. This suggests that feldspars have been derived both from acid and basic sources, being more abundant when the material is derived mainly from a basic source area. Sedimentary rock fragments are present throughout the succession in subordinate amounts and are essentially of intra-basinal origin (greywackes, shales, siltstones and cherts). Sporadic arkosic clasts occur in the Hazelbank, Fountainhall and Buckholm Formations.

6.2.1 ORDOVICIAN SUCCESSION

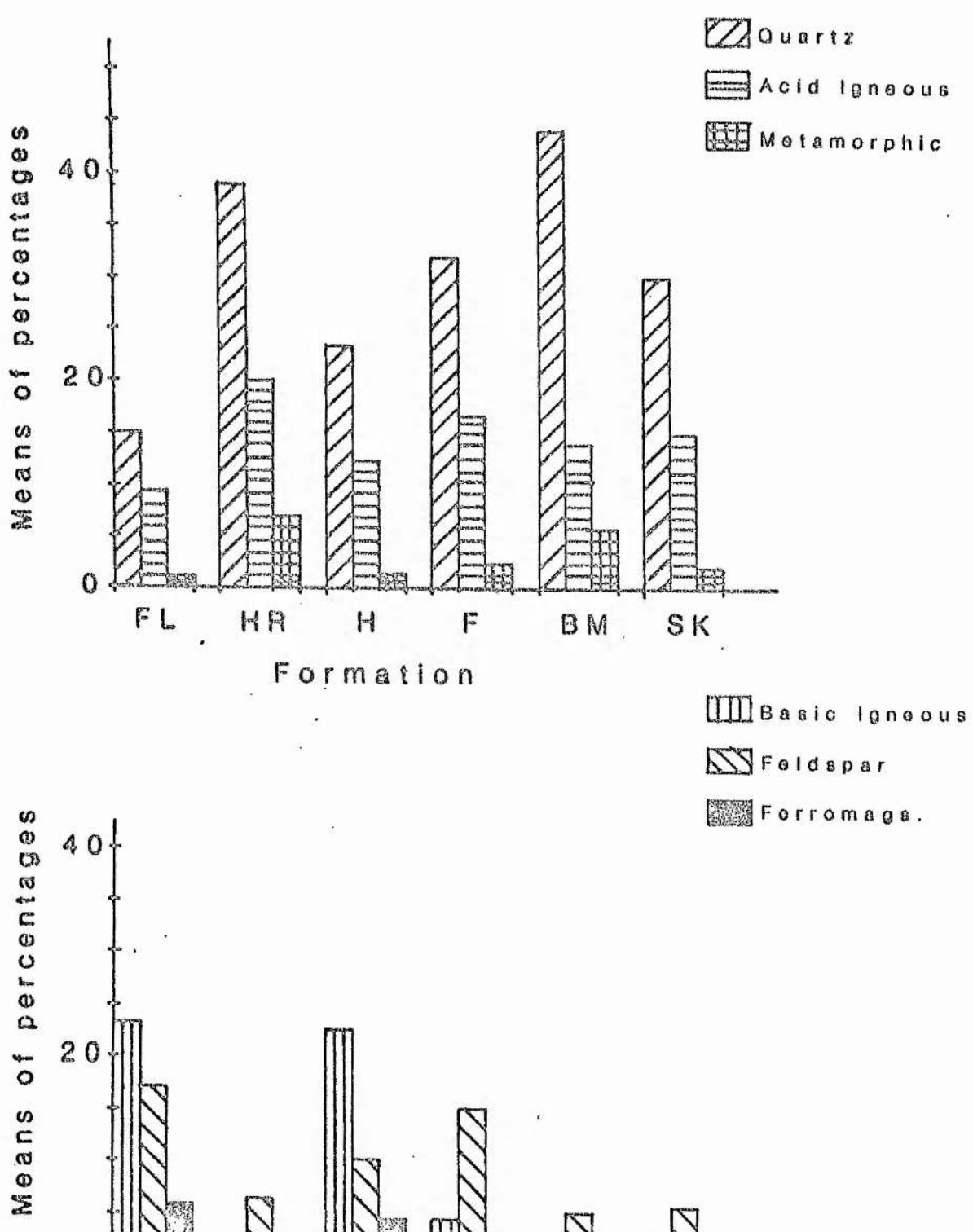

Fig. 6.4: Histograms of the formation means; FL =Falahill, HR =Heriot, H =Hazelbank, F =Fountainhall, BM =Buckholm, SK =Selkirk.

Falahill Formation

At the time when the Falahill Formation was being deposited the source area was dominated by basic volcanic rocks with subordinate contributions from acid igneous and metamorphic sources. Garnet, glaucophane and chrome spinel are dominant among the heavy minerals. Glaucophane is restricted to the Falahill Formation, also being reported in the Scar Formation of West Nithsdale (Floyd 1975). Glaucophane is a characteristic mineral of high T&P metamorphic belts which are believed to mark the site of convergent lithospheric plate boundaries and are considered (Ernst 1975) as indicators of subduction zone complexes. The coexistence of mafic and ultramafic fragments, e.g. serpentinite, dolerite/gabbro and chrome spinel in association with glaucophane, supports the idea of the presence of a subduction zone complex in the source area. The characteristics of the pyroxenes (Fig.8.9; Chapter 8) show that they have most probably been derived from the andesites of a volcanic arc. Although metamorphic rock fragments in the Falahill Formation are greatly subordinate to basic igneous clasts, garnet is more abundant than in any other formation. The source of metamorphic fragments (quartzite, mica-schist and foliated granite) was probably a Dalradian basement, and the acidic igneous contribution is probably from the two phases of granitic plutonism (560 Ma and 470 Ma; see below under Source area, p. 70) of the Midland Valley basement (Longman & Bluck 1979).

Heriot Formation

In the Heriot Formation the main source switched to acid igneous and metamorphic terrains, though a basic igneous source continued to provide minor amounts of material. The heavy mineral content is now dominated by apatite and tourmaline. Glaucophane disappears, though garnet remains prominent, emphasizing the elimination of the blueschist source and the increasing significance of the regional metamorphic, inferentially a Dalradian-like source. Sedimentary detritus now appears in significant quantity, and is largely of intra-basinal origin (greywacke, shale, chert).

6.2.2 GALA GROUP

Hazelbank Formation

A basic igneous terrain now becomes the dominating source area for the Hazelbank Formation, material derived from acid igneous and metamorphic terrains now being subordinate. Epidote and chrome spinel join apatite as the commonest heavy minerals. In contrast to the Heriot Formation, garnet is scarce, reflecting the essential contrast with the acid igneous and metamorphic dominance in the Heriot Formation.

Fountainhall Formation

In the Fountainhall Formation the acid igneous source again

resumes prominence, whilst the basic igneous source, though reduced proportionately, retains significance. Metamorphic fragments also increase, though less so than the acid igneous. A slight increase in apatite at the expense of chrome spinel by comparison with the Hazelbank Formation is taken to reflect the dominance of the igneous over the metamorphic terrain. Arkose fragments now appear, in addition to the normal intra-basinal sedimentary assemblage, implying the emergence of an extraneous sedimentary source. A source to consider is the Torridonian Series; though the northwestward location would fit, a considerable transport distance would be implied. Comparable arkoses also occur within the Highland Border Group at Aberfoyle, due NW of the present area; these, though volumetrically small, constitute a more plausible source.

Buckholm Formation

The Buckholm Formation shows a continued increase in the proportion of metamorphic fragments, a slight reversal of the increase in acid igneous clasts, and a drastic decrease in basic igneous fragments. Garnet reappears in association with tourmaline and apatite. The clast content denotes a reversion to sources comparable to those of the Heriot Formation.

6.2.3 HAWICK GROUP

Selkirk Formation

The major source for the Selkirk Formation was an acid igneous terrain, though metamorphic and basic igneous sources continued to provide minor contributions of material. Apatite, tourmaline and chrome spinel are now the common heavy minerals, with garnet now subordinate. The matrix is mostly carbonate which has partially (in places completely) replaced almost all types of detritus including quartz. Some carbonate grains are probably of detrital origin as their grain boundaries are sharp, and display exsolution of limonite along the grain boundaries.

6.3 NATURE OF THE SOURCE AREA

In most of the Silurian succession the axial palaeocurrents suggest a NE derivation. The transverse depositional palaeocurrents (erosional and depositional) are persistently from the NW throughout the succession, suggesting that the source area remains the same, i.e. the northeastern marginal landmass 'Cockburnland' (Walton 1963), which presumably had a covering of both acid and basic Lower Ordovician lavas over plutonic rocks comparable to those of the Ballantrae Igneous Complex (Walton 1965b). McMurtry (1980) claims that andesitic fragments from Southern Uplands 'basic-clast' greywackes generally, resemble in texture and mineralogy those of the Bail Hill Volcanic Group near Sanquhar, Nithsdale, and that clinopyroxene grains are also optically comparable. The chemistry of the Bail Hill clinopyroxenes (Chapter 8; Fig. 8.8, 8.9b) indicates alkaline affinities appropriate to lavas of seamounts. McMurtry thus deduced that the Bail Hill Volcanics (or other comparable

seamounts) would furnish a suitable sediment source. On the other hand, the detrital pyroxenes of the Falahill and Hazelbank Formations of the Gala area (present thesis), the Elvan Formation of the Abington area (Hepworth 1981) and the Red Island Formation of the Longford-Down Inlier (Sanders & Morris 1978) are non-alkaline, and thus more probably derived from a volcanic arc.

It is agreed that certain of the ferromagnesian minerals may have properties comparable to Bail Hill Volcanics, yet may have been derived from different sources. In support of this proposal, it is significant that clinopyroxenes of the Gala area do not show any evidence of sector-zoning as reported by McMurtry (1980) in the Bail Hill pyroxenes. Although the succession of the Southern Uplands and Longford-Down can not be strictly correlated with complete confidence, due to geographic separation and uncertainity over lateral equivalence of the fault blocks, the greywacke inputs, especially the 'basic-clast' type, are in general petrographically comparable, and were thus derived from equivalent or identical source areas. This deduction implies that the source rocks themselves formed belts extending for over 300 kilometres parallel to the strike. A volcanic arc source is therefore supported for these non-alkaline detrital clinopyroxenes, contrary to McMurtry's proposition; the Bail Hill seamount was obviously able completely or exclusively to dominate the local sediment supply, but did not extend its influence laterally to any significant extent. The Marchburn Formation of West Nithsdale (Floyd 1975) and the Corsewall Formation of the

Rhinns (Kelling 1962), lower in the succession than any unit proposed in the Gala area, also contain andesitic and clinopyroxene fragments; whereas these formations are either older or of comparable age (Llandeilo) to the Bail Hill volcanics, it seems unlikely that their detritus was derived from the Bail Hill area, especially since palaeocurrents from those areas are consistent in indicating a northwestward source.

It seems more plausible that a subduction complex, for instance the Ballantrae Igneous Complex, has contributed a significant proportion of the detritus of the 'basic-clast' greywackes, which also include lavas of volcanic arc origin (Lewis & Bloxam 1977; Church & Gayer 1973; Wilkinson & Cann 1974; Bluck et al. 1980). It must, of course, be noted that the origin of the Ballantrae lavas is at present under debate; it has been argued that some sections of the lava in the Ballantrae complex also show oceanic affinities (Lewis & Bloxam 1977; Jones 1977) and may have been tectonically juxtaposed with volcanic arc types. It has also been suggested (Ryan et al. 1983) that the Deer Park Complex, West Ireland, represents a dismembered ophiolite, presumably a lateral correlative of the Ballantrae Ophiolites, and may have contributed as a source area for the 'basic-clast' greywackes in the Irish sector (Sanders & Morris 1978).

The granitic fragments are mainly of two types: a) a foliated and sheared type which is likely to suggest either a Dalradian or a Grenvillian basement (Longman & Bluck 1979); and

b) unfoliated granites, some of which contain microcline and some micrographic and/or perthitic texture. It should be noted, however, that the reported Grenvillian age of the sheared granites is currently disputed; dating of first-cycle zircons have recently hinted at a 480 Ma (Grampian) date (B. J. Bluck, pers. comm. to J. A. Weir). Two types of unfoliated granite fragments have been recognized, contrasting both in petrography and age (Bloxam 1968; Longman & Bluck 1979) firstly, a non-perthitic, subsolvus type (560 Ma) and secondly, a microperthitic, subsolvus type (470 Ma). These unfoliated types are considered to have been derived from a source area to the SW margin of the Midland Valley. Some granites are free of K-feldspar and may represent the trondhjemitic granite of the Byne Hill, Girvan (Longman & Bluck 1979).

The acidic volcanic fragments (rhyolite, quartz-porphyry, quartz-keratophyre and volcanic glass), like the crystalline basement itself, are not represented in surface exposure in the present day Midland Valley. It is considered that these rocks were eruptives related to either or both of the granitic events, that as such they overlay the basement complex, and that they were totally removed by erosion (Walton 1983).

The metamorphic fragments including quartzite, muscovite-schist and muscovite-biotite-schist are appropriate to a Dalradian source, an attribution which is also appropriate for at least the 480 Ma unsheared microperthitic granites.

Sedimentary assemblages are essentially intrabasinal and locally derived, though minor limestone and arkosic fragments also occur.

6.4 CONCLUSIONS

The main source area for the Falahill Formation was the basic igneous rocks of a subduction complex and a volcanic arc, with minor contributions from acid igneous rocks of the Midland Valley basement and possiblly metamorphic area of the Dalradian basement. In the Heriot Formation the source area changed to a dominantly acid igneous and metamorphic terrain with subordination of the basic igneous source. This pattern was reversed within the Hazelbank Formation and re-established in the Fountainhall Formation, though with a lesser contribution from the metamorphic source. The metamorphic source in its turn assumed dominance in the Buckholm and Selkirk Formations, with progressive subordination of the basic contribution.

The main sources were a) a basic igneous source, partly subduction complex and partly volcanic arc; b) a metamorphic complex already unroofed to the level of the garnet isograd, inferentially the Dalradian basement; and c) an acidic igneous source, most probably granites of the Midland Valley basement of both 560 Ma and 470 Ma age (Longman & Bluck 1979). The possibility of the operation of a Grenvillian (1000 Ma) source awaits confirmation in the light of contrary, much younger indications, and must be regarded as not proven at present.

Dominance of submarine fans derived from the respective sources controlled clast composition within the various groups. Thus the basic source prevailed within the Falahill Formation; the metamorphic/acid igneous terrain supervened in the Heriot Formation; the Hazelbank Formation reverted to the basic source, and the Fountainhall Formation to metamorphic/acidic source, which increased its dominance with the Buckholm Formation. The strongly silicic Selkirk Formation probably arose by recycling out of earlier formations by then incorporated into the inferred growing accretionary prism.

7. STRUCTURE OF THE AREA

7.1 INTRODUCTION

The area displays marked contrasts in fold styles. To the NW, within the outcrops of the Falahill, Heriot, Hazelbank and Fountainhall Formations, the succession has been deformed into asymmetrical folds ranging from tight to open (Ramsay 1967) with modal trend of axial planes 030°-040° and dip 85-90° (Fig. 7.2b). Some are overturned (Plate 7.2) mainly to the SE and a few (3 in 79) are NW-facing monoclinal folds. To the SE, within the outcrops of the Selkirk Formation and the contiguous part of the Buckholm Formation. The fold style ranges from close to open (Ramsay 1967), with one tight and one monoclinal fold. The majority (53%) of the observed folds plunge gently (mode 0-10°) NE, and a small number (23%) plunge SW. SW plunges appear to be uniformly distributed, rather than being concentrated within localized areas. A small proportion (40%) of the folds are steeply plunging (plunge: 030-65°); of these, 29% plunge NE and 11% SW. It should be noted that these plunges are not as steep as have been recorded elsewhere in the Southern Uplands (Rust 1965a; Weir 1968, 1979; Floyd 1975). The succession throughout the area youngs dominantly to the NW; the folds verge mostly to the SE (Plate 7.1) and their long limbs young NW; the monoclinal folds face NW. The ratio of the long limbs to short in asymmetrical folds ranges between 2:3 and 1:20, and the modal ratio is approximately 1:3.

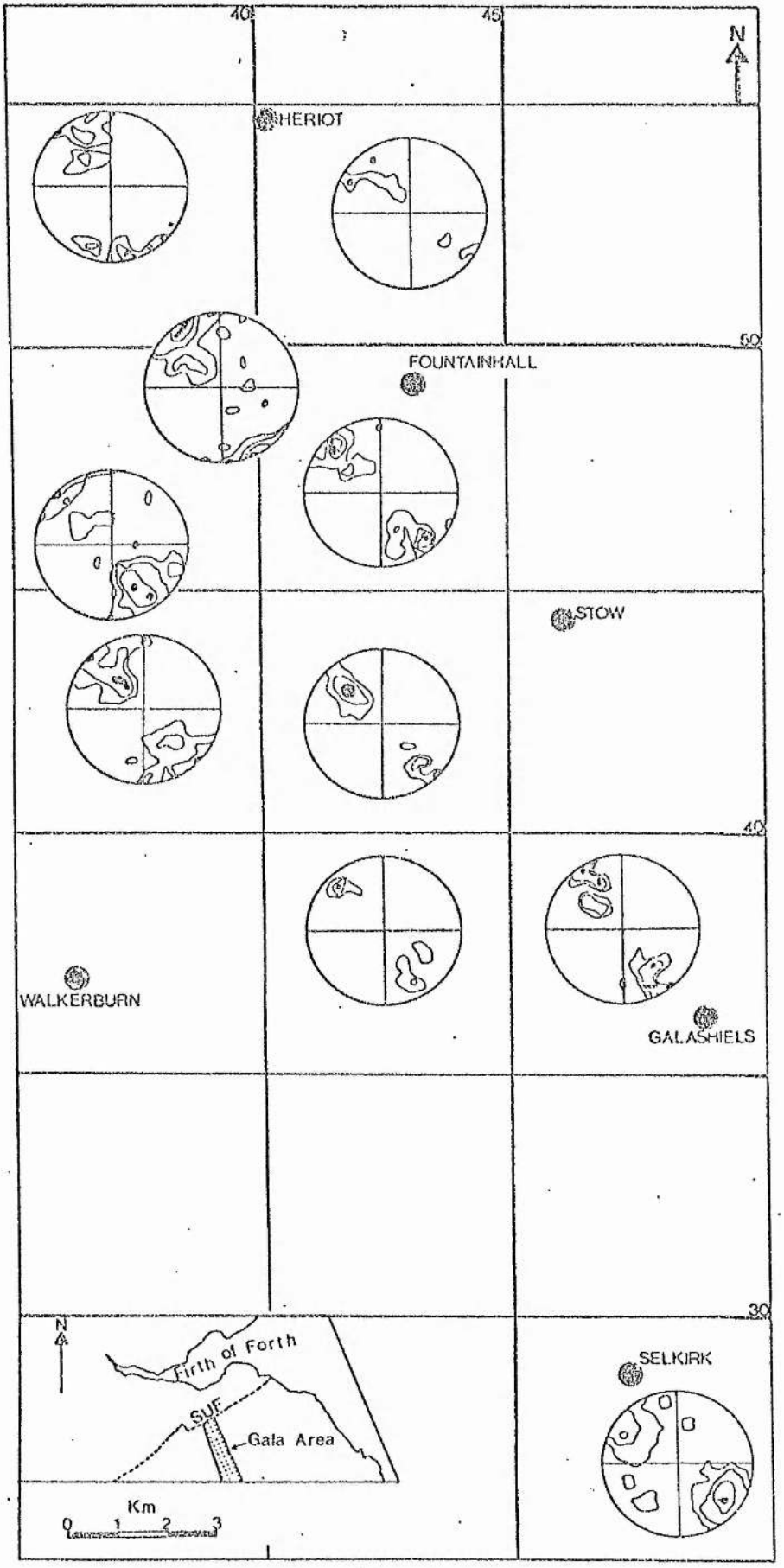

Fig. 7.1; Stereograms of poles to bedding attitudes in the designated subareas.

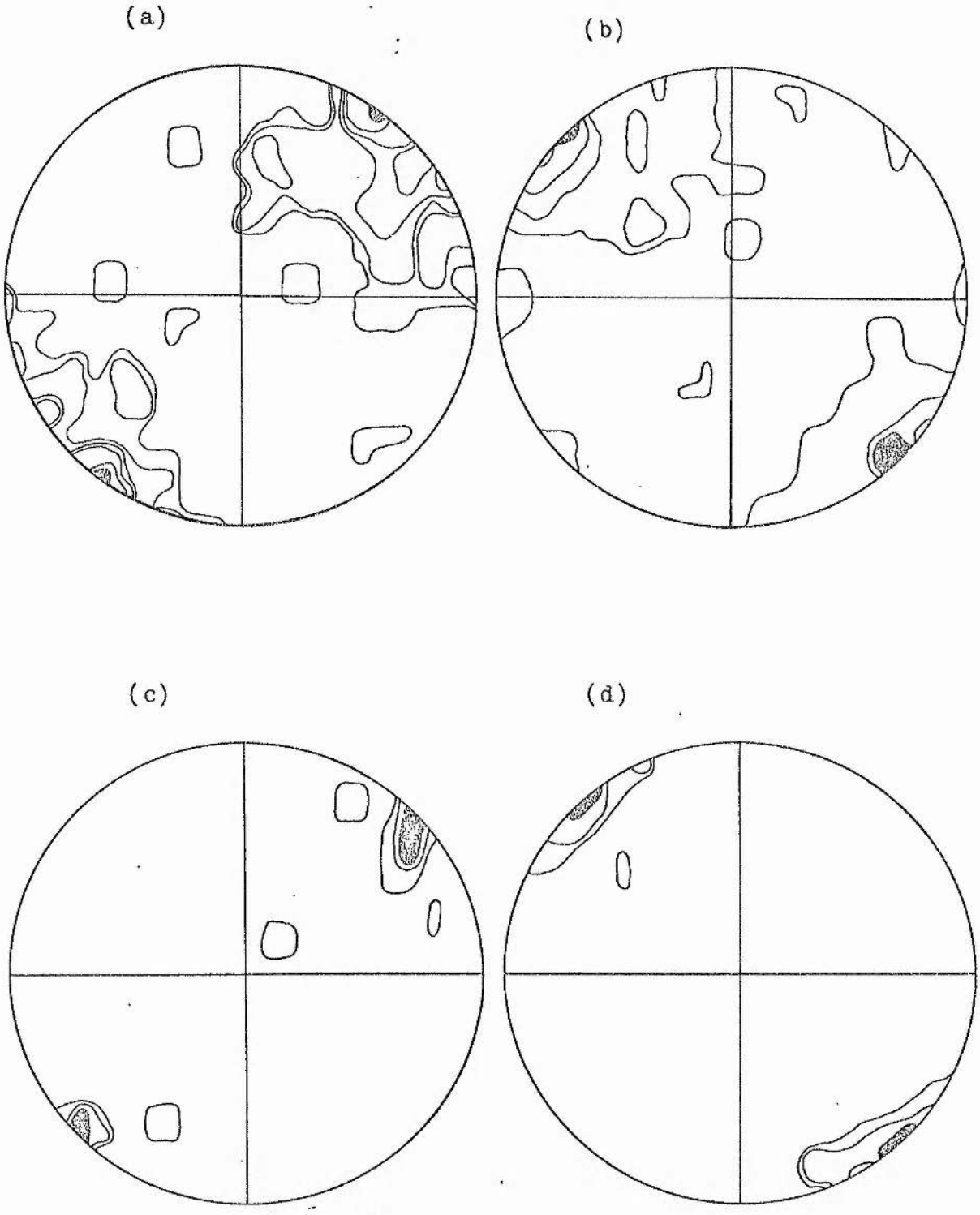

Fig. 7.2: (a) Equal area plot of all derived fold axes (n=81); contours at 1, 2, 4, 6, 8 and 11 points within 1% area. (b) Poles to the derived axial planes of all folds observed (n=81); contours at 1, 4, 7 and 11 points within 1% area. (c) Plot of derived axes from pi-diagrams of subareas (n=10); contours at 1, 2 and 3 points within 1% area. (d) Plot of derived axial planes from pi-diagrams of subareas (n=10); contours at 1, 2 and 3 points within 1% area.

Plate 7.1: Section showing SE-verging, asymmetrical folds in Selkirk Formation.

Plate 7.2: Tight asymmetrical fold showing overturning of SE limb.

Both minor folds (with amplitudes of 2 cm to 1 m) and folds of intermediate scale (having amplitudes of 1 m to 5 m) are present in the area. Minor folds characterize the pelitic sequences, which are more prevalent in the Fountainhall, Hazelbank, Heriot and Selkirk Formations. These minor folds are mostly of similar type, the ratio of the bed thickness at the limbs to that within the hinges ranging from 3:4 to 1:2. Axial thickening is more pronounced in minor folds, reflecting the lesser competence of the pelitic sequences, otherwise their style is comparable to that of the intermediate folds.

The formations occur within "blocks" (Hepworth 1981) bounded by strike faults, mostly associated with discontinuous outcrops of Moffat Shales which define the base of the blocks and are considered to furnish sliding surfaces. A conjugate set of wrench faults (Fig. 7.3c) cuts across the folded sequences and strike faults alike. Strike, as well as wrench faults show extreme diversity of pitch of their slickensides, suggesting reactivation; although not more than one set of slickensides was seen at any given locality (See Section 7.4.2 for detailed analysis).

The prevalence of imbrication in association with the major strike fault zones, the bounding of successive formations of markedly contrasting characteristics by these strike-fault zones, and the occurrence of younger formations progressively to the SE against a dominantly northeastward

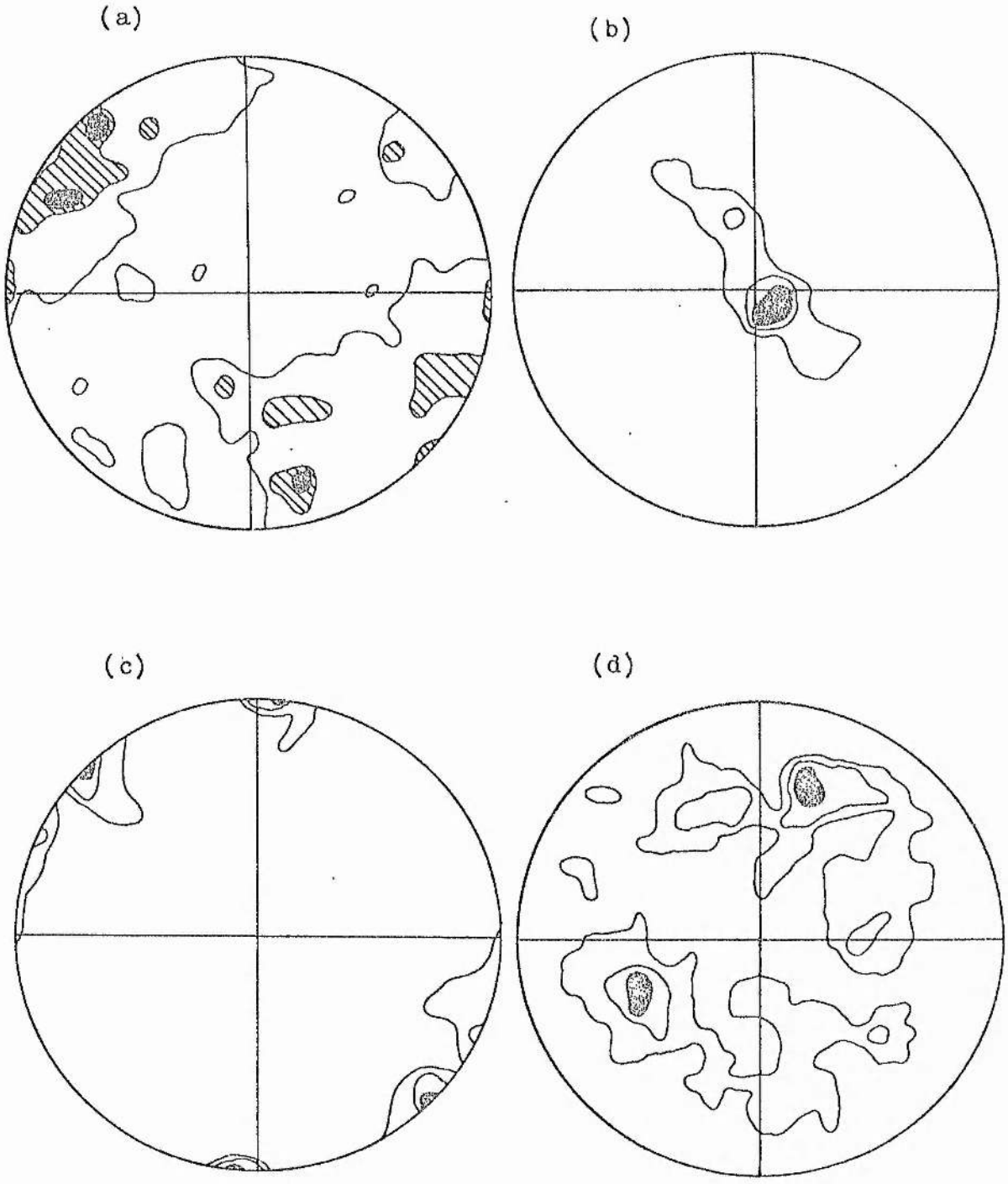

Fig. 7.3: (a) Poles to the attitude of fault planes, entire area (n=179); contours at 2, 5 and 7 points within 1% area. (b) Plot of slickenside plunges on dip slip faults (n=42); contours at 2, 4 and 8 points within 1% area. (c) Plot of slickenside plunges on wrench faults (n=32); contours at 2, 4 and 5 points within 1% area. (d) Plot of slickenside plunges on oblique slip faults (n=69); contours at 1, 3 and 5 points within 1% area.

younging, might be considered to support the Lower Palaeozoic accretionary prism model of McKerrow et al. (1977) for the Southern Uplands as a whole. On the other hand, there is no significant cross-strike variation in dips, and axial surfaces and related structures remain essentially vertical throughout. Under the accretionary model, dips and faults should show progressive northwestward overturning. Lack of these features is considered to call the prism hypothesis in question.

7.2 ANALYSIS OF FOLDS

Two techniques have been employed: a) Bedding plane attitudes were plotted on the Lambert Equal Area Stereographic Net, to analyse the major fold trends; b) Wherever fold closures are exposed or suspected, the limb attitudes of individual folds were plotted, and the disposition of axes and axial planes determined.

Apart from the larger quarries (Hazelbank, Caddonfoot etc.) limitation of exposure inhibits the recording of satisfactory quantities of directly-measured data for individual folds. Reliance has thus to be placed on plots of bedding plane attitudes, randomized according to the exposure distribution. The area was divided into subareas based on the 1:10,560 Ordnance Survey toposheets and pi-diagrams for each area constructed (Table 7.1; Fig. 7.1). Bedding attitude readings for each block were also plotted as poles, and

Table 7.1: Summary of the plot of bedding plane attitudes in subareas.

KEY

S/No	Serial Number
Sa No	Subarea Number
Pg Ax	Plunge of Axis
A Ax Pl	Attitude of Axial Plane
Mg St D	Direction of Maximum Stress

S/No	Sa No	Pg Ax	A Ax Pl	Mx St D
1	NT 35 SE	a) 18 to 75	76/80N	166-346
	NT 35 SE	b) 75 to 44	76/80N	166-346
2	NT 45 SW	25 to 208	40/55S	130-310
3	NT 44 SW	45-225/Hor	40/86S	130-310
4	NT 34 NE-a	22 to 59	57/85S	147-327
5	NT 34 NE-b	15 to 50	52/82N	142-322
6	NT 35 SE	48-228/Hor	48/85S	138-318
7	NT 44 SW	45-225/Hor	48/85S	135-315
8	NT 44 SE	10 to 15	45/70S	135-315
9	NT 43 NE	10 to 238	62/70S	152-332
10	NT 33 NE	30-210/Hor	30/83N	120-300
11	NT 42 NE	12 to 32	30/Vert	122-302
12	NT 43 NW	12 to 51	53/88N	143-323

yielded results compatible with the subareas based on Ordnance Survey toposheets. The general axial trend and plunge for each subarea was derived by drawing great circle-traces corresponding approximately to the mid-points of pi-diagram maxima. Intersections of great-circle traces are considered to represent potentially developed fold axes. A plot of 10 derived axes and axial planes (Fig. 7.2c and 7.2d) show that the axial plunges vary from very low angles to horizontal and have a modal azimuth of N. 45-50 E. The occurrence of steeper axes is also suggested by a single point having a plunge of 75 towards 40. Derived axial planes show a near-vertical dip.

7.2.1 Folds individually recorded (Appendix No. 7.1)

Minor folds and folds of intermediate scale, as defined above (Section 7.1), are common throughout the area. Tight folding is prevalent in the northwest of the area. Overturning, mostly of the northwestward facing limbs, is not uncommon, 21 out of 79 (27%) being overturned. Certain pelitic horizons also display northwestward-facing monoclinal folds (amplitude: 2-5 cm). F_2 crenulations comparable to those described by Weir (1968, 1979) were not seen. The attitude of the strata in dark grey and black shale horizons in Calfhope Burn suggests tight, asymmetrical folding. In Still Burn the black shales display tight overturned folds and in one locality, a very small-scale (amplitude: 3-5 cm), NW facing monoclinal fold. To the SE, close folding again

dominates but overturning is not common, and monoclinal folds are also rare. An approximately axial-planar cleavage is associated with certain of these folds. Most of the folds verge SE and only a few verge NW.

A plot of derived axes (Fig. 7.2a) shows that the modal azimuth of axes is 037°/horizontal. A second maximum gives an orientation of 056°/horizontal. A third and relatively weak maximum indicate a group of steeper axes (modal plunge: 40° towards 10), probably to be ascribed to refolding. A plot of axial planar poles (Fig. 7.2b) shows a dip ranging from 85° to vertical towards 312°-320°.

7.2.2 Phases of Folds

The gently plunging folds predominate throughout the area which represent the main phase of deformation. They correspond in style and attitude to the F_1 and F_2 phases of Rust (1965), Weir (1968), and Floyd (1975): see also comments on the continuity of deformation by Stringer & Treagus (1980, 1981). The steeply-plunging folds show no significant contrasts in style to those of the gently-plunging types; neither are the plunge variations localized with any one block. Tightness variations are controlled by lithology, tighter and similar folds being related to thinly-bedded pelitic sequences, and close to open, and truly concentric styles to thickly bedded greywacke sequences. Plunges are, however, less steep than some "F_3" axes reported by Craig &

Walton (1959), Rust (1965), and Floyd (1975), which approach the vertical and even display localized overturning. Stringer & Treagus (1980, 1981) have concluded that plunge is related to localized discrepancies within the same set of compressive forces. The sporadic and apparently random distribution of steep plunges in the Gala area appears to support the Stringer & Treagus conclusion (1980, 1981) of a continuum of deformation. The modal azimuth is very strong within an otherwise widespread scatter, indicating the dominance of the main phase throughout.

7.3 MAJOR FAULTS (see map next page)

7.3.1 Strike Faults

CARCANT FAULT: This fault runs across the small reservoir [NS 365 527] about 300 m N of Carcant and represented by a zone of lenticularly sheared and broken greywackes more than 20 m wide, in which bedding is largely obscured. Some of the sheared surfaces are curved or undulatory. The main fault plane is not visible, but the strata on opposite sides of the fault zone are of contrasting characteristics, being allocated to the Falahill Formation to the NW and the Heriot Formation to SE. The attitude of the sheared surfaces and the associated slickensides suggests a reverse sense of movement; most of the minor sheared surfaces dip southwards. About 50 m south of the fault zone, light grey and brownish grey siltstones and silty shales correlated with the Upper Hartfell

Fig. 7.4: Geological map of the Gala area.

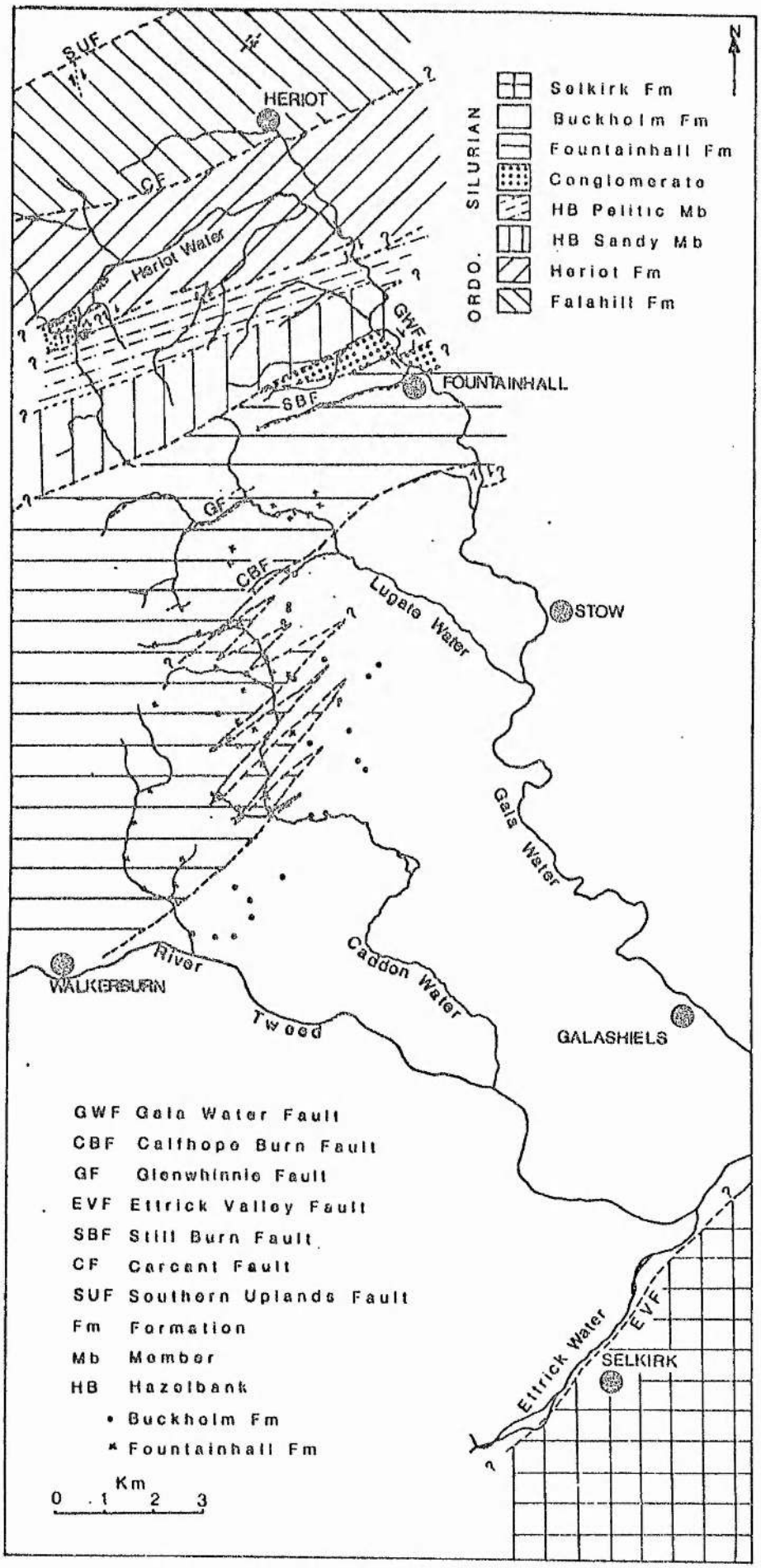

Shales (Chapter 4) are exposed. These are very tightly folded (see Appendix No. 7.2, for the style and type of folds).

STILL BURN FAULT: This fault runs along the entire length of the Still Burn [NS 428 493] to [NS 402 484], which is roughly parallel to the regional strike. Black shales representing the Lower Birkhill Shales again are exposed in the burn. These are highly distorted, sheared and display tight , asymmetrical folding with overturning of limbs facing NW, and NW facing monoclinal limbs. The exposures in the burn are not adequate either to reveal the nature and trend of movement or to show any evidence of imbrication. The black shales are exposed in several localities along the burn, and are consistent in being highly friable and sheared. This fault is within the Fountainhall Formation.

CALFHOPE BURN FAULT: This fault constitutes the boundary between the Fountainhall and Buckholm Formations, and determines the course of the Calfhope Burn between [NS 413 407] and [NS 399 401]. Its course can be traced westwards up to the high reaches of Ewes Water, where it is represented by two brecciated zones up to 1 m thick and about 50 m apart, cutting across the burn. These faults are associated with intensely weathered, highly sheared and broken, dark brownish grey and khaki siltstones, mudstones and silty shales of the sedgwickii or maximus Zones (Upper Birkhill Shales). Eastwards the fault probably coincides with the stream to the west of Pirn Knowe Lodge near Torquhan between [NS 432 474]

and [NS 431 473]. Greywackes at this locality are highly sheared and broken, though shales are not exposed.

GLENWHINNIE FAULT: This fault is named after Glenwhinnie Hill, SE of which, in the Lugate Water at [NS 395 466] a fault zone about 15 m wide is associated with dark grey siltstones and silty shales yielding a gregarius Zone fauna (Lower Birkhill Shales; Peach and Horne 1899). The fault marks the boundary between the pelite-dominated, lower levels of the Fountainhall Formation to the NW, and thickly-bedded, greywacke to the SE. A series of minor faults having steep NW hades forms the fault zone. These faults have imbricated the exposed siltstones and shales (Plate 7.3). The major fault plane is curved and dips NW under the imbricate faults; the dip steepens upwards from 15° up to almost vertical. The major fault is thus a listric fault (Plate 7.3) and the imbricate faults can be inferred to arise from it as a sole (cf. Cook 1976). Though the scale of the fault is small, on a scale of metres, its listric geometry reflects what has been observed in the major thrusts of the Fleet area (Cook 1976). In these, the geometry is on the scale of kilometres.

Although evidently a major strike fault, the Glenwhinnie Fault resembles the Still Burn Fault in being intraformational.

ETTRICK VALLEY FAULT: The contact between the Selkirk Formation and Buckholm Formation lines up with the known

Plate 7.3: Section of Glenwhinnie fault zone [NS 395 466] showing the curved fault plane and the steep imbricate faults above.

Plate 7.4: Steeply dipping strike faults in Hazelbank Quarry.

outcrop of the Ettrick Valley Thrust to the SW. No direct evidence of faulting is available from exposure within the Gala area, nor are black shales found along the contact between the two formations. The thrust in its known outcrop separates lateral correlatives of the Buckholm and Selkirk Formations, and is considered to extend northeastwards into the present area to separate the two formations. The lack of black shale occurrences contrasts with the type area in the Ettrick Valley (cf. Toghill 1970); though this lack may relate partly to a sparseness of exposure impressive enough even by Southern Uplands standards, it is equally likely to reflect a northeastwards descent of the tectonic profile and exposure of the higher levels of large scale imbricate slices (cf. Fyfe & Weir 1976; Webb 1983).

7.3.2 Wrench Faults

GALA WATER FAULT: The Gala Water follows, at least in part, the course of a major dextral fault which is clearly exposed N of Fountainhall. A thick conglomerate horizon cropping out within Dyker Law Plantation [NS 421 501] immediately W of Gala Water is displaced southwards to appear in the railway cutting near Allen Haugh [NS 435 495], E of Gala Water (Fig. 2.1, Chapter 2). The displacement of the fault is estimated as nearly 800 m.

Apart from above major wrench faults, several streams including especially Sit Burn at [NS 397 476], Ewes Water

between [NS 384 459] and [384 446], and an unnamed stream [NS 397 565] to E of Falahill Cottage, coincide with dextral displacements both of strata and of strike faults. Ladyside Burn between [NS 363 503] and [NS 367 486] and Whitelaw Cleugh between [NS 383 556] and [NS 364 553], coincide with the N-S alignment of the complementary sinistral displacements. The sense of movement is confirmed by small scale drag-folds. The movements involved in these cases are small though tectonically significant, ranging from 1.5 to 5 m.

7.4 ANALYSIS OF FAULTS

About 179 major and minor faults were recorded and classified (Appendix No. 7.3). The recorded data include attitude of fault planes, pitch of slickensides and apparent sense of movement if observable.

7.4.1 Attitude of Fault Planes

Poles to 179 fault planes (Fig. 7.3a) indicate a group of maxima in the NW and SE quadrants, the dip of which ranges from 75° to vertical. Though these faults show considerable variations in the azimuths of strike ranging from N. 30 E. to N. 60 E., they come sufficiently close to the range as to warrant classification as strike faults. Other maxima to NE, EW, SSE and SSW represent dextral wrenches, sinistral wrenches, northerly dipping strike faults and thrusts respectively. It is noteworthy that there is a considerable

difference between the strike of the north-dipping and south-dipping strike faults.

7.4.2 Pitch of Slickensides

On the basis of pitch of slickensides the faults can be divided into three main categories (Williams 1958): a) dip slips (including thrusts and reverse faults): b) oblique slips: and c) strike slips (wrenches).

a) Dip Slips

These includes faults in which the slickensides make an angle of 90° to the strike of the fault plane (Fig. 7.3b). A prominent maximum in the SE quadrant near the centre indicates that the slickensides mostly plunge very steeply to SE dispersing towards a small number with NW plunges of around 40°. The modal strike ranges between N. 40-50 E. This shows that the maximum stress direction σ_1 (taken perpendicular to modal strike of the fault planes) is N. 130-140 E., and is considered as horizontal.

b) Oblique Slips

Faults in which the pitch of slickensides ranges between $30\text{-}89^{\circ}$ are classified as oblique slips (Williams 1958; Fig. 7.3d). Weak (5%) maxima occur in the NE and SW quadrant, within two discrete fields widely dispersed in two opposed

great circles. Williams (1958) argues that slickensides pitching obliquely to the strike of the fault planes represent a planar swing of the intermediate σ_2 and minimum stress axes σ_3 about a horizontal maximum stress axis σ_1. This proposition appears less applicable to the Gala area on account of the wide dispersal of the poles. It is more plausible that obliquity is related to late-stage rotation of the early thrusts to steep angles (See section 7.3.1 and structural profile, Fig. 7.4), and dispersed due to the lack of (and loss of) parallelism on rotation (cf. Rust 1965a). A plot of slickenside plunges observed in the strike faults shows that in spite of the dip slip movements, strike slips and oblique slips have also taken place. Rust (1965a) concludes that strike faults moving initially as dip slips were re-activated by subsequent movements. It seams likely that re-activation occurred under most of the subsequent stress systems. Although great diversity of the pitch of slickensides within all trends of faults in the Gala area is evident, the fault planes show not more than one set of slickensides.

c) Strike Slips (Wrenches)

This group of faults includes those in which the pitch of slickensides ranges between 0-29° (Williams 1958; Fig. 7.3c). There are two main wrench fault groups: i) 1st order sinistral faults with a modal azimuth of 05°, dipping vertically; ii) 1st order dextral faults with a modal azimuth

of 135°, dipping 80° SW to vertical (Fig. 7.3a). These azimuths indicate an orientation of σ_1 as 150°, a clockwise rotation of about 15° as compared with σ_1 for the strike faults. As with the strike faults, the wrench faults also display re-activation showing an oblique sense of subsequent movement.

Comparison of the trends of faults and the plots of the plunges of slickensides with other areas of the Southern Uplands (Williams 1958; Weir 1968; Rust 1965a; Floyd 1975), confirm that the orientation of the stress axes is essentially comparable throughout the area.

7.5 STRUCTURAL PROFILE

The structural profile of the area (Fig. 7.5) is based on the attitude of bedding planes and 'way up' criteria in widely scattered and discontinuous outcrops, and shows that to SE of the area (the Selkirk Formation and part of the Buckholm Formation) the folds verge SE (Plate 7.1), displaying no overturning. In the northern part of the Buckholm Formation, by contrast, the vergence is opposite. Further northwestwards, although the Buckholm Formation is very poorly exposed, irregularity of the attitude and inconsistency in younging directions suggests shearing and imbrication of the strata. Still further north, the Fountainhall Formation is cut by a series of three major strike faults; the Calfhope Burn Fault, the Glenwhinnie Fault and the Still Burn Fault.

Fig. 7.5: Schematic structural profile across the Gala area

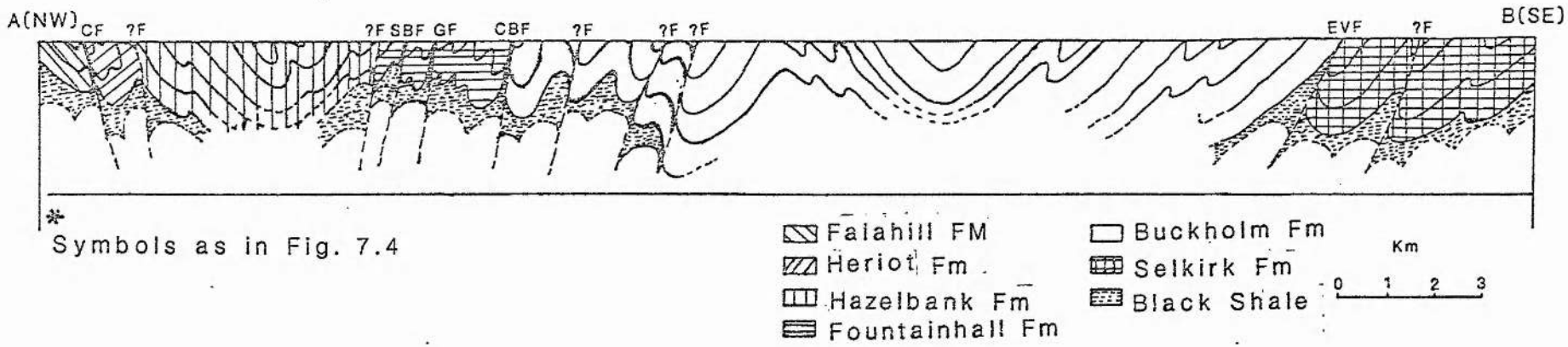

* Symbols as in Fig. 7.4

The strata within these faults show close to tight and asymmetrical folds verging SE, with overturning of the SE limbs. The fault planes show a progressive change in the attitude from SE to NW. The Ettrick Valley Thrust and the postulated minor imbricate fault are interpreted to have NW hades. The group of faults centred on the Calfhope Burn Fault displays NW hades which become steeper in northwestward succession, whilst the Carcant Fault reverses the hade. This progressive steepening and ultimate reversal of th hade may be ascribed to overturning of an erstwhile northwesterly hade, again mplying continuity of deformation (Eales 1979). Such progressive steepening and ultimate overturning would equally offset fold axial surfaces. Certain of the strike faults, e.g. the Carcant Fault, the Still Burn Fault, the Glenwhinnie Fault and the Calfhope Burn Fault, are associated with outcrops of pelagic and hemipelagic Moffat Shales. Webb (1983) observes that there is a direct relationship between the widths of the imbricate slices and the dominant thicknesses of the beds forming the packages. Raising of the structural profile and exposure of slices of Moffat Shales appears to be associated with short and therefore closely packed imbricate slices, i.e. with successions dominated by thin beds and pelitic sequences. This appears to be the case in the Gala area, in which Moffat Shale outcrops are associated especially with the Fountainhall, Hazelbank and Heriot Formations, whilst the thickly-bedded Buckholm Formation lacks such occurrences.

7.6 HISTORY OF DEFORMATION

It has been observed in Ewes Water [NS 384 447], Sit Burn [NS 399 535] and the road cutting near Hazelbank Quarry [NS 424 506] that the strike faults have been cut and displaced by wrench faults, indicating that wrench faults belong to a late stage of deformation. Eales (1979) suggests that, as part of a continuum of shortening, the major strike faults originated as shallow-dipping thrusts and shared in the overall rotation and steepening. The F_1 folds of Rust (1965) were coeval with the thrusts and were likewise rotated and modified by F_2. On this basis it seams likely that the Caledonian deformation took place in following steps:

1) Initiation of folding and early thrusts.
2) Subsequent rotation of folds and steepening of thrusts.
3) Re-activation of faults by subsequent movements probably in association with 'wrench' phase - variations in stress azimuths.

All the above structures are considered to have been formed under comparable stress conditions, with σ_1 orientated NNW-SSE throughout, though inherently variable within limits.

7.7 CONCLUSIONS

The structural pattern is consistent with that of other areas of the Southern Uplands, i.e in displaying variable

sequences, mainly of turbidites, deformed initially by a D_1 phase of folding and thrusting, steepened and further modified with a culmination in a wrench-fault phase.

The prevalence of imbrication in association with major strike fault zones, bounding formations of markedly contrasting characteristics which become successively younger to the SE against a dominantly northeastward younging, might be considered to support the Lower Palaeozoic accretionary prism model of McKerrow et al. (1977) for the Southern Uplands as a whole. But systematic steepening of dips and overturning of axial surfaces was not clearly found.

8. METAMORPHISM AND MINERAL CHEMISTRY

This chapter deals with the metamorphic history of the succession following deposition, in relation to the Caledonian deformation, and the mineral chemistry. The following techniques were employed:

a) Optical petrography
b) XRD analyses of the clay fraction of the greywacke matrix
c) Arising from b), assessment of illite crystallinity
d) Mineral chemistry (electron microprobe analyses)

8.1 OPTICAL PETROGRAPHY

Thin section studies of the greywackes show that most belong to the lithic type of Pettijohn (1957), (Fig. 3.3b; Chapter 3), with a range between feldspathic and quartzose (silicic). A chlorite - illite - albite matrix is characteristic of the silicic formations (Buckholm, Heriot, and Fountainhall Formations), with secondary carbonate prominent in the Selkirk Formation. Chlorite - illite - prehnite - albite and chlorite - illite - pumpellyite - albite assemblages are typical of the 'basic clast' formations (Falahill and Hazelbank Formations). The matrix content is always notably high (>15%). Veins are commonly present and are extensively developed near zones of intense deformation, showing more than one phase of deformation by cross-cutting relationship. Most are only a few mm wide and are compositionally related to the matrix. In silicic greywackes

the veins consist mostly of quartz and calcite, locally accompanied by opaque minerals. The sequence of development of the minerals in the quartz-calcite veins (Plate 8.1) is as follows:

a) Crystallization of quartz.
b) Invasion of calcite, replacing quartz. Some isolated relicts of quartz crystals remain in a calcite groundmass show the same optical orientation.
c) Minor sulphide mineralization: incoming of pyrite replacing quartz and calcite equally.

The same sequence of diagenetic events is also evident in the host greywackes (Plate 8.2); calcite commonly replaces feldspars and other susceptible minerals including quartz, especially in the calcite-rich Selkirk Formation. Other fine grained detrital components in the matrix are also replaced.

The 'basic clast' greywackes (the Falahill and Hazelbank Formations) are relatively richer in matrix (Fig. 3.3; Chapter 3), and show a correspondingly extensive development of phyllosilicates (chlorite and illite), and grain boundaries tend to be correspondingly more diffuse. Corroded boundaries of quartz are apparent in thin sections (Plate 3.1). Prehnite and pumpellyite are largely confined to veins, rarely occurring as groundmass components. Crystals of these minerals tend to grow oblique to vein walls. In the Falahill Formation, prehnite is also seen to have developed within flakes of white mica

Plate 8.1: Photomicrograph of greywacke from Falahill Formation showing diagenetic history of veins; calcite replacing quartz and pyrite replacing both quartz and calcite, X100, cross polars.

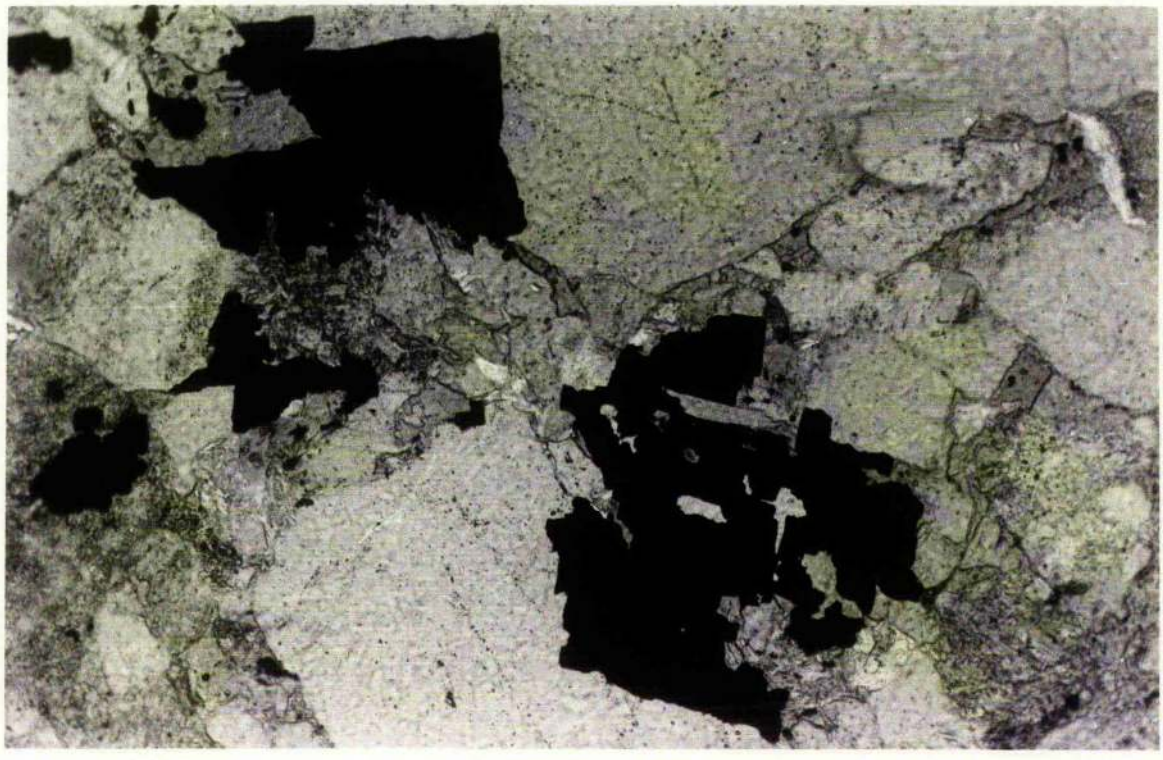

Plate 8.2: Photomicrograph of greywacke from Falahill Formation showing pyrite replacing matrix and detrital grains alike, X100, plane polarized light.

(phengite). Prehnite grows perpendicularly to the basal cleavage, disrupting the mica flakes (Plates 8.3-8.4; Appendix 8.15). In other contexts (Oliver and Leggett 1980; Oliver et al. 1984; Hepworth 1981) metamorphism and deformation are considered to have occurred synchronously. The textural similarity to the other areas of the Southern Uplands suggests that the same relationship holds good for the Falahill Formation.

8.2 XRD ANALYSES OF GREYWACKE MATRIX

The clay fraction of the greywacke matrix was separated according to the procedures described in Appendix 8.2 and prepared as:

a) dry (untreated), orientated mounts
b) Ethylene glycolated mounts
c) HCl treated mounts
d) Heated mounts
e) Dimethylsulphoxide (DMSO) treated mounts

Peak positions on diffraction charts were determined using quartz as an internal standard, and the minerals identified using the ASTM card index system (Berry et al. 1974).

8.2.1 Mineral Assemblages

The mineral assemblages identified by XRD are quartz, albite, 10 Å mica, chlorite, calcite and kaolinite.

Plate 8.3: Photomicrograph of greywacke from Fountainhall Formation showing prehnite growing within mica flakes causing disruption of mica flakes, X100, cross polars.

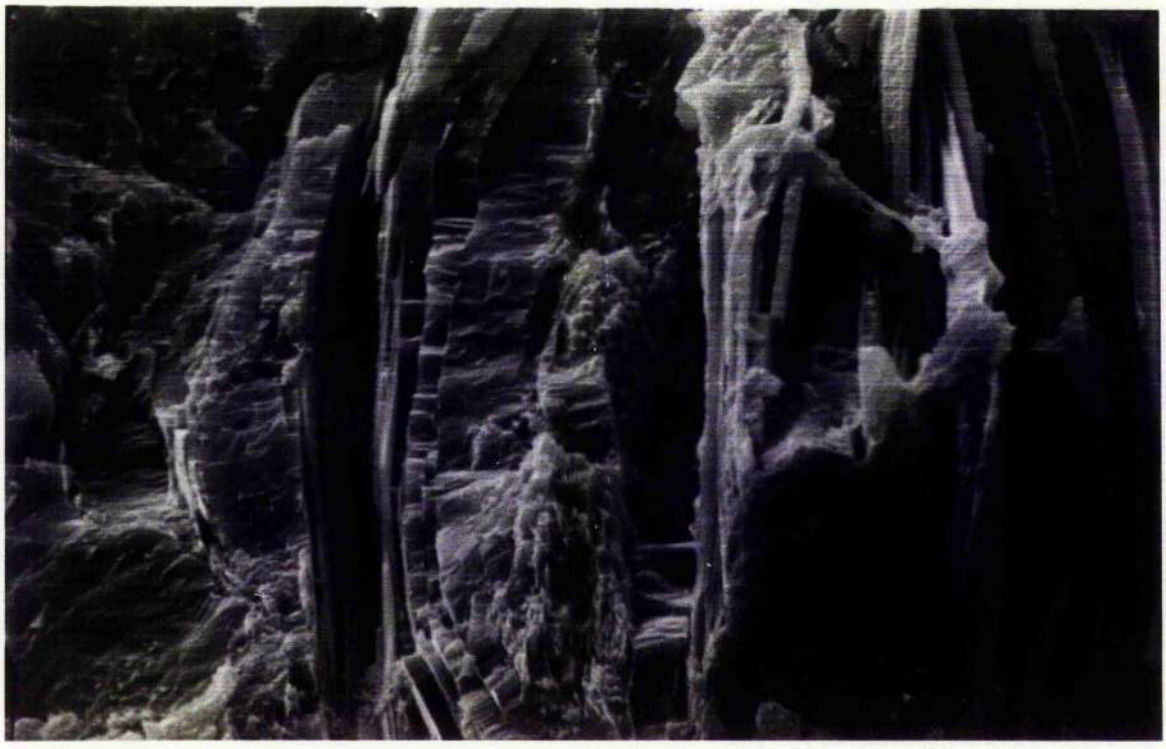

Plate 8.4: Scanning electron photomicrograph showing growth of prehnite within mica flakes.

10 Å Mica:

Strong peaks at 10 Å and 5 Å are attributed to the basal reflections [001] and [002] of white mica (M, Fig. 8.1 and 8.2). Most of the 10 Å peaks are asymmetrical towards low angles with the foot of the asymmetry situated at ~10.64 Å. Treatment with ethylene glycol (Fig. 8.1, 8.2) usually produces peak enhancement accompanied by a very slight increase in basal spacing though not enough to justify classification as smectite. The persistence of the [002] reflection after heat treatment confirms that the mineral is illite (Fig. 8.1, 8.2). Analyses of representative samples from the formations (Appendix 8.6) show that d(001) spacings range from 9.93 to 10.66 Å about a mean of 10.04 Å. This is larger than values previously reported by Hepworth (1981) for the Abington area (X = 9.988 Å), while values comparable with the Gala area have been reported by Watson (1976) for mudstones of Dob's Linn and Hartfell, Moffat, probably transitional between low anchezone and diagenetic (X = 10.01 and 10.04 Å respectively).

bo spacing: It has been found (Cipriani et al. 1968) that the measured peak position of d[060] is directly related to the bo parameter of the crystal lattice, i.e bo=d[010], which is dependent on the chemical composition of the octahedral layer. Values of d[060]~1.50 Å, bo~9.00 Å indicate dioctahedral micas. Parameter bo also permits distinction between muscovite and phengites. Substitution of Fe and Mg for Al in the octahedral

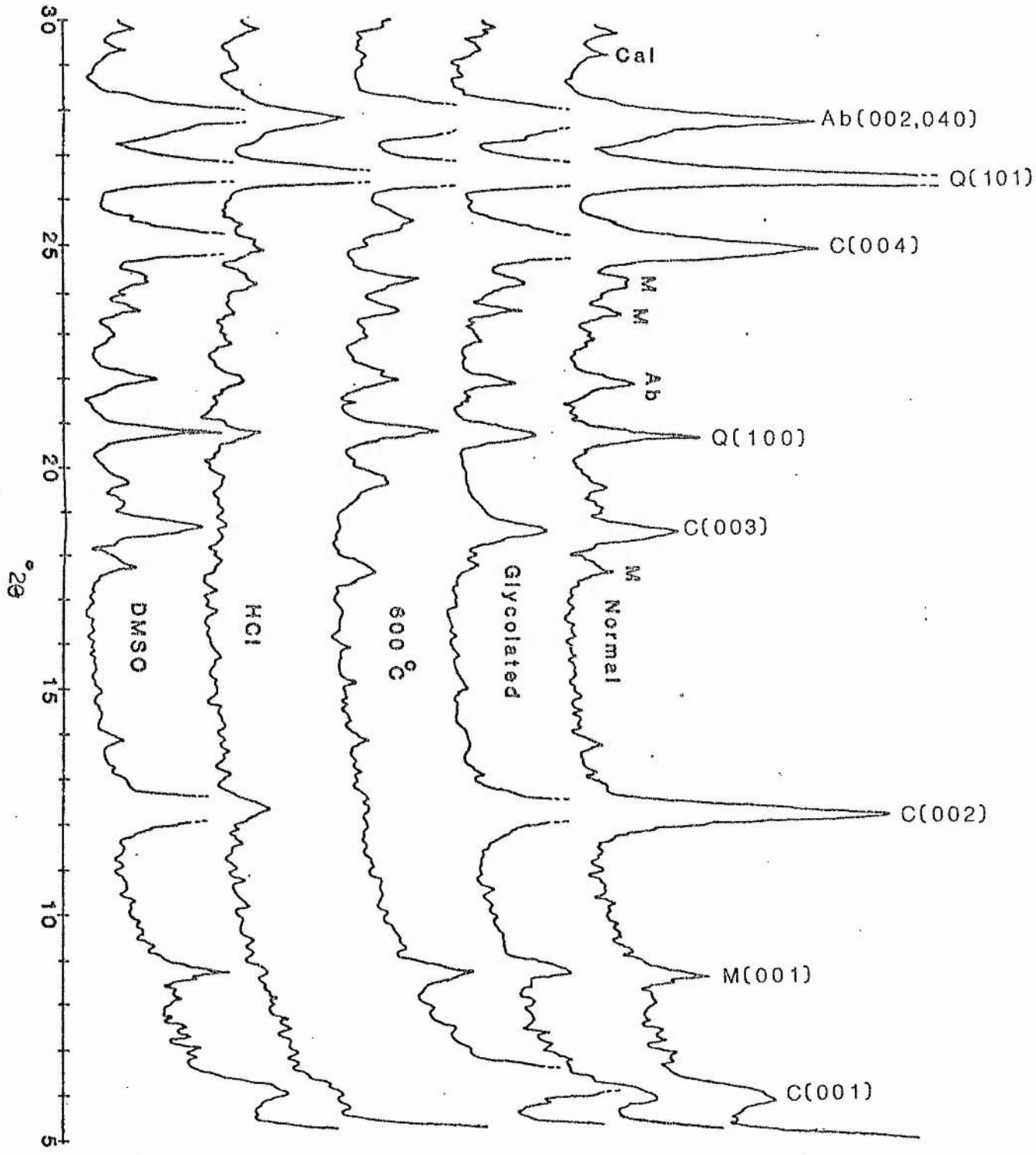

Fig. 8.1: XRD. scans of clay fraction of greywacke matrix showing effects of different treatments on clay minerals.

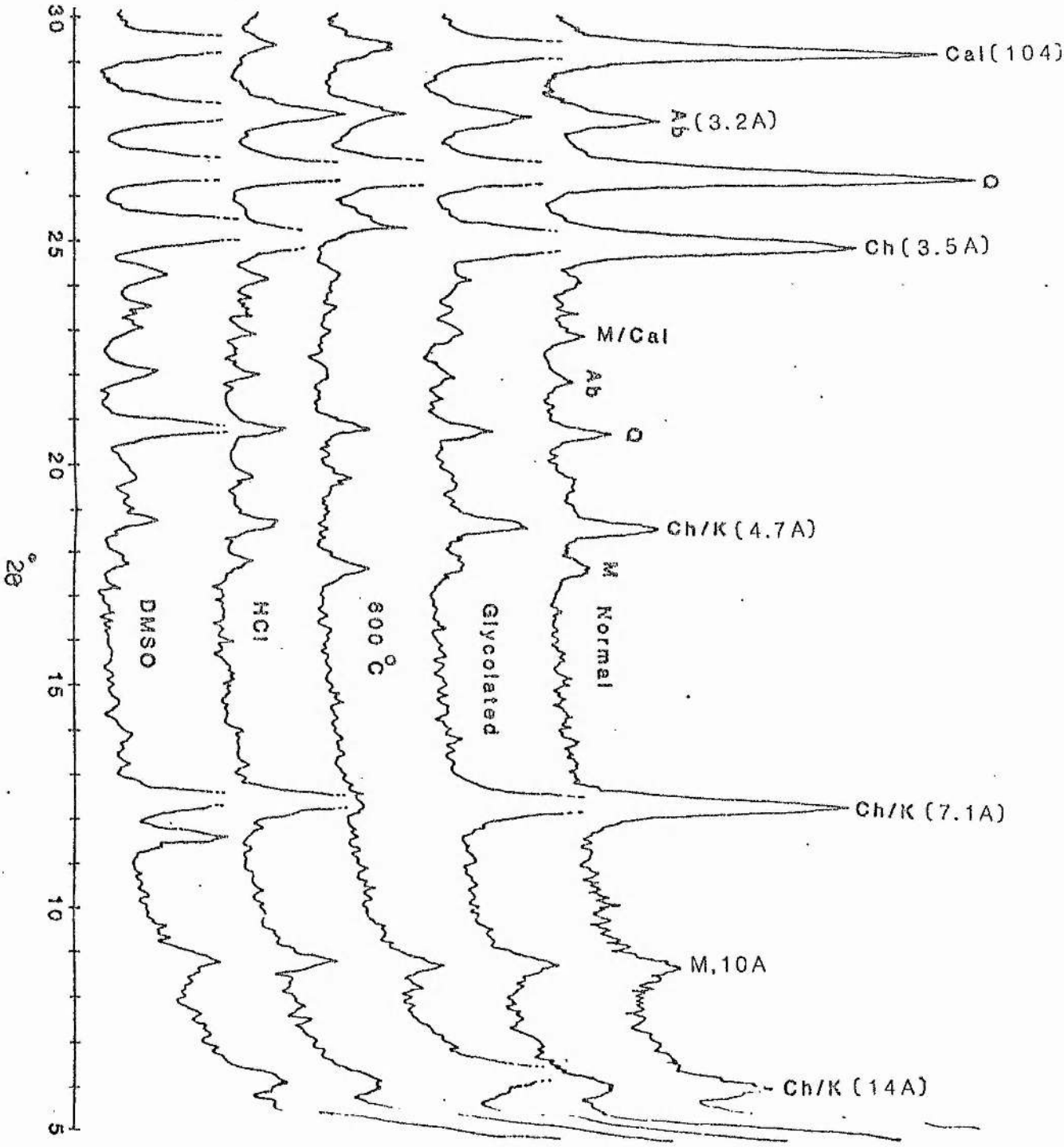

Fig. 8.2: XRD. scans of clay fraction of greywacke matrix showing effects of different treatments on clay minerals.

sites expands the lattice, bo being greater in phengites than in muscovites (Cipriani et al. 1968). In the greywackes of the Gala area, bo values range between 9.009 and 9.060 Å (Appendix 8.6), with a median of 9.032 and mode between 9.04 and 9.05 Å (Fig. 8.2). The bo parameter of white micas have been used as an indicator of relative geobarometry accompanying low grade metamorphism (Sassi and Scolari 1974; Padan et al. 1982). Such estimates have also been carried out elsewhere in the Southern Uplands (Hepworth 1981; Oliver et al. 1984). Values estimated in the Gala area closely correspond to them (Fig. 8.3).

Chlorite

The presence of chlorite is confirmed by strong reflections at 14 Å [001], 7 Å [002], 4.7 Å [003] and 3.5 Å [004] (Fig. 8.1; Appendix 8.7). The d-spacings were not effected by ethylene glycol treatment. Heat treatment enhances the 14 Å [001] reflection whilst causing the collapse of the 7 Å and 4.7 Å peaks and the depression of 3.5 Å peak (Fig. 8.1). This effect probably relates to the presence of unstable interlayer spaces in the chlorite lattice (?Mg-vermiculite; Thorez 1976). Some samples (Appendix 8.7), particularly those from the Selkirk Formation, show neither any change in their 14 Å reflection after HCl treatment, nor collapse after heat treatment, suggesting the coexistence of kaolinite, while in most other cases the [001], [002], [003], and [004] reflections of chlorite collapse after the HCl treatment confirming the presence of chlorite only. The even-order basal reflections [002] and [004] are always very

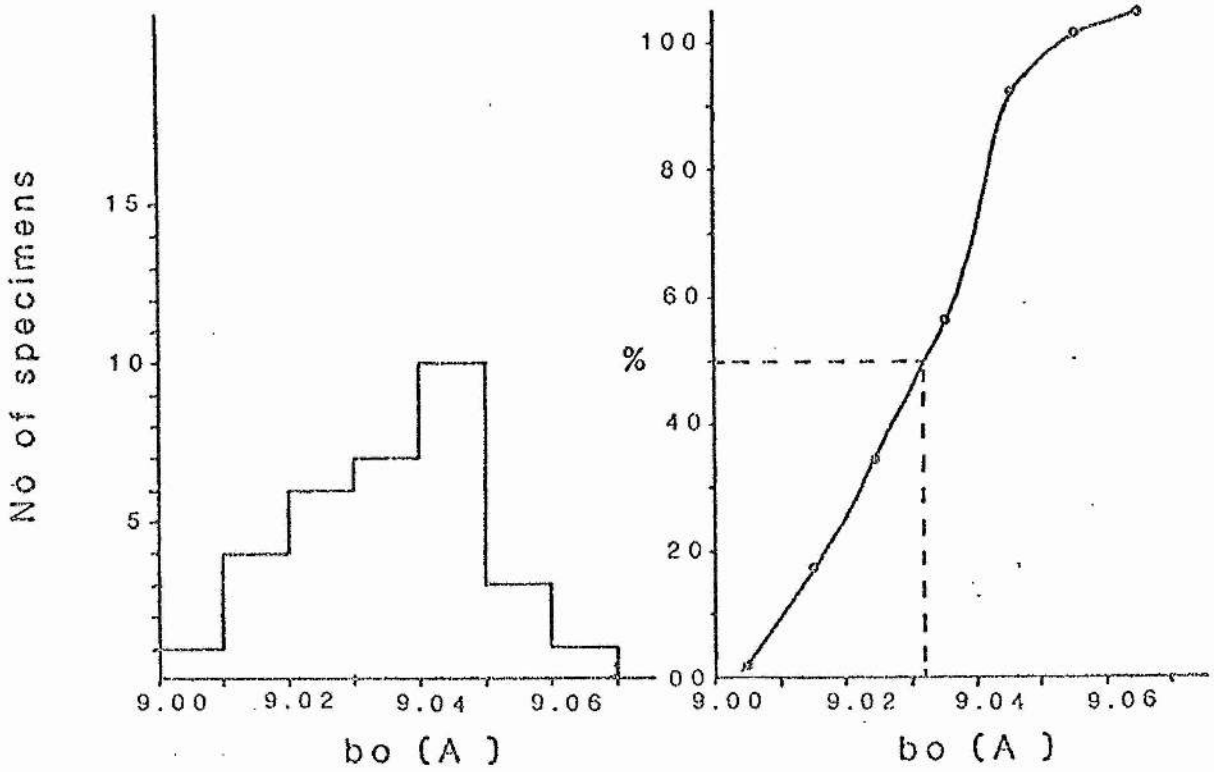

Fig. 8.3: Histogram and cumulative curve of bo values of illite.

strong, [002] being the strongest. This characteristic has been attributed to richness in iron (Hepworth 1981, and references cited therein). However, microprobe analyses show that 19 out of 31 from the Gala area (Appendix 8.7) and 9 out of 14 in the Abington area (Hepworth 1981) are strongly magnesian. Moreover, the probe analyses demonstrate that even within the same thin section, the composition of chlorite ranges from Mg-rich to Fe-rich (Appendix 8.7). The dioctahedral chlorites typically have more intense [003] reflections and retain their [002] peaks after heat treatment. Lack of these characters in the studied samples implies that trioctahedral chlorite is dominant.

Kaolinite

It was found that almost in all specimens from the Selkirk Formation, and in several from other formations (Fig. 8.2, Appendix 8.7), that [001] reflections are enhanced and the the remaining reflections are not affected by the HCl treatment, other than [004] which is slightly depressed. Heat treatment causes the enhancement of 14 Å peak and collapse of other peaks (3.55, 4.7 and 7.15 Å), suggesting the presence of kaolinite in coexistence with chlorite. DMSO treatment confirms the presence of kaolinite by shifting its 7.15 Å reflection to 7.5 Å position, while the 7.15 Å reflection for chlorite remains uneffected (Fig. 8.2; Appendix 8.7).

Calcite

Calcite is detected by the presence of its 3 Å [104] and 3.85 Å [102] reflections (Fig. 8.1, 8.2). These reflections are present in all the samples analysed, but 3 Å is the strongest (R.I. up to 100%) in the Selkirk Formation. The collapse of both peaks after HCl treatment confirms them as calcite.

Albite

The presence of 3.2 Å, 4 Å and 3.7 Å peaks in diffractograms of all samples (Fig. 8.1) correspond to the [001], [201] and [130] faces of albite respectively.

8.2.2 Illite Crystallinity

Illite crystallinity (IC) has been extensively used in recent years as a quantitative parameter to measure the degree of advancement of burial diagenesis or anchimetamorphism (Kubler 1967a; Dunoyer de Segonzac 1970; Frey 1970; Weber 1972; Kisch 1978). With increasing incipient metamorphism, the crystallite size increases concurrently with the progressive removal of expandable mixed layer clay minerals, the X-ray diffraction peaks of the 10 Å mica (illite, [001]) reflecting this change by becoming narrower. This effect corresponds to the loss of interlayer water, the absorption and fixing of potassium between the layers and the rearrangement of ions within the layers (Dunoyer de Segonzac 1970). In addition to temperature, the degree of crystallinity depends on initial chemical composition, hydrostatic pressure and chemical composition of the interstitial

water (Dunoyer de Segonzac 1970). The following two methods have been used to quantify the illite crystallinity:

a) Kubler index

This method involves the measurement of the width (mm or in 2θ) of the illite [001] peak at half peak height (L1/2h) above the background radiation (Kubler 1964, 1968; Kisch 1978).

IC = (L1/2h)

b) Weber index

Weber (1972) modified Kubler's method by defining (Hbrel) as the ratio of the width of illite [001] peak at half peak height above the background radiation to that of an external standard (quartz, [100]).

Both indices were determined in the analysed samples. Untreated orientated samples were run five times in succession under specified XRD conditions (Appendix 8.4) followed by three runs of quartz [100] as an external standard. Widths of illite [001] peaks were measured exactly half way between the top of the peaks and the level of background radiation and their means determined in mm and 2θ. The mean width of the quartz [100] peak was then likewise determined and Hbrel calculated.

c) Illite crystallinity results

All illite crystallinity values (Appendix 8.5) lie within the anchizone, which is equivalent to the prehnite-pumpellyite facies of metamorphism (Esquevin 1969; Kisch 1974). IC values based on Hbrel are closely comparable with those of other areas of the Southern Uplands (cf. Oliver et al. 1984; Hepworth 1981; Fig. 8.4). It has been suggested (Oliver et al. 1984) that both illite crystallinity and increase systematically northwards (See section 8.3), an increase attributable either directly to the increasing amount of D_1 folding and cleavage formation northwards at constant P & T, or to the apparent increase in grade of metamorphism, folding and cleavage in progressively deeper levels of the accretionary pile (Leggett et al. 1979). On the contrary distribution of IC values in the Gala area (Fig. 8.4) do not show any progressive increase in the IC values which include a cross-strike distance of over 30 Km. This suggests that metamorphism may not be controlled by an accretionary process as suggested by Oliver et al. (1984) and Legett et al. (1979); deep burial of the southern parts of the blocks might be expected to result in a southward, as opposed to a northward, increase in metamorphic grade. Neither is observed within the area.

8.3 MINERAL CHEMISTRY

The chemistry of certain of the more complex minerals, and especially those belonging to isomorphous series, was determined using the energy dispersive electron microprobe at the Grant Institute of Geology, University of Edinburgh. Instrument

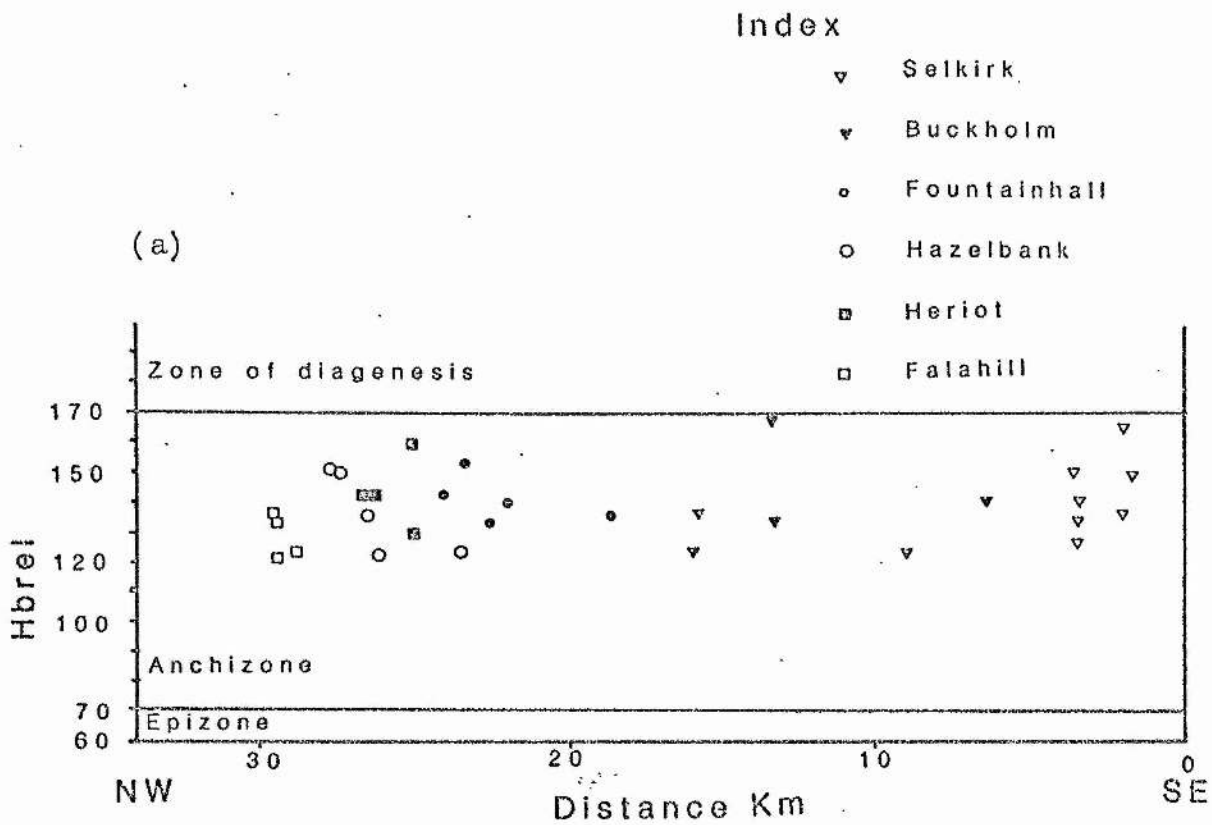

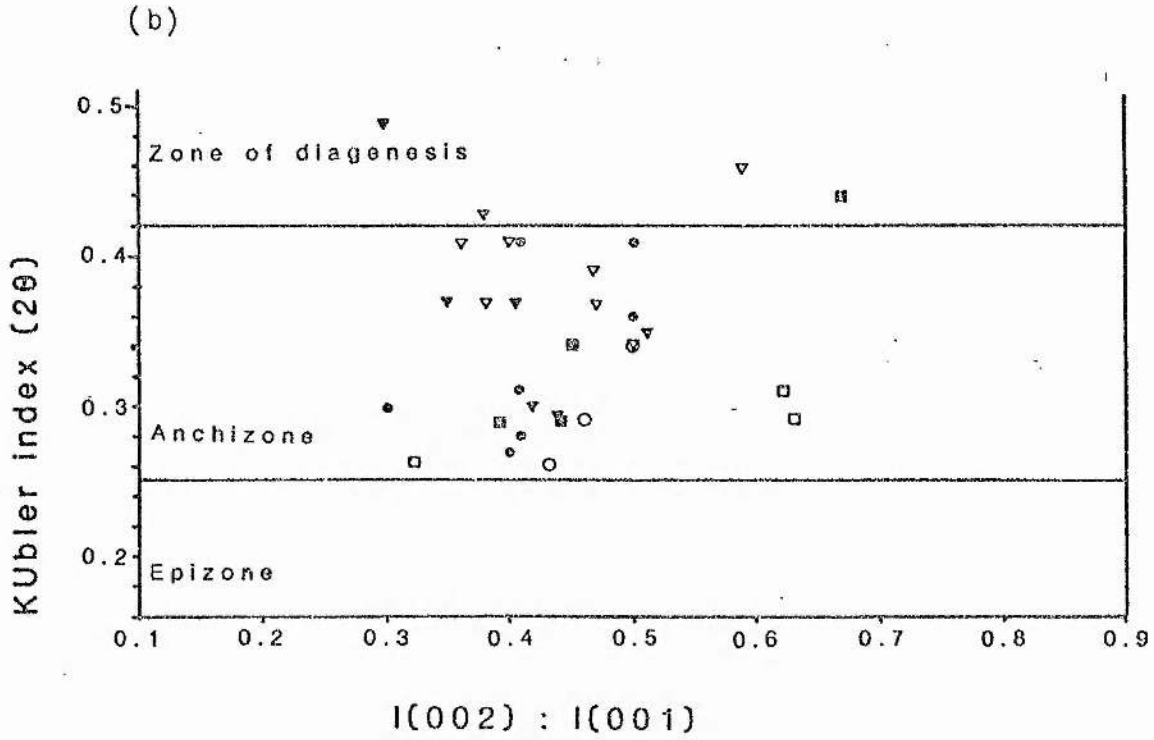

Fig. 8.4: Illite crystallinity results. (a) Hbrel values against the distance from SE extreme of the area. (b) Kubler index against the intensity ratio; I(002):I(001).

conditions are given in Appendix 8.19 results are given in Appendices 8.8 to 8.18.

8.3.1 Pumpellyite

Certain veins and localized patches of matrix display a spongy texture characteristic of pumpellyite aggregates, though pumpellyite could not be confirmed optically. Probe analyses show high levels of Ca, Al and Mg (Appendix 8.8) and are richer in Na_2O than the standard pumpellyite (Deer et al. 1965). This probably shows the presence of a soda rich mineral (presumably albite) in association with pumpellyite.

8.3.2 Prehnite

Analyses of the vein prehnite (1,2,3, Appendix. 8.9) and a single detrital prehnite (4, Appendix 8.9) and their Ca-Al-Fe plot (Fig. 8.5) show that they are comparable to prehnite found elsewhere in the Southern Uplands (Hepworth 1981; Oliver et al. 1984).

8.3.3 Chlorite

With a few exceptions, most of the chlorite analysed was in the groundmass. One detrital grain (Analysis 13, AK 336, Appendix 8.10), and one vermicular inclusion in a quartz grain (Analysis 15, AK 159, Appendix 8.10) were also analysed. The detrital chlorite falls within the sheridanite field while most

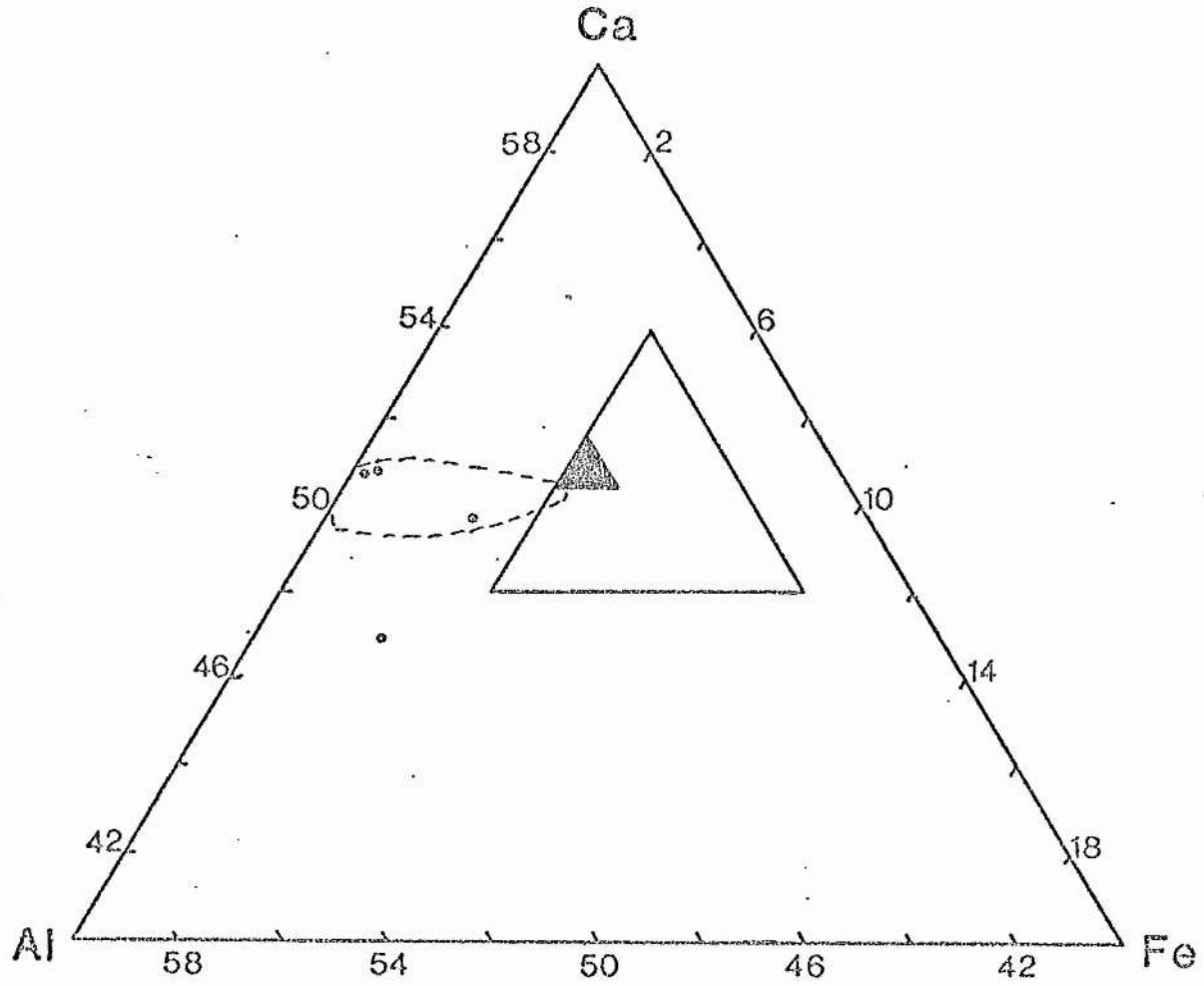

Fig. 8.5: Prehnite analyses; Al, Ca, Fe(tot) cation proportions.

of the groundmass chlorite ranges from ripidolite (mostly sub species aphrosiderite), through pycnochlorite to diabantite, with most falling within the pycnochlorite field (Fig. 8.6). A small proportion fits into the brungsvigite, penninite and talc-chlorite fields.

8.3.4 Plagioclase

Probe analyses of plagioclase grains distributed throughout the succession show that all are albite (Ab91 - Ab100) (Appendix. 8.11; Fig. 8.7). The analyses also include one plagioclase phenocryst in a spilite clast. The results are consistent with those for sandstones of the Elvan Formation of the Abington area (Hepworth 1981). These results confirm the XRD analyses (Fig. 8.1; Section 8.2.1).

8.3.5 Pyroxene

Detrital pyroxenes from the Falahill and Hazelbank Formations were analysed. Most (22 out of 26) are calcic augite two are salite and two diopsidic-augite (Appendix 8.12; Fig. 8.8). The pyroxenes of both formations presumably have been derived from a similar source rocks as their compositions are closely comparable. These pyroxenes are also comparable with the pyroxenes of the Elvan Formation of the Abington area (Hepworth 1981) but differ from the pyroxenes of the metadolerite of the Raven Gill Formation of Abington area (Hepworth 1981) and the Bail Hill Volcanic Group (McMurtry 1980a). It has been concluded

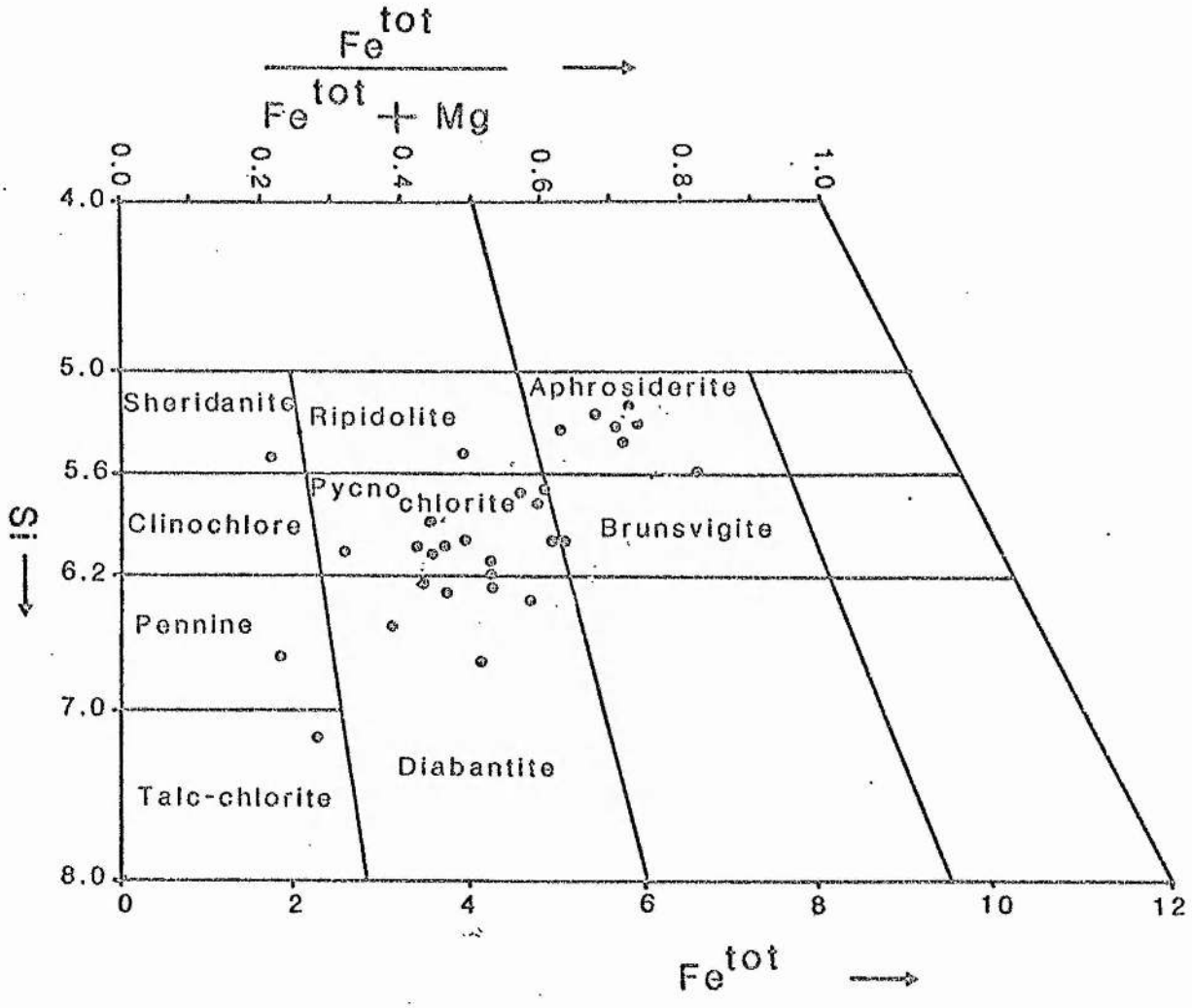

Fig. 8.6: Chlorite analyses; diagram after Hey (1954).

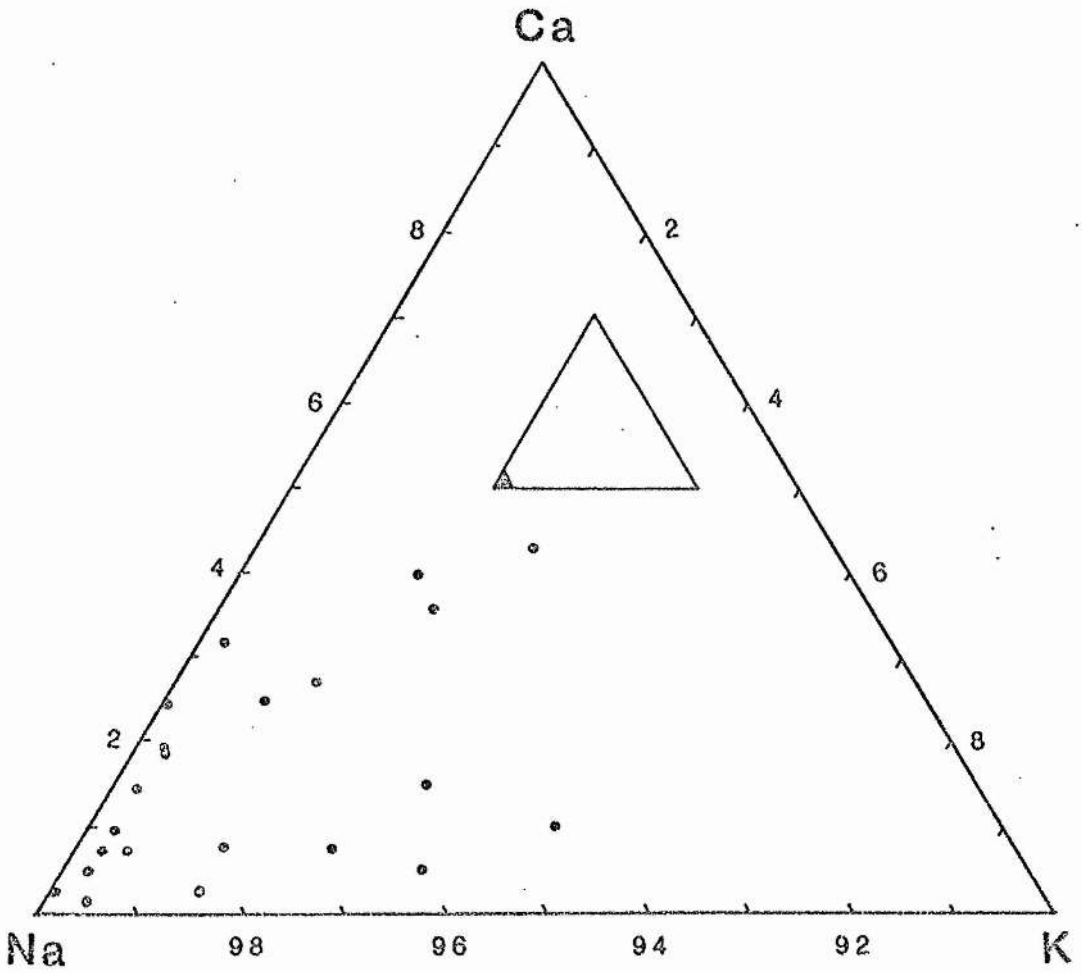

Fig. 8.7: Plagioclase analyses; Na, Ca, K cation proportions.

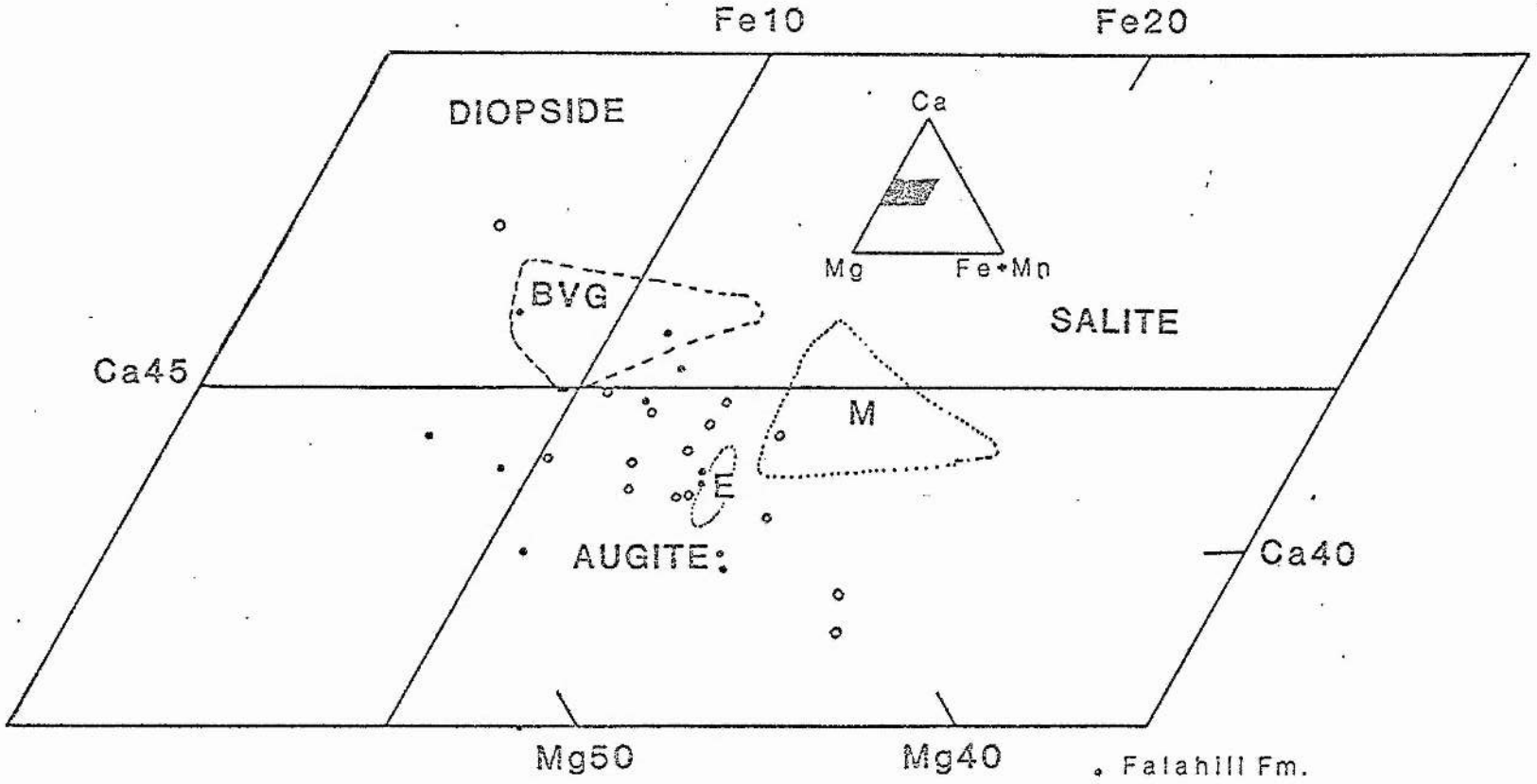

Fig. 8.8: Pyroxene analyses plotted on part of the pyroxene quardrilatral (inset) and comparison with other areas using the same numbering system.

that the Bail Hill Volcanics represent an alkali basalt of hawaiite-mugearite-trachyte series of an oceanic-island (seamount), which are also comparable to salites and Ca-rich augites of hypabasal rocks derived from alkali olivine basalt magmas, and from which high Al salites have been recorded.

The detrital pyroxenes of the Falahill and Hazelbank Formations of the Gala area are different from those of the Bail Hill Volcanic Group in two respects; a) textures of the grains, as no zoning was found as have frequently been observed in the pyroxenes of the of the Bail Hill Volcanic Group; b) non-alkaline nature of the pyroxenes (Fig. 8.9), (Nisbet & Pearce 1977; Le Bas 1962; Kushiro 1960). Covariation plots of TiO_2-Al_Z (Fig. 8.9b, after Le Bas 1962) of pyroxenes show that 22 out of 26 fall into the nonalkaline field. A plot of the discriminant functions, F1 & F2 [Fig. 8.9a; Appendix 8.12, after Nisbet & Pearce (1977)] suggest that the pyroxene may have been derived from a volcanic arc region. This suggestion is supported by the fact that in all the above plots the pyroxenes closely resemble the known volcanic arc basalt plots of Nisbet & Pearce (1977). Thus it can be concluded that the detrital pyroxenes of the Falahill and Hazelbank Formations are non-alkaline and have been derived from a source outside the depositional basin, most likely a volcanic arc.

8.3.6 Amphibole

The majority of the amphiboles (Appendix 8.13) were

(a)

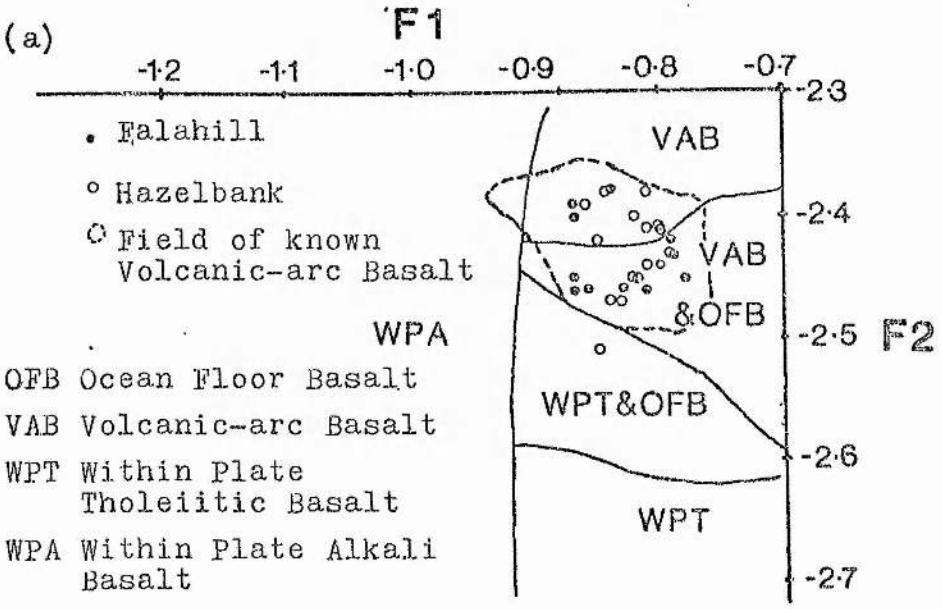

(b)

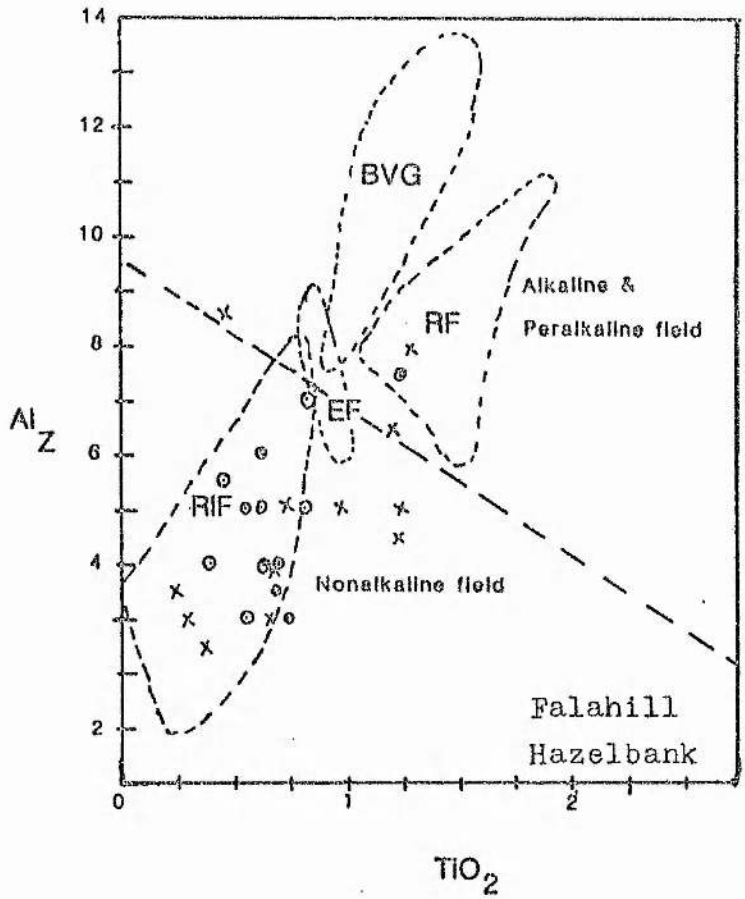

Fig. 8.9: Pyroxene analyses: (a) Plot of discriminant functions, F1 against F2 (after Nisbet & Pearce 1977). (b) Plot of Al_Z agaibst TiO_2 (after Le Bas 162);

BVG, Bail Hill Volcanic Group (McMurtry 1980), RF, Raven Gill Formation (metadolerite); EF, Elvan Formation, Abington area (Hepworth 1981); RIF, Red Island Formation, Longford-Down Inlier (Sanders & Morris 1977).

classified as calcic class B (Leake 1978), whilst only four out of 19 grains are of the calcic class A (Fig. 8.10). Three other analysed grains, considered to belong to the glaucophane group, were classified as calcic-sodic class A and B, and one again as calcic class B. The mineral species covered by these classifications include ferro-pargasitic hornblende, pargasite, ferroan-pargasite, edenite, edenitic hornblende, ferro-edenitic hornblende, actinolite hornblende and magnesio-hornblende. The majority of the amphiboles from the Gala area fall into the fields of ferroan-pargasite hornblende, pargasite and ferroan-pargasite and edenitic hornblende. Two grains were classified as magnesio-horblende and another two as actinolite-hornblende. One grain from the Falahill Formation is classified as magnesian-hastingsitic hornblende and one as ketophorite. The Al^{vi} - Na+K covariation plot (Fig. 8.11a; after Deer *et al.* 1965) show that most of the amphiboles are similar to pargasite-ferrohastingite and hornblende. Fe^{3+} ions were calculated using Papike's *et al.* (1974) charge balance equation.

A comparison with the amphiboles of the Elvan Formation (Hepworth 1981) show that the majority are, by contrast, calcic class A (Leake 1978), and none is either pargasitic, ferro-pargasitic hornblende or ferroan-pargasite. However, edenite-hornblende and magnesio-hornblende do occur. The primary magmatic amphiboles from the Bail Hill Volcanic Group (McMurtry 1980a) are mostly pargasites and ferroan-pargasites and as such are more comparable to amphiboles from the Falahill and Hazelbank

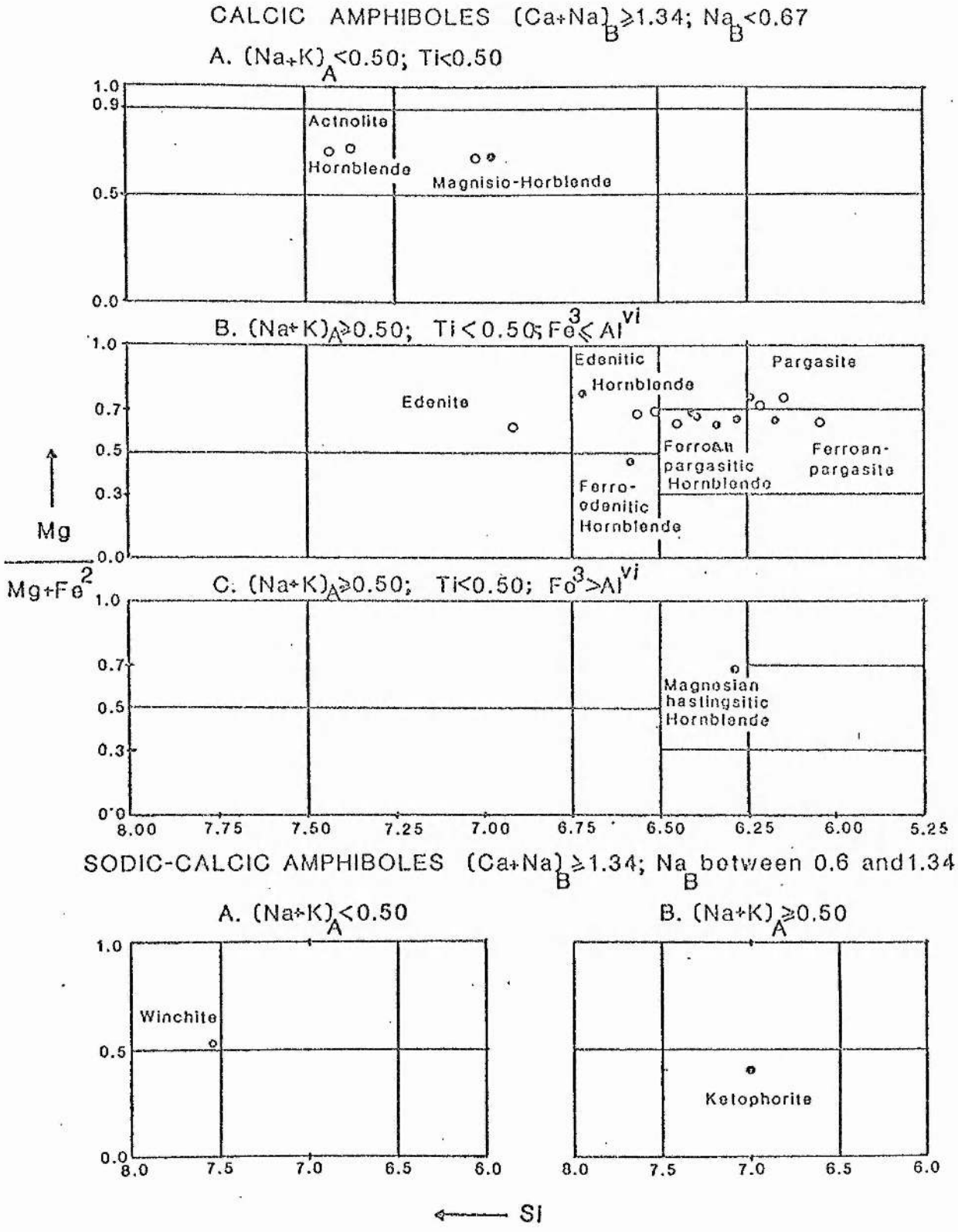

Fig. 8.10: Classification of amphiboles (after Leake 1978).

Formations. Magnesio-hornblende and ferroan - pargasitic - hornblende were also found with some components of the Ballantrae Complex (Spray and Williams 1980) and are closely comparable with the detrital hornblende of the Falahill and Hazelbank Formations.

8.3.7 Glaucophane

Only four grains of glaucophane were analysed (Appendix 8.14) and are classified as ferro-glaucophane (Leake 1978; Fig. 8.11b). Two optically comparable grains are calcic-sodic amphiboles, one in class A and one in Class B. The presence of glaucophane indicates a subduction complex in the source area (Ernst 1975).

8.3.8 White mica

Analyses of white mica (Appendix 8.15) show that both muscovite (tetrahedral Si:Al, less than 4:1) and phengites (tetrahedral Si:Al, more than 4:1) occur. It is also noticeable that the ratio of phengite to muscovite in the Falahill, Heriot and Hazelbank Formations is higher (7:5), while all five white micas analysed in the Buckholm, Fountainhall and Selkirk Formations were found to be muscovite (Appendix 8.15). A covariation plot of Al_2O_3 and Fe(tot) (Fig. 8.12a; after Miyashiro 1973, p.202) show that phengite falls into the field of the glaucophane-schist facies while muscovite enters the field of the chlorite, biotite and almandine zone. The Al-poor nature of

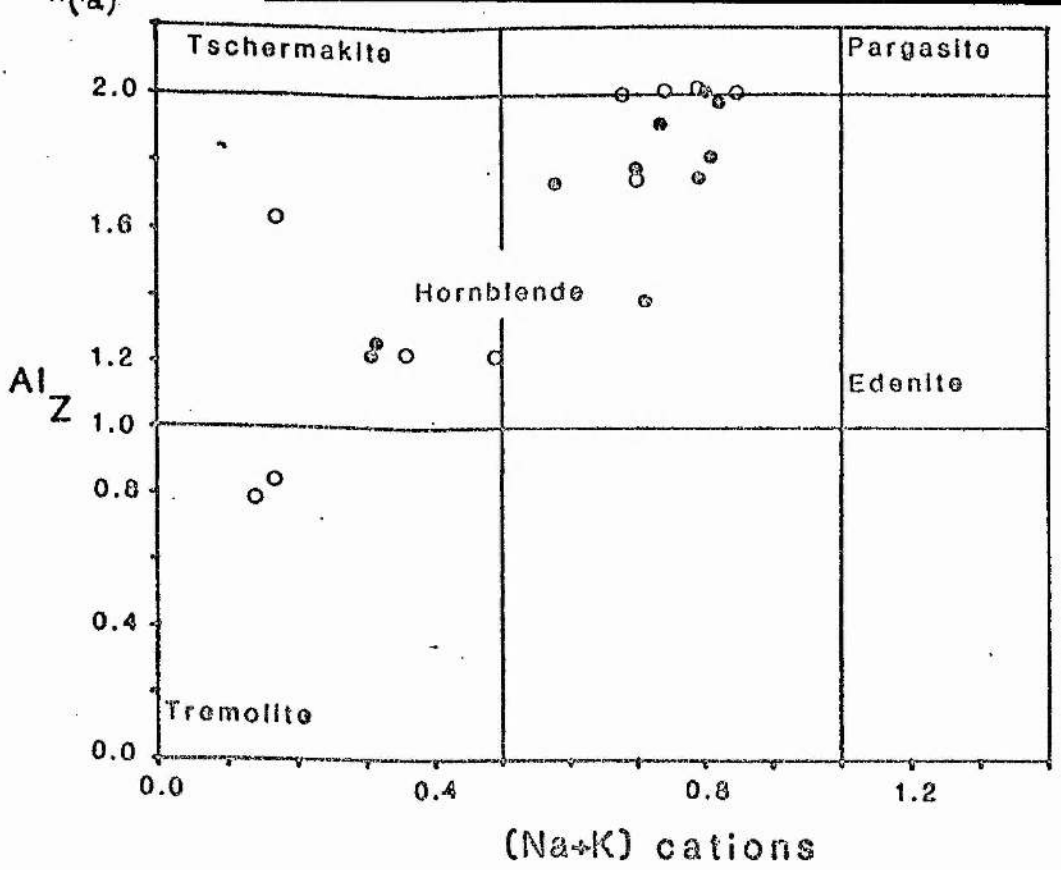

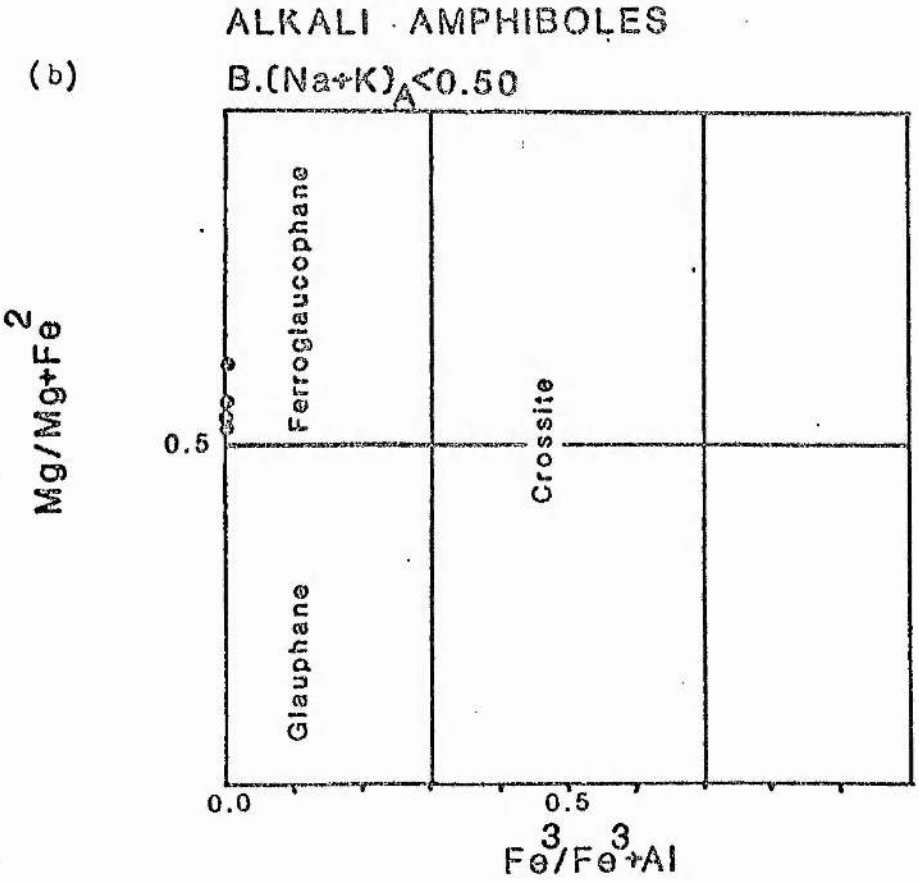

Fig. 8.11: Amphibole analyses. (a) Al_Z against (Na+K) (after Dear et al. 1965). (b) Classification of alkali amphiboles (after Leake 1978).

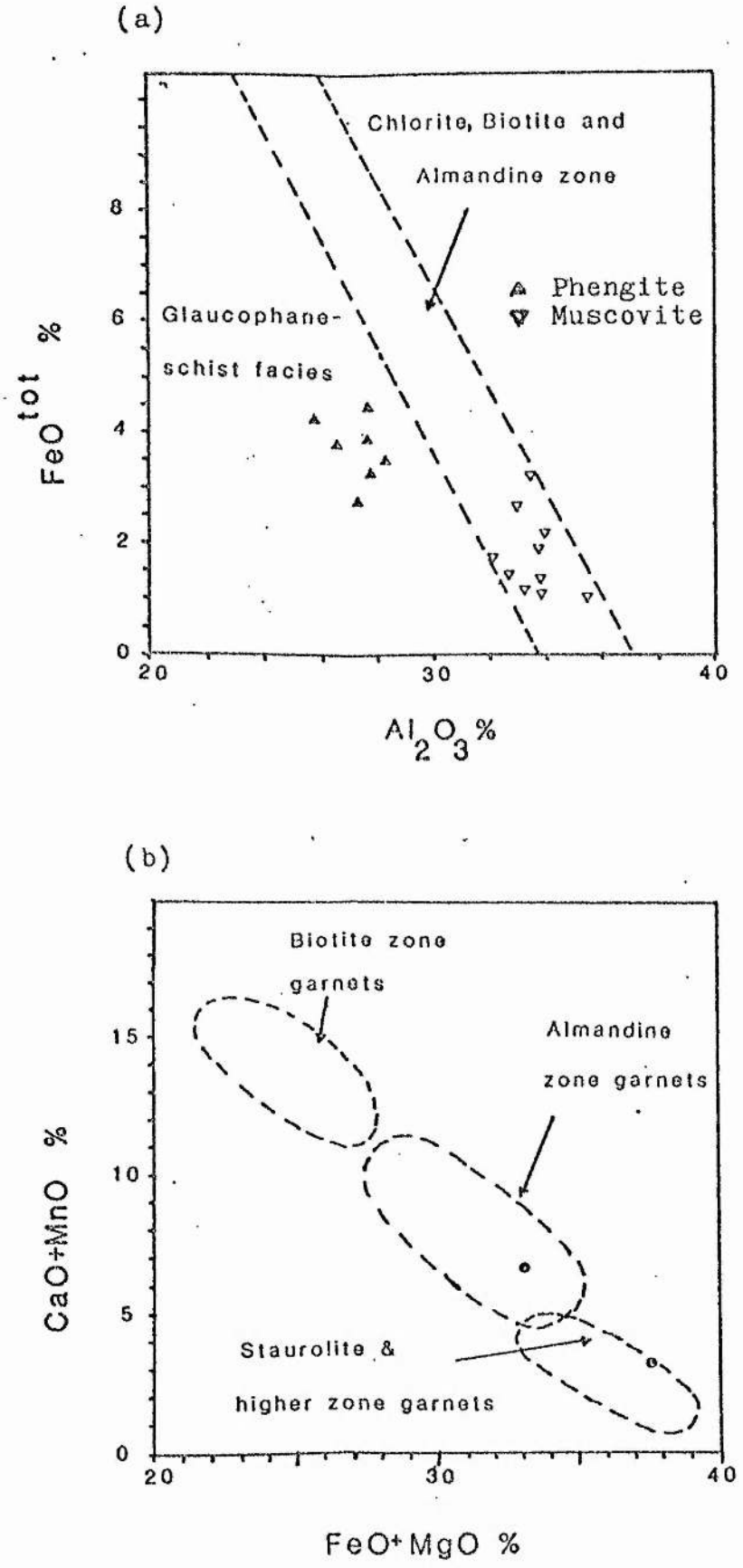

Fig. 8.12: (a) Plot of white mica (after Miyashiro 1973). (b) Plot of garnet (adopted from Sturt 1962).

phengite (Fig. 8.12a; Appendix. 8.15) is a characteristic of white mica from the glaucophane-schist facies (Miyashiro 1973, p.202).

8.3.9 Biotite

Analyses of biotite (Appendix. 8.16), plotted on a MgO - FeO - Al_2O_3 triangular diagram (Fig. 8.13, after Nockolds 1947) shows that they are comparatively rich in MgO and Al_2O_3, and resemble the biotite of calc-alkaline igneous rocks. The plot shows that biotite comes from mafic as well as acidic sources. The calc-alkaline affinity of these biotites (Nockolds 1947) is also supported by the analyses of associated pyroxenes (Appendix. 8.7; Fig. 8.8 and 8.9) which also display calc-alkaline characteristics (Nisbet & Pearce 1977; Le Bas 1962; Sanders and Morris 1978).

8.3.10 Calcite

Analyses of the carbonate matrix, and also some grains interpreted as detrital (Appendix 8.17) show that they are almost pure calcite with the following range in composition:

CaO	48-54%
MgO	0.09-0.64%
MnO	0.01-0.42%
FeO	0.02-0.23%

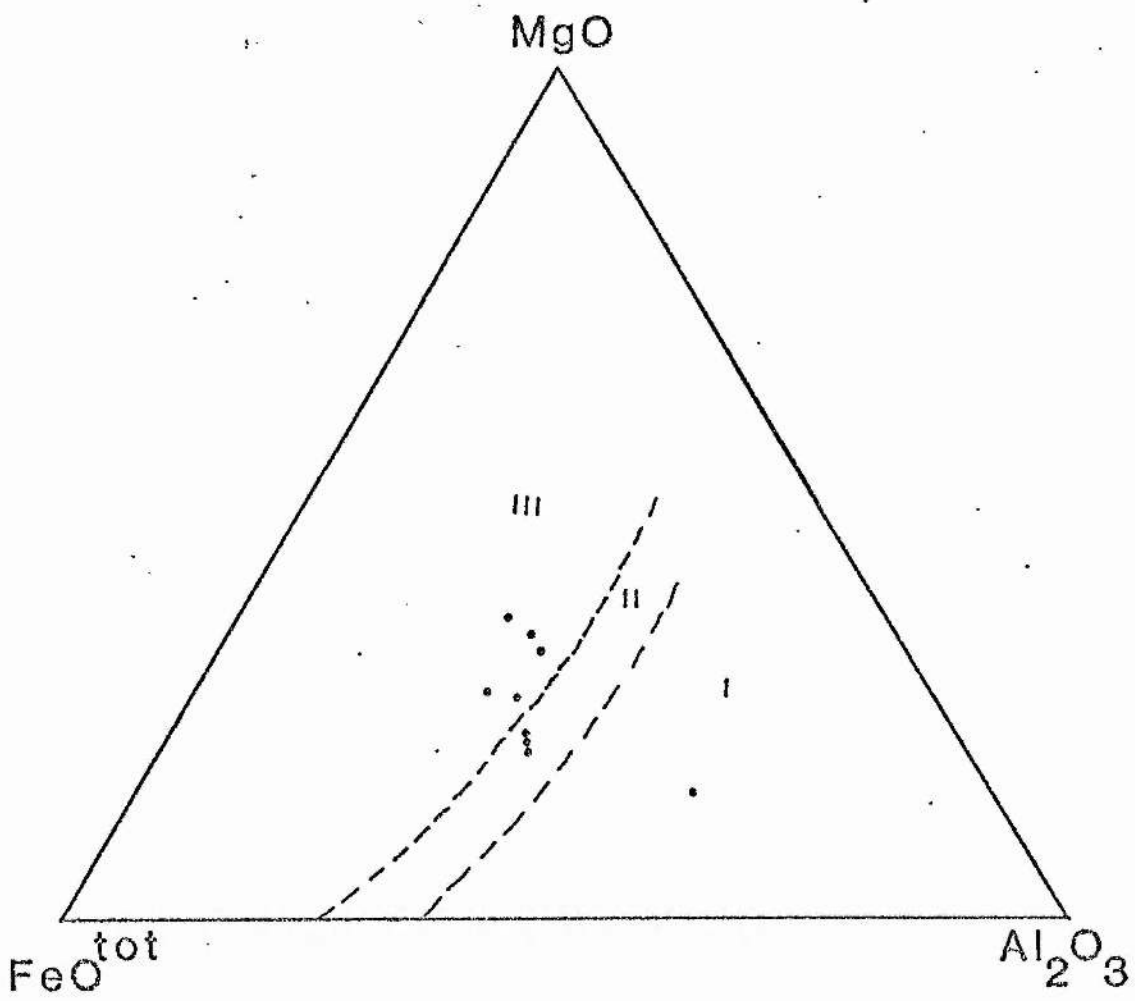

Fig. 8.13: MgO-Fe(tot)-Al_2O_3 plot for biotite from calc-alkali igneous rocks (after Nockolds 1947).

I = biotite associated with muscovite etc.

II = biotite associated with hornblende, pyroxene or olivine.

III = biotite unaccompanied by other mafic minerals.

This finding again confirms the XRD analyses. Though the Selkirk Formation is notably carbonate rich, its carbonates are similar in composition to those of the other formations.

8.3.11 Heavy Minerals

Analyses of heavy minerals are given in Appendix 8.18. Two garnet grains were analysed in a specimen of the Buckholm Formation which correspond to almandine (Deer et al. 1965). When plotted in FeO+MgO - CaO+MnO covariation diagram Fig. 8.12b, they fall into the field of almandine and higher grade garnets (Sturt 1962).

Three chrome spinel grains were analysed and found to be exceptionally rich in CrO_2 (42-47% $>Al_2O_3$). The Fe:Mg ratio is equal to or less than one.

Two detrital grains of epidote were also analysed and found to correspond to clinozoisite (ana. 8 & 9, p.198) and piemontite (ana. 1, p.200) of Deer et al. 1965).

8.4 CONCLUSION

Clay minerals are mainly chlorite and illite with or without the association of kaolinite. Illite crystallinity and b_0 values suggest the anchizone of metamorphism without showing any progressive increase in grade to NW. Mineral assemblages suggest a prehnite-pumpellyite facies of metamorphism.

Detrital pyroxenes are different from those of the Bail Hill Volcanic Group and by contrast show a volcanic arc affinity. Amphiboles are closely comparable with some components of the Ballantrae Complex. White mica is of two types: a) muscovite; b) phengite, which tends to increase to the NW. The presence of chrome spinel indicate ultrabasic rocks in source area which is further supported by the glaucophane fragments, also characteristic of the subduction zone.

9. SUMMARY, CONCLUSIONS AND DISCUSSION

9.1 SUMMARY

The Ordovician and Silurian succession of the Gala area commences with representatives of the Moffat Shale Group which pass conformably upwards into turbidite successions of highly variable age. The succession crops out within a number of strikewise-orientated fault blocks, and in general there is a progressive delay in initiation of turbidite sedimentation within successive fault blocks to the southeast. Thus within the two northwestern fault blocks, turbidite deposition began within the Caradoc Series, and within successively higher levels of the Llandovery and possibly Wenlock Series in the more southeasterly blocks. The proven Llandovery turbidites are the stratotypes of the Gala Group (Lapworth 1870). The Ordovician turbidite sequence includes two formations, not formally combined as a Group; the Gala Group is divided into three formations within the present area, and one formation is ascribed to the overlying Hawick Group. The divisions are differentiated primarily on the basis of micropetrography.

The Falahill Formation is the oldest Ordovician turbidite subdivision in the Gala area, and is characterized by dark grey 'basic-clast' greywackes distinctive in having garnet and scarce blue amphiboles of the glaucophane group. The succeeding Heriot Formation is characterized by medium dark grey 'silicic' greywackes. Ferromagnesian minerals and basic

igneous clasts are notably deficient, indicating a change of source. The above formations are correlated respectively with the Scar and Shinnel Formations of West Nithsdale and the Portpatrick Basic-clast and Portpatrick Acid-clast `Divisions` of the Rhinns of Galloway. A Lower Hartfell (Upper Caradoc) age is suggested, on the basis of lateral correlation.

The Gala Group commences with the 'basic-clast' greywackes of the Hazelbank Formation. Three members are recognized, spanning the interval between the P. acuminatus and C. cyphus Zones (L. Birkhill). The succeeding 'intermediate' greywackes of the Fountainhall Formation range from the P. acuminatus Zone to the M. sedgwickii or the R. maximus Zone (Lower to Upper Llandovery).

The Buckholm Formation is highly siliceous, suggesting a reversion to a source area similar to the Heriot Formation. Graptolite faunas indicate the M. turriculatus Zone (U. Birkhill, Upper Llandovery). The upper part of the Buckholm Formation shows interdigitation with the Fountainhall Formation, suggesting overlapping of turbidite fans; a western fan depositing the Fountainhall facies and an eastern fan laying down the Buckholm facies.

The Selkirk Formation represents the Hawick Group, and is highly siliceous and compositionally mature. This formation is correlated with the Carghidown Beds of Whithorn. Estimates of the age of the group as a whole range between Upper

Llandovery and Wenlock (Clarkson, Craig and Walton 1975); more recent findings (A. Kemp, pers. comm.) denote a wholly Llandovery age.

The fault blocks within which successive formations crop out are bounded by steep thrusts. Commonly one formation occupies a single block, though the Fountainhall Formation, which occupies the largest time span, is associated with three fault blocks, the southernmost of which also limits the outcrop of the Buckholm Formation, by virtue of including the merging of two interfering fans. The blocks are successively younger towards the SE, and strata within the blocks young dominantly to the NW.

Most formations correspond to lithic greywackes. They display a compositional range from `basic-clast` to highly siliceous, the latter trend probably being related to recycling as well as a change in source. `Basic-clast` greywackes are derived partly from ophiolitic and partly from volcanic arc sources, `Intermediate` types reflect a mixed source, with the incoming of a contribution from a plutonic and metamorphic terrain. This terrain becomes the major first-cycle contributor for the silicic (`acid-clast`) varieties.

Basic, intermediate and acidic eruptives dominate the `basic-clast` formations. Schists up to garnet grade characterize the `silicic` formations, which are otherwise

dominated by more durable clasts of granitic origin.

Detrital pyroxenes of the Gala area are comparable with those of the the Red Island Formation of the Longford-Down area, and the Elvan Formation of Leadhills - Abington area and differ from those of the Bail Hill Volcanic Group. The latter are suggested to have been derived from alkali-basalt hawaiite - mugearite - trachyte lava series typical of volcanic seamounts. By contrast, the detrital pyroxenes of the Gala area are non-alkaline and may therefore have been derived from a volcanic arc region.

On the other hand, amphiboles are comparable to those of the Bail Hill Volcanic Group (McMurtry 1980), and even more closely to those of the Ballantrae ophiolites, suggesting derivation from this or a similar ophiolitic source, with which an initial blueschist source may have been associated.

Palaeocurrents show preferred orientations (Fig. 6.1). Evidence from the Ordovician succession is weak. Erosional currents in the Silurian were from the NE. Depositional currents, by contrast, consistently have directions from NW to SE throughout the succession, again agreeing with observations elsewhere in the Southern Uplands. This supports Rust's (1965b) postulation of longitudinal scour allied to transverse depositional currents. The consistency of the direction of depositional currents suggest derivation from a marginal landmass 'Cockburnland' of Walton (1963) to the NW, which is

considered to have had a covering of both acid and basic Lower Ordovician lavas over plutonic rocks resembling those of the Ballantrae Igneous Complex (Walton 1965). This is different from the 'Cockburnland' of Leggett et al. (1979) which represents a trench-slope break bounded northwards by the Southern Uplands Fault. Derivation from the NW including the Highland type metamorphic material and the acid igneous rocks of the Midland Valley basement, and persists through the 'intermediate' and 'silicic' formations. Reactivation of the basic source took place in the Hazelbank Formation.

The area is divisible into at least six contrasting zones of facies associations ranging from inner-fan to outer-fan (fringe) and ocean floor environment. Two turbidite fans were active during the deposition of Zone 5. The occurrence of closely comparable facies associations (channelized mid-fan) along with indications of contrasting palaeocurrent trends suggests opposed fan fringes.

Although there is no evidence either of positive (fining upwards) or negative (coarsening upwards) trends of second order cycles (megasequences), the columnar profile of the whole area (Fig. 5.1) suggests at least three retrogressions of the fan from inner-fan to outer-fan (fringe) positions followed by rapid progressions to an inner-fan/mid-fan position.

The area displays marked contrasts in fold styles. To

the NW, affecting the outcrop of the Heriot, Hazelbank and Fountainhall Formations, the succession has been deformed into asymmetrical folds mostly verging SE and some NW, and ranging from tight to open; the latter are commonly overturned. There are also a few monoclinal folds facing NW. To the SE, within the Selkirk Formation and the adjacent part of the Buckholm Formation, the deformation is less intense, folding ranging from close to open with only a few tight folds. Monoclinal folds occur rarely, but are consistent in facing NW. The derived axial planes for the whole area show a modal azimuth of N. 45° E. and a nearly vertical dip. A small proportion of axial surfaces have a modal attitude of 038/40°SE. Plunges are mainly low, with very subordinate steep plunges both to SW and NE. The folds are mostly similar in style, with a maximum limb : hinge thickness ratio of 1:2. Thickening is more pronounced in minor folds (amplitude: 2 cm to 1 m).

Variations in style cannot be attributed to any particular formation or block, but may be observed within a single block. All observations agree in supporting the conclusion of Stringer & Treagus (1980, 1981) that both steeply and gently plunging folds may form in response to localized discrepancies within the same set of compressive forces.

Stringer & Treagus follow Eales (1979) in suggesting that most if not all the Caledonian structures of the Southern Uplands can be explained by a common but evolving stress

system. Faulting is an important element in the deformation of the succession; indeed, faulting is more important than folding in controlling distribution of the outcrops of the various formations. The faults are divisible into three categories: a) dip slips (modal strike: N.040-050E.), b) oblique slips c) strike-slips (wrenches). The boundary thrusts are complex structures, and where favourably exposed (as in the Glenwhinnie Fault) are seen to be associated with imbricated zones, in which the imbricate faults arise from the main thrust plane as a sole. The wrenches are again divisible into dextral (azimuth 135, dip 80-90 to SW) and sinistral (azimuth 005-185°/vertical) sets (Fig. 7.3). It is noticeable that all the three categories of fault show diversity of the pitches of slickensides, supporting Rust's (1965a) conclusion that faults moving initially as dip-slips were reactivated as oblique slips by subsequent movements under reoriented stress systems.

It is concluded that the initial folds and thrusts were interlinked, and were rotated during a continuum of deformation, initially flat-lying thrusts being reoriented at this stage into steeply dipping strike faults. This was followed by wrench faulting. Reactivation of the faults was probably the last event. It seems likely that all these structures formed under substantially homogeneous stress conditions sustained over a prolonged interval of time.

The succession has suffered low-grade thermodynamic

metamorphism. The mineral assemblages include chlorite - illite - albite in siliceous formations, with chlorite - prehnite - albite and chlorite - prehnite - pumpellyite - albite in basic-clast greywackes. These indicate a position within the anchizone, with a small proportion in the diagenetic zone. There is no suggestion of overall northward increase in grade within the anchizone, in correspondence with observations elsewhere within the Southern Uplands - Longford-Down sector.

9.2 DISCUSSION

9.3.1 Fore-arc Tectonics

It has been proposed that the succession of the Southern Uplands was deposited in a trench to the south of a northwestern continent. The existence of the `Iapetus Ocean` of Harland and Gayer (1972) (the `proto-Atlantic Ocean` of Wilson 1966), first indicated by faunal evidence (Williams 1976; McKerrow & Cocks 1976) is now supported by palaeomagnetic (Briden *et al.* 1973; Piper 1978) and structural (Phillips *et al.* 1976; McKerrow *et al.* 1977) evidence.

A number of contrasting subduction models has been proposed, including those of Dewey (1969) who postulated a NW-dipping subduction zone, extended upwards to outcrop as the Southern Uplands Fault; Fitton & Hughes (1970), who postulated a southerly subduction under the broad area of the

paratectonic Caledonides of Dewey (1969); Gunn (1973), who invoked paired NW-dipping subduction zones, one Dewey's `Southern Uplands` Zone and the other now represented by the Highland Boundary Fault, separated by the continental crust of the Midland Valley. Phillips et al. (1976) modified both the `Dewey` and the `Gunn` proposals by suggesting divergent subduction systems, NW under the Southern Uplands and SE under the Lake District, with oblique closure and substantial components of sinistral strike-slip (Max et al. 1983).

Northwesterly subduction led to the development of the Southern Uplands as an accretionary prism formed as material (sediments and volcanics of the ocean floor) was scraped off and imbricated at the continent-ocean interface (Mitchell 1974; McKerrow et al. 1977; Seely et al. 1974; Kulm & Fowler 1974; Webb 1983). Detachment of the underlying basement is proposed to have taken place along fault planes, initiated as low-angle thrusts and progressively rotated towards verticality as subduction continued (Seely et al. 1974; Karig and Sharman 1975). This accounts for the dominance of northwesterly younging strata within the blocks and persistence of the younger pelagic/hemipelagic ocean-floor facies into successively higher fault blocks southeastwards (Mitchell 1974; Mitchell and McKerrow 1975; Anderson and Cameron 1979).

Initiation of the faulting probably occurred along an inclined plane of high shear stress extending for some tens of

km through the trench-wedge sediments, inferentially through episodic subduction (Cowan 1974, 1978; Karig & Sharman 1975 and references therein). Accretionary complexes may also form during oblique subduction, e.g. the Taupo-Hi Kurangi Subduction system, New Zealand (Cole & Lewis 1981), and the Sunda (Nias) arc system off Sumatra (G. F. Moore & Karig 1980). Strike-slip faults are considered to be characteristic of oblique subduction; significant, probably even dominant, strike-slip components now appear to be well established for most or all major crustal fractures within the Caledonides, strongly supporting obliquity of subduction. Thrust nappes and SE-verging folds were propagated within the inner wall of the accretionary complex. Folds of opposing vergence are also present (also noted in the Gala area); such folds have been inferred to have formed towards the end of the subduction during continental collision (Cameron 1977); it should be noted, however, that there is not universal agreement on the collision along the proposed Iapetus suture (Max et al. 1983).

9.3.2 Trench sedimentation

Clastic sediments of the Southern Uplands have been interpreted as trench deposits because of their axial sediment dispersal (NE-SW), lack of evidence for any southeasterly source (Dewey 1971; Piper 1972; Leggett 1980), and consistency of conformable contacts between turbidite sequences and underlying Moffat Shales (McMurtry 1980; Hepworth 1981).

In the Southern Uplands axial and lateral transport was principally by turbidity currents, with interdigitation of turbidite fans of NW derivation. In the Gala area the distributary system is mostly channelized; vertical distribution of facies shows at least three main progression and regression cycles, from a inner-fan to outer-fan (fringe) position during the time span covered (Chapter 5). Sediment transport mechanisms include debris flows (A1), high concentration sediment gravity flow (C1) and low density turbidity current flow (D1). The transition from lateral to axial flow in the trench is logically considered to have resulted from deflection of the turbidity current by the outer slope (Piper 1972; Schweller & Kulm 1978). Although restricted exposure inhibits observation of lateral and vertical facies variations of turbidite facies (Mutti & Ricci Lucchi 1975), individual components of the fan model can be recognised with reasonable confidence, and assembled to produce an acceptable fan model.

Comparison of the clastic rocks of the Southern Uplands with present day analogues (Piper 1972) suggests a comparison with Recent turbidites within the Aleutian Trench off Alaska. Comparison shows (Piper 1972) that both basins are characterized by high sedimentation rates, association of pelagic and hamipelagic sediments with turbidites, minor slumps and dominance of axial erosional currents over the lateral depositional currents. The scale of the present area

is also comparable with the Alleutian Trench.

ACKNOWLEDGEMENTS

I am gratefully indebted to my supervisors, Prof. E. K. Walton and Dr. J. A. Weir for suggesting the project and for their kind advice, stimulating discussions and encouragement throughout my study period.

Parts of the manuscripts were read by Dr. G. J. H. Oliver, Dr. A. M. Hopgood and Dr. I. Strachan (University of Birmingham). I am thankful for their stimulating comments and discussions and for correcting my errors. The help of Dr. W. E. Stephens for computing work, Dr. A. R. MacGregor for the identification of fossil fragments and Dr. I. Strachan for graptolite identification is highly appreciated.

I am also thankful to Dr. G. C. Saigal and Dr. N. Saigal, M. Al-Rubaii, L. J. Evans, L. J. Thomas and J. R. Baldwin for their advice, especially the help of L. J. Evans in XRD analyses is gratefully acknowledged.

Thanks are also due to Mr. S. Bateman and Mr. D. Herd for general help, Mr. A. Mackie for thin section and polished section work, Mr. A. J. Reid and Mr. R. A. Batchelor for help in XRD studies, Mrs. J. A. Kinnaird for inclusion study, Mr. J. Allan for photography and Mrs J. Galloway and Miss C. H. Finlay for their help in typing part of the

manuscript. Thanks to Mr. and Mrs. J. Lyons for providing me home comforts during the field season.

I am very thankful to Br. Agha Akbar Shah, V.C., the University of Baluchistan for my nomination and for granting me study leave; and the Ministry of Education, Government of Pakistan for financial support. I am equally thankful to the staff of the Education Division, Embassy of Pakistan for their cooperation and encouragement.

REFERENCES

ANDERSON, T. B. & CAMERON, T. D. J. 1979. A structural profile of Caledonian deformation in Down. In: Harris, A. L., Holland, C. H. & Leake, B. E. (eds) The Caledonides of the British Isles - rewiewed. Spec. Publ. geol. Soc. London. 8, 236-7.

ATKINS, F. B. 1969. Pyroxenes of the Bushveld intrusions, South Africa. J. Petrology 10, 222-49.

BENTON, M. J. 1982. Trace fossils from the Lower Palaeozoic ocean-floor sediments of the Southern Uplands of Scotland. Trans. R. Soc. Edinburgh: Earth Sciences 73, 67-87.

BERRY, L. G., POST, B., WEISSMAN, S., McMURDIE, H. F. & McCLUNE, W. F. 1974. Selected Powder Diffrection Data for Minerals. (1st ed). Joint Committee on Powder Diffrection Standards, Swarthmore, Pennsylvania.

BLATT, H. & CHRISTIE, J. M. 1963. Undulatory extinction in quartz of igneous and metamorphic rocks and its significance in provenance studies of sedimentary rocks. J. Sediment. Petrol. 33, 559-79.

BLOXAM, T. W. 1968. The petrology of Byne Hill, Ayreshire. Trens. R. Soc. Edinburgh: Earth Sciences 68, 16-9.

BLUCK, B. J. 1978. Sedimentation in a late orogenic basin: the Old Red Sandstone of the Midland Valley of Scotland. In: Bowes, D. R. & Leake, B. E. (eds) Crustal evolution in northern Britain and the adjacent regions, 249-78. Geol. J. Spec. Issue 10.

BLUCK, B. J., HALLIDAY, A. N., AFTALION, M. & MACINTYRE, R. M. 1980. Age and origin of Ballantrae ophiolite and its significance to

to the Caledonian orogeny and Ordovician time scale. Geology 8, 492-5.

BOUMA, A. H. 1962. Sedimentology of some flysch deposits: A graphic approach to facies interpretation. Elsevier Amsterdam.

BRIDEN, J. C., MORRIS, W. A. & PIPER, J. D. A. 1973. Palaeomagnetic studies in the British Caledonides - VI: Regional and global implications. Geophys. J.R. astron. Soc. 34, 107-34.

CAMERON, T. D. J. 1977. The stratigraphy, sedimentology and structural geology of the Silurian rocks of east Lecale, Co.Down. Ph.D. thesis, Queen's University, Balfast (Unpubl.).

CHURCH, W. R. & GAYER, R. A. 1973. The Ballantrae ophiolite. Geol. Mag. 100, 497-510.

CIPRIANI, C., SASSI, F. P. & VITERBO BASSANI, C. 1968. La Composizione delle miche chiare in rapporto con le constanti reticolari e col grado metamorphico. Rend. Soc. Ital. mineral. petrogr. 24, 153-87.

CLARKSON, C. M., CRAIG, G. Y. & WALTON, E. K. 1975. The Silurian rocks bordering Kirkcudbright Bay, South Scotland. Trans. R. Soc. Edinburgh, 69, 313-25.

COLE, J. W. & LEWIS, K. B. 1981. Evolution of Taupo-Hikurangi subduction system. Tectonophysics 72, 1-21.

COOK, D. R. 1976. The geology of Cairnsmore of Fleet granite and and its environments, southwest Scotland. Ph.D. thesis, University of St. Andrews (Unpubl.).

COOK, D. R. & WEIR, J. A. 1979. Structure of the Lower Palaeozoic rocks around Cairnsmore of Fleet, Galloway. Scott. J. Geol. 15, 187-202.

COWAN, D. S. 1974. Deformation and metamorphism of the Franciscan subduction zone complex northwest of Pacheco Pass, California. Bull. geol. Soc. Am. 85, 1623-34.

COWAN, D. S. 1978. Origin of blue-schist bearing chaotic rocks in the Franciscan Complex, San Sameon, California. Bull. geol. Soc. Am. 89, 1415-23.

CRAIG, G. Y. & WALTON, E. K. 1959. Sequence and structure in the Silurian rocks of Kirkcudbrightshire. Geol. Mag. 96, 209-20.

CRAIG, G. Y. & WALTON, E. K. 1962. Sedimantary structures and palaeocurrent directions from the Silurian rocks of Kirkcudbrightshire. Trans. geol. Soc. Edinburgh 19, 100-19.

CUMMINS, W. A. 1962. The greywacke problem. Lpool Manchr. geol. J. 3, 51-72.

DEER, W. A., HOWIE, R. A. & ZUSSMAN, J. 1965. Rock forming minerals. Vols. 1-5 (4th ed). Longmans, London.

DEWEY, J. F. 1969a. Structure and sequence in the paratectonic Caledonides. In: Kay, M. (ed) North Atlantic: geology and continental drift. Mem. Am. Assoc. Petrol. Geol. 12, 309-35.

DEWEY, J. F. 1969b. Evolution of the Appalachian/Caledonian orogen. Nature, London 222, 124-9.

DEWEY, J. F. 1971. A model for the Lower Palaeozoic evolution of the southern margin of the early Caledonides of Scotland and Ireland. Scott. J. Geol. 7, 219-40.

DICKINSON, W. R. 1970. Interpreting detrital modes of greywackes and arkose. J. Sediment. Petrol. 40, 695-707.

DICKINSON, W. R. & SEELY, D. R. 1979. Structure and stratigraphy of

forearc regions. Bull. Am. Assoc. Petrol. Geol. 63, 2-31.

DUNOYER DE SEGONZAC, G. 1970. The transformation of clay minerals during diagenesis and low grade metamorphism: a review. Sedimentology 15, 281-346.

DZULYNSKI, S., & RADOMSKI, A. 1955. Origin of groove casts in the light of turbidity current hypothesis. Acta Geol. Polonica 5, 47-66.

EALES, M. H. 1979. Structure of the Southern Uplands. In: Harris, A. L., Holland, C. H. & Leake, B. E. (eds) The Caledonides of the British Isles - reviewed. Spec. Publ. Geol. Soc. London No. 8, 269-73.

ERNST, W. G. 1975. Introduction In: Ernst, W. G. (Ed) Subduction zone metamorphism. Dowden, Hutchinson and Ross Inc., Stroudsburg, Pennsylvania, 1-14.

ESQUEVIN, J. 1969. Influence de la composition chimique des illites sur leur crystallinite. Bull. Centr. Resh. Pau, 3, 147-53.

FITTON, J. G. & HUGHES, D. J. 1970. Volcanism and plate tectonics in the British Ordovician. Earth planet. Sci. Lett. 8, 223-8.

FLOYD, J. D. 1975. The Ordovician rocks of West Nithsdale. Ph.D. thesis, University of St. Andrews (Unpubl.).

FREY, M. 1970. The step from diagenesis to metamorphism in pelitic rocks during the Alpine Orogenesis. Sedimentology 15, 261-79.

FYFE, T. B. & WEIR, J. A. 1976. The Ettrick Valley thrust and the upper limit of the Moffat Shales in Craigmichan Scaurs (Dumfries and Galloway Regon: Annandale and Eskadale District). Scott. J. Geol. 12, 93-102.

GEIKIE, A. 1871a. On the order of succession among the Silurian rocks of Scotland. Trans. geol. Soc. Glasgow, 3, 74-95.

GEIKIE, A. 1871b. Explanation of Sleet 15 - geology of Dumfriesshire (nort-west part), Lanarkshire (south part), Ayreshire (south-east part). Mem. geol. Surv. Scotland.

GORDON, A. J. 1962. The Lower Palaeozoic rocks around Glenluce, Wightownshire. Ph.D. thesis, University of Edinburgh (Unpubl.).

GUNN, P. J. 1973. Location of the proto-Atlantic suture in the British Isles. Nature, London 242, 111-2.

HARKNESS, R. 1851. On the Silurian rocks of Dumfriesshire and Kirkcudbright. Q. J. geol. Soc. London 7, 46-58.

HARKNESS, R. 1856. On the lowest sedimentary rocks of the south of Scotland. Q. J. geol. Soc. London 12, 238.

HARLAND, W. B. & GAYER, R. A. 1972. Arctic Caledonides and earlier oceans. Geol. Mag. 109, 289-314.

HARLAND, W. B., AGER, D.V., BALL, H. W., BISHOP, W. W., CURRY, D., DEER, W. A., GEORGE, T. N., HOLLAND, C. H., HOLMES, S. C. A., HUGHES, N. F., KENT, P. E., PITCHER, W. S., RAMSBOTTOM, W. H. C., STUBBLEFIELD, C. J., WALLACE, P. & WOODLAND, A. W. 1972. A concise guide to stratigraphic procedure. J. geol. Soc. London 128, 296-305.

HEPWORTH, B. C. 1981. Geology of the Ordovician rocks between Leadhills and Abington, Lanarkshire. Ph.D. thesis, University of St. Andrews (Unpubl.).

HEY, M. H. 1954. A new review of the chlorites. Mineralog. Mag. London 30, 277-92.

HOLLAND, C. H., AUDLEY-CHARLES, M. G., COWIE, U. W., CURRY, D., FITCH, F. J., HANCOCK, J. M., HOUSE, M. R., INGHAM, J. K., KENT, P. E., MORTON, N., RAMSBOTTOM, W. H. C., RAWSON, P. F., SMITH, D. B., STUBBLEFIELD, C.J., TORRENS, H. S., WALLACE, P.

& WOODLAND, A. W. 1978. A guide to stratigraphical procedure. Geol. Soc. London Spec. Rep. No. 11.

HUBERT, J. F., SCOTT, K. M. & WALTON, E. K. 1966. Composite nature of Silurian flysch sandstones shown by groove molds on intra-bed surfaces, Peeblesshire, Scotland. J. Sediment. Petrol. 36, 237-241.

JONES, C. M. 1977. The Ballantrae Complex as compared to the ophiolites of Newfoundland. Ph.D. thesis, University of Wales, Cardiff (Unpubl.).

KARIG, D. E. & SHARMAN, G. F. 1975. Subduction and accretion in trenches. Bull. geol. Soc. Am. 86, 377-89.

KELLING, G. 1961. The stratigraphy and structure of the Ordovician rocks of the Rhinns of Galloway. Q. J. geol. Soc. London 117, 37-35.

KELLING, G. 1962. The petrology and sedimentation of Upper Ordovician rocks in the Rhinns of Galloway, southwest Scotland. Trans. R. Soc. Edinburgh 65, 107-37.

KELLER, W. D. & LITTLEFIELD, R. F. 1950. Inclusions in quartz of igneous and metamorphic rocks. J. Sediment. Petrol. 20, 74-84.

KISCH, H. J. 1974. Anthracite and meta-anthracite coal ranks associated with 'anchimetamorphism' and 'very-low-stage' metamorphism I, II and III. Proc. Kon. ned. Akad. Wet. Amsterdam Ser. B, 77, 89-118.

KISCH, H. J. 1978. Incipient metamorphism of Cambro-Silurian rocks from the "Eastern Complex" Caledonides of Jamtland, western Sweden: illite crystallinity and vitrinite reflectance. Rep. joint German Israeli Res. Proj. E12, 1-49.

KUBLER, B. 1964. Las angiles, indicateurs de metamorphisme. Rev. Inst. Fr. Pet. Paris 19, 1093-113.

KUBLER, B. 1967a. La cristallinite de l'illite et les zones tout a fait superieures du metamorphisme. In: Etages tectoniques, 105-122. A La Baconniere, Neuchatel (Suisse).

KUBLER, B. 1968. Evaluation quantitative de metamorphisme per la crystallinite de l'illite. Bull. Centr. Rech. Pau 2, 385-95.

KUENEN, Ph. H. 1953a. Significant features of graded bedding. Bull. geol. Soc. Am. 37, 1044-66.

KUENEN, Ph. H. 1953b. Graded bedding, with observations on the Lower Palaeozoic rocks of Britain. Verh. K. ned. Akad. Wet. 20, 1-47.

KUENEN, Ph. H. 1958. Experiments in geology. Trans. geol. Soc. Glasgow 23, 1-28.

KULM, L.D. & FOWLER, G. A. 1974. Oregon continental margin structure and stratigraphy: a test of imbricate thrust model. In: Burke, C. A. & Drake, C. L. (eds) The geology of continental margins, 261-83. Springer-Verlag, New York.

KUSHIRO, I. 1960. Si-Al relation in clinopyroxenes from igneous rocks. Am. J. Sci. 258, 548-54.

LAPWORTH, C. 1870. On the Lower Silurian Rocks of Galashiels. Geol. Mag. 7, 204-9.

LAPWORTH, C. 1874. On the Silurian of the south of Scotland. Trans. geol. Soc. Glasgow 4. 164-74.

LAPWORTH, C. 1878. The Moffat Series. Q. J. geol. Soc. London 34, 240-346.

LAPWORTH, C. & WILSON, j. 1870a. The Lower Silurian rocks in the neighbourhood of Galashiels. Trans. geol. Soc. Edinburgh 2, 46-58.

LAPWORTH, C. & WILSON, J. 1870b. On the Silurian rocks of the counties of Roxburgh and Selkirk. Geol. Mag. 8. 456-64.

LEAKE, B. E. 1978. Nomenclature of amphiboles. Mineralog. Mag. London 42, 533-63.

LeBAS, M. J. 1962. The role of alumina in igneous clinopyroxenes with relation to their parentage. Am. J. Sci. 260, 267-88.

LEGGETT, J. K. 1980a. The sedimentological evolution of a Lower Palaeozoic accretionary fore-arc in the Southern Uplands of Scotland. Sedimentology 27, 401-17.

LEGGETT, J. K. 1980b. British Lower Palaeozoic black shales and their palaeo-oceanographic significance. J. geol. Soc. London 137, 139-156.

LEGGETT, J. K., McKERROW, W. S. & EALES, M. H. 1979. The Southern Uplands of Scotland: A Lower Palaeozoic accretionary prism. J. geol. Soc. London 36, 755-70.

LEWIS, A. D. & BLOXAM, T. W. 1977. Petrotectonic environments of the Girvan-Ballantrae lavas from rare earth element distribution. Scott. J. Geol. 13, 211-22.

LONGMAN, C. D. & BLUCK, J. B. 1979. Ordovician conglomerates and the evolution of the Midland Valley. Nature, London 280, 578-80.

MACKIE, W. 1896. The sands and sandstones of east Moray. Trans. geol. Soc. Edinburgh 7, 148-72.

MAX, M. D., RYAN, P. D. & INAMDAR, D. D. 1983. A magnetic deep structural geology interpretation of Ireland. Tectonics 2, 431-51.

McKERROW, W. S. & COCKS, L. R. M. 1976. Progressive faunal migration across the Iapetus Ocean. Nature, London 263, 304-5.

McKERROW, W. S., LEGGETT, J. K. & EALES, M. H. 1977. An imbricate

thrust model for the Southern Uplands of Scotland. Nature, London 267, 237-9.

McMURTRY, M. J. 1980a. The Ordovician rocks of the Bail Hill Area, Sanquhar, South Scotland: Volcanism and Sedimentation in the Iapetus Ocean. Ph.D. thesis, University of St. Andrews (Unpubl.).

McMURTRY, M. J. 1980b. Discussion of: Evidence for Caledonide subduction from greywacke detritus in the Longford-Down inlier. J. Earth Sci. R. Dublin Soc. 2, 209-12.

MITCHELL, A. H. G. 1974. Flysch-ophiolite successions: polarity indicators in arc and collision type orogens. Nature, London 248, 747-9.

MITCHELL, A. M. G. & McKERROW, W. S. 1975. Analogous evolution of the Burma orogen and the Scottish Caledonides. Bull. geol. Soc. Am. 86, 305-15.

MIYASHIRO, A. 1973. Metamorphism and metamorphic belts. George Allen and Unwin Ltd., London.

MOORE, G. F. & KARIG, D. E. 1980. Structural geology of Nias Island, Indonesia: Implications for subduction zone tectonics. Am. J. Sci. 280, 193-223.

MURCHISON, R. I. 1851. On the Silurian rocks of the south of Scotland. Q. J. geol. Soc. London 7, 139-69.

MUTTI, E. & RICCI-LUCCHI, F. 1975. Turbidite facies and facies associations. In: Mutti, E., Parea, G. C., Ricci-Lucchi, F., Sagri, M., Zanzucchi, G., Ghibaudo, G. & Jaccarino, S. Examples of turbidite facies associations from selected formations of the northern Apennines. IX Int. Congr. Sedim. (Nice), Field Trip. A-II, 21-36.

NICOL, J. 1848. On the geology of Silurian rocks in the valley of

the Tweed. Q. J. geol. Soc. London 4, 195-209.

NISBET, G. & PEARCE, A. 1977. Clinopyroxene composition in mafic lavas from different tectonic settings. Contrib. Mineral. Petrol. 63, 149-60.

NOCKOLDS, S. R. 1947. The relation between chemical composition and paragenesis in the biotite micas of igneous rocks. Am. J. Sci. 245, 401-20.

OLIVER, G. J. H. & LEGGETT, J. K. 1980. Metamorphism in an accretionary prism: prehnite-pumpellyite facies metamorphism of the Southern Uplands. Trans. R. Soc. Edinburgh: Earth Sciences 71, 235-46.

OLIVER, G. J. H., SMELLIE, J. L., THOMAS, L. J., CASEY, D. M., KEMP, A., EVANS, L. J. BALDWIN, J. R. & HEPWORTH, B. C. 1984. Early Palaeozoic metamorphic history of the Midland Valley, Southern Uplands - Longford-Down Massif and the Lake District, British Isles (in press).

PADAN, A., KISCH, H. J., & SHAGAM, R. 1982. The use of lattice parameter bo of dioctahedral illite/muscovite for the characterization of P/T gradients of incipient metamorphism. Contrib. Mineral. Petrol. 79, 85-95.

PAPIKE, J. J., CAMERON, K. I. & BALDWIN, K. 1974. Amphiboles and pyroxenes - characterization of other than quadrilateral components as estimates of ferric iron from microprobe data. Abstr. Prog. geol. Soc. Am. 6, 1053-4.

PEACH, B. N. & HORNE, J. 1899. The Silurian Rocks of Britain. Vol. 1, Scotland. Mem. Geol. Surv. Scotland.

PETTIJOHN, F. J. 1957. Sedimentary Rocks (2nd ed). Harper & Row, New York.

PHILLIPS, W. E. A., STILLMAN, C. J. & MURPHY, T. 1976. A Caledonian plate tectonic model. J. geol. Soc. London 132, 578-609.

PIASECKI, A. M. J. & VAN BREEMEN, O. 1983. Field and isotopic evidence a c. 750 Ma tectonothermal event in Moine rocks in the Central Highland region of the Scottish Caledonides. Trans. R. Soc. Edinburgh: Earth Sciences 73, 119-34.

PIPER, D. J. W. 1972. Trench sedimentation in the Lower Palaeozoic of Southern Uplands. Scott. J. Geol. 8, 289-91.

PIPER, D. J. W. 1978. Turbidite muds and silts on deep sea fans and abyssal planes. In: Stanley, D. J. & Kelling, G. (eds) Sedimentation in Submarine Canyons, Fans and Trenches, 163-76. Dowden, Hutchinson & Ross, Stroudsburg, Pa.

RAMSAY, J. G. 1960. The deformation of early linear structures in cases of repeated folding. J. Geol. 68, 75-93.

RAMSAY, J. G. 1961. The effect of folding upon the orientation of sedimentary structures. J. Geol. 69, 84-100.

RAMSAY, J. G. 1967. Folding and fracturing of rocks. McGraw Hill, New York and London.

RICCI-LUCCHI, F. 1975a. Depositional cycles in two turbidite formations of the northern Apennines (Italy). J. Sediment. Petrol. 45, 3-43.

RICCI-LUCCHI, F. 1975b. Sediment dispersal in turbidite basins: examples from the Miocene of the northern Apennines. Proc. IXth Int. Congr. Sedim. (Nice), Theme 5, 347-52.

RUST, B. R. 1963. The geology of area around Whithorn, Wigtownshire. Ph.D. thesis, University of Edinburgh (Unpubl.).

RUST, B. R. 1965a. The stratigraphy and structure of the Whithorn area of Wigtownshire, Scotland. Scott. J. Geol. 1,

101-33.

RUST, B. R. 1965b. The sedimentology and diagenesis of Silurian turbidites in southeast Wigtownshire, Scotland. Scott. J. Geol. 1, 231-246.

RYAN, P. D., SWAL, V. K. & ROWLANDS. 1983. Ophiolite melange separates ortho- and para-tectonic Caledonides in western Ireland. Nature, London 301, 50-2.

SANDERS, I. S. & MORRIS, J. H. 1978. Evidence for Caledonian subduction from greywacke detritus in the Longford-Down inlier. J. Earth Sci. R. Dublin Soc. 1, 53-62.

SASSI, F. P., & SCOLARI, A. 1974. The bo values of the potassic white micas as a berometric indicator in low-grade metamorphism of pelitic schists. Contrib. Mineral. Petrol. 45, 143-52.

SCHWELLER, W. J. & KULM, L. D. 1978. Depositional patterns and channellized sedimentation in active eastern Pecific trenches. In: Stanley, D. J. & Kelling, G. (eds), Sedimentation in Submarine Canyons, Fans and Trenches 311-24. Dowden, Hutchinson & Ross, Stroudsburg, Pa.

SEDGWICK, A. 1850. On the geological structure structure and relations of the frontier chain of Scotland. Edinb. New Phil. Journal 51, 250-8.

SEELY, D. R., VAIL, P. R. & WALTON, G. G. 1974. Trench slope model. In: Burke, C. A. & Drake, C. L. (eds) The Geology of the continental margins, 249-60. Spronger-Verlag, New York.

SEILACHER, A. 1974. Flysch trace fossils: evolution of behavorial diversity in the deep-sea. Neues. Jahrb. Geol. Palaeontol. Monatsh. 1974, 233-45.

SPRAY, J. G. & WILLIAMS, G. D. 1980. The sub-ophiolite metamorphic

rocks of the Ballantrae Igneous Complex, SW Scotland. J. geol. Soc. London 137, 359-68.

STRINGER, P. & TREAGUS, J. E. 1980. Non-axial planar S1 cleavage in the Hawick Rocks of Galloway area, Southern Uplands of Scotland. J. Struct. Geol. 2, 317-31.

STRINGER, P. & TREAGUS, J. E. 1981. Asymmetrical folding in the Hawick Rocks of Galloway area, Southern Uplands of Scotland. Scott. J. Geol. 17, 129-48.

STURT, B. A. 1962. The composition of garnets from pelitic schists in relation to the grade of regional metamorphism. J. Petrology 3, 181-91.

THOREZ, J. 1976. The practical identification of clay minerals. G. Lelotte, Dison, Belgique.

TOGHILL, P. 1970. The southeast limit of the Moffat Shales in the upper Ettrick valley region, Selkirkshire. Scott. J. Geol. 6, 233-42.

WALKER, R. G. 1967. Turbidite sedimentary structures and their relationship to proximal and distal depositional environments. J. Sediment. Petrol. 37, 25-43.

WALTON, E. K. 1955. Silurian greywackes in Peeblesshire. Proc. R. Soc. Edinburgh B, 65, 327-57.

WALTON, E. K. 1956a. Limitations of graded bedding: and alternate criteria of upwards sequence. Trans. geol. Soc. Edinburgh 16, 262-71.

WALTON, E. K. 1956b. Two Ordovician conglomerates in South Ayrshire. Trans. geol. Soc. Glasgow 22, 133-56.

WALTON, E. K. 1961. Some aspects of succession and structure in the Lower Palaeozoic rocks of the Southern Uplands of Scotland.

Geol. Rdsch. 50, 63-77.

WALTON. E. K. 1963. Sedimentation and structure in the Southern Uplands. In: M. R. W. Johnston & F. H. Stewart (eds) The British Caledonides, 71-97. Oliver & Boyd, Edinburgh.

WALTON, E. K. 1983. The Lower Palaeozoic - stratigraphy. In: Craig, G. Y. (ed) Geology of Scotland, 105-35, Scottish Acadmic Press, Edinburgh.

WALTON, E. K. 1983. Lower Palaeozoic - structure and palaeogeography. In: Craig, G. Y. (ed) Geology of Scotland, 139-66, Scottish Acadmic Press, Edinburgh.

WALTON, E. K. 1967. The sequence of internal structures in turbidites. Scott. J. Geol. 3, 306-17.

WALTON, E. K. & WEIR, J. A. 1974. Letter: 'The Upper Glenkiln-Hartfell cherts and mudstones of Broadlaw and their stratigraphical significance'. Scott. J. Geol. 9, 320-1.

WARREN, P. T. 1963. The petrology, sedimentation and provenance of the Wenlock rocks near Hawick, Roxburgshire. Trans. geol. Soc. Edinburgh 19, 225-55.

WARREN, P. T. 1964. The stratigraphy and structure of the Silurian (Wenlock) southeast of Hawick, Roxburgshire, Scotland. Q. J. geol. Soc. London 120, 193-222.

WATSON, S. W. 1976. The sedimentary geochemistry of the Moffat Shales: A carbonaceous sequence in the Southern Uplands. Ph.D. thesis, University of St. Andrews (Unpubl.).

WEBB, B. 1983. Imbricate structure in the Ettrick area, Southern Uplands. Scott. J. Geol. 19, 387-400.

WEBER, K. 1972. Note on the determination of illite crystallinity. Neues Jahrb. Mineral. Monatshefte, 6, 267-76.

WEIR, J. A. 1968. Structural history of Silurian west coast of Gatehouse, Kirkcudbrightshire. Scott. J. Geol. 4, 30-52.

WEIR, J. A. 1974a. The sedimentology and diagenesis of the Silurian rocks on the coast west of Gatehouse, Kirkcudbrightshire. Scott. J. Geol. 10, 165-86.

WEIR, J. A. 1979. Tectonic contrasts in the Southern Uplands. Scott. J. Geol. 15, 169-186.

WELSH, W. 1964. The Ordovician rocks of northwest Wigtownshire. Ph.D. thesis, University of Edinburgh (Unpubl.).

WILKINSON, J. M. & CANN, J. R. 1974. Trace elements and tectonic relationships of basic rocks in the Ballantrae Igneous Complex, Ayrshire. Geol. Mag. 111, 35-41.

WILLIAMS, A. 1958. Oblique-slip faults and rotated stress systems. Geol. Mag. 95, 207-18.

WILLIAMS, A. 1959. A structural history of Girvan District, southwest Ayrshire. Trans. R. Soc. Edinburgh 63, 629-67.

WILLIAMS, A. 1962. The Barr and Lower Ardmillan Series (Caradoc) of the Girvan district, southwest Ayreshire. Mem. geol. Soc. London 3.

WILLIAMS, A. 1976. Plate tectonics and biofacies evolution as factors in Ordovician correlation. In: Bassett, M. G. (ed) The Ordovician System, 29-66. University of Wales Press and National Museum.

WILLIAMS, A., STRACHAN, I., BASSETT, D. A., DEAN, W. T., INGHAM, J. K., WRIGHT, D. A. & WHITTINGTON, H. B. 1972. A correlation of Ordovician rocks in the British Isles. Geol. Soc. London, Spec. Rep. No. 3.

WILSON, J. T. 1966. Did the Atlantic close and then re-open? Nature, London 211, 676-81.

YERMAKOV, N. P., DOLGOV, A. Yu., KALYUZHNYI, Vl., KOMOROV, O. P., LAZ'KO, Ye. M., NIKOLAYEV, V. A., SAFRONOV, G. M., KIYEVLENKO, Ye. Ya., BABANOV, G. V., VERSHININ, V. V. & KHOTENKOV, M. M. (eds) 1965. Research on the nature of mineral-forming solutions. Pergamon Press, Oxford.

ZIEGLER, A. M. & McKERROW, W. S. 1975. Silurian marine red beds. Am. J. Sci. 275, 31-56.

Appendix No 3.1: Results of 500 point counts

KEY

Q	= Quartz	F	= Feldspar
A	= Acid igneous	B	= Basic igneous
S	= Sedimentary	Mt	= Metamorphic
FM	= Ferromagnesian	Mx	= Matrix
S/No	= Serial Number	Sp No	= Specimen Number

FALAHILL FORMATION

S/No	Sp No	Q	F	A	B	S	Mt	FM	Mx	Grid Ref
1	320	14.6	26.2	11.6	19.6	0.2	0.2	3.4	24.6	3953 5446
2	322	12.4	17.0	4.4	24.6	0.4	0.0	6.0	35.6	3822 5431
3	80-b	16.9	8.9	15.5	29.5	1.1	1.3	8.3	18.5	3949 5539
4	338	18.4	13.6	12.4	21.6	1.0	4.0	6.4	22.6	4649 5315
5	341	10.6	20.2	8.4	27.2	0.0	1.4	6.2	25.9	3520 5263
6	80-a	10.0	19.4	4.8	29.4	0.6	0.6	6.4	29.4	3949 5539
7	328	18.8	12.2	4.2	27.0	0.0	0.6	5.2	32.0	3717 5357

HERIOT FORMATION

S/No	Sp No	Q	F	A	B	S	Mt	FM	Mx	Grid Ref
1	344	42.1	8.3	18.0	3.1	0.0	6.7	0.0	21.7	3573 5251
2	331	43.8	6.6	15.8	0.4	0.0	9.8	0.0	23.6	3657 5263
3	620	39.2	9.2	14.6	2.8	0.8	4.0	0.0	29.4	4409 5467
4	85	38.4	4.6	14.4	1.6	2.2	3.2	0.0	35.6	4125 5323
5	613	40.0	6.2	9.8	0.4	0.2	6.8	0.0	36.6	4339 5413
6	534	46.6	3.8	20.6	0.8	0.0	8.0	0.0	20.2	3674 4939
7	81	45.1	3.5	2.0	2.0	0.8	1.2	0.0	45.5	4189 5435
8	349	44.0	4.8	17.2	1.0	2.6	5.0	0.0	25.4	3979 5198
9	3-a	21.0	6.3	40.0	4.3	2.1	0.2	0.0	26.1	

HAZELBANK FORMATION

S/No	Sp No	Q	F	A	B	S	Mt	FM	Mx	Grid Ref
1	2-c	22.0	11.6	9.2	23.2	4.2	0.6	2.0	26.0	4238 5060
2	90	24.4	16.8	4.0	27.6	0.8	1.0	10.0	15.2	4293 7007
3	380	32.6	10.1	10.0	20.2	1.4	1.4	2.7	21.7	3970 4905
4	438	20.2	9.6	14.2	24.2	1.2	2.2	5.6	22.8	3677 4905
5	433	22.2	7.2	19.4	24.4	0.4	1.6	7.6	17.2	3442 4916
6	467	22.8	7.2	12.8	25.0	0.6	0.8	0.2	30.6	3635 4850
7	365	17.1	7.8	15.9	26.1	6.8	1.8	5.2	19.3	5099 3857
8	407-a	21.3	7.3	18.1	18.7	1.8	2.1	4.6	26.3	3643 4994
9	310	30.0	12.2	11.8	7.7	0.2	1.8	0.0	36.5	4062 5053
10	611	18.0	14.4	7.8	29.6	4.8	1.6	5.0	18.8	4362 5250

FOUNTAINHALL FORMATION

S/No	Sp No	Q	F	A	B	S	Mt	FM	Mx	Grid Ref
1	9	43.4	14.0	11.0	1.1	0.9	1.4	0.0	28.2	4362 4944
2	218	39.5	13.2	13.5	3.4	0.4	2.6	0.0	27.4	4848 4660
3	244	46.2	10.6	15.0	5.0	0.7	2.7	0.0	19.8	4332 4789
4	271	39.4	12.5	19.7	1.4	0.2	1.3	0.0	25.5	4153 4973
5	292	19.6	21.6	10.4	13.8	1.4	0.8	0.0	31.0	4017 4175
6	476-a	33.0	17.8	15.0	1.4	1.6	5.0	0.0	26.2	3651 4659
7	492	30.8	11.8	15.0	9.4	2.8	3.8	0.0	25.8	3829 4704
8	507	29.2	14.4	15.8	4.2	2.0	2.6	0.0	31.8	3961 4816
9	632	32.6	13.4	14.8	4.8	3.6	4.4	0.0	26.4	3796 4383
10	683	18.8	21.0	26.0	3.2	1.2	1.4	0.0	28.4	3777 3888
11	679	16.2	15.8	23.8	7.2	0.2	1.0	0.2	35.6	3827 4123

BUCKHOLM FORMATION

S/No	Sp No	Q	F	A	B	S	Mt	FM	Mx	Grid Ref
1	58	37.0	11.8	16.2	3.6	0.4	3.4	0.0	27.4	4782 3795
2	33	56.0	7.0	6.3	0.6	1.4	2.2	0.1	26.4	4383 4628
3	21	50.8	1.6	2.2	0.0	0.0	1.4	0.2	44.0	4718 3736
4	34	39.4	4.2	19.8	0.4	0.4	10.2	0.0	25.6	4486 4342
5	159	45.4	3.6	14.4	2.0	1.4	2.8	0.0	30.4	4165 4594
6	124	43.0	3.8	17.8	1.2	0.6	6.0	0.2	27.4	4121 4327
7	289	36.8	6.8	11.8	4.2	1.6	2.4	0.2	36.2	4034 4205
8	19	43.0	7.4	3.6	1.2	2.0	7.6	0.0	35.2	4393 3943
9	729	43.8	4.4	15.8	0.2	0.2	7.8	0.0	27.8	4918 3247
10	27	46.6	3.8	11.4	0.2	0.6	8.8	0.2	28.4	4228 3780
11	720	40.2	5.8	20.4	0.4	0.6	7.8	0.0	24.8	4140 3690
12	653	45.0	5.2	17.0	3.8	1.4	2.2	0.0	25.4	3841 3830
13	716	47.4	4.2	18.6	0.4	0.6	4.6	0.4	23.8	4035 3836

Appendix No 3.1: Results of 500 point counts - continued

DUCKHOLM FORMATION - continued

S/No	Sp No	Q	F	A	B	S	Mt	FM	Mx	Grid Ref
14	67	45.4	8.0	10.2	1.8	1.2	2.4	0.0	31.0	4482 3691
15	712	33.8	7.6	18.0	3.6	0.8	6.2	0.0	30.0	4790 3392
16	43	45.6	2.4	13.6	0.4	0.4	11.0	0.0	26.6	4633 4145

SELKIRK FORMATION

S/No	Sp No	Q	F	A	B	S	Mt	FM	Mx	Grid Ref
1	755	30.0	4.0	23.4	2.6	0.6	1.5	0.0	37.7	4916 2638
2	730	38.3	2.6	6.6	0.8	0.5	1.4	0.0	49.6	4867 2909
3	779	35.1	2.5	9.9	1.0	0.0	1.7	0.0	49.7	4975 2790
4	745	32.6	5.0	21.7	2.1	0.3	1.1	0.0	37.1	4778 2728
5	748	28.4	5.6	21.2	2.8	1.1	2.1	0.1	38.8	4801 2591
6	738	26.0	8.0	5.2	0.6	0.8	1.0	0.0	58.4	4810 2708
7	777	22.8	9.2	9.6	1.8	1.4	2.6	0.0	52.6	4950 2841
8	759	26.6	6.0	18.0	2.2	1.6	2.2	0.0	43.4	4923 2637

Appendix 3.2: Results of 1000 point counts (repetition of 9 samples)

S/No	Sp No	Q	F	A	B	S	Mt	FM	Mx
1	58	39.5	13.2	13.57	3.4	0.4	2.5	0.0	27.4
2	2-c	23.6	9.3	6.6	24.0	4.4	1.1	7.8	23.4
3	90	22.8	17.6	5.1	25.0	1.6	1.1	9.8	17.0
4	320	15.1	27.4	14.8	13.5	0.1	0.4	2.4	26.5
5	21	50.6	1.5	3.0	0.0	0.0	1.9	0.1	42.8
6	3-a	16.3	6.54	49.0	4.0	2.8	0.6	0.0	20.71
7	81	43.4	3.2	2.1	0.7	2.0	2.9	0.0	45.7
8	318	32.7	11.1	13.1	8.0	1.1	1.4	0.0	32.6
9	322	12.6	16.2	5.4	17.9	0.4	0.1	6.8	40.6

Appendix No 3.3: Results of granule counts

KEY

Q	= Quartz	F	= Feldspar
AP	= Acid plutonic	AV	= Acid volcanic
BP	= Basic plutonic	BV	= Basic volcanic
S	= Sedimentary	Mt	= Metamorphic
S/No	= Serial Number	Sp No	= Specimen Number

FALAHILL FORMATION

S/No	Sp No	Q	F	AP	AV	BP	BV	Mt	S	Grid Ref
1	340	20.5	1.2	12.0	8.5	10.7	27.8	12.0	7.3	3611 5324
2	337	7.5	8.5	11.7	15.9	7.5	33.0	0.0	15.9	3649 5303

HERIOT FORMATION

S/No	Sp No	Q	F	AP	AV	BP	BV	Mt	S	Grid Ref
1	334-a	29.0	3.0	23.0	5.0	2.0	4.0	27.0	7.0	3648 5276
2	3-b	18.3	8.2	31.2	22.9	2.7	9.2	3.7	3.7	5403 4068
3	400	22.0	2.0	16.0	15.0	5.0	12.0	14.0	14.0	3697 5063
4	532	19.8	3.5	29.1	8.1	4.6	10.5	3.5	20.9	3678 5140
5	340	24.0	6.0	19.0	4.0	0.0	14.0	23.0	10.0	3611 5324

HAZELBANK FORMATION

S/No	Sp No	Q	F	AP	AV	BP	BV	Mt	S	Grid Ref
1	389	9.0	3.0	17.0	10.0	13.0	21.0	20.0	7.0	4397 4290
2	2-c	18.0	2.1	5.2	6.4	17.3	29.8	13.4	7.4	4238 5060
3	390-a	14.5	5.3	1.3	1.3	35.5	28.9	2.6	10.5	3587 5038
4	390	11.9	5.9	18.6	2.6	5.9	17.8	0.0	37.3	3587 5038
5	318	19.0	6.0	20.0	12.0	5.0	25.0	7.0	6.0	4062 5055
6	408	15.0	2.0	6.0	3.0	3.0	34.0	4.0	33.0	3640 5000
7	358	23.0	11.0	6.0	6.0	2.0	33.0	3.0	16.0	3871 5064
8	433	13.0	5.6	11.3	1.0	20.7	35.8	19	10.4	3585 4941
9	316	22.4	5.3	9.2	1.3	5.3	35.5	3.9	17.1	4010 5028
10	422	12.0	2.7	6.6	4.0	6.7	30.7	4.0	34.6	3667 4937
11	398	20.0	2.2	8.9	3.3	2.2	20.0	23.3	20.0	3693 5082

FOUNTAINHALL FORMATION

S/No	Sp No	Q	F	AP	AV	BP	BV	Mt	S	Grid Ref
1	259	28.0	12.0	12.0	9.8	4.9	17.1	9.8	6.1	4213 4987
2	228	19.2	6.7	0.8	7.5	17.5	22.5	2.5	23.3	4280 4886
3	688	40.9	3.4	12.4	9.0	4.5	9.0	20.2	1.1	4014 4029
4	501	20.5	8.9	17.0	6.2	0.9	17.8	22.3	6.2	3849 4655
5	479	33.7	6.3	14.7	4.2	1.0	5.3	27.4	7.4	3690 4651
6	191	28.9	9.0	16.2	7.2	2.7	16.2	14.4	5.4	4039 4649
7	502	30.0	9.0	19.0	3.0	4.0	11.0	19.0	5.0	3817 4645
8	506	28.0	26.0	13.0	6.0	5.0	11.0	6.0	5.0	3948 4849
9	630	26.1	9.1	6.8	10.2	0.0	30.6	13.6	3.4	3836 4305
10	186	34.0	8.0	15.0	9.0	1.0	12.0	11.0	10.0	4094 4692
11	483	22.9	5.3	10.7	6.9	5.3	25.9	9.2	13.7	3710 4653
12	476	32.1	6.2	19.6	5.4	0.9	3.6	15.2	17.0	3651 4659

BUCKHOLM FORMATION

S/No	Sp No	Q	F	AP	AV	BP	BV	Mt	S	Grid Ref
1	649-a	18.5	1.2	9.9	6.2	6.2	7.4	12.3	38.3	3957 3895
2	270-a	16.7	10.3	16.7	12.8	5.1	14.0	12.8	11.5	4137 4979
3	283	32.4	8.4	9.9	8.4	8.4	22.5	4.2	5.6	4106 4212
4	112	31.5	4.1	9.6	9.6	1.4	6.8	21.9	15.1	4248 4360
5	66-a	21.0	1.0	20.0	2.0	6.0	7.0	26.0	17.0	4489 3577
6	63	21.3	1.6	36.2	0.0	2.4	5.5	21.3	11.8	4490 3521
7	52	28.0	7.0	8.0	3.0	3.0	11.0	33.0	7.0	4681 3733
8	27-a	29.3	2.4	4.9	6.1	3.7	3.7	28.0	25.6	4228 3780
9	30-a	12.3	5.7	39.6	24.5	0.9	7.5	2.8	6.6	4461 4382
10	33	34.8	5.4	17.4	4.3	1.1	5.4	20.6	10.9	4383 4628
11	35	34.1	3.3	23.1	4.4	1.1	6.6	18.7	8.8	4400 4462
12	22-a	31.0	3.0	17.0	3.0	3.0	11.0	22.0	10.0	4494 4172
13	4	29.7	2.7	19.8	3.6	6.3	9.0	24.3	4.5	4441 4615
14	706	27.0	1.0	8.0	2.0	7.0	11.0	34.0	10.0	4608 3440

SELKIRK FORMATION

S/No	Sp No	Q	F	AP	AV	BP	BV	Mt	S	Grid Ref
1	781	11.6	0.9	10.7	35.7	5.4	18.7	5.4	11.6	5020 2750

Appendix No. 3.4: DESCRIPTION OF ROCK FRAGMENTS

1. IGNEOUS ROCK FRAGMENTS

Spilite: These consist mainly of a mosaic of plagioclase laths which may show alignment and in some instances variolitic texture. Rounded vesicles subsequently filled with chlorite are a common feature. Sporadic phenocrysts of plagioclase up to 1mm long occur. Ferromagnesian minerals are fine grained, optically indeterminable. They attain up to nearly 30% by volume, and occur mainly as groundmass components.

Rhyolite/Quartz-porphyry: The rhyolites are porphyritic (Plate 3.1), with subhedral to anhedral quartz and orthoclase phenocrysts set in a quartzo-feldspathic groundmass. In quartz-porphyry, quartz phenocrysts are set in a highly siliceous microcrystalline groundmass.

Trachyte: This is a porphyritic rock consisting of K-feldspar and plagioclase (sodic) phenocrysts having the form of elongate laths and displaying flow alignment. Ferromagnesian minerals are absent.

Volcanic Glass: This is a common rock type made up of non-crystalline glassy material which is very clear in plane polarized light and isotropic in crossed polars. Devitrified quartz growths occur sporadically. Some have a distinctly brown tinge; irregular black and dark brown spots are

characteristic of these. Others are characterized by sporadic feldspar microlites set in the dominantly isotropic groundmass. Devitrification textures and microlites in variety are characteristic of pitchstones.

Granite: These are equigranular, hypocrystalline, and comparatively coarse grained, and consist mostly of feldspar (both orthoclase and plagioclase, ocasssionally microcline), with or without perthite. Quartz is essentially present, but subordinate. Ferromagnesian minerals are absent within the dimensions of the clasts. Some fragments show micrographic intergrowths of quartz and feldspars (Plate 3.11). Some fragments are foliated and display a development of mica (chlorite and ?illite) along the grain boundaries and probably derived from a high grade metamorphic terrain.

Diorite: These consist of equigranular intergrowths of quartz, sodic plagioclase, brownish green hornblende and clinopyroxenes. Poikilitic intergrowths of feldspar and hornblende are also present. In some cases, large phenocrysts of greenish brown hornblende and altered plagioclase up to 1mm long are present in a groundmass of biotite, quartz and feldspar. Apatite, epidote and zircon occur as accessory minerals.

Dacite: This is a very fine grained quartzo-feldspathic, hypocrystalline rock type containing a small proportion of quartz grains along with a lesser proportion of unidentifiable

black and dark brown spongy spots.

Andesite/Basalt: These are porphyritic rock fragments consists mostly of phenocrysts of greenish brown hornblende, clinopyroxenes (Plate 3.9) and plagioclase in a groundmass of very fine plagioclase laths. In some instances the amphibole and pyroxene phenocrysts are completely pseudomorphed in chlorite and/or carbonates. Apatite is present as an accessory mineral.

2. METAMORPHIC ROCK FRAGMENTS

Metaquartzite: Metaquartzite consists of equigranular quartz grains with occasional muscovite flakes. In some the quartz grains may be lensoid or elongated. Some fragments display corrosion and partial replacement of the quartz grains by micaceous minerals, recalling diagenetic replacement textures within the greywackes.

Schists: Quartz-schist clasts predominate, and consist mainly of quartz in detached, lensoid grains, and micas. Alignment of the quartz grains and the mica flakes defines a strong fabric (Plate 3.12). Quartz-muscovite schist is the most common. Others include quartz-muscovite-biotite schist, chlorite-schist, garnet-schist, glaucophane-schist (Plate 3.13) and ?kyanite-schist. There are only a few examples of garnet-schist and a single doubtful example referred to kyanite-schist.

Epidosite: Epidosite fragments consists of equigranular aggregates of anhedral, weakly pleochroic, greenish to brownish-yellow epidote, intergrown in some cases with quartz which may dominate epidote and show alignment. Epidosite is most common in the Hazelbank and Falahill Formations.

Epidote-amphibolite: These consist of equigranular intergrowths of epidote, mid-green to pale green hornblende, and plagioclase which have been subsequently altered. Epidote is present as equigranular aggregates and as individual inclusions within hornblende.

3. SEDIMENTARY ROCK FRAGMENTS

Siltstone: These are the commonest sedimentary fragments, and range in size from less than 1mm to up to 10cm, occurring in all the formations. They are mostly more or less deformed (Plate 3.15). Many display alignment of the mica flakes and some show parallel lamination. The clast tenor of the siltstone fragments closely resembles that of the host rocks. Some of the fragments are very rich in carbonate, to the extent of having only a few relict detrital grains floating in the carbonate matrix. Siltstone fragments commonly have a much higher proportion of carbonate than the host rock, suggesting that they were incorporated late in their diagenetic history.

Greywackes: Fine grained greywacke fragments show characters similar to those of the host rocks and are deformed by compaction, as are the siltstones (Plate 3.15).

Sandstone: Sandstone fragments consist of subangular to subrounded grains of quartz and feldspar cemented by calcite or quartz (Plate 3.14). Quartz fragments may be supported by the calcite matrix; adjacent fragments may show the same optical orientation, suggesting that the quartz grains have been partially replaced along fractures and grain boundaries. Other sedimentary clasts include black shales and limestones.

Fossil fragments: Fossil fragments are very rare in the greywackes; only five fragments were found throughout the area, three in the Hazelbank Formation, one in the Heriot Formation and one in the Buckholm Formation. Those in the Hazelbank Formation include an indeterminate impunctate brachiopod (Plate 3.16), radiolaria enclosed in a chert fragment and an algal fragment which is possibly Dasycladacean; this is a shallow water marine organism (A. R. MacGregor, pers. comm.). The Heriot Formation yielded a solitary echinoderm plate, carrying an encrusting bryozoan; again these are indeterminate. A single phosphatic fish scale recorded from the Buckholm Formation is is probably of thelodont origin. All were probably derived from a shallow marine environment.

APPENDIX No 7.1: List of all folds recorded in the area

Key

S/No = Serial Number
Ax Pl = Attitude of Axial Plane
Ovt = Overturned
Tt = Tight
Grid Ref = Grid Reference
Op = Open
Mono = Monoclinal
Dr = Drag

Q = Quarry
H = Hill
Cl = Cleugh
C = Common
B = Burn
W = Water
Gr = Grain

S/No	Locality	Grid Ref	Axis	Ax Pl	Type
1	Blindlee Q	7418 3736	15 to 53	38/42S	Ovt
2	Nithershiels	4075 4411	14 to 63	70/70N	Op
3	Long Hangman R	3931 4544	44 to 93	80/77S	Op
4	Stagehall H	-	2 to 237	46/84S	Op
5	Bow Castle	-	6 to 238	59/85S	Tt
6	Caddonhead	4026 4114	56-235/Hor	49/40S	Ovt
7	Brockhouse B	4077 5134	20 to 144	104/20S	Ovt
8	Lg Hangman B	4946 4660	10 to 216	82/80S	Op
9	Brockhouse B	3948 5060	60-240/Hor	60/44S	Mono
10	Corsehope B	3938 5136	10 to 90	84/60S	Mono
11	Lugate W	3806 4691	26 to 12	27/75N	Ovt
12	Lugate W	3723 4671	38 to 07	40/56N	Ovt
13	Lugate W	-do-	44 to 33	24/80S	Ovt
14	Lugate W	-do-	61 to 02	40/80N	Ovt
15	Lugate W	-do-	38 to 12	40/60N	Ovt
16	Lugate W	-do-	38 to 07	40/56N	Ovt
17	Lugate W	3660 4698	30 to 349	110/39N	Ovt
18	Lugate W	3810 4690	48 to 16	04/85E	Op
19	Ladyside B	3629 4970	05 to 83	78/55S	Ovt
20	Ladyside B	3606 4955	32 to 82	84/86N	Tt
21	Ladyside B	3587 4941	15 to 206	26/Ver	Op
22	Ladyside B	3653 4892	38 to 228	49/47S	Ovt
23	Ladyside B	3691 4883	04 to 32	30/58S	Ovt
24	Ladyside B	3660 4845	41 to 70	49/67S	Ovt
25	Ladyside B	3622 4820	26 to 57	50/74S	Ovt
26	Sole B	3690 4651	37 to 47	47/Ver	Tt
27	Shank Cleugh	3806 3638	13 to 139	139/Ver	Op
28	Sit B	3802 4811	42 to 279	108/80S	Dr
29	Sit B	3921 4785	58 to 02	62/62N	Ovt
30	Sit B	3911 4788	35 to 70	65/85S	Op
31	Heathery B	3950 4779	37 to 80	60/66S	Op
32	Ewes W	3860 4622	20 to 238	44/80N	Op
33	Ewes W	3839 4585	10 to 244	61/80N	Tt
34	Trously B	3792 4885	12 to 218	35/75N	Tt
35	Trously B	3788 4582	23 to 62	92/40N	Op
36	Trously B	3750 4552	04 to 248	68/85S	Op
37	Ewes W	3775 4488	02 to 60	59/60S	Op
38	Ewes W	3769 4471	18 to 224	53/68S	Tt
39	Ewes W	3771 4465	06 to 36	32/74S	Tt
40	Trously B	3788 4500	65 to 246	48/82N	Tt
41	Trously B	3788 4500	32 to 20	55/48N	Tt
42	Ewes W	3837 4486	38 to 221	49/78S	Tt
43	Merlin's Cl	3977 4311	30 to 92	75/60S	Op
44	Armet W	4348 5405	10 to 43	38/40S	Ovt

APPENDIX No 7.1: List of all folds recorded in the area - continued

45	Armet W	4357 5395	10 to 36	27/42S	Ovt
46	Hazelbank	4238 5060	45 to 05	24/72N	Tt
47	Hazelbank	-do-	50 to 30	30/Ver	Op
48	Caddon W	3850 4391	36 to 53	30/59S	Ovt
49	Ewes W	3772 4437	46 to 35	45/80N	Op
50	Ewes W	3870 4498	20 to 50	63/60N	Op
51	Ewes W	3877 4498	30 to 60	60/Ver	Op
52	Caberston Gr	3736 4173	90-180/Hor	90/65S	Ovt
53	Caddon W	3938 4232	10 to 204	25/85S	Op
54	Falahill	3949 5539	68 to 79	79/Ver	Op
55	Selkirk H	4790 2782	20 to 40	42/85N	Tt
56	Selkirk C	4757 2770	44-224/Hor	44/Ver	Tt
57	Selkirk C	-do-	08 to 48	49/85N	Tt
58	Selkirk C	4759 2760	20 to 224	45/Ver	Tt
59	Selkirk C	-do-	32-312/Hor	32/Ver	Tt
60	Selkirk C	-do-	34-214/Hor	34/Ver	Tt
61	Selkirk C	-do-	54 to 08	176/82F	Tt
62	Selkirk C	7460 2755	40-220/Hor	40/Ver	Tt
63	Selkirk C	-do-	32 to 56	48/79S	Tt
64	Selkirk C	-do-	40 to 54	52/87S	Tt
65	Selkirk C	-do-	02 to 211	31/80N	Tt
66	Selkirk C	-do-	30-210/Hor	30/78N	Tt
67	Selkirk C	-do-	34-214/Hor	34/Ver	Tt
68	Selkirk C	-do-	35-215/Hor	35/Ver	Tt
69	Selkirk C	4778 2728	38 to 238	68/76S	Op
70	Selkirk C	-do-	40 to 236	66/78S	Op
71	Selkirk C	4800 2616	04 to 32	30/78S	Tt
72	Selkirk C	-do-	28 to 46	43/84S	Tt
73	Selkirk C	4853 2589	04 to 221	42/77S	Tt
74	Selkirk C	4916 2638	03 to 07	10/55N	Mono
75	Bell H	4888 2870	42 to 239	47/78N	Ovt
76	Whitemuir H	4975 2790	24 to 29	29/Ver	Tt
77	Whitemuir H	-do-	29 to 27	30/86N	Tt
78	Selkirk C	9760 2755	33-213/Hor	33/Ver	Tt
79	Ewes W	-	42-222/Hor	42/Ver	

APPENDIX NO 7.2 Morphology of the exposed folds

Index:-
ILA = inter limb angle
LL = long limb
SL = short limb
BTL = bed thickness at limb
BTH = bed thickness at hinge
OV = overturned
NLL = Northern limb longer

S No	Locality	Grid Ref	(ILA)	Type	Vergence	Amplitude	Wavelength	SL:LL	BTL:BTH
1	212 Lugate water	395 467	?	Mono-clinal	SE	few cm	?	?	?
2	512 Sit Burn	392 478	50	close	SE	25 cm	70 cm	NLL	2:3
3	516 Sit Burn	388 481	65	close	?	8-25 cm	35-1 cm	1:1	1:1
4	585-a Lugate Water	399 439	45	close	?	40 cm	60 cm	2:3	2:3
5	585-b Lugate Water	-do-	125	Gentle	?	5 cm	1.5 m	?	1:2
6	585-c Lugate Water	-do-	42	close (ov)	NW	30 cm	1 m	2:3	1:1
7	538	386 462	90	open	?SE	?	?	?	?
8	542	384 458	80	open	?SE	?	40-50 m	?	?
9	565-b	378 449	50-55	close	?NW	1 m	2 m	?	?
10	570	384 449	55-65	close	?NW	?	?	?	?
11	175	401 452	40	close	?SE	?	?	?	?
12	257	426 492	150	Gentle Monoclinal	SE	2 cm	6 cm	?	?
13	250	409 486	60-70	close (ov)	SE	6-10 cm	20-30 cm	NLL	1:2
14	02	424 506	40	close (ov)	SE	50 cm - 2 m	3 - 5 m	2:15	1:1-1:2
15	305-a	407 513	30	Tight (ov)	SE	?	2.5 cm	NLL	1:2
16	305-b	-do-	130-140	Gentle	?	4-5 cm	55 cm	?	?
17	309	402 510	40-45	close (ov)	?NW	?	2.5-3 m	2:3	?
18	417	361 496	45-55	close (ov)	NW	25 cm	50 cm	1:5	1:2
19	333	465 527	40-50	close (ov)	SE	20 cm	65 cm	1:3	1:2
20	615	435 540	40	close (ov)	SE	28 cm	68 cm	1:4	2:3
21	615	436 540	45	close (ov)	SE	13 cm	32 cm	1:20	2:3
22	30	395 554	85	open (ov)	?SE	?	?	?	?
23	742	476 276	45-60	close	SE	1.5-2 m	20-30 m	1:3	2:3
24	743	476 275	40-60	close	?NW	2-5 m	20-30 m	2:3-1:4	2:3
25	745	478 273	80	open	SE	75 - 1 m	20-30 m	1:18	2:3
26	739	479 278	60	close	?SE	several metres	?50-100 m	2:3	2:3

APPENDIX No 7.3: Details of all faults recorded in the area

Key

S/No	= Serial Number	Grid Ref	= Grid Reference
At F Pl	= Attitude of Fault Plane	Sin	= Sinistral
Pc	= Pitch Angle	OS	= Oblique Slip
Ty	= Type		
Dex	= Dextural		
Rev	= Reverse		
Q	= Quarry	B	= Burn
Tl	= Tunnel	Cl	= Cleugh
W	= Water	Cr	= Graig
C	= Common	H	= Hill

S/No	Locality	Grid Ref	At F Pl	Pc	Ty
1	Hazelbank	4238 5060	35/72N	15 N	Dex
2	Hazelbank	-do-	105/76N	?	Rev
3	Hazelbank	-do-	20/80N	30 N	OS
4	Hazelbank	-do-	42/79N	07 N	Dex
5	Hazelbank	-do-	10/Ver	25 N	Sin
6	Hazelbank	-do-	30/77N	47 N	OS
7	Hazelbank	-do-	40/35N	45 S	OS
8	Hazelbank	-do-	360/Ver	21 N	Sin
9	Hazelbank	-do-	85/40N	?	?
10	Hazelbank	-do-	70/51N	0	Sin
11	Hazelbank	-do-	150/77N	70 S	OS
12	Hazelbank	-do-	175/Ver	?	?
13	Hazelbank	-do-	55/76N	39 S	OS
14	Hazelbank	-do-	120/76N	57 N	OS
15	Hazelbank	-do-	85/66N	12 N	?
16	Hangingshaw Q	5403 4068	170/Ver	90	Rev
17	Hangingshaw Q	-do-	40/65S	?	?
18	Craigend H Q	4441 4615	30/84S	30 S	OS
19	Craigend H Q	-do-	135/80S	24 N	Sin
20	Craigend H Q	-do-	136/80S	25 N	Sin
21	Craigend H Q	-do-	20/71S	20 S	?
22	Craigend H Q	-do-	130/80S	10 N	Sin
23	Craigend H Q	-do-	130/40S	35 S	OS
24	Craigend H Q	-do-	150/80S	35 S	OS
25	Craigend H	4604 4424	15/65S	60 S	OS
26	Allan's Haugh	4362 4944	50/81S	90	Rev
27	Allan's Haugh	-do-	120/61N	21 N	Sin
28	Allan's Haugh	-do-	115/68N	58 N	OS
29	Allan's Haugh	-do-	172/70E	00	Dex
30	Knowes Dean	4367 3933	60/68S	23 S	Sin
31	Bow Bridge	4494 5172	32/77S	80 N	OS
32	Bow Bridge	-do-	120/30N	11 S	Sin
33	Watherston B	4383 4628	85/63N	20 S	Sin
34	Bowshank Tl	4540 4113	08/65S	65 N	OS
35	Whitelee Q	4605 3983	170/72W	20 S	Dex
36	Whitelee Q	-do-	150/70N	40 S	OS
37	Blindlee	4677 3730	75/74N	60 N	OS
38	Buckholm	4782 3795	80/75N	20 S	Dex
39	Buckholm	4787 3805	80/75N	50 S	OS

APPENDIX No 7.3: Details of all faults recorded in the area - continued

40	Caddonlee	4491	3516	150/74S	20 N	Sin
41	Whytbank	4482	3691	75/80N	30 N	OS
42	Whytbank	-do-		05/Ver	?	Dex
43	Whytbank	4477	3737	65/50N	77 N	OS
44	Whytbank	-do-		360/35W	70 S	OS
45	Falahill	3972	5645	25/75S	?	Dex
46	Falahill	3961	5638	50/83S	50 N	OS
47	Whitelaw Cl	3636	5532	05/Ver	?	Sin
48	Hazelbank	4242	5096	75/42N	30 N	OS
49	Hazelbank	-do-		52/45N	45 N	OS
50	Hazelbank	-do-		60/45N	50 N	OS
51	Hazelbank	-do-		25/45N	45 N	OS
52	Hazelbank Q	5041	4266	82/67S	05 S	Sin
53	Hazelbank Q	-do-		65/80N	?	Sin
54	Hazelbank Q	-do-		10/85S	?	?
55	Hazelbank Q	-do-		02/40S	60 S	OS
56	Hazelbank Q	-do-		140/70S	0	Sin
57	Hazelbank Q	-do-		70/75S	10 N	Sin
58	Hazelbank Q	4259	5048	175/60W	30 N	OS
59	Hazelbank Q	4250	5050	10/80S	0	Sin
60	Hazelbank Q	-do-		80/Ver	06 N	Sin
61	Hazelbank Q	-do-		15/Ver	90	Rev
62	Hazelbank Q	4257	5060	40/Ver	0	Sin
63	Hazelbank Q	-do-		15/75S	?	?
64	Hazelbank Q	-do-		65/70S	56 S	OS
65	Hazelbank Q	4256	5057	25/86N	30 N	OS
66	Hazelbank Q	-do-		175/80W	45 N	OS
67	Hazelbank Q	-do-		170/60"	?	?
68	Hazelbank Q	-do-		50/88S	?	?
69	Hazelbank Q	-do-		60/80S	40 N	OS
70	Hazelbank Q	4261	5051	140/84N	44 N	OS
71	Hazelbank Q	-do-		30/45N	?	?
72	Cortleferry Q	4293	5007	70/Ver	50 N	OS
73	Cortleferry Q	-do-		115/85N	20 N	Dex
74	Watherston	4423	4625	15/61S	52 N	OS
75	Coller Cl	3676	5085	100/80S	?	Dex
76	Coller Cl	3693	5072	40/80N	30 N	OS
77	Ladyside B	3643	4994	95/20N	40 S	OS
78	Ladyside B	3640	5000	60/60S	07 N	Dex
79	Ladyside B	3630	4995	140/Ver	?	Sin
80	Ladyside B	-do-		100/42N	73 S	OS
81	Ladyside B	-do-		160/80E	10 S	Sin
82	Ladyside B	3637	4985	65/75S	50 N	OS
83	Ladyside B	-do-		80/75S	50 N	OS
84	Ladyside B	-do-		85/80S	40 N	OS
85	Ladyside B	-do-		70/85S	45 N	OS
86	Ladyside B	-do-		80/Ver	40 N	OS
87	Ladyside B	-do-		90/75S	30 S	OS
88	Ladyside B	-do-		75/85S	45 N	OS
89	Ladyside B	3613	4961	80/70N	?	?Rev
90	Ladyside B	3597	4945	20/Ver	50 N	OS
91	Ladyside B	3512	4942	55/30N	60 S	OS
92	Ladyside B	3587	4941	50/Ver	?	?
93	Ladyside B	3632	4960	360/40E	55 N	OS
94	Ladyside B	3649	4939	55/75S	25 S	Sin
95	Ladyside B	-do-		65/85S	45 N	OS

APPENDIX No 7.3: Details of all faults recorded in the area - continued

96	Ladyside B	3653	4892	135/50S	?	Dex
97	Ladyside B	-do-		80/60N	?	Rev
98	Glentress B	3760	4891	20/Ver	45 N	OS
99	Raw B	3712	4806	25/75N	30 N	OS
100	Sole B	3690	4651	135/80N	30 S	OS
101	Lugate W	3710	4653	130/Ver	0	Sin
102	Lugate W	3795	4693	10/80S	90	Rev
103	Lugate W	-do-		130/65N	90	Rev
104	Lugate W	-do-		45/80S	90	Rev
105	Sit B	3943	4766	40/80N	?	Rev
106	Sit B	-do-		60/60N	?	?Rev
107	Sit B	3970	4706	80/50N	?	?Rev
108	Toathieknowe B	3585	5254	170/30E	30 N	OS
109	Falahill	3949	5539	50/85S	?	?Rev
110	Falahill	-do-		30/80S	?	?Rev
111	Ewes W	3855	4619	80/80S	?	?Rev
112	Ewes W	3832	4520	60/75N	05 S	Sin
113	Lugate W	3946	4664	60/36N	90	Rev
114	Lugate W	-do-		60/75N	90	Rev
115	Lugate W	-do-		110/70S	?	?Rev
116	Lugate W	-do-		70/65N	?	?Rev
117	Caddon W	4032	4297	30/85S	90	Rev
118	Birehope B	3983	4318	50/80N	70 S	OS
119	Merlin's Cl	3955	4300	75/25S	80 N	OS
120	Merlin's Cl	-do-		75/55S	90	Rev
121	Ewes W	3770	4459	10/60N	60 N	OS
122	Trously B	3788	4582	50/Ver	?	?Rev
123	Raeshaw Q	3587	5038	115/60N	?	?
124	Raeshaw Q	-do-		90/75S	65 N	OS
125	Hoppringle W	4267	5112	360/65E	?	?Rev
126	Armet W	4360	5391	80/40N	70 S	OS
127	Armet W	4381	5480	05/?E	80 N	OS
128	Ewes W	3841	4460	30/85S	70 N	OS
129	Ewes W	3839	4467	80/65S	?	?Rev
130	Holylee	3989	3707	360/85W	40 S	OS
131	Holylee	-do-		28/65S	70 S	OS
132	Holylee	-do-		35/70S	90	Rev
133	Holylee	-do-		160/70W	35 S	OS
134	Stony Knowe	3957	3895	20/25S	90	Rev
135	Holylee B	3921	3789	5/75S	15 S	Sin
136	Seathope H	3760	3971	10/45W	90	Rev
137	Gatehope B	3733	3919	10/50E	90	Rev
138	Seathope B	3826	4130	30/45S	90	Rev
139	Seathope B	3830	4095	90/60S	00	Dex
140	Caddon W	4017	4075	40/70S	70 S	OS
141	Hersie B	3914	4176	105/35S	90	Rev
142	Hersie B	3902	4167	50/60S	90	Rev
143	Hersie B	3897	4170	50/55S	90	Rev
144	Plora B	3642	3642	50/65S	55 S	OS
145	Plora B	3625	3549	60/65S	20 N	Sin
146	Whytbank Q	4482	3691	70/70N	35 S	OS
147	Whytbank Q	-do-		95/40N	90	Rev
148	Thornylee Cr	4013	3690	25/20N	90	Rev
149	Thornylee Cr	-do-		30/15S	90	Rev
150	Touting H	4911	3377	70/45N	70 S	OS
151	Touting H	-do-		25/65S	70 N	OS

APPENDIX No 7.3: Details of all faults recorded in the area - continued

152	Touting H	-do-	100/45N	60 S	OS
153	Falahill	3949 5539	60/55N	?	?Rev
154	Selkirk H	4790 2782	45/Ver	00	Dex
155	Selkirk H	-do-	25/Ver	10 N	Sin
156	Selkirk H	-do-	45/60S	?	?Rev
157	Selkirk H	-do-	25/60N	50 N	OS
158	Selkirk C	4757 2770	45/60N	00	Dex
159	Selkirk C	4759 2760	40/72N	30 S	OS
160	Selkirk C	-do-	55/45N	90	Rev
161	Selkirk C	4759 2760	35/65N	00	Sin
162	Selkirk C	-do-	30/60N	05 S	Sin
163	Selkirk C	-do-	20/65N	05 S	Sin
164	Selkirk C	-do-	35/70S	35 N	OS
165	Selkirk C	4760 2755	20/70N	90	Rev
166	Selkirk C	-do-	360/75E	00	Dex
167	Selkirk C	-do-	110/80N	?	?Rev
168	Selkirk C	-do-	165/70N	20 S	Sin
169	Selkirk C	-do-	360/60W	00	Sin
170	Selkirk C	4778 2728	30/55S		?Rev
171	Selkirk C	-do-	100/Ver	20 S	Sin
172	Selkirk C	4916 2638	50/75S	00	Sin
173	Selkirk C	-do-	20/75N	20 N	Sin
174	Linglee H	4623 3027	75/35N	45 N	OS
175	Hog Knowes	4933 2834	10/85S	00	Sin
176	Hog Knowes	-do-	140/70S	00	Sin
177	Black Law	4115 4819	115/30N	00	Dex
178	Black Law	-do-	110/32N	00	Dex
179	Black Law	-do	115/35N	00	Dex

Appendix 8.1: Grid references of specimens selected for XRD analysis.

S/No	Sp No	Formation	Grid Reference
1	Ak-80	Falahill	3949 5539
2	Ak-336	"	3650 5289
3	Ak-338	"	3642 5315
4	Ak-340	"	3611 5324
5	Ak-03	Heriot	4068 5403
6	Ak-81	"	4189 5435
7	Ak-85	"	4125 5323
8	Ak-328	"	3717 5357
9	Ak-334	"	3648 5276
10	Ak-535	"	4055 5340
11	Ak-620	"	4409 5467
12	Ak-02	Hazelbank	4238 5060
13	Ak-84b	"	4266 5041
14	Ak-387b	"	3808 4991
15	Ak-407a	"	3643 4994
16	Ak-440	"	3710 4923
17	Ak-228	Fountainhall	4280 4886
18	Ak-259	"	4213 4987
19	Ak-292	"	4017 4175
20	Ak-498	"	3770 4686
21	Ak-567	"	3792 4503
22	Ak-4a	Buckholm	4441 4615
23	Ak-48	"	4605 3983
24	Ak-74	"	4354 3726
25	Ak-641	"	3989 3707
26	Ak-686	"	3929 4066
27	Ak-769	"	4605 3025
28	Ak-734	Selkirk	4803 2840
29	Ak-739	"	4790 2782
30	Ak-741	"	4757 2770
31	Ak-742	"	4759 2760
32	Ak-748	"	4801 2591
33	Ak-752	"	4853 2589
34	Ak-763	"	4829 6220

Appendix 8.2 Separation of clay fraction from greywacke matrix

Unweathered parts of the samples (approximately 300g) were chosen and any visible weathering and secondary effects were removed using the 6 inch diamond wheel. The material was crushed to chips (1-2 cm) and washed by distilled water, dried, then ground in a Teema mill for 1 minute. Further disaggregation was obtained by placing the powder/water mixture in ultrasonic bath for 10 minutes. The slurry was then transferred to a water-filled glass test tube and shaken well to ensure thorough mixing. Four samples at a time were centrifuged for 40 seconds at a speed setting of 5, and the suspension transferred into other clean test tubes, again centrifuged for 40 seconds at a setting of 7. This time the suspension was removed and the settled fraction is the required clay fraction (2-6 μm) for X.R.D. analysis.

Appendix 8.3 Instrumental conditions of X.R.D. for clay mineral determination

Source Cu K(α): normal focus: Ni filter

Slit 1^{o}-0.2-1^{o} : Chart speed: 1200 mm/h

Angular goniometer speed: 1^{o}/min

Scan: 3-35^{o} 2θ Time constant: 2S: Z=3

36KV, 18mA

Glycolated and Heated Specimens

Runs of glycolated and heated specimens were made to check for the presence of mixed layering. The samples were treated with ethylene glycol for one hour, and heated up to 600^{o}C for 1 hour.

HCl treatment

Approximately 10 g of the powdered sample were mixed with 20 ml of HCl (18%), thoroughly mixed and heated up to 80^{o}C for 8 hours. The sample was then washed and transferred to water filed 50 ml test tube, shaken well and left for 30 minuts. The uppermost sedimented layer was then mounted on a glass slide for X.R.D. run.

DMSO treatment

Approximately 10 g of the powdered samples were mixed with 20 ml of dimethylsupphoxide (DMSO) and heated up to 180°C for 72 hours. The samples were then washed and put into a 50 ml water filled test tube, shaken well and and left for 30 minutes to settle down. The uppermost layer (~8 μm) was mounted on glass slide for X.R.D. run.

Appendix 8.4 Illite crystallinity: measurement

The samples prepared for clay mineral analysis (~6 μm) mounted on glass slides were also used for illite crystallinity measurements (separation methods described in Appendix 8.2). The instrumental conditions used are as follows.

Source: Cu K(α): normal focus: Ni filter

Slit: 1^{o}-0.2-1^{o}

Chart speed: 600 mm/h

Angular goniometer speed: 0.5^{o}/min

Time constant: 4S : Z=3

Rate meter speed: 4 x 10^{2} counts/sec

Phillips PW1012/20 diffractometer.

At least 5 measurements were taken per specimen, scanning from 7.5^{o} to 10^{o} 2θ, followed by three runs of quartz standard from 20 to 21.5^{o} 2θ. The widths of 5 illite peaks for each sample were taken exactly half way between the level of background reflection and the top of the peak, and their mean calculated. The mean of the 1/2 peak width of quartz (100) was also determined in a similar way and the Weber index calculated using the following equation.

Hbrel = [Hb (001) Illite (mm)/ Hb (100) Quartz (mm)] X 100

where Hbrel= Halbwertbreite relative (after Weber 1972b)

Appendix 8.5: Illite crystallinity results

Sp No	Kubler Index	Weber Index	I(002)/I(001)
FALAHILL			
Ak-80	0.31	137.2	0.62
Ak-328	0.29	137.2	0.63
Ak-336	0.26	123.2	-
Ak-338	0.29	137.2	0.63
HERIOT			
Ak-81	0.44	160.0	0.67
Ak-85	0.31	143.1	0.39
Ak-334	0.29	135.5	0.43
Ak-535	0.28	143.3	0.41
Ak-620	0.34	129.0	0.45
HAZELBANK			
Ak-02	0.26	123.6	0.43
Ak-387b	0.34	150.9	0.38
Ak-407a	0.43	150.0	0.38
Ak-440	0.29	136.3	0.46
FOUNTAINHALL			
Ak-228	0.39	140.0	0.50
Ak-259	0.41	154.0	0.36
Ak-292	0.27	136.4	0.40
Ak-498	0.31	143.6	0.41
Ak-567	0.36	143.0	0.50
Ak-686	0.30	136.2	0.30
BUCKHOIM			
Ak-4a	0.35	123.0	0.52
Ak-48	0.49	168.0	0.30
Ak-74	0.29	134.5	0.44
Ak-641	0.37	124.0	0.41
Ak-718	0.37	137.0	0.35
Ak-769	0.30	140.0	0.42
SELKIRK			
Ak-734	0.41	150.0	0.36
Ak-739	0.34	127.0	0.50
Ak-741	0.39	140.0	0.47
Ak-742	0.37	134.0	0.46
Ak-748	0.37	136.0	0.38
Ak-752	0.41	149.0	0.40
Ak-763	0.46	164.0	0.59

NB Locality and Grid references of samples are given in Appendix 7.1.

Appendix 8.6: Parameters of illite

Sp No	Position of (001)			d (060)$^{2\theta}$	bo A^{o}
	Normal	Glycolated	600 ^{o}C		
Ak-02	10.04	10.04	10.04	61.62	9.023
Ak-4a	10.12	10.05	9.93	61.40	9.052
Ak-48	10.04	10.04	10.04	61.43	9.026
Ak-74	9.98	10.04	10.04	61.60	9.026
Ak-80	9.93	10.04	-	61.70	9.013
Ak-81	9.99	9.97	10.13	61.62	9.023
Ak-85	9.98	9.99	10.04	61.44	9.047
Ak-228	9.93	9.94	-	61.47	9.043
Ak-259	10.02	9.93	10.08	61.60	9.026
Ak-292	10.10	9.93	10.04	61.50	9.039
Ak-328	10.12	10.09	10.04	61.48	9.042
Ak-334	9.98	10.05	10.04	61.53	9.035
Ak-336	9.83	10.04	10.04	61.33	9.062
Ak-338	10.04	10.12	10.04	61.50	9.039
Ak-387b	10.12	9.88	9.98	61.39	9.044
Ak-407a	9.98	9.93	-	61.39	9.055
Ak-440	10.04	10.05	9.99	61.68	9.016
Ak-498	9.99	9.93	10.10	61.73	9.009
Ak-535	10.04	9.98	9.93	61.66	9.018
Ak-567	9.99	9.97	10.04	-	-
Ak-620	9.98	9.97	9.88	61.49	9.041
Ak-641	9.99	10.02	9.99	61.72	9.010
Ak-686	9.98	10.04	10.09	61.47	9.043
Ak-718	10.10	9.93	10.09	61.53	9.035
Ak-734	10.12	10.04	9.98	61.53	9.037
Ak-739	9.99	9.98	10.04	61.48	9.042
Ak-741	9.93	9.99	10.04	61.56	9.031
Ak-742	10.09	9.93	10.04	61.58	9.029
Ak-748	10.04	9.99	10.09	61.61	9.025
Ak-752	10.04	10.05	10.01	61.36	9.058
Ak-763	9.98	9.88	10.04	61.53	9.037
Ak-769	9.98	9.88	9.99	61.47	9.043

NB Localities and Grid references of the samples are given in Appendix 7.1.

Appendix 8.7: Position of first four basal reflections of Chlorite/Kaolinite in normal run, and position of reflection at 7 ^{o}A, after HCl, Heat, Ethyline Glycole and DMSO treatment.

Sp No	Untreated run				/001/ /002/ A^{o} of Chlorite/Kaolinite			
	(001)	(002)	(003)	(004)	HCl	EG	600 ^{o}C	DMSO Ch K
Ak-02	14.48	7.13	4.74	3.55	7.13, d	7.1C	cps	7.05, 7.44
Ak-4a	14.24	7.11	4.74	3.54	7.09	7.11	cps	7.05, 7.46
Ak-48	14.50	7.17	4.87	3.55	7.1C	7.13	cps	-
Ak-74	14.24	7.10	4.73	3.54	7.13	7.08	cps	-
Ak-80	14.24	7.11	4.74	3.55	cps	7.09	cps	-
Ak-81	14.24	7.08	4.79	3.55	cps	7.09	cps	-
Ak-85	14.36	7.13	4.75	3.55	7.09, d	7.13	cps	7.01 only
Ak-228	14.36	7.10	4.74	3.55	cps	7.11	cps	-
Ak-259	14.22	7.15	4.75	3.55	cps	7.10	cps	-
Ak-292	14.36	7.34	4.73	3.55	cps	7.13	cps	7.13, 7.62
Ak-328	14.38	7.04	4.74	3.56	7.11, d	7.10	cps	-
Ak-334	14.24	7.11	4.74	3.56	7.18, d	7.13	cps	-
Ak-336	14.38	7.11	4.74	3.57	7.22, d	7.11	cps	7.10 only
Ak-338	14.48	7.10	4.74	3.56	7.12, d	7.11	cps	7.10 only
Ak-340	14.48	7.1C	4.75	3.66	cps	7.13	cps	-
Ak-387b	14.62	7.22	4.75	3.55	7.09, d	7.11	cps	-
Ak-407a	14.38	7.10	4.74	3.55	cps	7.13	cps	-
Ak-440	14.70	7.13	4.76	3.55	cps	7.11	cps	7.16, 7.65
Ak-498	14.38	7.11	4.73	3.53	cps	7.10	cps	-
Ak-535	14.24	7.1C	4.73	3.53	7.C6	7.1C	cps	7.1C, 7.43
Ak-567	14.36	7.1C	7.74	3.54	7.07	7.C9	cps	-
Ak-62C	14.24	7.1C	4.74	3.55	cps	7.09	cps	7.13, 7.59
Ak-641	14.37	7.09	4.74	3.52	cps	7.09	cps	-
Ak-686	14.48	7.21	4.73	3.56	7.C5, d	7.13	cps	7.13, 7.59

Appendix 8.7 - continued

Sp No	Untreated run				[001]/[002] A° of Chlorite/Kaolinite			
	(001)	(002)	(003)	(004)	HCl	EG	600 °C	DMSO Ch K
Ak-718	14.48	7.10	4.74	3.54	7.12, d	7.09	cps	-
Ak-734	14.38	7.11	4.74	3.54	7.07	7.10	cps	7.13, 7.62
Ak-739	14.38	7.11	4.74	3.54	7.10	7.07	cps	7.10, 7.59
Ak-741	14.24	7.11	4.74	3.53	7.10	7.11	cps	-
Ak-742	14.48	7.16	4.73	3.56	7.08	7.07	cps	7.10, 7.68
Ak-748	14.48	7.10	4.74	3.53	cps	7.11	cps	7.07 only
Ak-752	14.24	7.13	4.74	3.56	7.05	7.11	cps	7.05, 7.55
Ak-763	14.24	7.11	4.74	3.54	cps	7.05	cps	7.13 only
Ak-769	14.24	7.10	4.74	3.55	7.14	7.13	cps	7.07 only

d = depressed

NB Locality and Grid references are of the specimens given in Appendix 7.1.

cps = collapsed

APPENDIX No 8.8: Electron probe microanalyses of pumpellyite

	1 Ak 80a	2 Ak 412	3 Ak 337
SiO_2	56.31	51.89	69.60
Al_2O_3	16.61	15.53	13.16
FeO*	5.42	5.45	1.55
TiO	1.24	0.78	0.01
MgO	4.23	3.78	3.33
MnO	0.09	0.11	0.08
K_2O	0.73	0.54	1.84
F_2O	-	-	-
CaO	4.15	9.93	3.02
Na_2O	7.65	6.22	3.19
Total	96.44	94.25	95.78
*All iron as FeO Ions based on 26 oxygens			
Si	8.76	8.45	10.26
Al	3.05	2.98	2.29
Fe	0.70	0.74	0.19
Ti	0.15	0.10	-
Mg	0.98	0.92	0.73
Mn	0.01	0.02	0.01
K	0.14	0.11	0.35
F	-	-	-
Ca	0.69	1.73	0.48
Na	2.31	1.96	0.91
Total	16.80	17.01	15.23

APPENDIX 8.9: Electron probe microanalyses of prehnite

	1 Ak 338	2 Ak 338	3 Ak 80-b	4 Ak 80-b
SiO_2	54.25	79.97	42.94	43.52
Al_2O_3	19.00	8.36	22.62	23.68
FeO*	0.10	0.12	1.85	1.57
MgO	0.01	0.03	0.01	0.22
MnO	0.04	0.04	0.05	0.03
CaO	21.57	9.52	26.06	24.14
Total	95.02	98.12	93.58	94.23
*All iron as FeO Ions based on 26 oxygens				
Si	8.53	11.23	7.18	7.19
Al	3.52	1.38	4.46	4.62
Fe	0.01	0.01	0.26	0.23
Mg	0.01	0.01	-	-
Mn	0.01	0.00	0.01	-
Ca	3.63	1.43	4.67	4.28
Total	15.72	14.09	16.60	16.59

APPENDIX No 8.10 Electron probe microanalyses of chlorites

	1 Ak 60-a	2 Ak 8-a	3 Ak 8-a	4 Ak 8-a	5 Ak 80-b	6 Ak 2L	7 Ak 214	8 Ak 365	9 Ak 3/11	10 Ak 780	11 Ak 380	12 Ak 316	13 Ak 336	14 Ak 337	15 Ak 159	16 Ak 159	17 Ak 759	18 Ak 1	19 Ak 1
SiO_2	32.14	23.73	24.64	24.17	27.97	24.36	34.21	29.73	28.90	25.08	29.20	29.80	27.33	22.68	29.88	23.25	27.84	29.04	28.72
Al_2O_3	18.49	21.13	19.76	20.45	15.70	20.92	20.90	14.15	15.72	17.65	17.15	13.77	21.77	17.13	17.77	21.42	17.50	16.47	17.01
FeO*	23.32	29.43	30.23	31.77	27.81	30.83	10.97	21.11	23.07	32.35	24.43	26.25	10.42	22.73	15.38	31.42	26.99	23.96	20.35
TiO_2	0.12	0.05	0.04	0.04	-	0.05	0.02	-	0.03	0.04	-	-	-	-	-	0.02	0.01	-	-
MgO	10.19	11.52	12.02	10.14	14.52	10.73	18.19	19.83	16.72	10.88	15.16	16.70	25.00	17.48	22.60	9.78	13.47	16.08	19.97
MnO	1.00	0.36	0.54	0.30	0.32	0.33	0.23	0.31	0.30	0.25	0.23	0.26	0.18	0.24	0.07	0.46	0.28	0.21	0.20
K_2O	1.96	0.00	-	0.00	-	-	2.88	0.02	0.05	0.04	0.52	0.01	-	0.06	0.01	-	0.27	0.16	0.01
Na_2O	0.51	0.02	0.01	0.01	0.08	0.01	0.04	0.04	0.05	0.02	0.05	0.07	0.01	0.04	0.02	0.01	0.01	0.06	0.02
CaO	0.17	0.01	0.02	0.02	0.15	0.04	0.09	0.16	0.45	0.03	0.19	0.11	-	0.14	0.09	-	0.22	0.23	0.22
Total	87.44	86.30	87.32	86.99	86.57	87.27	87.54	85.35	85.44	86.37	86.94	86.98	85.52	86.75	85.83	86.04	86.61	86.21	85.51
Ions based on 28 oxygens * All iron as FeO																			
Si	6.71	5.23	5.40	5.34	6.06	5.33	6.66	6.30	6.20	5.62	6.71	6.36	5.45	6.05	6.07	5.19	6.00	6.17	6.04
Al	4.55	5.49	5.09	5.33	4.01	5.40	4.80	3.53	3.96	4.66	4.27	3.46	5.12	4.23	4.25	5.64	4.45	4.13	4.21
Fe	4.07	5.42	5.52	5.88	5.04	5.64	1.78	3.74	4.13	6.06	4.32	4.69	1.74	3.99	2.61	5.81	4.86	4.26	3.58
Ti	0.02	0.01	0.01	0.01	-	0.01	0.00	-	0.00	0.01	-	-	-	-	-	-	-	-	-
Mg	3.17	3.79	3.92	3.34	4.69	3.50	5.28	6.26	5.33	3.63	4.77	5.31	7.66	5.46	6.84	3.26	4.33	5.09	5.94
Mn	0.17	0.07	0.10	0.07	0.06	0.06	0.04	0.06	0.07	0.05	0.04	0.05	0.03	0.04	0.01	0.09	0.05	0.04	0.04
K	0.52	0.00	-	0.00	-	-	0.71	0.01	0.01	0.01	0.14	0.00	-	0.02	-	-	0.07	0.04	-
Na	0.02	0.01	0.01	0.00	0.04	0.00	0.02	0.02	0.02	0.01	0.02	0.03	0.00	0.02	0.01	0.01	0.01	0.02	0.01
Ca	0.38	0.00	0.01	0.00	0.04	0.01	0.02	0.04	0.10	0.01	0.04	0.03	-	0.03	0.02	-	0.05	0.05	0.05
Total	19.27	20.02	20.06	19.99	19.95	19.96	19.31	19.95	19.84	20.06	19.78	19.83	20.00	19.85	19.82	20.00	19.82	19.81	19.87

	20 Ak 3	21 Ak 764	22 Ak 45	23 Ak 45	24 Ak 214	25 Ak 214	26 Ak 214	27 Ak 85	28 Ak 85	29 Ak 654-a	30 Ak 654-a	31 Ak 654-a
SiO_2	28.71	36.91	25.72	26.30	29.60	28.62	24.91	31.57	26.74	29.91	28.40	27.23
Al_2O_3	17.43	18.26	19.61	21.77	17.95	17.68	20.04	16.57	19.44	17.84	18.02	18.79
FeO*	21.25	13.36	22.26	26.97	20.27	21.21	30.98	18.15	25.43	23.97	20.56	25.09
TiO_2	-	-	0.03	0.10	0.04	0.02	0.10	0.02	0.05	0.04	0.03	0.04
MgO	18.05	15.43	17.57	10.09	17.84	18.28	11.31	18.20	14.28	14.23	19.37	14.79
MnO	0.19	0.16	0.04	0.28	0.18	0.19	0.24	0.15	0.15	0.16	0.26	0.32
K_2O	0.04	3.47	0.01	0.03	0.30	0.17	0.01	0.42	0.44	0.17	0.04	0.11
Na_2O	0.03	0.06	0.01	0.15	0.02	0.04	0.01	0.05	0.00	0.06	0.01	0.02
CaO	0.28	0.09	0.01	0.02	0.17	0.17	0.02	0.39	0.02	0.38	0.09	0.09
Total	85.98	86.75	85.60	87.00	86.47	86.39	87.63	85.52	86.57	86.78	86.78	86.48

Ions based on 28 oxygens
* All iron as FeO

Si	6.03	7.14	5.48	5.66	6.14	5.98	5.43	6.52	5.72	6.28	5.89	5.81
Al	4.31	4.28	4.93	5.51	4.38	4.35	5.15	4.03	4.90	4.41	4.40	4.73
Fe*	3.73	2.22	3.97	4.85	3.51	3.71	5.65	3.13	4.55	4.21	3.56	4.78
Ti	-	-	0.01	0.01	0.01	0.00	0.02	0.00	0.01	0.01	0.00	0.01
Mg	5.64	4.57	5.59	3.35	5.50	5.69	3.67	5.60	4.55	4.45	5.98	4.70
Mn	0.03	0.03	0.07	0.05	0.03	0.03	0.05	0.03	0.03	0.03	0.05	0.06
K	0.01	0.88	0.00	0.23	0.08	0.05	0.00	0.11	0.12	0.05	0.01	0.03
Na	0.01	0.02	0.00	0.06	0.01	0.02	0.00	0.02	0.00	0.03	0.00	0.01
Ca	0.06	0.02	0.00	0.00	0.04	0.04	0.01	0.09	0.01	0.09	0.02	0.02
Total	19.83	19.17	20.05	19.72	19.71	19.87	19.98	19.53	19.89	19.55	19.92	19.84

Ions based on 28 oxygens
* All iron as FeO

Appendix 8.11 Electron probe microanalyses of plagioclase feldspar

	1 Ak 338	2 Ak 80-a	3 Ak 2-c	4 Ak 8-a	5 Ak 80-a	6 Ak 80-b	7 Ak 412	8 Ak 365	9 Ak 370	10 Ak 370	11 Ak 380	12 Ak 336
SiO_2	65.55	59.81	67.02	67.63	67.16	67.13	65.89	65.85	68.48	67.99	65.88	68.09
Al_2O_3	20.02	23.71	19.93	19.77	19.94	20.02	19.60	20.31	19.37	19.33	20.29	18.85
*FeO	0.15	0.95	0.31	0.35	0.20	0.19	0.63	0.65	0.02	0.01	0.18	0.07
MgO	0.02	0.73	0.58	0.13	0.09	0.19	0.31	0.30	0.02	0.02	0.03	-
K_2O	0.32	4.25	0.19	0.45	0.82	0.54	0.25	1.06	0.06	0.03	0.49	0.01
Na_2O	11.05	7.17	11.36	11.36	10.97	11.11	11.15	10.35	11.86	11.68	10.71	11.59
CaO	0.78	0.68	0.51	0.18	0.19	0.33	0.56	0.46	0.33	0.19	0.87	0.03
Total	97.98	97.32	99.41	99.88	99.40	99.52	98.40	99.06	100.17	99.28	98.46	98.65
Ions based on 32 oxygens, Total iron as FeO												
Si	11.75	11.01	11.83	11.88	11.85	11.83	11.78	11.71	11.96	11.97	11.75	12.05
Al	4.23	5.14	4.15	4.09	4.15	4.16	4.13	4.26	3.99	4.01	4.26	3.93
*Fe	0.02	0.15	0.05	0.05	0.03	0.03	0.09	0.10	-	-	0.03	0.01
Mg	0.03	0.20	0.02	0.04	0.03	0.05	0.08	0.08	0.01	-	0.01	-
K	0.07	1.00	0.04	0.10	0.18	0.12	0.06	0.24	0.01	0.01	0.11	-
Na	3.84	2.56	3.89	3.87	3.75	3.79	3.87	3.57	4.02	3.99	3.70	3.98
Ca	0.15	0.135	0.10	0.03	0.04	0.06	0.11	0.09	0.06	0.04	0.17	0.01
Total	20.10	20.20	20.07	20.06	20.04	20.05	20.12	20.06	20.06	20.02	20.03	19.98

APPENDIX 8.12 Electron probe microanalyses of pyroxenes

Falahill Formation

	Sp No AK 338			Sp No AK 80-a				Sp No AK 80-b				
	1	2	3	1	2	3	4	1	2	3	4	5
SiO_2	52.18	50.65	50.57	49.32	50.57	48.84	51.04	49.12	50.67	50.90	52.19	50.32
TiO_2	0.25	0.64	0.73	1.18	0.98	1.27	0.63	0.46	1.21	0.29	0.36	1.24
Al_2O_3	2.27	2.75	3.06	3.90	2.84	4.60	2.63	6.12	2.57	2.23	1.64	2.71
Cr_2O_3	0.31	0.03	0.49	0.01	0.01	0.01	0.07	0.43	1.15	0.02	0.15	0.13
FeO*	5.44	6.49	4.56	6.90	7.15	7.18	9.74	4.25	8.48	9.03	6.55	8.68
MnO	0.19	0.18	0.10	0.17	0.34	0.20	0.28	0.35	0.21	0.46	0.19	0.24
MgO	17.30	15.55	15.66	14.22	15.14	14.47	15.33	15.15	14.81	14.92	17.28	14.79
CaO	20.88	19.04	22.63	21.90	21.48	21.91	19.16	22.66	20.13	19.04	19.87	19.91
Na_2O	0.26	0.26	0.32	0.40	0.40	0.40	0.32	0.16	0.39	0.47	0.13	0.38
Total	99.09	95.61	98.12	98.01	98.80	98.89	99.20	98.45	98.63	97.37	98.38	98.39
Number of cins based on 6 oxygens												
Si	1.93	1.94	1.90	1.87	1.90	1.84	1.92	1.83	1.91	1.94	1.95	1.90
Al	0.10	0.12	0.14	0.17	0.13	0.20	0.19	0.27	0.11	0.10	0.07	0.12
Ti	0.01	0.02	0.03	0.03	0.03	0.04	0.02	0.01	0.03	0.01	0.01	0.04
Mn	0.01	0.01	0.00	0.01	0.01	0.01	0.01	0.00	0.01	0.02	0.01	0.01
Fe	0.17	0.21	0.14	0.21	0.22	0.23	0.31	0.13	0.27	0.29	0.21	0.27
Cr	0.01	0.00	0.01	0.00	0.00	0.00	0.00	0.01	0.00	0.00	0.00	0.00
Mg	0.95	0.89	0.88	0.80	0.84	0.81	0.86	0.84	0.83	0.85	0.96	0.83
Ca	0.83	0.78	0.91	0.89	0.86	0.88	0.77	0.91	0.81	0.78	0.79	0.81
Na	0.02	0.02	0.02	0.03	0.03	0.03	0.02	0.01	0.03	0.04	0.01	0.03
Total	4.02	3.99	4.02	4.03	4.03	4.04	4.02	4.03	4.02	4.02	4.01	4.02
Al^{IV}	0.07	0.06	0.10	0.13	0.10	0.16	0.08	0.17	0.09	0.06	0.05	0.10
Al^{VI}	0.03	0.06	0.04	0.04	0.03	0.04	0.08	0.10	0.02	0.04	0.02	0.02
$F1^{\ddagger}$	-0.79	-0.79	-0.84	-0.87	-0.87	-0.87	-0.81	-0.83	-0.87	-0.80	-0.78	-0.86
$F2^{\ddagger}$	-2.43	-2.42	-2.38	-2.39	-2.45	-2.40	-2.46	-2.46	-2.46	-2.44	-2.45	-2.46

* Total iron as FeO

‡ F1 and F2 calculated after Nisbet & Pearce (1977)

APPENDIX 8.12: Electron probe microanalyses of pyroxenes - continued

2 HAZELBANK FORMATION

	Sp Ak-2-C				Sp Ak-412				
	1	2	3	4	1	2	3	4	5
SiO_2	51.36	50.20	51.93	50.51	50.21	51.42	53.34	50.32	50.69
TiO_2	0.62	0.63	0.41	0.65	0.70	0.39	0.50	0.47	0.69
Al_2O_3	2.75	3.74	1.71	3.65	2.08	2.52	0.56	3.32	1.95
Cr_2O_3	-	0.26	0.01	0.08	0.03	0.30	0.02	0.40	0.04
FeO	8.68	7.41	8.25	7.22	12.06	5.95	3.46	6.43	11.85
MnO	0.35	0.18	0.39	0.17	0.38	0.17	0.11	0.18	0.35
MgO	15.34	15.02	15.12	14.92	14.34	16.45	16.22	15.30	14.30
CaO	20.17	21.32	20.87	19.16	18.05	20.92	25.14	21.65	18.60
Na_2O	0.30	0.29	0.44	0.23	0.31	0.33	0.03	0.35	0.34
Total	99.57	99.06	99.13	96.58	98.17	98.45	98.93	98.43	98.82
Number of ions based on 6 oxygens * All iron as FeO									
Si	1.92	1.88	1.95	1.92	1.92	1.92	1.98	1.89	1.93
Ti	0.02	0.02	0.01	0.02	0.02	0.01	0.00	0.01	0.02
Al	0.12	0.17	0.08	0.16	0.09	0.11	0.02	0.15	0.09
Cr	-	0.01	0.00	0.00	0.00	0.01	0.00	0.01	0.00
Fe	0.27	0.23	0.26	0.23	0.39	0.19	0.01	0.20	0.38
Mn	0.01	0.01	0.01	0.01	0.01	0.01	0.00	0.01	0.01
Mg	0.85	0.84	0.84	0.85	0.82	0.92	0.90	0.86	0.81
Ca	0.81	0.86	0.84	0.78	0.74	0.84	1.00	0.87	0.76
Na	0.02	0.02	0.03	0.02	0.02	0.02	0.00	0.03	0.02
Total	4.02	4.03	4.02	3.99	4.02	4.02	4.02	4.03	4.02
Al^{IV}	0.10	0.12	0.08	0.08	0.08	0.08	0.02	0.11	0.07
Al^{VI}	0.04	0.05	0.03	0.08	0.01	0.03	-	0.04	0.02
$*^2F1$	-0.83	-0.82	-0.84	-0.79	-0.81	-0.80	-0.84	-0.81	-0.82
$*^2F2$	-2.47	-2.40	-2.45	-2.43	-2.44	-2.41	-2.38	-2.38	-2.45

2* F1 and F2 calculated after Nisbet & Pearce (1977) (see text)

APPENDIX 8.12: Electron probe microanalyses of pyroxenes - continued

2 HAZELBANK FORMATION - cont

	Ak Sp Ak-365					Sp Ak-380
	1	2	3	4	5	1
SiO_2	51.58	49.18	50.32	50.54	52.25	48.41
TiO_2	0.57	0.84	0.82	0.55	0.74	1.23
Al_2O_3	1.81	5.44	3.12	3.47	1.92	4.62
Cr_2O_3	0.02	0.03	0.05	0.11	0.01	-
FeO*	10.16	7.98	9.56	7.38	8.81	8.24
MnO	0.42	0.18	0.23	0.18	0.35	0.21
MgO	14.59	13.96	13.89	15.36	15.33	13.88
CaO	19.86	19.97	20.87	20.37	20.31	20.82
Na_2O	0.30	0.31	0.38	0.33	0.29	0.44
Total	99.31	97.90	99.25	98.29	100.01	97.84
Number of irons based on 6 oxygens * All iron as FeO						
Si	1.94	1.86	1.90	1.90	1.94	1.85
Ti	0.02	0.02	0.02	0.02	0.02	0.04
Al	0.08	0.34	0.14	0.15	0.08	0.21
Cr	0.00	0.00	0.00	0.00	0.00	-
Fe	0.32	0.25	0.30	0.23	0.27	0.26
Mn	0.01	0.01	0.01	0.01	0.01	0.01
Mg	0.82	0.78	0.78	0.86	0.85	0.79
Ca	0.80	0.81	0.84	0.82	0.81	0.85
Na	0.02	0.02	0.03	0.02	0.02	0.03
Total	4.02	4.01	4.03	4.02	4.01	4.04
Al^{IV}	0.06	0.14	0.10	0.10	0.06	0.15
Al^{VI}	0.02	0.20	0.04	0.05	0.02	0.06
$*^2F1$	-0.84	-0.81	-0.85	-0.80	-0.85	-0.86
$*^2F2$	-2.47	-2.41	-2.42	-2.41	-2.51	-2.39

* Total iron as FeO

*2 F1 and F2 calculated after Nisbet & Pearce (1977)

Appendix 8.13

Electron probe microanalyses of amphiboles - Falahill

	Ak-338			Ak-80-a		Ak-80-b				
	1	2	3	4	5	6	7	8	9	10
SiO_2	47.42	40.68	42.62	42.02	40.35	42.87	42.92	42.14	45.81	42.05
TiO_2	6.87	2.06	1.68	3.34	1.95	2.74	2.46	2.74	2.21	0.32
Al_2O_3	7.34	12.41	11.78	11.76	9.75	10.44	10.63	11.87	8.37	12.45
FeO*	13.39	13.37	13.65	12.25	14.93	11.25	12.10	10.88	11.27	19.12
MnO	0.32	0.17	0.24	0.20	0.26	0.32	0.20	0.12	0.15	0.12
MgO	13.90	12.64	13.07	13.39	13.71	14.27	14.08	14.64	15.35	9.04
CaO	12.03	11.33	11.16	11.19	8.91	11.22	11.17	11.08	11.12	6.37
Na_2O	0.75	2.26	2.27	2.24	1.5	2.23	2.21	2.39	2.02	4.14
K_2O	0.53	0.87	0.57	1.05	0.71	0.96	0.50	0.89	0.87	0.36
F_2O	0.03	0.10	0.18	0.13	0.17	0.16	0.21	0.19	0.27	0.22
Total	96.67	95.91	97.22	96.59	92.25	96.47	96.50	96.95	97.45	94.23

* All iron as FeO
* Ions based on 22 oxygens

Si	6.72	5.91	6.08	6.03	6.10	6.12	6.13	6.97	6.45	6.28
Ti	0.09	0.23	0.18	0.36	0.22	0.29	0.26	0.29	0.23	0.04
Al^{IV}	1.23	2.09	1.92	1.82	1.74	1.76	1.79	1.98	1.39	1.72
Al^{VI}	-	0.04	0.06	-	-	-	-	-	-	0.48
Fe^{tot*}	1.59	1.62	1.63	1.47	1.89	1.34	1.45	1.29	1.32	2.39
Fe^{3+}*	0.244	0.180	0.114	0.00	0.540	0.00	0.00	0.00	0.00	0.00
Fe^{2+}	1.406	1.511	1.584	1.537	1.411	1.405	1.511	1.349	1.384	2.49
Mn	0.04	0.02	0.03	0.02	0.03	0.04	0.02	0.01	0.02	0.02
Mg	2.93	2.74	2.78	2.86	3.09	3.04	3.00	3.09	3.21	2.01
Ca	1.83	1.76	1.71	1.72	1.44	1.72	1.70	1.68	1.67	1.02
Na	0.21	0.64	0.63	0.62	0.44	0.62	0.61	0.66	0.55	1.20
K	0.10	0.16	0.10	0.19	0.14	0.17	0.09	0.16	0.16	0.07
F	0.01	0.05	0.08	0.06	0.08	0.07	0.10	0.09	0.12	0.11
Total	14.77	15.25	15.20	15.17	15.18	15.18	15.17	15.24	15.19	15.33

Appendix 8.13 - continued

Electron probe microanalyses of amphiboles - Hazelbank

	Ak-2-c			Ak-412			Ak-365			Ak 380
	11	12	13	14	15	16	17	18	19	20
SiO_2	48.31	42.57	50.75	41.64	44.10	40.36	50.86	43.57	46.56	46.82
TiO_2	0.36	1.91	0.48	1.11	1.63	2.17	0.31	1.73	1.67	3.03
Al_2O_3	7.83	13.81	5.17	14.46	9.78	13.40	4.82	10.52	7.25	12.19
FeO*	12.33	9.54	11.91	10.16	12.12	14.17	12.39	13.89	14.45	11.05
MnO	0.24	0.14	0.26	0.13	0.32	0.22	0.33	0.30	0.39	0.15
MgO	14.66	14.33	16.43	14.12	14.66	12.17	15.38	13.19	13.38	14.03
CaO	11.41	11.77	10.78	11.69	10.76	11.46	11.43	10.99	11.31	11.58
Na_2O_3	1.31	2.70	0.55	2.49	2.40	2.41	0.45	2.09	1.31	2.36
K_2O	0.02	0.05	0.08	0.01	0.54	0.66	0.11	0.64	0.70	1.05
F_2O	0.66	0.03	0.02	-	0.11	0.35	0.03	0.11	0.10	0.11
Total	96.54	96.86	95.45	96.82	97.42	96.36	97.12	97.04	97.12	96.36

* All iron as FeO
* Ions based on 22 oxygens

Si	6.77	5.96	7.06	5.91	6.28	5.81	7.13	6.22	6.62	5.85
Ti	0.04	0.20	0.05	0.12	0.17	0.24	0.03	0.19	0.18	0.33
Al^{IV}	1.23	2.04	0.85	2.09	1.64	2.19	0.80	1.77	1.22	2.06
Al^{VI}	0.06	0.24	-	0.33	-	0.08	-	-	-	-
Fe^{tot}*	1.45	1.12	1.39	1.21	1.44	1.70	1.45	1.66	1.72	1.33
Fe^{3+}	0.039	0.00	0.116	0.242	0.00	0.244	0.079	0.040	0.00	0.00
Fe^{2+}	1.471	1.168	1.329	1.011	1.510	1.529	1.436	1.692	1.797	1.285
Mn	0.03	0.02	0.03	0.02	0.04	0.03	0.04	0.04	0.05	0.02
Mg	3.06	2.99	3.41	2.98	3.11	2.61	3.21	2.81	2.84	3.00
Ca	1.72	1.76	1.61	1.78	1.64	1.77	1.72	1.68	1.72	1.78
Na	0.36	0.73	0.15	0.68	0.06	0.67	0.12	0.58	0.36	0.66
K	-	0.01	0.02	-	0.10	0.12	0.02	0.12	0.13	0.19
F	0.03	0.01	0.01	-	0.05	0.16	0.01	0.05	0.05	0.05
Total	14.75	15.09	14.57	15.12	15.16	15.38	14.53	15.11	14.88	15.27

Fe^{3+} calculated using the charge balance equation of Papike et al. (1974).

APPENDIX 8.14 Electron probe microanalyses of glaucophane

Falnhill Formation

	Ak-338		Ak 80-a			Ak-80-b
	1	2	3	4	5	6
SiO_2	52.5	46.35	54.38	50.98	52.37	54.13
TiO_2	0.77	0.18	0.05	0.14	0.12	0.04
Al_2O_3	7.81	11.10	8.94	9.93	8.57	6.72
FeO*	17.25	19.73	18.19	17.00	15.54	18.29
MnO	0.18	0.18	0.11	0.11	0.19	0.25
MgO	8.82	7.39	6.18	8.40	9.72	8.32
CaO	1.80	5.71	0.76	2.12	3.35	1.11
Na_2O	6.45	5.34	7.08	6.26	6.03	6.98
K_2O	0.01	0.35	0.07	0.13	0.11	0.03
F_2O	0.06	0.15	0.04	0.09	0.19	0.07
Total	95.65	96.49	95.81	95.16	96.20	95.95
*All iron as FeO Ions based on 22 oxygens						
Si	7.41	6.72	7.63	7.24	7.33	7.63
Ti	0.08	0.02	0.01	0.01	0.01	-
Al^{IV}	0.59	1.28	0.37	0.76	0.67	0.37
Al^{VI}	0.71	0.62	1.11	0.90	0.74	0.75
Fe^{tot*}	2.04	2.39	2.13	2.02	1.82	2.16
Fe^{3+}	0.00	0.00	0.00	0.00	0.00	0.00
Fe^{2+}	2.12	2.50	2.23	2.11	1.90	2.25
Mn	0.02	0.02	0.01	0.01	0.02	0.03
Mg	1.85	1.60	1.29	1.78	2.02	1.75
Ca	0.27	0.89	0.11	0.32	0.50	0.17
Na	1.76	1.50	1.93	1.72	1.64	1.91
K	-	0.06	0.01	0.02	0.02	0.01
F	0.03	0.07	0.02	0.04	0.08	0.03
Total	14.77	15.17	14.62	14.84	14.87	14.80

* Fe^{3+} calculated using the charge balance equation of Papike et al. 1974.

APPENDIX No 5.15: Electron probe microanalyses of white mica NB 12, 2, 2a, 6 and 6a are prehnite grown within mica fiamwes

	Ak-338 1	1a	2 Ak 80-a	2a Ak 80-a	3 Ak 80-a	4 Ak 2C	5 Ak 2C	6 Ak 80-b	6a Ak 80-b	7 Ak 412	8 Ak 365	9 Ak 370	10 Ak 380
SiO_2	48.19	43.80	44.01	46.41	48.32	45.51	46.25	42.84	43.13	49.38	50.29	46.42	45.82
Al_2O_3	26.6	23.59	24.00	26.69	25.77	33.90	33.78	23.10	24.02	27.90	27.31	33.93	32.13
FeO	3.71	3.54	1.76	2.19	4.24	2.19	1.90	1.10	0.87	3.20	2.27	1.07	1.73
TiO_2	0.16	0.13	0.13	0.28	0.22	0.20	0.23	0.07	0.06	0.21	0.20	0.67	0.47
MgO	2.90	5.84	0.59	1.67	3.02	1.16	0.88	0.08	0.43	2.17	2.93	0.99	1.61
MnO	0.01	0.05	0.02	0.01	0.02	-	-	0.02	0.23	0.01	0.01	-	0.01
K_2O	10.41	4.69	2.05	6.61	9.97	9.14	9.66	0.06	0.31	10.58	10.65	9.35	10.40
Na_2O	0.06	0.42	0.30	0.67	0.82	1.43	0.96	0.03	0.04	0.24	0.22	0.90	0.65
CaO	0.03	9.03	21.04	9.38	0.14	-	-	26.08	25.24	-	-	0.05	-
Total	92.62	91.10	93.91	93.93	92.52	93.54	93.68	93.38	94.13	93.71	93.89	93.39	92.82

* All iron as FeO, Ions based on 22 oxygens

Analysis No	1	1-a	2	2-a	3	4	5	6	6-a	7	8	9	10
Si	6.69	6.25	6.16	6.39	6.73	6.18	6.26	6.05	6.02	6.73	6.81	6.26	6.29
Al	4.36	3.97	3.96	4.34	4.23	5.43	5.39	3.85	3.96	4.49	4.36	5.40	5.20
Fe	0.43	0.42	0.21	0.25	0.49	0.25	0.21	0.13	0.10	0.37	0.26	0.12	0.20
Ti	0.02	0.01	0.01	0.03	0.02	-	0.02	0.01	0.01	-	0.02	0.07	0.05
Mg	0.60	1.24	0.12	0.34	0.63	0.23	0.18	0.02	0.09	0.04	0.59	0.20	0.33
Mn	-	0.01	-	-	-	-	-	-	-	-	-	-	-
K	1.85	0.85	0.37	1.16	1.77	1.58	1.67	0.01	0.06	1.84	1.84	1.61	1.82
Na	0.16	0.12	0.09	0.16	0.22	0.38	0.25	0.01	0.01	0.07	0.06	0.24	0.17
Ca	-	1.38	3.15	1.38	0.02	-	-	3.95	3.78	-	-	0.01	-
Total	14.12	14.25	14.07	14.08	14.13	14.07	13.99	14.03	14.03	13.96	13.94	13.90	14.06

Analyses No	11 Ak 337	12 Ak 159	13 Ak 759	14 Ak 3	15 Ak 764	16 Ak 334	17 Ak 214	18 Ak 85	19 Ak 654
SiO_2	47.96	45.63	46.27	47.27	44.38	43.63	44.14	46.01	46.33
Al_2O_3	28.34	33.82	33.24	27.69	35.51	25.79	33.45	32.97	32.64
FeO	3.44	1.35	1.19	4.45	1.03	3.93	3.22	2.67	1.46
TiO_2	0.43	1.21	1.23	0.58	0.04	0.47	0.57	0.37	1.37
MgO	2.29	0.76	1.07	2.15	0.56	1.86	1.84	1.10	1.20
MnO	-	0.2	-	-	-	0.04	0.06	0.05	0.06
K_2O	9.69	10.75	9.39	9.66	7.91	8.34	7.19	9.70	11.00
Na_2O	0.91	0.39	0.93	1.08	0.49	1.02	0.60	1.12	0.48
CaO	0.03	0.02	0.04	-	-	0.06	0.07	0.07	0.05
Total	93.09	93.96	93.35	92.80	89.92	85.15	91.15	94.07	94.59

Ions based on 22 oxygens

* All iron as FeO

Si	6.59	6.18	6.26	6.57	6.15	6.57	6.11	6.24	6.25
Al	4.59	5.4	5.30	4.53	5.80	4.50	5.46	5.27	5.19
Fe	0.40	0.15	0.13	0.52	0.12	0.49	0.37	0.30	0.16
Ti	0.04	0.12	0.13	0.05	-	0.05	0.06	0.04	0.14
Mg	0.47	0.15	0.22	0.45	0.12	0.42	0.38	0.22	0.24
Mn	-	-	-	-	-	-	0.01	0.01	0.01
K	1.70	1.86	1.62	1.71	1.40	1.60	1.27	1.68	1.89
Na	0.24	0.10	0.24	0 29	0.13	0.30	0.16	0.29	0.13
Ca	-	-	0.01	-	-	0.01	0.01	0.01	0.01
Total	14.04	13.98	13.91	14,12	13.72	14.04	13.83	14.07	14,03

APPENDIX 8.16 Electron probe microanalysis of biotite

	1 Ak 338	2 Ak 370	3 Ak 370	4 Ak 336	5 Ak 337	6 Ak 159	7 Ak 85	8 Ak 654	9 Ak 654
SiO_2	28.81	29.75	28.03	31.17	32.46	29.27	48.38	31.28	27.38
Al_2O_3	13.93	19.20	18.53	15.40	16.30	16.90	21.84	18.86	16.10
FeO*	20.43	23.24	23.99	18.80	18.73	22.14	11.98	22.85	25.04
TiO_2	2.32	1.68	1.57	3.22	1.87	3.17	0.12	2.28	2.50
MgO	19.04	11.98	12.86	17.24	16.12	13.79	5.83	10.20	15.12
MnO	0.34	0.07	0.05	0.29	0.29	0.13	0.08	0.11	0.19
K_2O	0.24	1.54	0.94	2.75	0.56	1.03	4.62	4.86	0.07
F_2O	0.02	0.10	0.13	0.06	0.04	0.16	0.08	0.15	0.03
CaO	0.41	0.21	0.29	0.86	0.17	0.12	0.02	0.05	0.12
Na_2O	0.07	0.05	0.05	0.06	1.23	0.04	0.23	0.06	0.02
Total	85.61	87.82	86.45	89.86	87.77	86.77	93.17	90.72	86.59
Ions based on 23 oxygens									
Si	5.01	5.08	4.90	5.16	5.40	5.05	7.06	5.25	4.81
Al	2.86	3.87	3.82	3.01	3.20	3.44	3.76	3.73	3.34
Fe	2.97	3.32	3.51	2.61	2.61	3.20	1.46	3.21	3.68
Ti	0.30	0.22	0.21	0.40	0.23	0.41	0.01	0.29	0.33
Mg	4.94	3.05	3.35	4.26	4.00	3.55	1.27	2.55	3.96
Mn	0.05	0.01	0.01	0.04	0.04	0.02	0.01	0.02	0.03
K	0.05	0.34	0.21	0.58	0.12	0.23	0.86	1.00	0.02
F	0.01	0.05	0.07	0.32	0.02	0.09	0.04	0.08	0.02
Ca	0.08	0.04	0.06	0.15	0.03	0.02	-	0.01	0.02
Na	0.02	0.02	0.02	0.12	0.40	0.01	0.06	0.02	0.01
Total	16.31	16.00	16.17	16.27	16.05	16.03	14.55	16.21	16.22

* All iron as FeO

APPENDIX 8.17 Electron probe microanalyses of Carbonate

	(AK 159) 1	(AK 759) 2	(AK 759) 3	(AK 759) 4	(AK 3) 5	(AK 370) 6
CaO	53.42	52.62	49.71	53.52	48.33	54.45
MgO	0.09	0.26	0.28	0.64	0.05	0.64
MnO	0.15	0.15	0.42	0.02	0.12	0.01
FeO*	0.09	0.26	0.16	0.02	0.03	0.03
SiO_2	-	0.11	4.65	-	0.17	-
Total	53.77	53.37	55.90	54.21	48.88	55.13
Ions based on three oxygens * All iron as FeO						
CaO	2.98	2.95	2.50	2.95	2.96	2.95
Mg	0.01	0.02	0.02	0.05	-	0.05
Mn	0.01	0.01	0.02	-	0.01	-
Fe	-	0.01	0.01	-	-	-
Si	-	0.01	0.22	-	0.01	-
Total	3.00	3.00	2.78	3.00	2.99	3.00

APPENDIX 8.18 Electron probe microanalyses of heavy minerals

	Garnet		Epidote		Ilmenite			Apatite
	AK 159	AK 159	AK 380	AK 380	AK 85	AK 85	AK 85	AK 380
SiO_2	37.11	37.98	37.46	37.69	0.02	0.05	0.03	-
Al_2O_3	21.08	21.93	22.62	24.82	26.91	23.60	19.29	-
FeO*	34.16	25.99	12.54	9.70	16.35	16.31	19.98	0.29
TiO_2	0.06	0.65	0.01	0.01	0.01	-	0.05	-
Cr_2O_3	-	-	-	-	42.24	46.04	47.72	-
MgO	3.34	7.05	0.04	0.02	13.41	12.79	11.11	0.13
MnO	0.41	0.92	0.60	0.10	0.59	0.64	0.70	0.01
P_2O_5	-	-	-	-	-	-	-	36.40
F_2O	-	-	-	-	-	-	-	4.92
K_2O	-	-	0.15	-	-	-	-	-
Na_2O	-	0.01	0.01	0.02	-	0.01	0.01	-
CaO	2.87	5.68	21.63	23.13	-	-	-	53.54
Total	99.04	99.54	95.07	95.51	99.53	99.45	98.91	95.30
*All iron as FeO O = 24			O = 6		O = 6			O = 25
Si	5.99	1.48	1.50	1.48	-	-	-	-
Al	4.01	1.00	1.07	1.15	1.44	1.29	1.09	-
Fe	4.62	0.85	0.42	0.32	0.62	0.63	0.80	0.04
Ti	0.01	-	-	-	-	-	-	-
Cr	-	-	-	-	1.52	1.68	1.81	-
Mg	0.80	0.41	-	-	0.91	0.88	0.80	0.04
Mn	0.06	0.03	0.02	-	0.02	0.02	0.03	-
P	-	-	-	-	-	-	-	5.71
F	-	-	-	-	-	-	-	2.88
K	-	-	-	-	-	-	-	-
Na	-	-	-	-	-	-	-	-
Ca	0.50	0.24	0.93	0.98	-	-	-	10.63
Total	15.99	4.02	3.96	3.94	4.52	4.52	4.55	19.32

Appendix 8.19: Precision of electron microprobe data

All analyses were performed at the Grant Institute of Geology, University of Edinburgh, using the energy dispersive electron microprobe. Calebration was monitored by a cobalt standard; accuracy was estimated by analysing a jadeite stanard prior to the commencement of each session. Precision is 1% at 50% concentration level, 2% at 10% concentration level and 10% at 2% concentration level (P. G. Hill, pers comm 1984).